Convergent-Beam Electron Diffraction

Convergent-Beam Electron Diffraction

by
Michiyoshi Tanaka
Masami Terauchi

Physics Department,
Faculty of Science,
Tohoku University

JEOL LTD.

Published by JEOL LTD.
1418 Nakagami, Akishima, Tokyo, 196 Japan

Printed in Japan

Contents

Preface

In recent years, analytical electron microscopy has been taking rapid strides. Among the important functions of analytical electron microscopy is included the convergent-beam electron diffraction (CBED) method, which is now in the course of development. This book surveys the CBED methods, using a plenty of photographs taken by them.

My first motivation to publish it was that I was requested to bring out a publication composed of photographs taken by CBED. The second was that I wished to publish, in some form or other, many of our CBED photographs which, although not included in any paper so far, are of high scientific value and quite worth seeing. And the third motivation was that I was incited by the recent publication of "Convergent Beam Electron Diffraction of Alloy Phases" by the Bristol Group under the direction of Professor Steeds.

The present work is not intended to describe in detail the complicated theories of the point-group and space-group determination methods. It briefly illustrates a wide variety of CBED techniques by using ray-path diagrams of our electron microscope and patterns obtained from (111) Si crystals, and gives an easy-to-understand description of point-group and space-group determination procedures, using examples of real-crystals. I have also included as much application data as possible in the hope that the reader will see what can be done by CBED and appreciate the beauty of crystal symmetries revealed by CBED.

CBED techniques and their application to materials science are still under development. There are other techniques and many application data which I want to include in this book, but I have given up doing so because I, being a slow writer, have not yet announced them in scientific publications. I wish to add such techniques and data in future subsequent editions of this publication, to make it more complete.

I admit that this first edition is not entirely well balanced with regard to space allotment to the individual chapters, which I would like to correct step by step. I considered it better to take the first, although incomplete, step rather than to delay the publication of this book by attaching too much importance to its completeness and best editorial balance. The references were limited to a necessary minimum, then even those papers which should necessarily be referred to when reviewing CBED in a scientific journal were omitted. Most of the photographs included in this publication were taken with a JEM-100CX, which has lately been equipped with an FEG. Others were taken with a JEM-200CX, JEM-1200EX and JEM-2000FX by courtesy of JEOL LTD. It is noted that the photographs without any indication were taken at an accelerating voltage of 100kV.

The data shown herein was obtained with the cooperation of successive graduate students in the Master Course of Physics Department of Tohoku University. Those people are Mr. R. Saito (presently at Hitachi Research Lab, Hitachi Ltd.), Mr. S. Matsuda (Textile Research Lab, Asahi Chemical Industry Co., Ltd.), Mr. H. Sekii (Central R & D Lab, Omuron Tateishi Electrics Co.), Mr. T. Nagasawa, Mr. H. Takayoshi (Komukai Works, Toshiba Co.), Mr. K. Kaneyama (Master Course, Phys. Dept., Tohoku Univ.) and Mr. M. Terauchi (Master Course, Phys. Dept., Tohoku Univ.), who is the co-author of this book. I am deeply indebted to these people for their cooperation in this work.

I express my cordial gratitude to JEOL LTD's staff, especially Mr. T. Eto, Mr. Y. Harada, Mr. K. Ueno, Mr. Y. Hirata, Mr. T. Tomita and Mr. Y. Kondo for their devoted collaboration in developing the CBED techniques. I thank Mr. F. Sato for his highly skilled photograph printing and for the maintnance of the JEM-100CX-FEG. And I express my heartfelt thanks to Prof. D. Watanabe for allowing me and the graduate students to concentrate on this work.

I am indebted to the following for permission to use illustrations: The Japanese Society of Electron Microscopy (p.12, 14 ~ 18, 28, 59, 64, 66, 67, 80 ~ 86, 88, 90 ~ 93), the Publication Office, Japanese Journal of Applied Physics (pp.30, 31), International Union of Crystallography (pp.46, 47, 51 ~ 53, 152, 153, 156 ~ 159) and the Royal Society of London (pp.154, 155).

This work was supported financially by the Grant-in-Aid of Scientific Research (No. 142009, No. 346033, No. 57420014) and the Grant-in-Aid for Developmental Scientific Research (No. 56840016) from the Ministry of Education, Science and Culture, and by the Kurata Research Grant.

Sendai, Spring 1985

Michiyoshi Tanaka

Introduction

The methods to investigate crystal structures by electron microscopy and electron diffraction can be divided into two categories. The first is aimed at obtaining microscopic images of high spacial resolution by illuminating a specimen with a parallel incident beam. Experimental and theoretical studies on crystal structure images have been developed, and then this method, phase-contrast microscopy, has been applied to the study of crystal structures of a great many materials. The second is aimed at obtaining diffracted intensity profiles with high angular resolution by illuminating a specimen with a convergent beam. This method has recently been developed and is called convergent-beam electron diffraction (CBED).

The method corresponding to CBED in the field of light optics is that with a conoscope. Using a conoscope, we can identify a crystal to be isotropic, uniaxial or biaxial, and determine the optical axis and the signs of birefringence. When using CBED — a conoscope method with an electron beam accompanied by the diffraction effect — we can determine more basic properties of a crystal: crystal point-groups and space-groups.

Point- and space-group determinations have so far been carried out by the X-ray diffraction method. This method, to which the kinematical diffraction theory is applicable, can not determine whether a crystal is polar or non-polar unless the anomalous dispersion effect is utilized. As a result, the X-ray diffraction method can only identify 11 Laue groups among 32 point groups. CBED, based fully upon the dynamical diffraction, can distinguish polar crystals from non-polar crystals, thus allowing the unique identification of point groups. Furthermore, it enables us to know the presence of a 2_1 screw axis and glide planes. CBED is much superior to the X-ray method in determining crystal point-groups and space-groups.

When combined with electron microscopy, CBED can identify small areas down to 1 nm in diameter and determine the symmetries of the areas. In recent years, the microanalysis using an electron microscope (analytical electron microscopy) has been rapidly developed by combining various analyzing methods. CBED has been established as one of the important functions in analytical electron microscopy.

CBED obtains diffraction patterns using a conical electron beam with an angle of more than 10^{-3} rad. on a uniform and non-bending specimen area about 10 nm in diameter (a JEM-100CX equipped with a field emission gun can illuminate an about 1-nm-diameter specimen area). Instead of usual diffraction spots, diffraction disks are produced. All the point groups can be determined uniquely by inspecting the symmetries appearing in the disks. For the theory of point-group determination, the reader is referred to the references [1] and [2].

A 2_1 screw axis and glide planes are identified by CBED through a conspicuous dynamical diffraction effect. When a crystal has the axis or the planes, special extinction lines can appear in kinematically forbidden reflections, the lines being called dynamic extinction lines or GM lines. By examining whether GM lines are formed or not in kinematically forbidden reflections, most space groups can be identified. For the theory of space-group determination, the reader is referred to the references [3] and [4].

The observation of a crystal defect by CBED was first carried out for a stacking fault parallel to the foil surface of a graphite specimen[5], where some of the symmetries observed for a perfect crystal were lost. The identification of the Burgers vector of a dislocation was recently performed by CBED[6]. A theory has been proposed for the CBED symmetries expected from a bicrystal like a twinned crystal, whose interface lies parallel to the specimen surface at the midpoint of the specimen[7]. A convenient method for determining the specimen thickness using the two-beam dynamical theory has been given in the reference[8]. Low-order crystal structure factors can be determined by bringing simulated intensity profiles computed by using the many-beam dynamical theory into good agreement with the observed intenisty profiles[9].

The basic method to obtain CBED patterns is that by CTEM, where a clean vacuum of less than 2×10^{-7} Torr and a condenser-objective (C-O) lens are required to avoid the contamination of specimens and to suppress the distortion of CBED disks, respectively. The identification of the specimen area from which a CBED pattern is obtained is performed by varying the excitation of a mini lens placed just above the C-O lens or by the additive use of a STEM attachment.

In CBED at the present stage, element beams in the incident beam are assumed to be incoherent with each other. Then, CBED patterns can be alternatively obtained by rocking a parallel incident beam with a point on a specimen as the fulcrum, instead of a convergent beam[10]. In the beam rocking (BR) method, electrical signal processing[11] can be performed to make clear CB-

ED pattern symmetries, since diffracted intensities are converted into electrical signals.

In ordinary CBED, the angular size of a diffraction disk is limited by a neighbouring disk. The techniques to obtain a larger non-overlapping disk by overcoming the limitation were developed for both the CTEM and BR methods [12], [13], [14]. When the hollow-cone beam (HCB) method is applied to CTEM-CBED, a large-angle whole pattern is obtained [15], [16], [17]. When the angle of HCB against the optical axis is set to the Bragg angle of a HOLZ reflection, a whole pattern consisting only of HOLZ reflections is obtained.

A bright electron source is quite effective for CBED. The BR-CBED method would not have reached the level of practical use if a field emission gun (FEG) had not been equipped on an electron microscope. In CBED, an accelerating voltage as low as 20 kV is quite useful to reveal three-dimensional symmetries in contrast to high resolution microscopy, where a higher accelerating voltage is advantageous to obtain higher resolution. The FEG supplies an intense beam sufficient for taking CB-ED patterns at a low accelerating voltage. In application fields, the FEG is also effective, for example, to obtain CBED patterns of weak superlattice reflections and weak incommensurate reflections.

In the next chapter various techniques to obtain CB-ED patterns are illustrated and a description is given of a drawing method for HOLZ lines, the accelerating voltage and lattice parameter determination methods and a specimen-thickness determination method. In the following chapters, the point-group and space-group determination methods are demonstrated. In the last chapter, various application data is collected. In the appendices, figures, tables necessary for point- and space-group determinations, and computer programs for drawing HOLZ lines, etc. are given to help understand the CBED method.

References

Point Groups

[1] B.F. Buxton, J.A. Eades, J.W. Steeds and G.M. Rackham: *Phil. Trans. R. Soc. London,* **281** (1976) 171.

[2] M. Tanaka, R. Saito and H. Sekii: *Acta Cryst.*, **A39** (1983) 357.

Space Groups

[3] J. Gjønnes and A.F. Moodie: *Acta Cryst.*, **19** (1965) 65.

[4] M. Tanaka, H. Sekii and T. Nagasawa: *Acta Cryst.*, **A39** (1983) 825.

Defects

[5] A.W.S. Johnson: *Acta Cryst.*, **A28** (1972) 89.

[6] F.W. Schapink, S.K.E. Fogany and B.F. Buxton: *Acta Cryst.*, **A39** (1983) 805.

[7] R.W. Carpenter and J.C.H. Spence: *Acta Cryst.*, **A38** (1982) 55.

Specimen Thickness

[8] P.M. Kelly, A. Jostsons, R.G. Blake and J.G. Napier: *phys. stat. sol. (a),* **31** (1975) 771.

Structure Factors

[9] P. Goodman and G. Lehmpfuhl: *Acta Cryst.*, **22** (1967) 14.

Techniques

Beam-Rocking

[10] M. Tanaka: *Prac. Met.*, **20** (1983) 201.

Signal Processing

[11] M. Tanaka, K. Ueno and Y. Hirata: *Jpn. J. Appl. Phys.*, **19** (1982) L201.

LACBED

[12] J.A. Eades: *Inst. Phys. Conf. Ser.*, **52** (1980) 9.

[13] M. Tanaka, R. Saito, K. Ueno and Y. Harada: *J. Electron Microsc.*, **29** (1980) 408.

[14] M. Terauchi and M. Tanaka: *J. Electron Microsc.*, **34** (1985) in the press.

Hollow-Cone Beam

[15] Y. Kondo, T. Ito and Y. Harada: *Jpn. J. Appl. Phys.*, **23** (1984) L178.

[16] M. Tanaka, H. Takayoshi, M. Terauchi, Y. Kondo, K. Ueno and Y. Harada: *J. Electron Microsc.*, **33** (1984) 195.

[17] M. Tanaka and M. Terauchi: *J. Electron Microsc.*, **34** (1985) 52.

Techniques

The CBED techniques are listed in the diagram. The techniques are divided into two branches — the CTEM and STEM & BR methods. The CTEM method is the basic one. The BR method, an alternative method to obtain CBED patterns, is for rather advanced or special use, since an additional electronic device, the STEM unit, is needed and the incident beam is inefficiently used. In the following, each technique is illustrated using diagrams together with CBED patterns obtained mainly from (111) Si specimens.

CTEM-CBED consists of six techniques. The most fundamental technique to obtain CBED patterns by CTEM is firstly described. Various shaped condenser apertures are introduced to obtain the intensity distribution over the entire Brillouin zone, instead of a circular aperture normally used. The LACBED technique allows obtaining non-overlapping disks whose angular size is larger than that limited by a neighbouring disk. By LACBED I, a large-angle bright-field pattern and large-angle dark-field patterns are recorded on different films. These patterns are obtained simultaneously on a film by LACBED II.

Hollow-cone beam techniques using an electrical and an aperture method enable us to obtain a large-angle whole pattern. The FEG is very important for obtaining CBED patterns at low accelerating voltages and BR-CBED patterns with a shorter exposure time. An α-selector technique is useful in CBED experiments. This technique can change the angle of a convergent incident-beam to a certain extent keeping the probe size on the specimen constant by varying the excitation of the illumination lens system with other conditions unchanged.

STEM- and BR-CBED consist of four techniques. The STEM technique enables us to identify the specimen position from which a CBED pattern is obtained. The beam-rocking method is an alternative technique to obtain CBED patterns. The LACBED technique by the BR method is described. Signal processing to make clear the symmetries of CBED patterns is an especially advantageous technique in the BR method. Since scattered electrons are converted to electrical signals in this method, signal processing can be done in a fairly unrestricted manner.

The other three techniques useful for CBED study are described. The first is the simulation of HOLZ lines, by which indices of HOLZ lines are identified and the basis of the second technique is given. The second determines crystal lattice spacings and accelerating voltages by using HOLZ lines. The third is quick specimen-thickness determination based upon the two-beam dynamical theory.

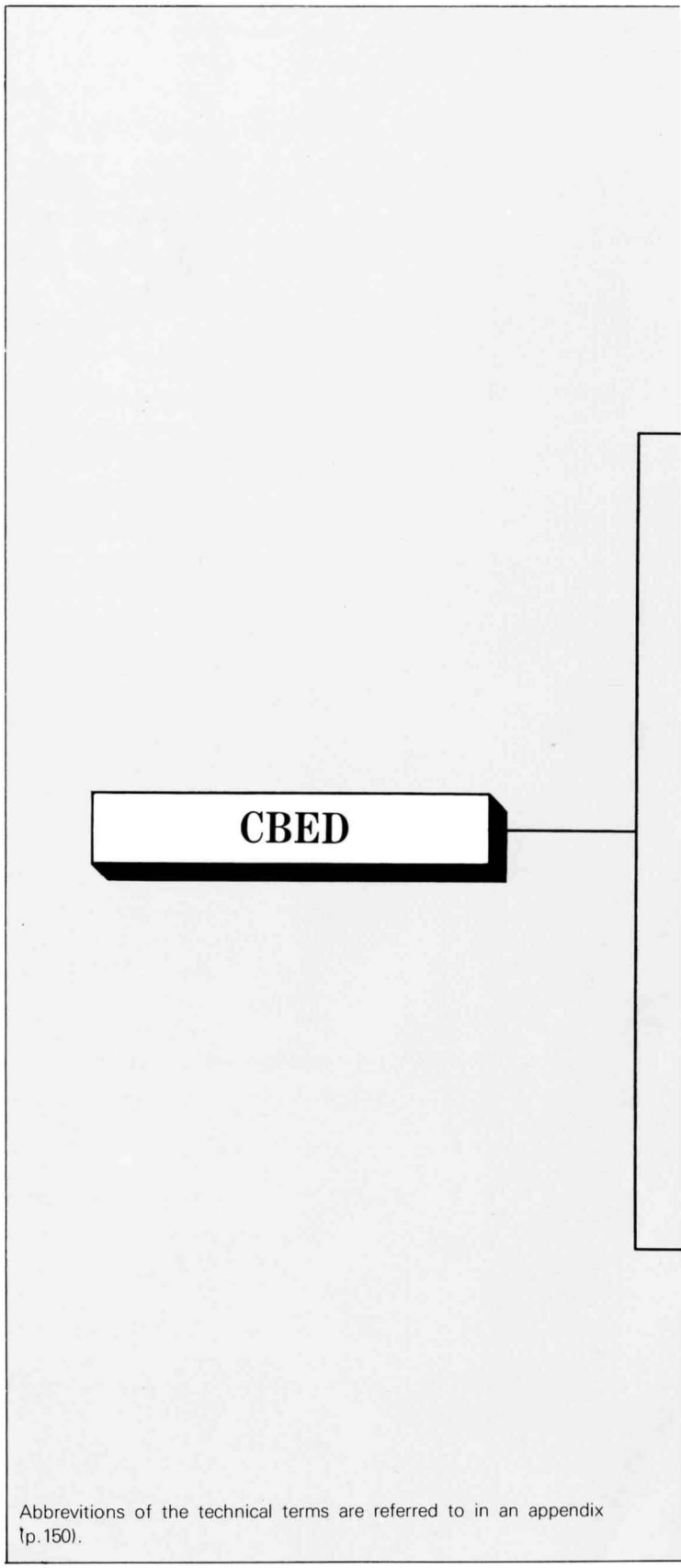

Abbrevitions of the technical terms are referred to in an appendix (p. 150).

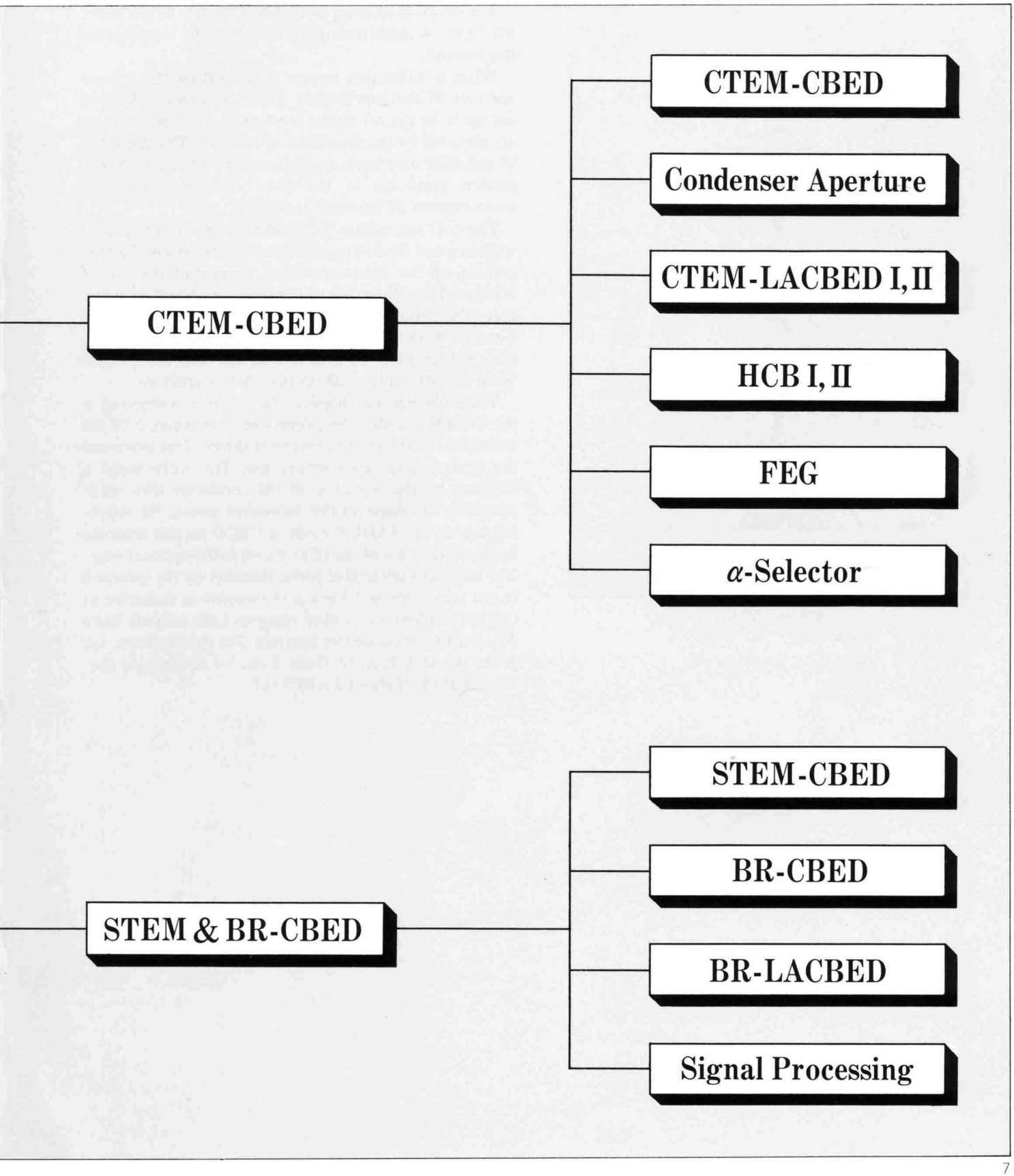
CTEM-CBED
CTEM-CBED
Condenser Aperture
CTEM-LACBED I, II
HCB I, II
FEG
α-Selector
STEM & BR-CBED
STEM-CBED
BR-CBED
BR-LACBED
Signal Processing

Various CBED Methods

CTEM-CBED

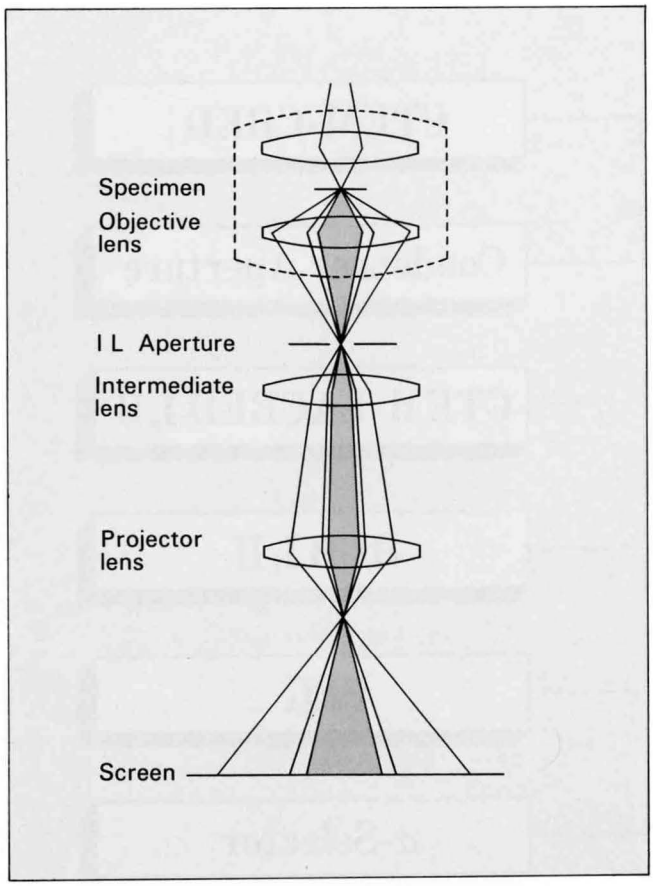

CBED by CTEM

The ray-path diagram of CTEM-CBED is shown in the left figure. A condenser-objective (C-O) lens is needed for this method.

When a diffraction pattern is formed on the selector aperture of the intermediate lens, high-order reflections are apt to be cut off by the aperture and diffraction disks are distorted by the aberration of this lens. The distortion of the disks may introduce serious errors in knowing the pattern symmetry in the disks and in quantitative measurements of intensity profiles.

The C-O lens makes the incident beam converge on a specimen and forms a microscopic image (not a diffraction pattern) on the selector aperture, eliminating the cut-off effect and the distortion of the disks. It should be noted that these two effects occur also in the microscopic image when the C-O lens is used, but these account for nothing since the image of an area illuminated with the incident beam is sufficiently small on the selector aperture.

The probe size and shape on the specimen is observed in the SAMAG mode. The probe size is determined by the excitations of the lenses converging the incident beam and the second-condenser aperture size. The probe shape is adjusted by the stigmator of the condenser lens, while observing the shape on the fluorescent screen. By switching over to the SADIFF mode, a CBED pattern from the illuminated area is obtained as shown in the opposite page. The minimum obtainable probe diameter on the specimen in our instrument is 3.5 nm at the maximum excitation of the 2nd condenser lens when using an LaB_6 cathode and a 40 μm diameter condenser-aperture. For routine work, the probe diameter is set to about 8 nm for obtaining a convergent angle of about 2×10^{-2} rad.

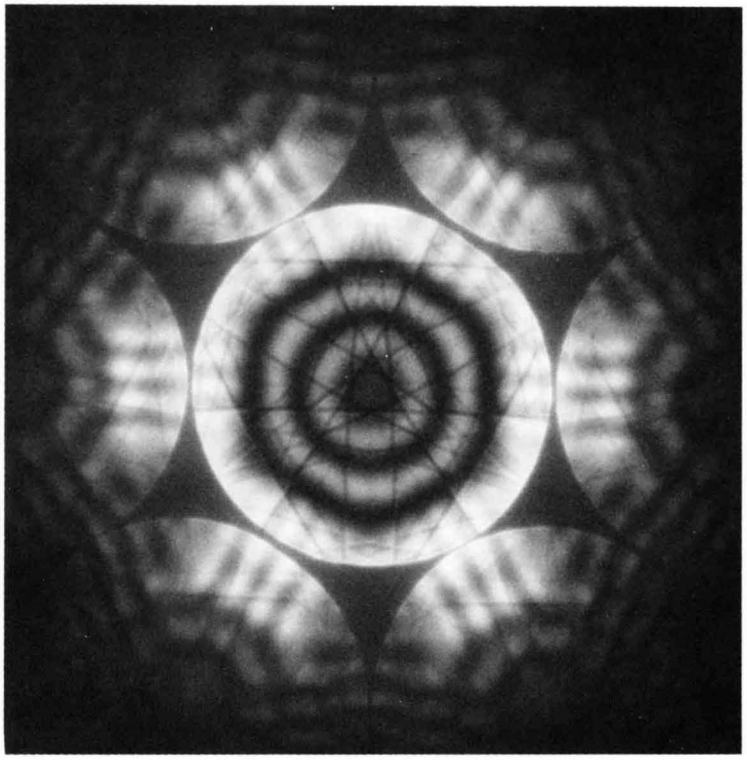

(a)

Zone-axis pattern (ZAP) obtained from a (111) Si specimen.

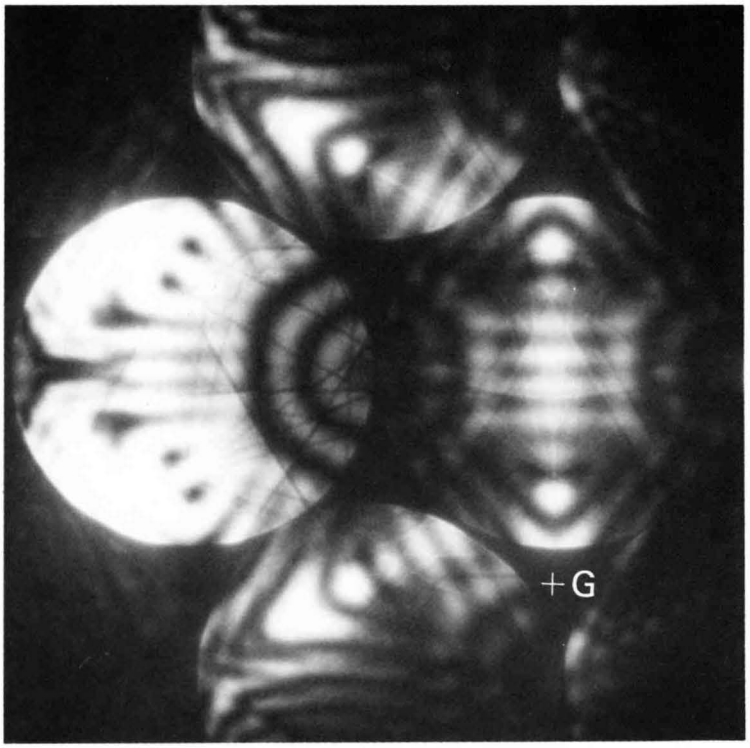

(b)

$2\bar{2}0$ Dark-field pattern (DP).

Condenser Aperture

In the study of crystal symmetries, it is desirable to obtain diffracted intensities over the whole area of a zone determined by Bragg reflections. For crystal-structure-factor determination, the background due to inelastic scattering must be reasonably subtracted. For these requirements, square, hexagonal and rectangular apertures of 30, 40, 70 and 120 μm were made in copper plates by the electroforming method. The photographs of these apertures are shown in the figure. The CBED patterns obtained by using these apertures are seen to cover almost the entire area of the zone as shown in Photos (a), (b) and (c), and to allow the reasonable subtraction of the background as shown in (d).

The apertures were formed so that one of their shadow edges coincides with one of the tilt axes of the side entry goniometer at an accelerating voltage of 100 kV. It is necessary to repeat specimen setting a few times until the desired crystallographic direction of the specimen coincides with the tilt axis.

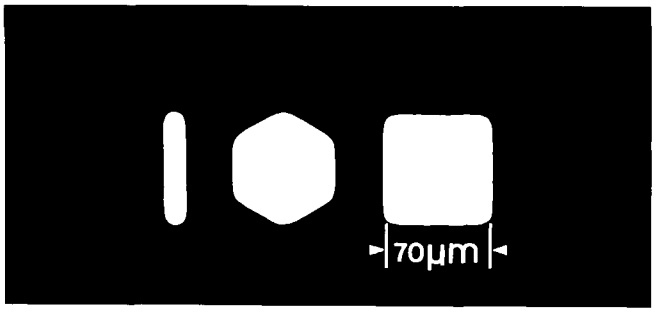

M. Tanaka: *JEOL News*, **16E** (1978) 13.
M. Tanaka: 10th Intern. Cong. Electron Microscopy, Humburg, 1982, p.625.

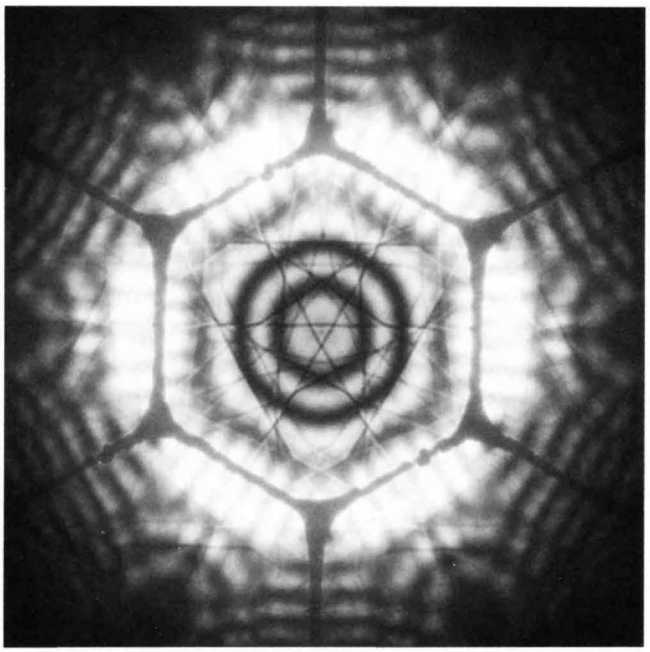

(a) 111 ZAP.

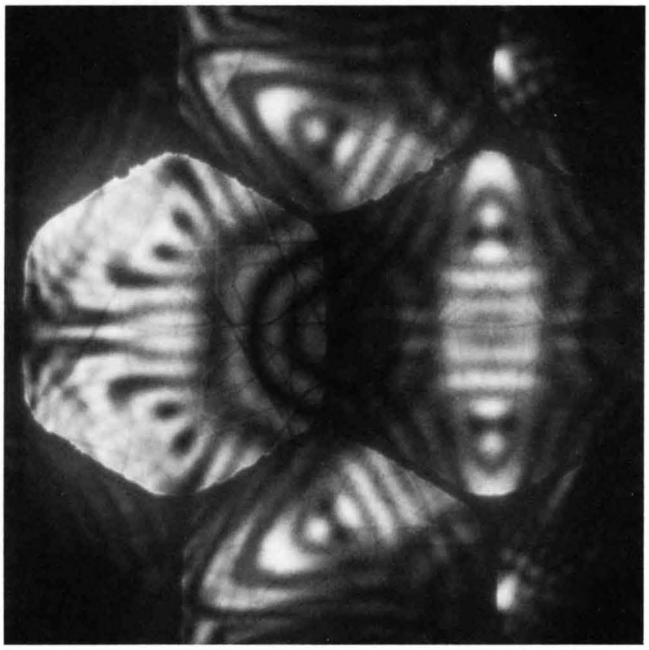

(b) $2\bar{2}0$ DP.

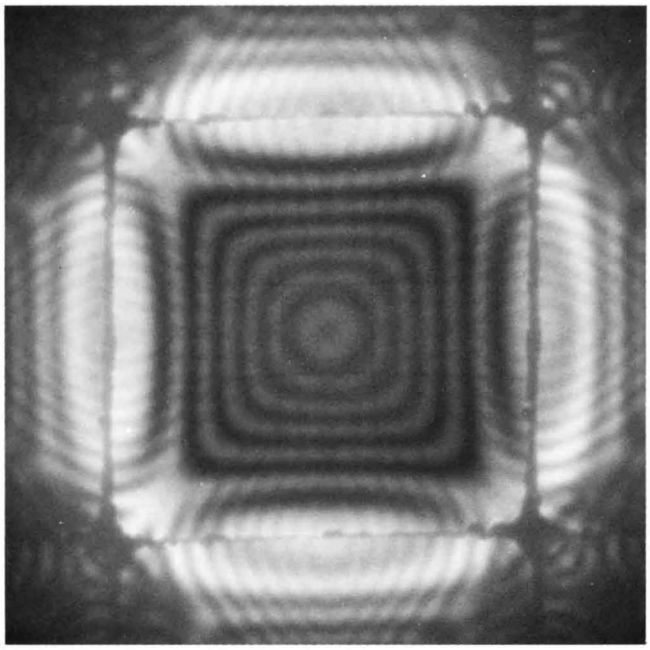

(c) 100 ZAP.

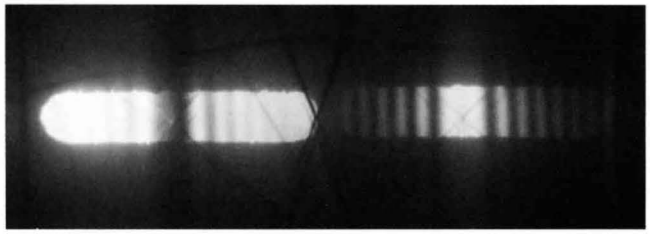

(d) 000 and $2\bar{2}0$ disks, $h\bar{h}0$ systematic reflections being excited.

CTEM-LACBED I

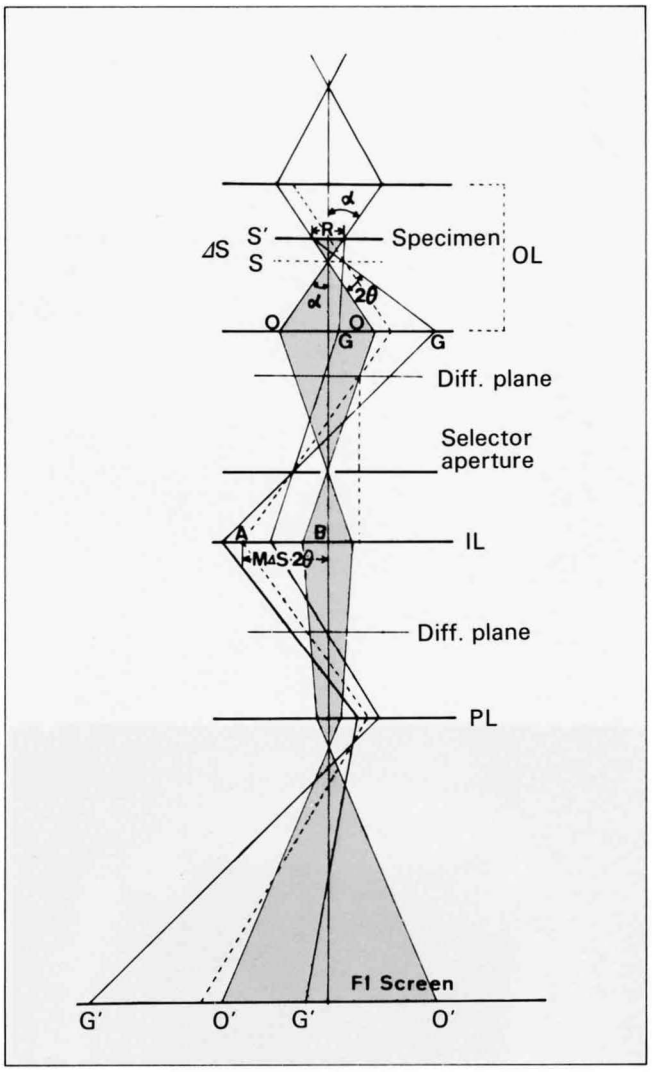

LACBED by CTEM

The diameter of a non-overlapping disk in a CBED pattern is limited by the Bragg angle of the nearest reflection. When the thickness of a crystal specimen is small, or its Fourier potential is large, or its lattice spacing is large, intensity oscillation sufficient to find symmetries of a pattern is not observed in the disk. The large-angle (LA) techniques make it possible to obtain non-overlapping disks extending to a larger angle than the Bragg angle.

An LACBED pattern by CTEM is obtained without the use of any additional device. The ray path of this technique is shown in the figure. A specimen is placed at a focussed position S of the incident beam. The intermediate lens is focussed on the selector aperture in the SAMAG mode. The transmitted and diffracted beams form their images at nearly the same position on the selector aperture. The specimen is shifted effectively to a defocussed position S' from S using, for example, the height control of the side-entry goniometer. Then, the transmitted and diffracted images are separated from each other on the selector aperture. One of them, for example, the transmitted image is chosen with the selector aperture, and the SAMAG mode is switched over to the SADIFF mode. The LACBED pattern O'O' is obtained on the fluorescent screen without the disturbance of the reflected beam G'G'. The obtained pattern is shown in the photograph, its angular size being about four times that of the photogrphs in previous pages.

An inevitable disadvantage of this technique is to require a large flat specimen area — several hundreds of nm in diameter.

M. Tanaka, R. Saito, K. Ueno and Y. Harada: *J. Electron Microsc.*, **20** (1980) 408.

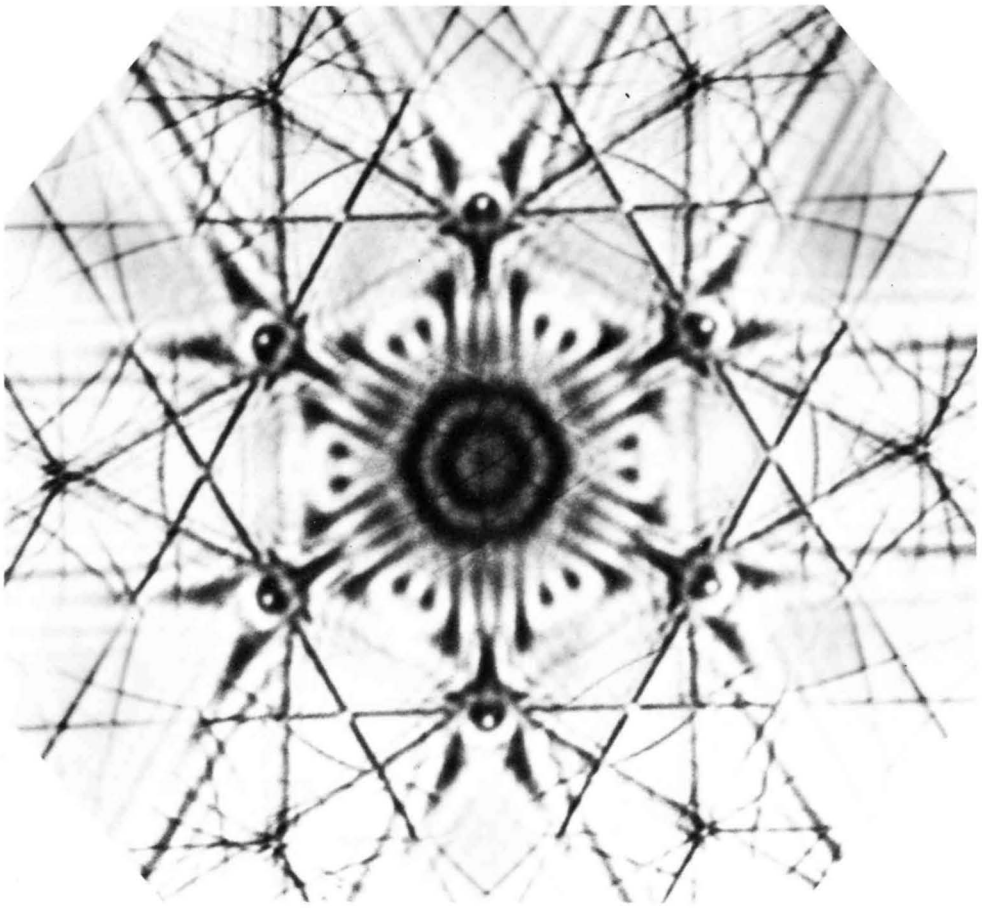

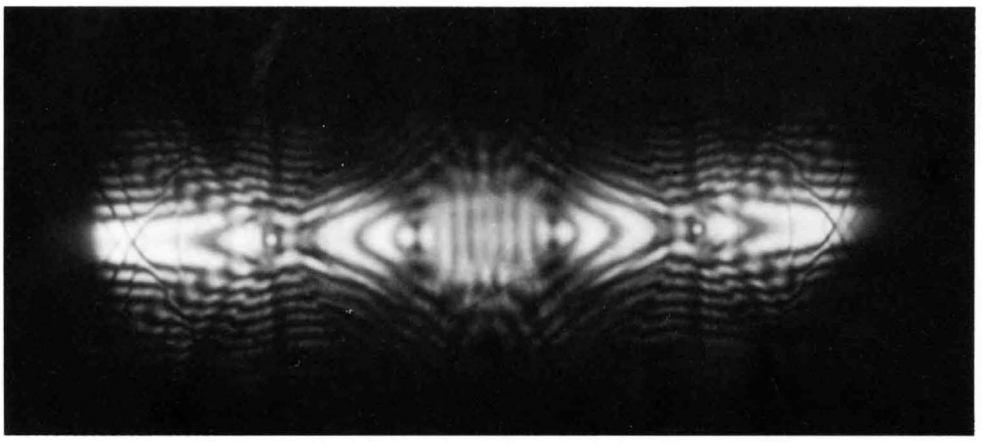

LACBED patterns obtained by CTEM.

CTEM-LACBED II

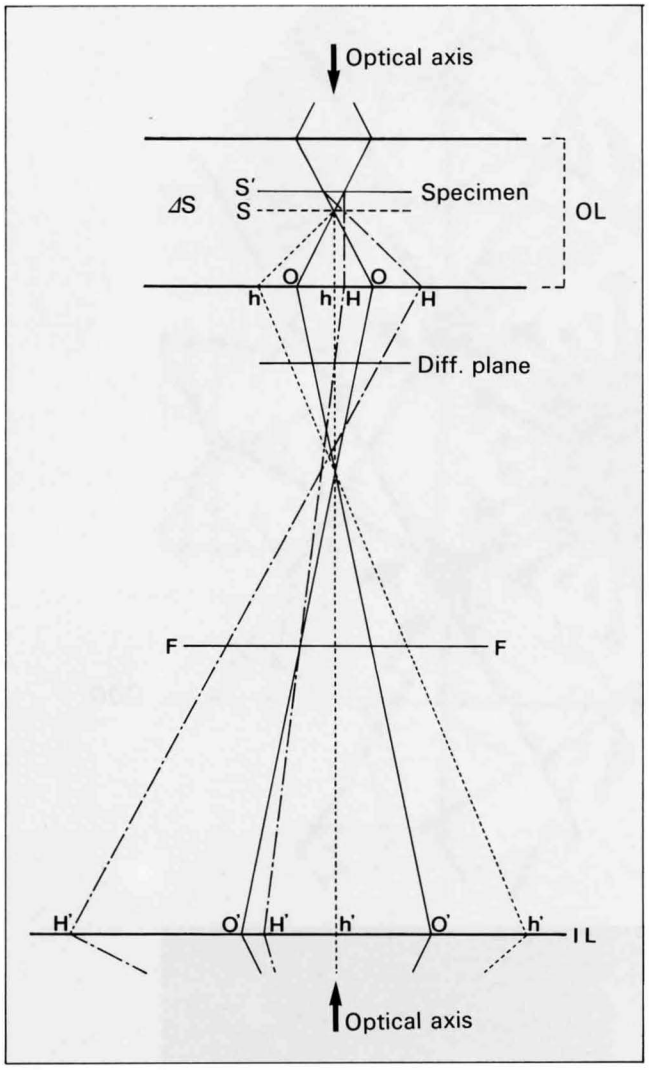

LACBED by CTEM

The LACBED I technique obtains the bright-field pattern (BP) and dark-field patterns (DP), each on a different film at a different time for a different crystal setting.

When the intermediate lens is not focussed on the back focal plane (the diffraction plane) but on an image at a plane F shown in the figure with other conditions kept the same as with the LACBED I technique, large-angle bright-field and dark-field patterns are produced without overlapping each other on the fluorescent screen. Using this technique, the symmetries of BP and DP are simultaneously observed. Since the excitation of the illumination-lens system in this technique is the same as that in the LACBED I technique, the size of an illuminated specimen area is essentially the same between these two techniques. It should be noted that the present technique requires the excitation of the intermediate and projector lenses to be variable continuously over wide ranges.

M. Terauchi and M. Tanaka: *J. Electron Microsc.*, **34** (1985) in the press.

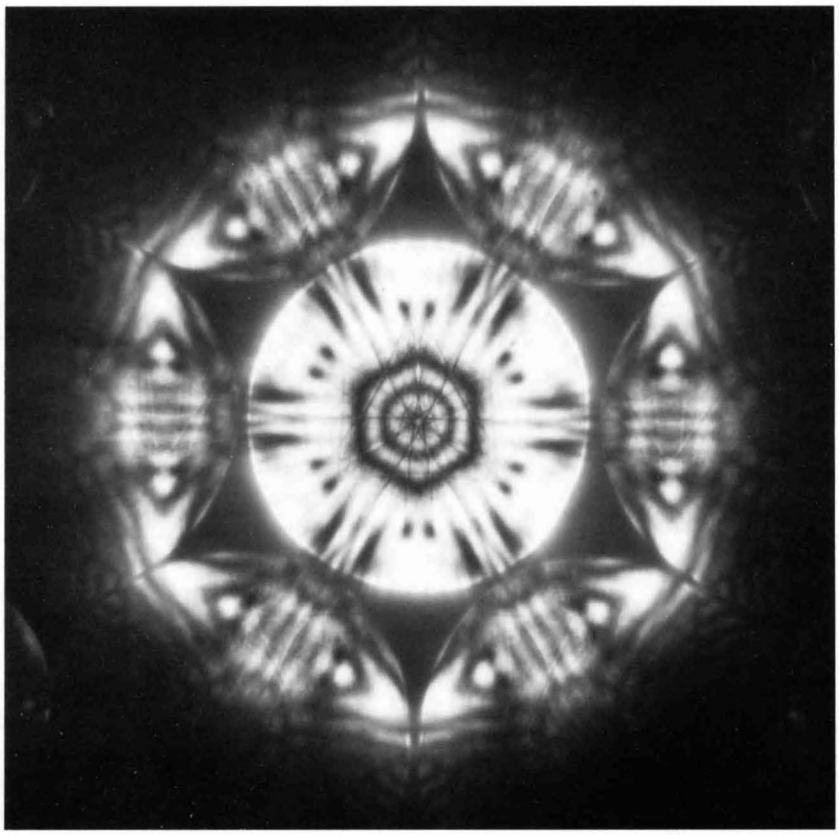

LACBED pattern obtained by CTEM. BP and DPs are simultaneously observed.

Hollow-Cone Beam I (Electrical Method)

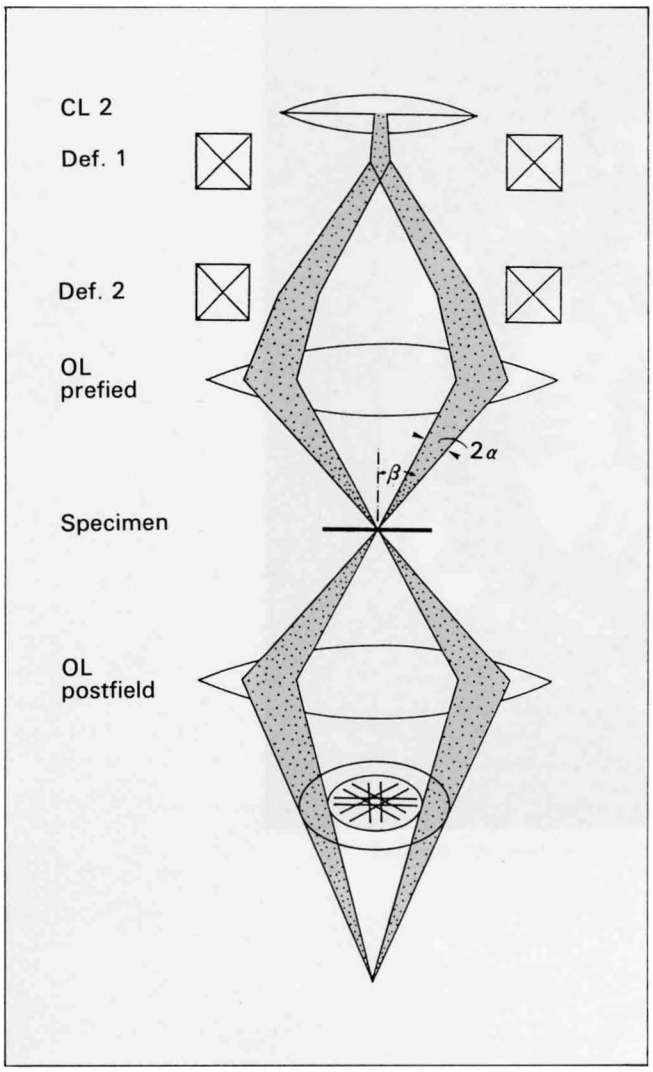

HCB method

The hollow-cone beam (HCB) technique can reveal the symmetry with respect to a zone axis or whole pattern symmetry. The ray path illustrates the electrical hollow-cone beam method. The incident beam of convergent angle 2α focussed on a point of a specimen is tilted by angle β against the optical axis and rotated around the optical axis.

Photo (a) shows an oridnary zone-axis pattern (ZAP). To find the symmetry of the whole pattern, it is necessary to find symmetries due to the dark-field disks about the center of the bright-field disk. This symmetry is not always easy to find in a ZAP. The HCB technique can find the whole pattern symmetry more easily. Photo (b) shows an HCB-CBED pattern, the tilt angle β being set to twice the angle of the nearest Bragg reflection, 220. The bright ring corresponds to the incident beam. The whole pattern symmetry $3m$ is seen in the ring. Since the pattern extends over a larger angle than the convergent beam angle 2α, this pattern is a large-angle whole pattern.

When the tilt angle β is set to a reflection on a higher-order Laue-zone (HOLZ) ring, only HOLZ reflection lines appear around the optical axis (Photo (c)). Therefore, this pattern is regarded as a three-dimensional large-angle whole pattern. It is noted that owing to the spheircal aberration of the objective lens, the illuminated specimen area becomes larger as the tilt angle β increases.

Y. Kondo, T. Ito and Y. Harada: *Jpn. J. Appl. Phys.*, **23** (1984) L178.
M. Tanaka, H. Takayoshi, M. Terauchi, Y. Kondo, K. Ueno and Y. Harada: *J. Electron Microsc.*, **33** (1984) 195.
M. Tanaka and M. Terauchi: *J. Electron Microsc.*, **34** (1985) 52.

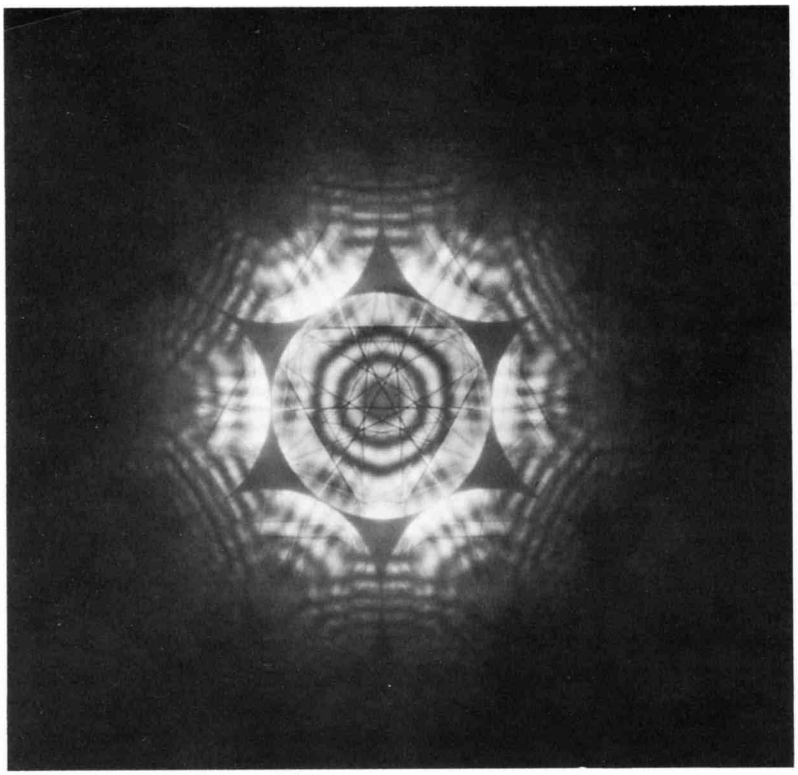

(a)

Ordinary 111 ZAP.

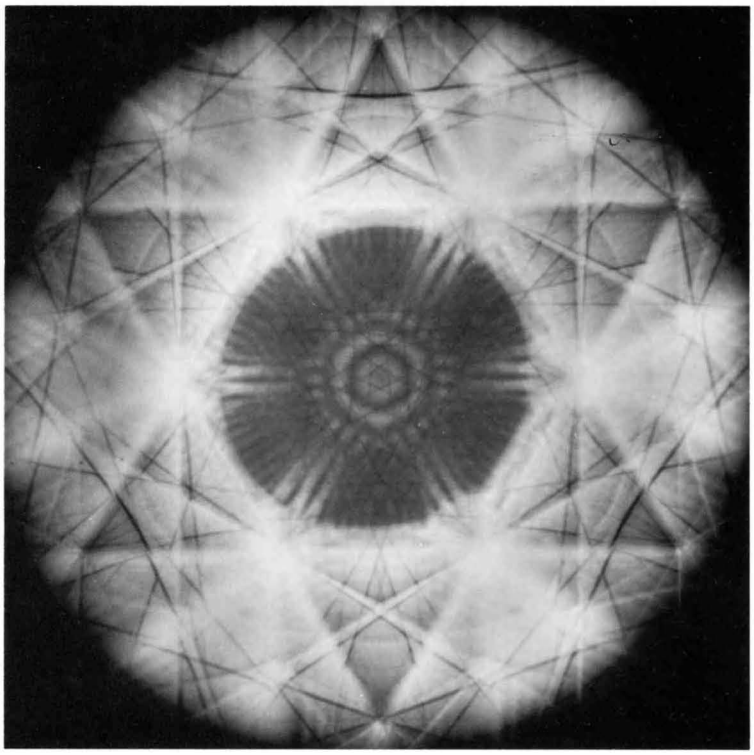

(b)

111 HCB whole pattern; tilt angle β was set to twice the Bragg angle of 220 reflection.

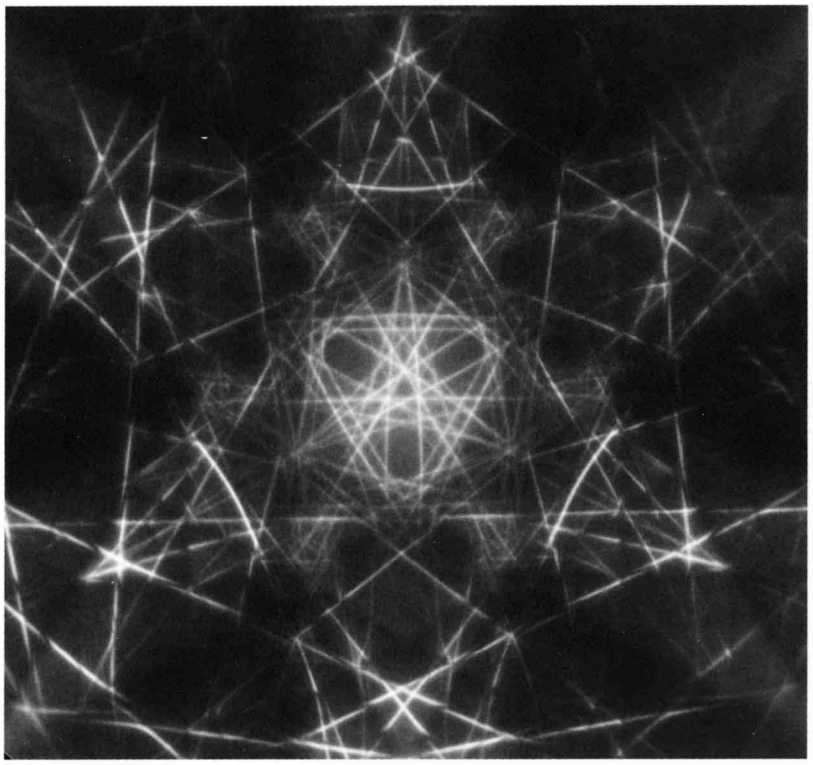

(c)

111 HCB-HOLZ pattern obtained by the electrical method; tilt angle β was set to a HOLZ reflection.

Hollow-Cone Beam II (Aperture Method)

An alternative technique to obtain HCB-HOLZ patterns is one using an annular condenser aperture. The incident beam passing through the annular condenser aperture is converged on a specimen area by the prefield of the objective lens. The tilt angle of the incident beam against the optical axis is adjusted by a weak lens placed just above the objective lens. A sketch of an aperture now to hand and an obtained pattern are shown on the figure and the photograph, respectively.

When the pattern is compared with one obtained by the electrical method (Photo (c) on the opposite page), the quality of the $3m$ symmetry in the pattern on this page is found a little inferior to that in Photo (c). When an aperture with narrower supporting bridges or with threefold symmetrical bridges is used, the quality of the symmetry is improved.

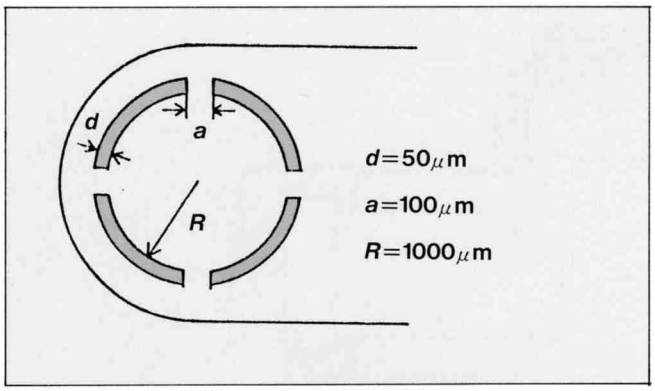

Sketch of the annular aperture used.

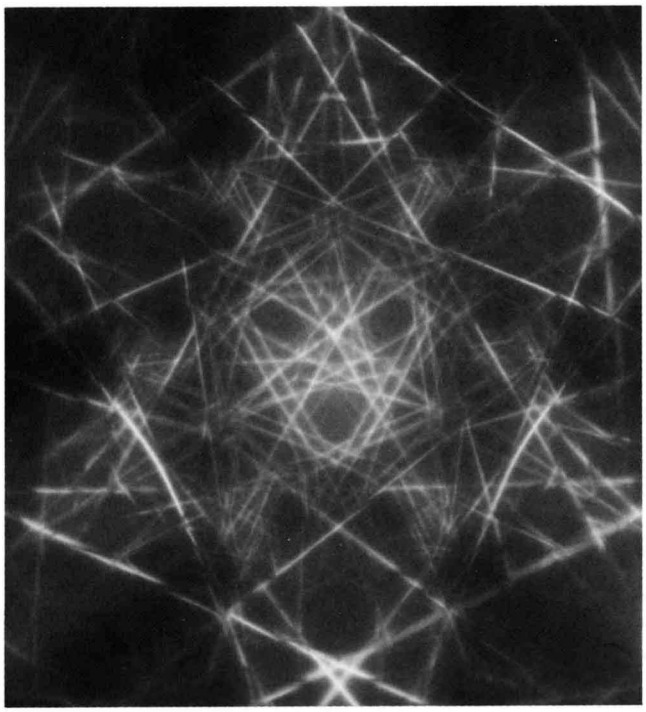

111 HCB-HOLZ pattern obtained with an annular aperture.

M. Tanaka, H. Takayoshi, M. Terauchi, Y. Kondo, K, Ueno and Y. Harada: *J. Electron Microsc.*, **33** (1984) 195.

Field Emission Gun (FEG)

A bright and small electron source is realized by a field emission gun (FEG). A thermal type FEG with a [100] tungsten emitter was installed in our JEM-100CX electron microscope. An electronically controlled automatic evacuation system was newly developed for gun chamber evacuation instead of the previous system using manual operation. This new system makes it possible to start from rough pumping, bake the chamber over a desired period and reach a high vacuum of 4×10^{-10} Torr without manual operation.

The brightness of the FEG is 2×10^8 A/cm^2 str. at an accelerating voltage of 80 kV. The virtual source diameter is about 40 nm and the minimum probe diameter on a specimen is 1 nm.

This FEG system has three anodes as shown in the figure. To obtain the maximum brightness, the positive voltages of the first and second anodes can be varied independently of the final accelerating voltage. As a result, we can observe CBED patterns even at an accelerating voltage as low as 20 kV, whereas with an ordinary 100 kV electron microscope it is quite difficult to observe the patterns at a voltage lower than 40 kV.

Photos (a), (b), (c) and (d) are CBED patterns taken at 80, 60, 40 and 20 kV, respectively. On account of the small electron source size, the HOLZ lines in these patterns are much sharper than those obtianed with an LaB_6 cathode. The FEG enables us to observe the symmetries of CBED patterns of weak reflections such as superlattice reflections and obtain the patterns by the beam rocking method (shown below) with a shorter exposure time.

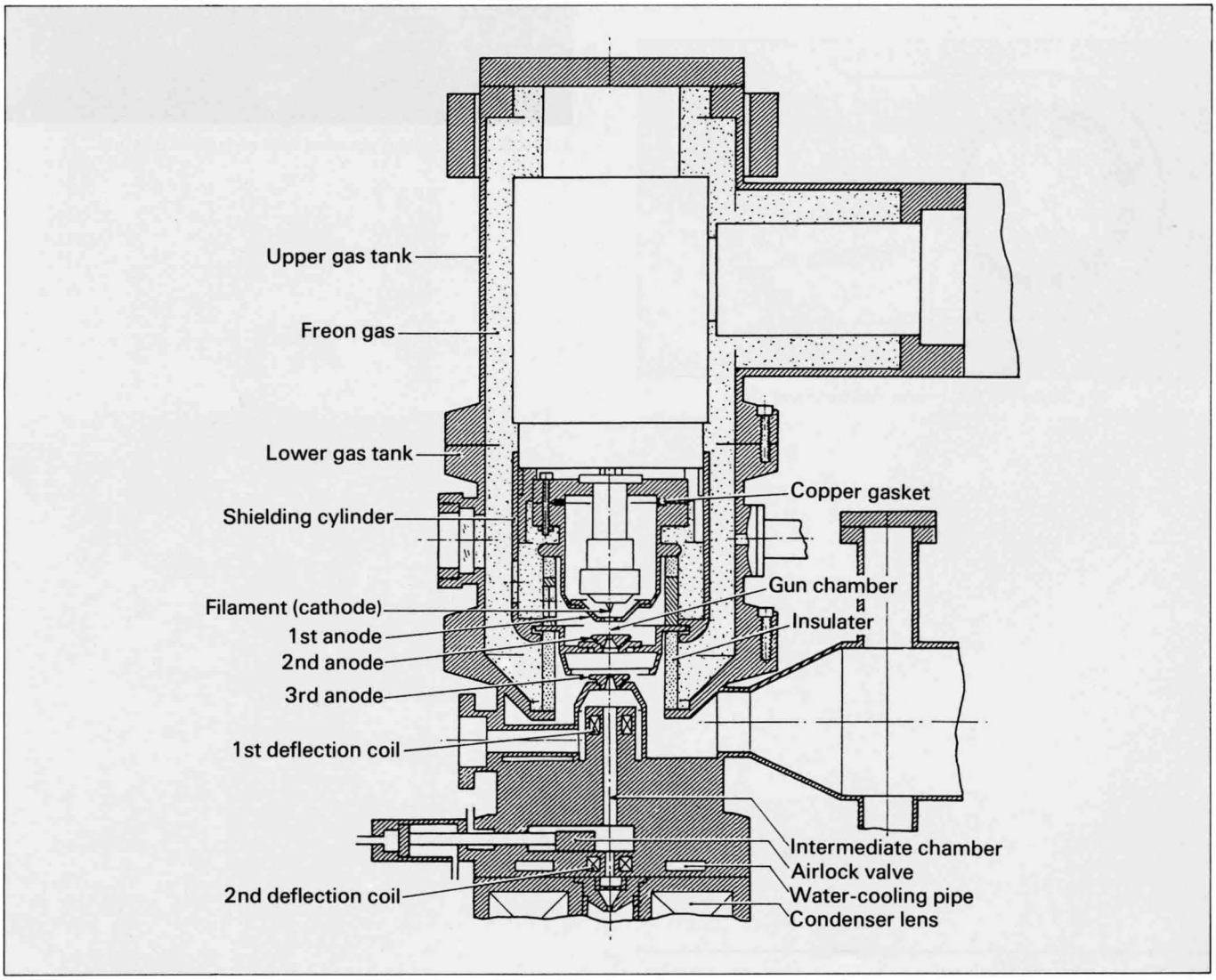

Cross section of Field Emission Gun

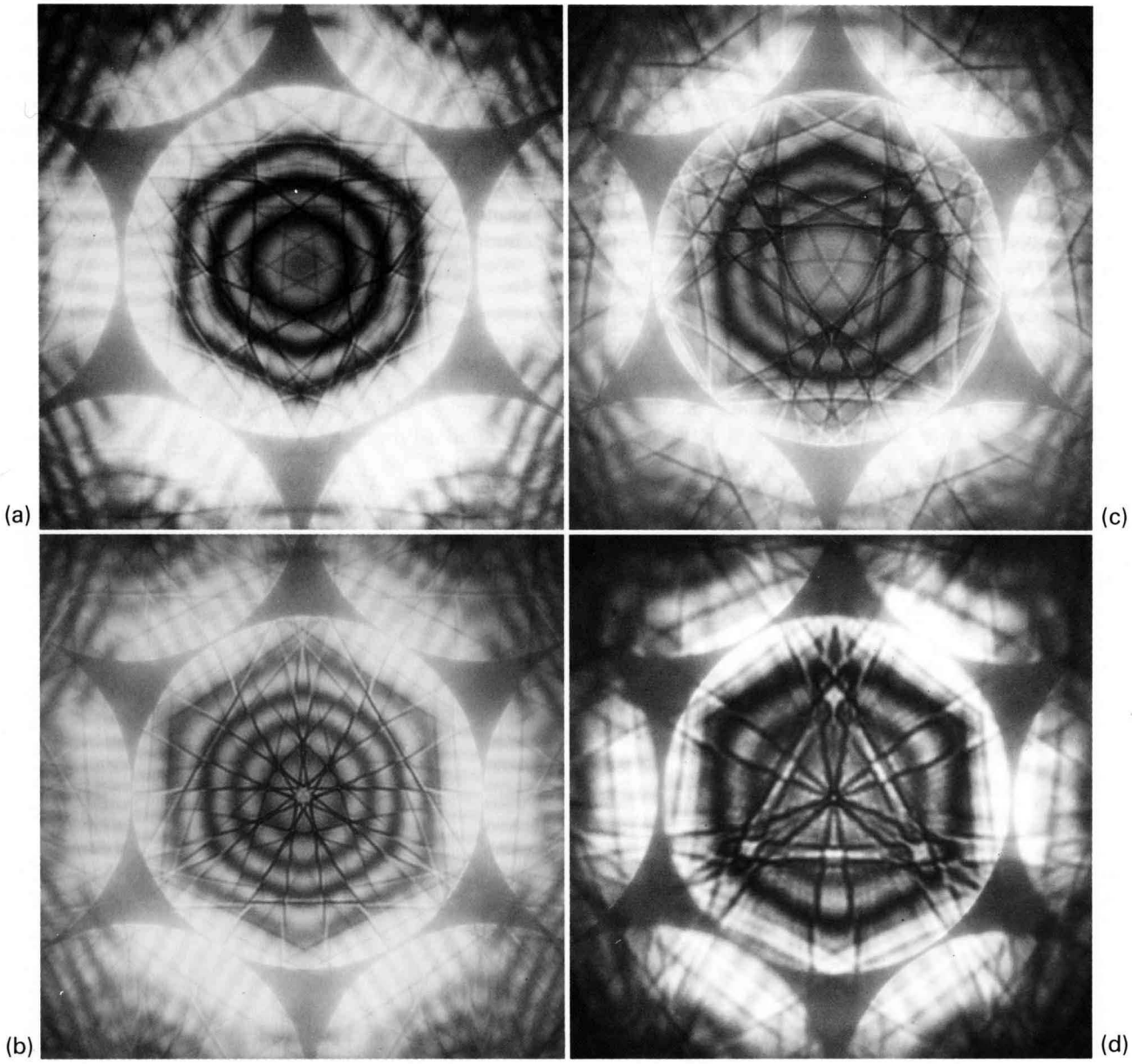

111 ZAP; (a) 80kV, (b) 60kV, (c) 40kV and (d) 20kV.

α-Selector

In CBED experiments, the convergent angle (2α) of the incident beam on a specimen needs to be varied. The angle can be changed by using condenser apertures of different sizes, but is changed discontinuously according to their sizes. When the angle is varied continuously by changing the excitations of the illumination lens system and occasionaly of the objective lens, the incident beam is defocussed on the specimen and the minimum probe size itself is also changed.

For CBED, electron microscopes should have a function to vary the angle α continuously, keeping the probe size on the specimen constant. This function is called the "α-selector".

The figures illustrate the action of the "α-selector". The size of the condenser aperture and the excitation of the objective lens are kept the same in the three diagrams. While the values of the convergent angle 2α differs among these figures, the same size virtual image of the electron-beam source is formed on the object plane A of the objective lens, by properly selecting the excitations of the condenser lens system. Thus, we can vary the convergent angle of the incident beam continuously over a certain range with a condenser aperture of a definite size, keeping the probe size on the specimen constant. The photographs shown on the opposite page were taken by changing the convergent angle in a JEM-2000FX with an "α-selector" device, operated at 200kV.

T. Tomita, M. Iwatsuki, Y. Arai, Y. Ishida, K. Ibe and Y.Harada: Proc. 8th European Cong. on EM, Budapest, **1** (1984) 57.

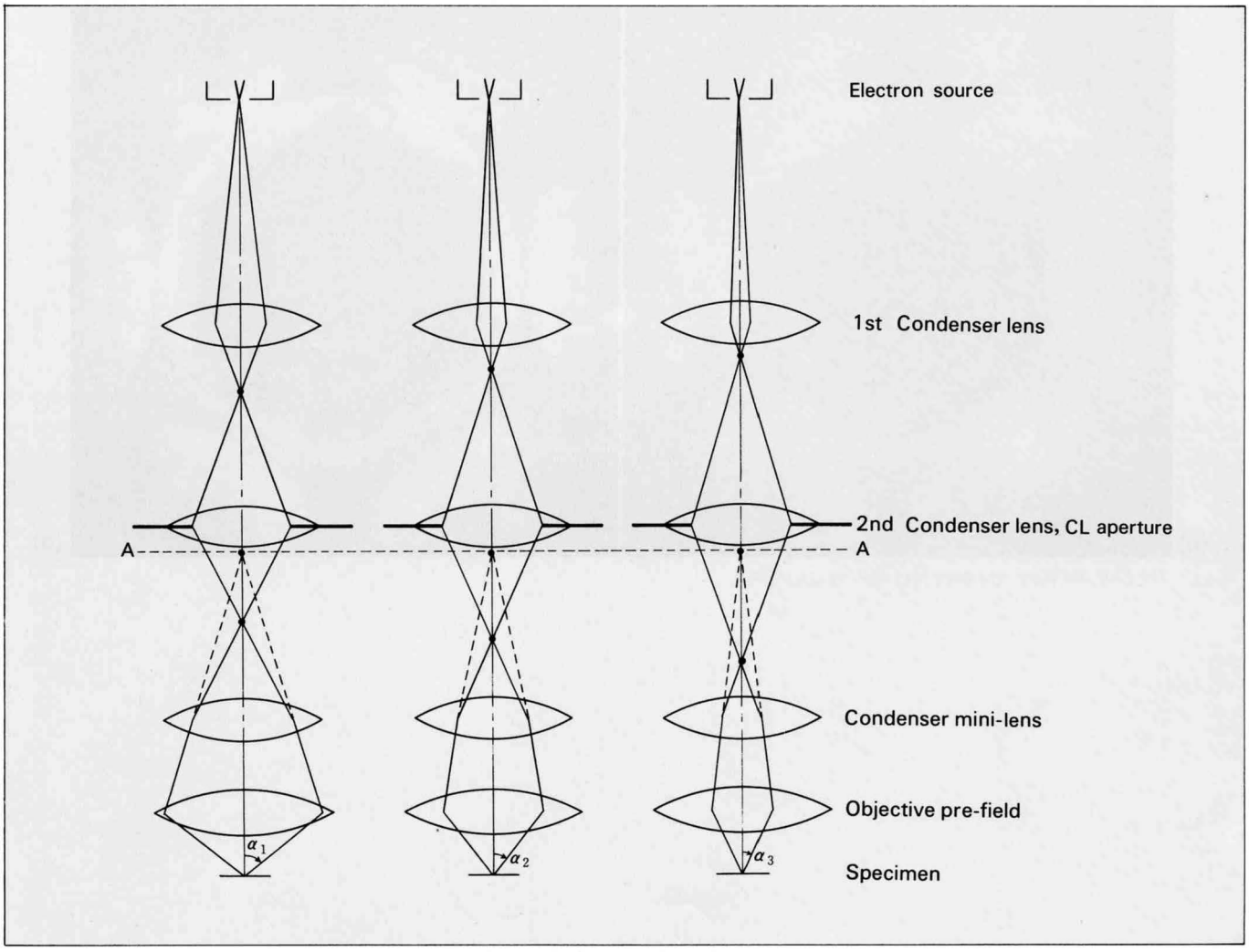

Ray-path diagrams of α-selector

FeS_2 [100]

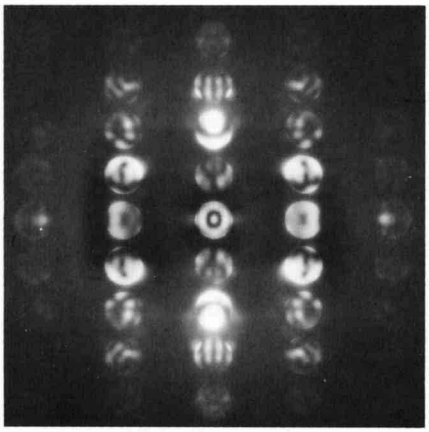

$2\alpha = 3.9$ mrad

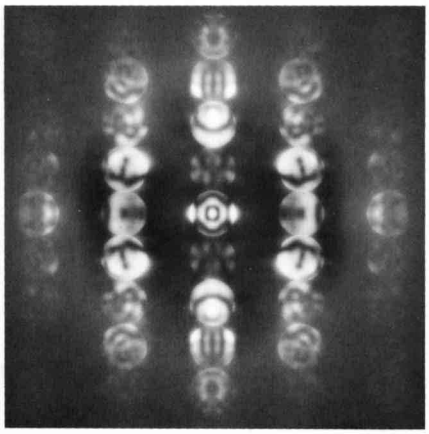

4.6 mrad

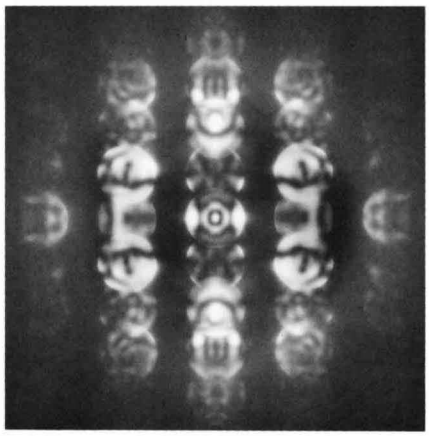

6.0 mrad

Si [111]

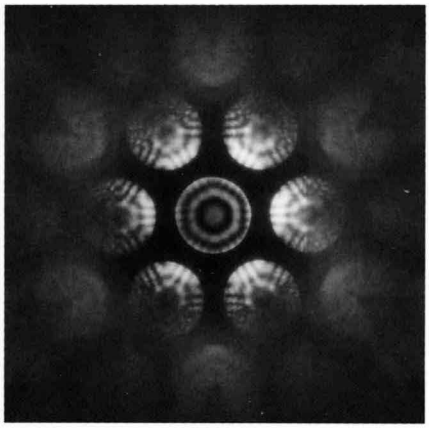

$2\alpha = 10.3$ mrad

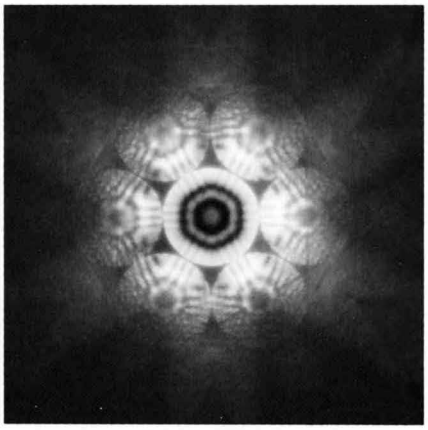

13.1 mrad

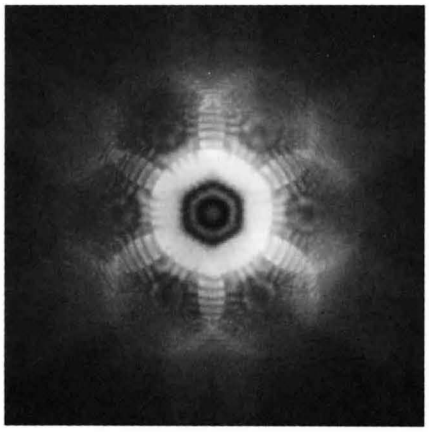

16.3 mrad

MgO [111]

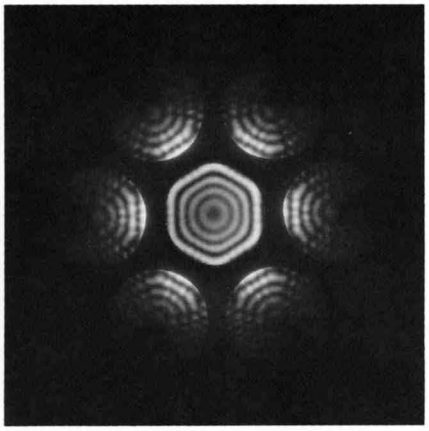

$2\alpha = 14.3$ mrad

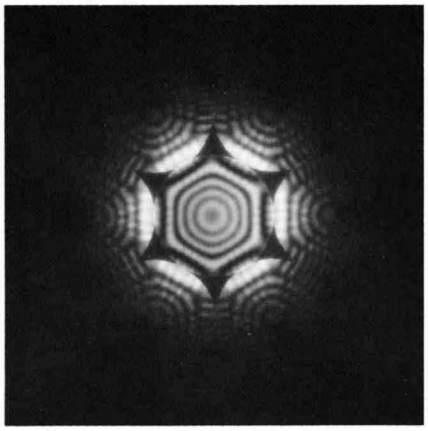

16.8 mrad

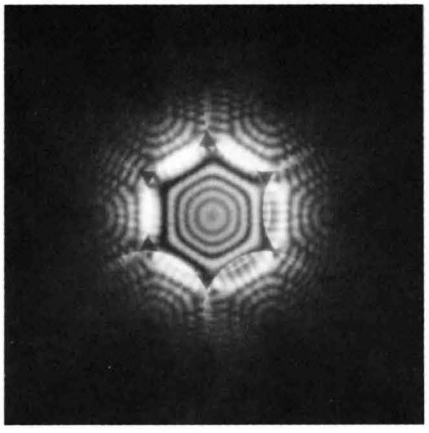

17.8 mrad

STEM-CBED

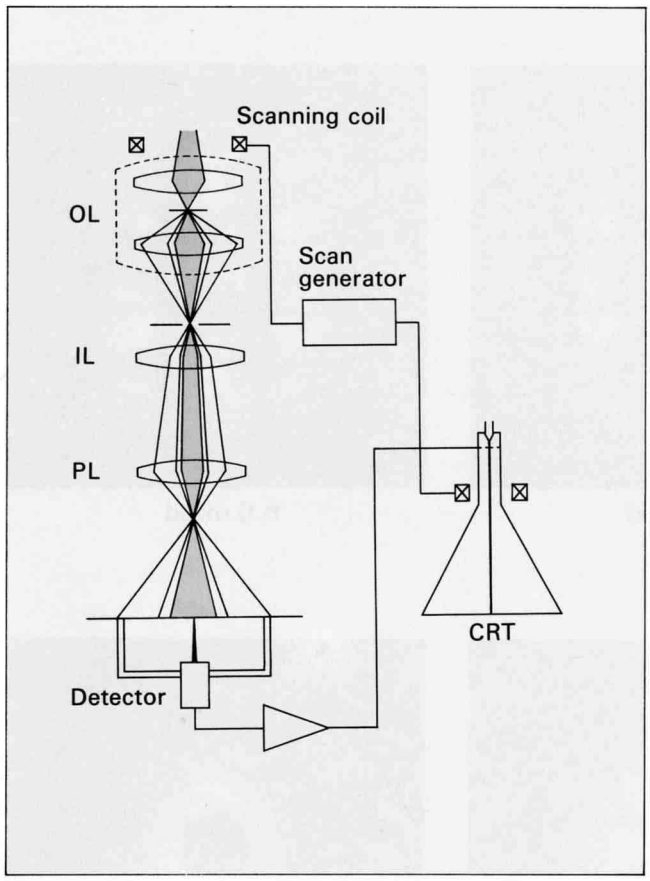

STEM-CBED with C-O lens

By introducing a STEM attachment, we can obtain a CBED pattern on the fluorescent screen and a microscopic image on the CRT screen. That is, the lens conditions of the microscope are set so as to obtain a CBED pattern by the CTEM method. Then, a specimen area is scanned with a convergent beam using the scanning coil. The transmitted or diffracted beam is detected by the STEM detector. The corresponding image is displayed on the CRT.

The desired position from which a CBED pattern is obtained can be selected by manually stopping the scanning and positioning of the bright spot on the CRT image. The positioning has to be finished before the after-image on the long-persistence CRT screen fades out. A recent STEM attachment has a preset function which can assign a specimen position for obtaining a CBED pattern while observing a STEM image. The seven CBED photographs on the opposite page were obtained from the image areas of the corresponding numbers.

M. Tanaka: *JEOL News,* **16E** (1978) 13.

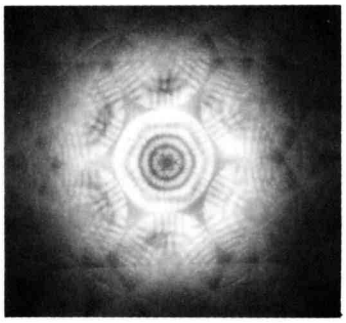

1

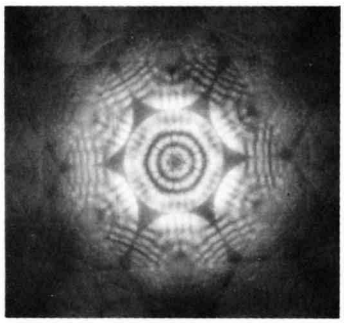

2

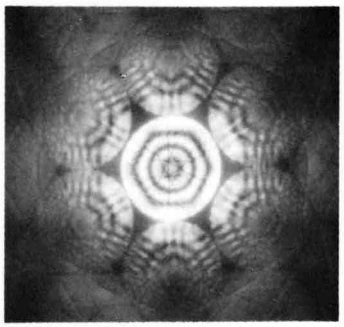

3

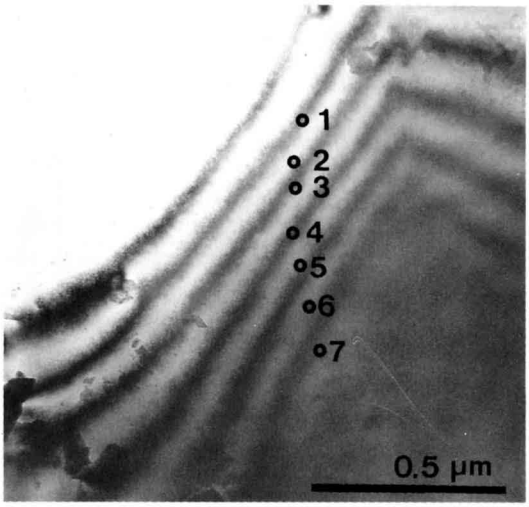

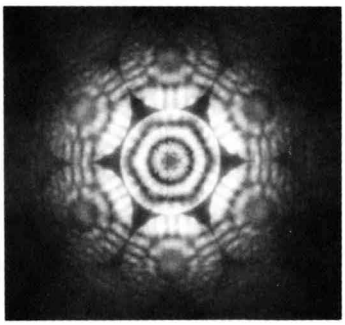

4

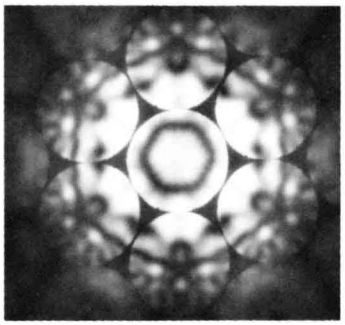

5

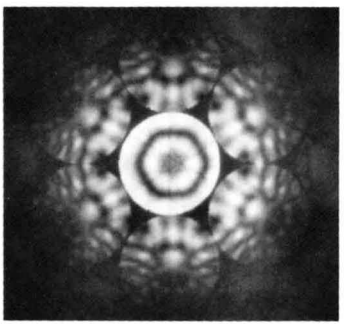

6

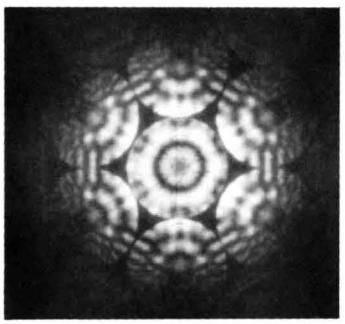

7

BR-CBED

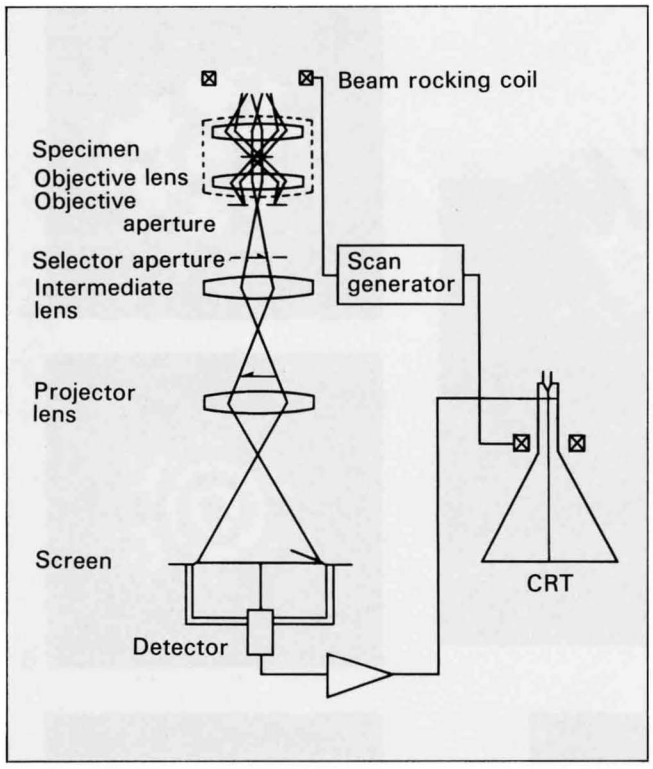

BR-CBED with C-O lens

When the parallel incident beam is rocked by the action of the rocking coil placed above the C-O lens with an point on a specimen as the fulcrum, a virtual convergent beam is produced, although its diameter on the specimen is a few micrometers. With the rocked beam, an image is formed in the SAMAG mode on the fluorescent screen. The rocked beam passing through a hole bored in this screen is received by the STEM detector and is output to the CRT screen synchronously with the rocking angle of the incident beam. Then a CBED pattern is obtained on the CRT.

Photo (a) shows a CBED pattern obtained by this beam-rocking (BR) method, using an LaB_6 cathode, an incident beam with a divergence angle of 8×10^{-5} rad. and an exposure time of 250 sec. The image area from which the pattern was obtained is indicated in Photo (b) with a circle formed by a hole in the fluorescent screen. It should be noted that in the BR method, the disk size of the pattern is determined by the objective aperture size, instead of the condenser-aperture size in the CTEM method. The divergence angle of the incident beam should be less than 1×10^{-4} rad. for clearly resolving fine lines due to HOLZ reflections, since the angular breadths of these lines are usually about 2×10^{-4} rad.

The advantages of the BR method are as follows:

1) Electrical signal processing can be used to enhance the symmetries in the patterns.
2) Owing to the low current density of the incident beam, specimen contamination is insignificant, and specimen damage is greatly reduced, allowing extensive application to materials susceptible to strong convergent-beam illumination.

M. Tanaka: *JEOL News* **16E** (1978) 13.

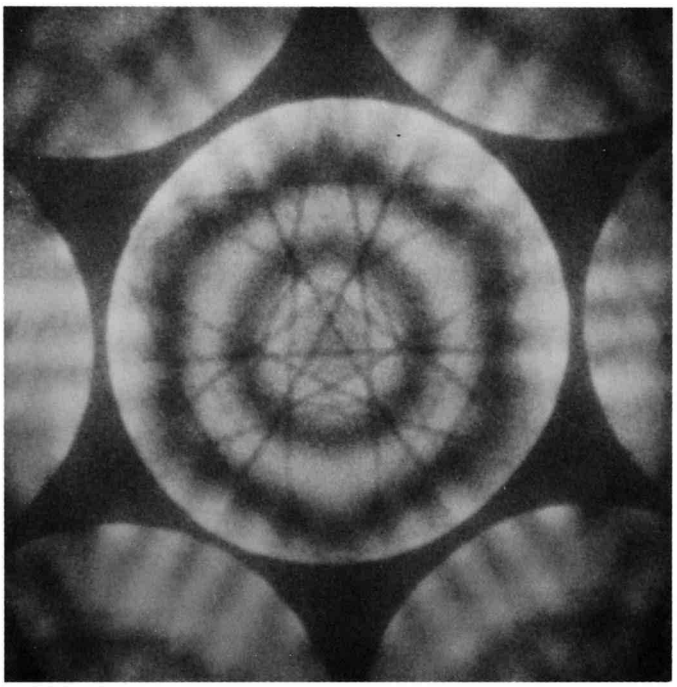

(a)

111 ZAP obtained by the BR method.

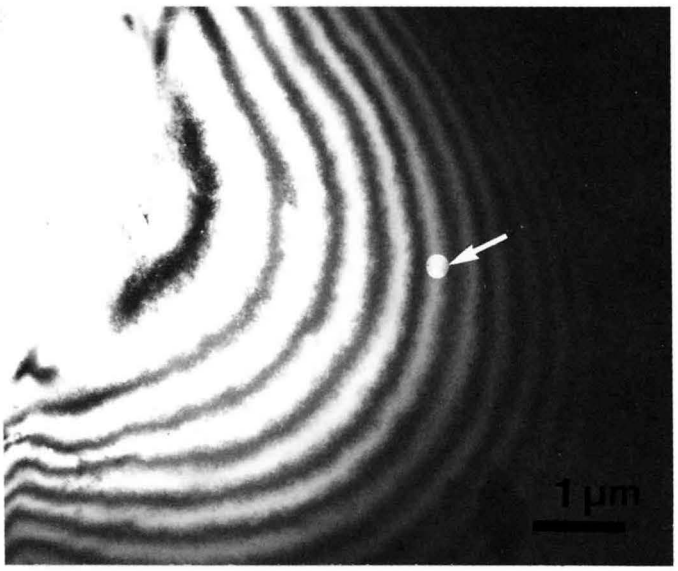

(b)

Photo (a) was obtained from the area indicated with an arrow

BR-LACBED

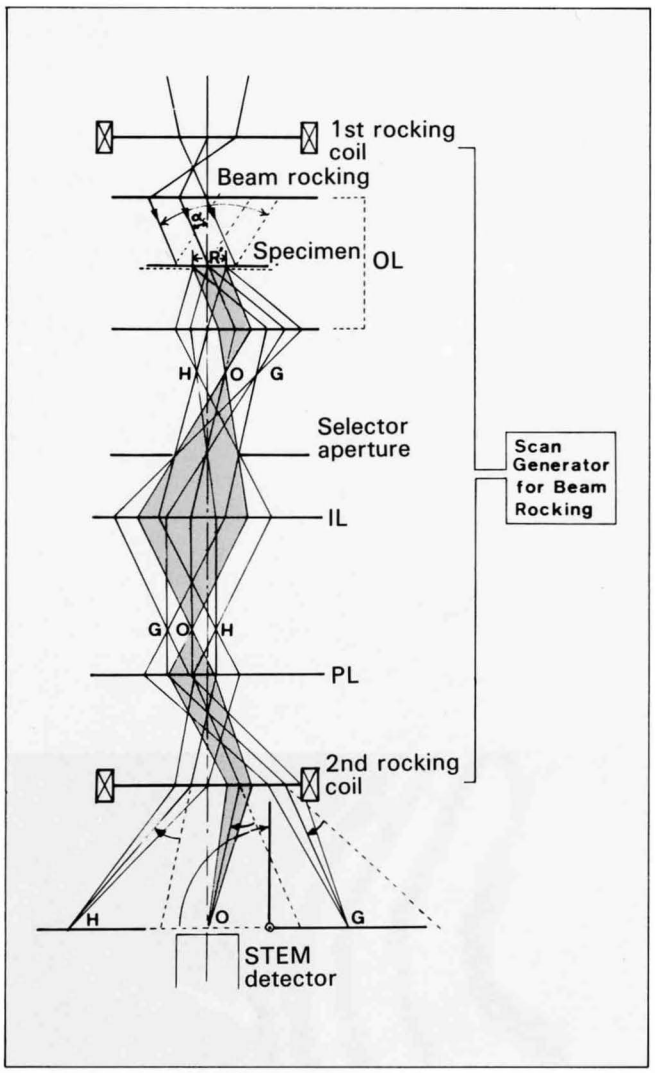

LACBED by BR method.

The LACBED pattern is obtained alternatively by the BR method. The ray path of this technique is illustrated in the figure. The parallel incident beam is rocked by the first rocking coil, with a point on the specimen as the fulcrum. The objective aperture used in the BR-CBED method described in the previous pages is removed from the ray path. The second rocking coil is placed under the projector lens. An arbitrary bias potential can be applied to the second coil to bring a desired beam to the STEM detector. The second coil is synchronously driven with the first rocking coil so that the beam always falls on the STEM detector while the incident beam is being rocked. Other beams are cut off by the fluorescent screen. When the distance between neighbouring beams is large enough, the receiving window of the STEM detector is utilized instead of the hole. Then, an LACBED pattern is displayed on the CRT. The photographs show the bright (a) and $2\bar{2}0$ dark-field (b) LACBED patterns obtained by this method.

J.A. Eades: *Inst. Phys. Conf. Ser.*, **52** (1980) 9.
M.Tanaka, R. Saito, K. Ueno and Y. Harada: *J. Electron Microc.*, **20** (1980) 408.

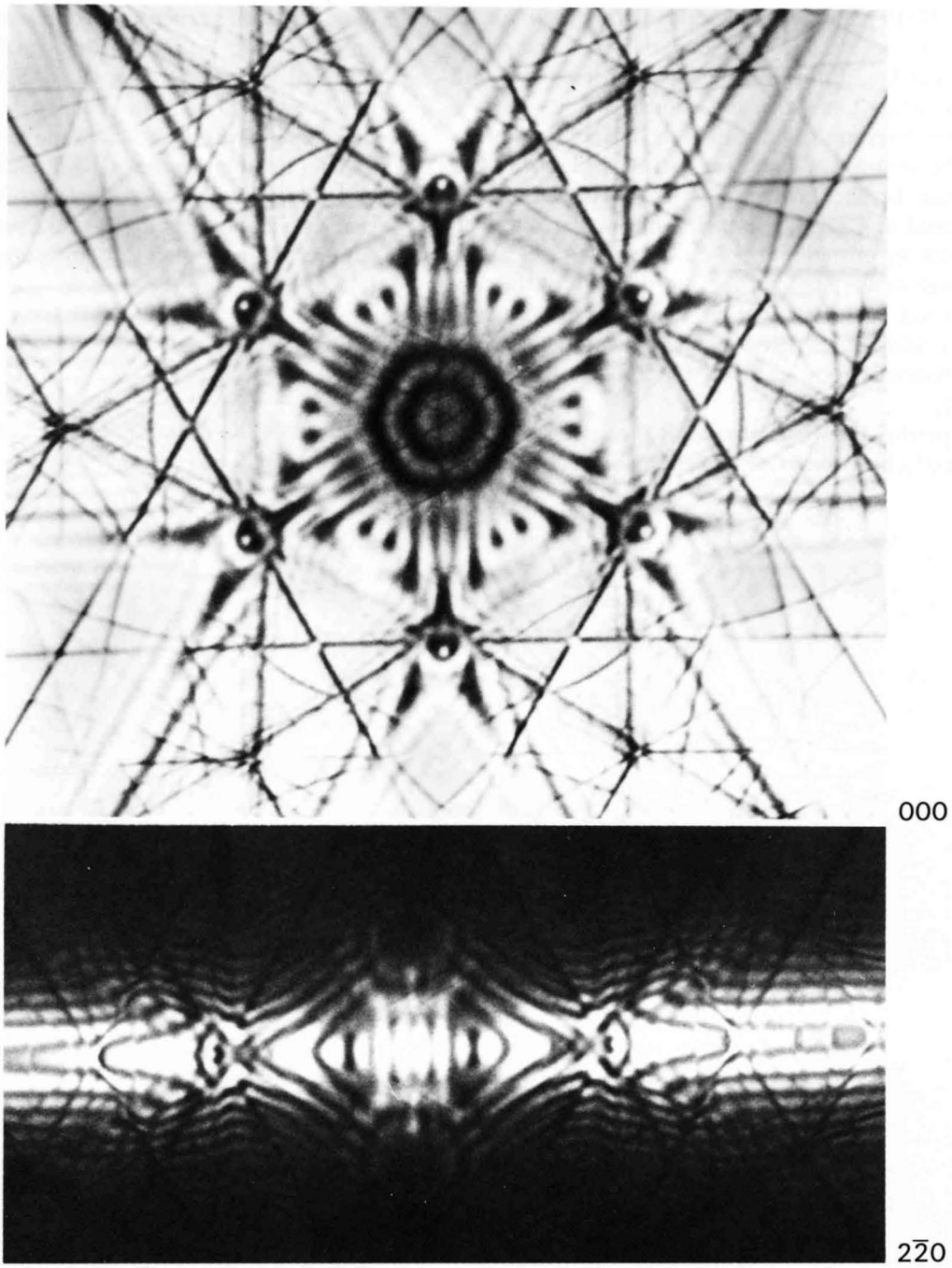

LACBED patterns obtained by the BR method.

Signal Processing

Most CBED patterns are composed of broad fringes formed by the interaction between 0-th Laue-zone reflections and fine lines formed by the interaction between 0-th and higher-order Laue-zone reflections.

When the high contrast due to broad fringes is suppressed and the contrast of fine lines is enhanced, their symmetries can be identified easily. In the photographic method used in CTEM, the high contrast is reduced to some extent by changing the γ-curve characteristics of a film through developing, but the improvement of the contrast is limited. In the BR method, signal processing can be done in a fairly unrestricted manner, since the electrical signal converted from scattered electrons can be easily processed.

To be precise, the signal processing is carried out by using a type of a band-pass filter which can be easily made by hand with little expense in contrast to computer processing. The main action of the signal processing is, as illustrated in the upper figure, to filter a certain frequency band of CBED patterns. The block diagram of the signal processing device is shown in the lower figure. Photos (a) and (c) show processed CBED patterns from a (111) Si and (111) Ge with appropriate settings of band frequencies, elucidating fine details of the patterns. Photos (b) and (d) are non-processed patterns corresponding to (a) and (c).

M. Tanaka, K. Ueno, Y. Hirata: *Jpn. J. Appl. Phys.*, **19** (1980) L201.

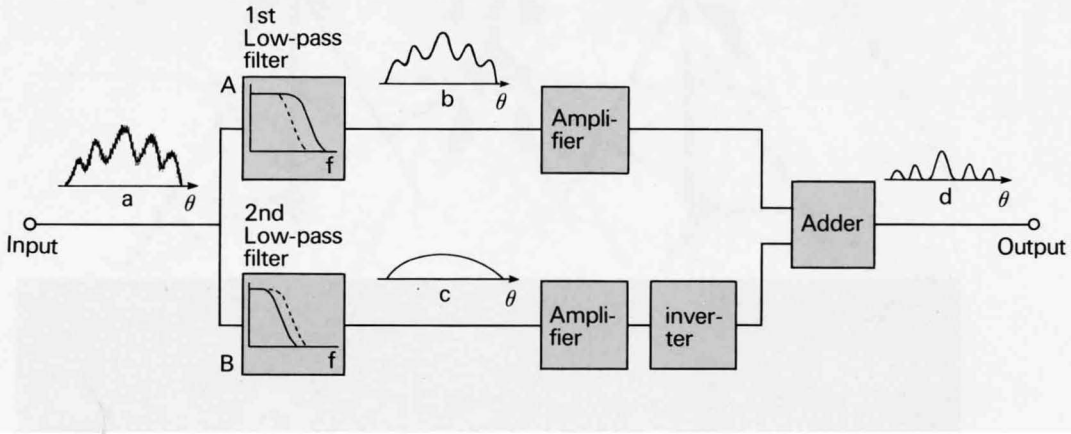

Sketch of signal-processing action.

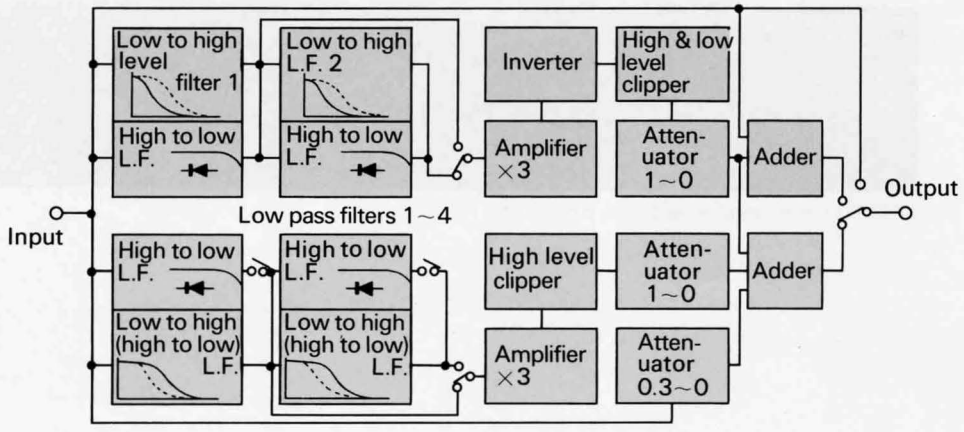

Block diagram of the signal-processing device.

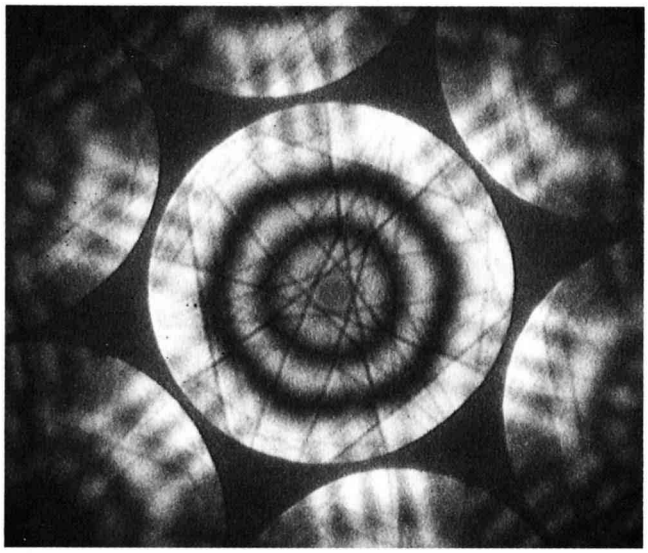

(a) with signal processing.

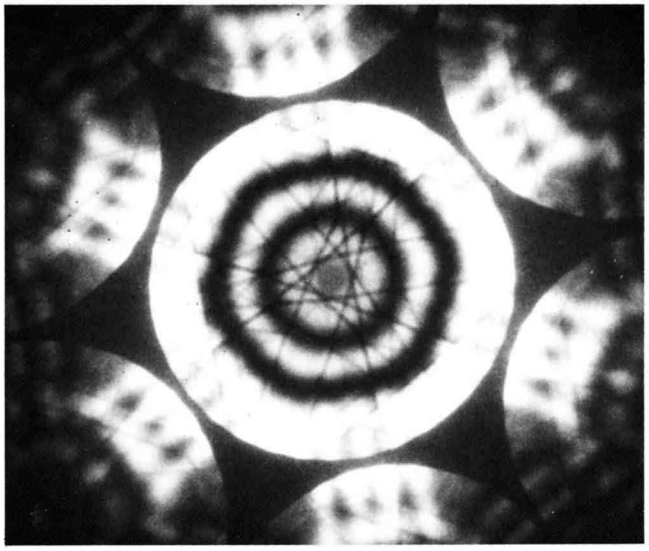

(b) without signal processing.

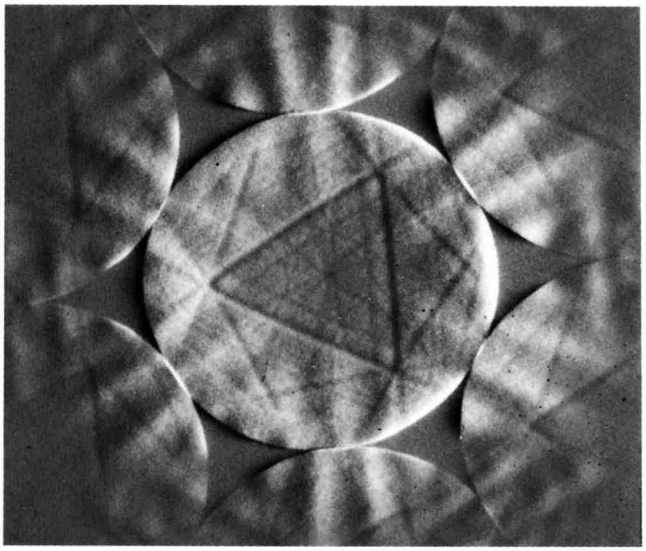

(c) with signal processing.

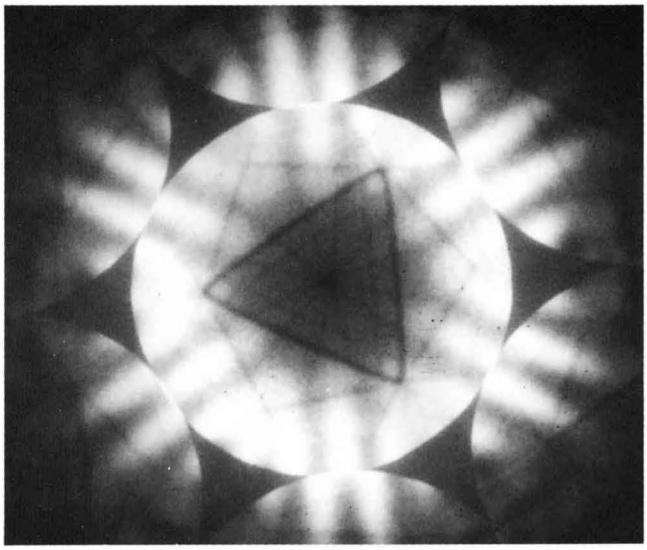

(d) without signal processing.

Simulation of HOLZ Lines

HOLZ lines appearing in CBED patterns are very important for knowing three-dimensional symmetries of crystals, accelerating voltage of the incident beam, crystal lattice parameters and Fourier potentials of crystals. For these purposes, the simulation of HOLZ lines is needed.

HOLZ lines appearing in a 0-th Laue-zone reflection are simulated by drawing the intersection arcs of the Eward sphere with HOLZ reflections.

The programs for two personal computers PC 8801 (NEC) and HP-86 (Hewlett-Packard) for drawing the HOLZ lines are listed in an appendix. The input data is shown here. Examples of outputs by these computers are printed out in the following pages. The dispersion effect due to the dynamical interaction is of course ignored. For comparison, the real $2\bar{2}0$ pattern taken from a (111) Si at 62.8 kV is shown.

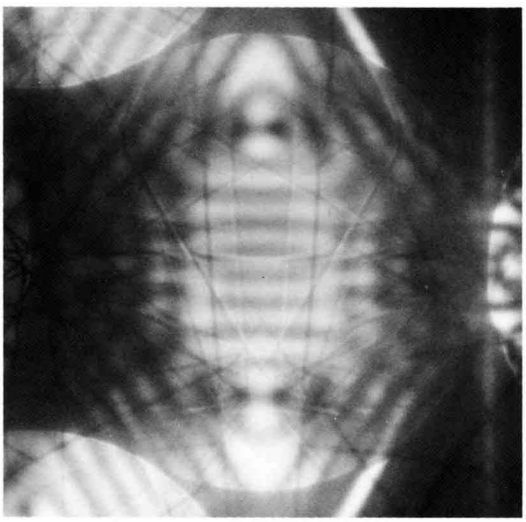

$2\bar{2}0$

Input Data

```
SPECIMEN NAME                                    ? Si
CRYSTAL SYSTEM
   cubic              ------------------ 1
   tetragonal         ------------------ 2
   rhombohedral
      (rhombohedral coordinates) --- 3
   hexagonal,trigonal,rhombohedral
      (hexagonal coordinates) ------ 4
   orthorhombic       ------------------ 5
   monoclinic         ------------------ 6
   triclinic          ------------------ 7
   diamond type       ------------------ 8
                                         ? 8
LATTICE PARAMETERS (A°)                  a=b=c= ? 5.43
ACCELERATING VOLTAGE in kV                      ? 62.8
ZONE AXIS  u,v,w                                ? 1,1,1
DOES EXCITE G-REFLECTION ? (y/n)                ? Y
INDEX OF G                                      ? 2,-2,0
ORDER OF LAUE ZONE                              ? 1
TWO NONLINEAR VECTORS V1 AND V2 BY WHICH ALL RECIPROCAL
LATTICE POINTS IN THE 0-TH LAUE ZONE ARE COVERED.
(V1 DETERMINES HORIZONTAL DIRECTION IN THE OUTPUT)
                        X1,Y1,Z1, X2,Y2,Z2 =? 1,-1,0,0,1,-1
TWO REFLECTIONS IN THE 0-TH LAUE ZONE (THEY DETERMINE
THE DISK SIZE)           H1,K1,L1, H2,K2,L2=? 2,0,-2,0,2,-2
DIAMETER OF DISKS MEASURED IN UNITS OF
MIN.[ABS(H1,K1,L1),ABS(H2,K2,L2),ABS(H1-H2,K1-K2,L1-L2)]
                                         ? 1
INDEX OF A RECIPROCAL LATTICE POINT IN THE N-TH
LAUE ZONE.                               ? 1,1,-1
```

Output by PC8801 (NEC)

Si

[1 1 1]

62.8 kV

1 st Laue Zone

G reflection :
(2 -2 0)

a = 5.43
b = 5.43
c = 5.43
alpha,beta,gamma
= 90 , 90 , 90

Radius of N-th Laue Zone
= 2.12937
Horizontal Direction
= (1 ,-1 , 0)

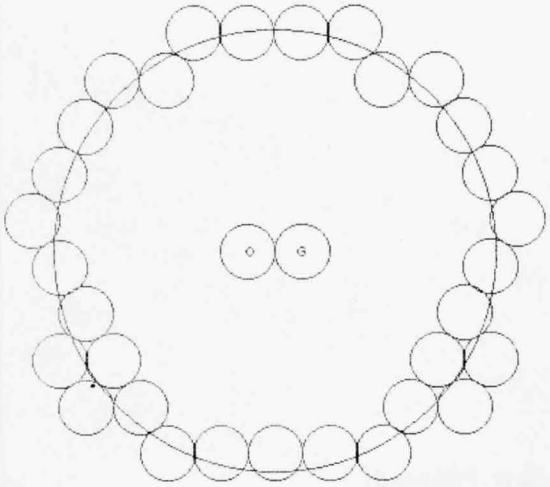

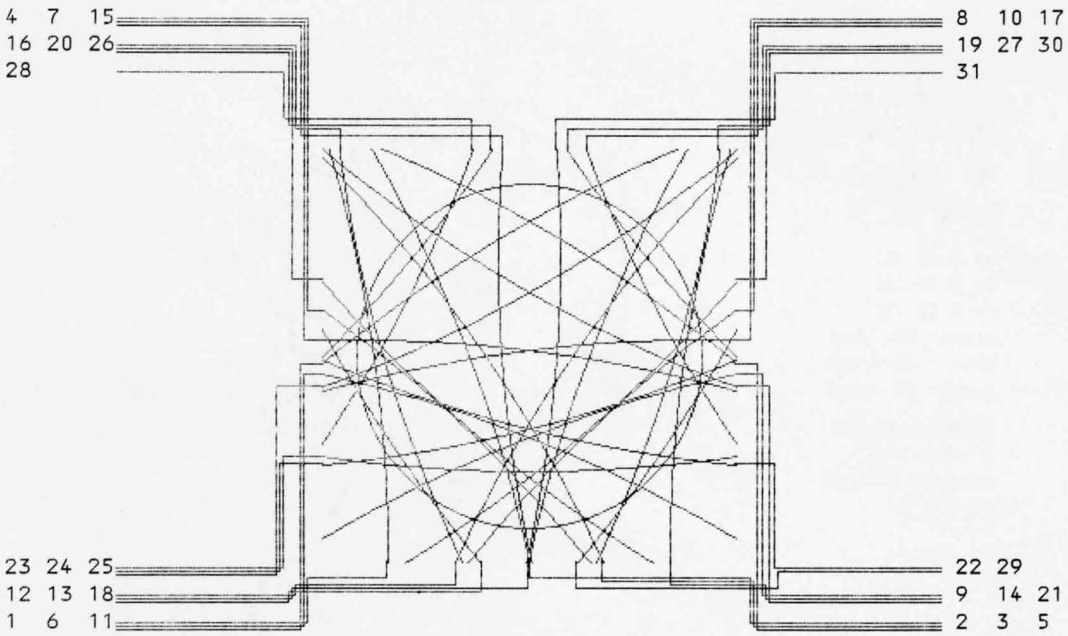

*Si (1 1 1) 1 st zone 62.8 kV

1 - (11 ,-9 ,-1)
2 - (11 ,-7 ,-3)
3 - (11 ,-5 ,-5)
4 - (11 ,-3 ,-7)
5 - (9 ,-1 ,-7)
6 - (9 , 1 ,-9)
7 - (7 , 3 ,-9)
8 - (5 , 5 ,-9)
9 - (3 , 7 ,-9)
10 - (-1 , 9 ,-7)
11 - (1 , 7 ,-7)
12 - (-3 , 9 ,-5)
13 - (-5 , 9 ,-3)
14 - (-7 , 9 ,-1)
15 - (-7 , 7 , 1)
16 - (-7 , 5 , 3)
17 - (-9 , 5 , 5)
18 - (-7 , 3 , 5)
19 - (-9 , 3 , 7)
20 - (-7 , 1 , 7)
21 - (-7 ,-1 , 9)
22 - (-5 ,-3 , 9)
23 - (-3 ,-5 , 9)
24 - (-1 ,-7 , 9)
25 - (1 ,-9 , 9)
26 - (5 ,-11 , 7)
27 - (3 ,-9 , 7)
28 - (7 ,-11 , 5)
29 - (5 ,-9 , 5)
30 - (7 ,-9 , 3)
31 - (9 ,-9 , 1)

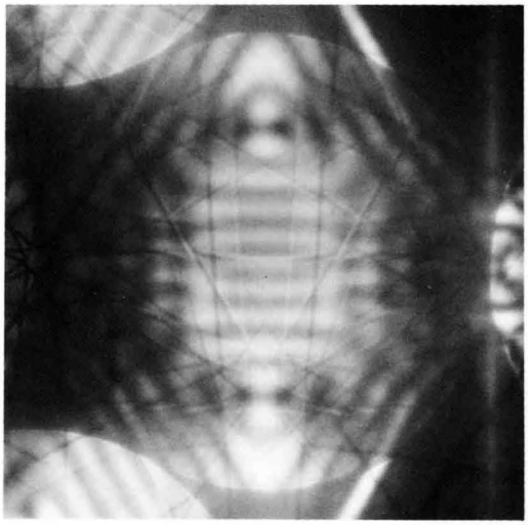

Output by HP-86(Hewlett-Packard)

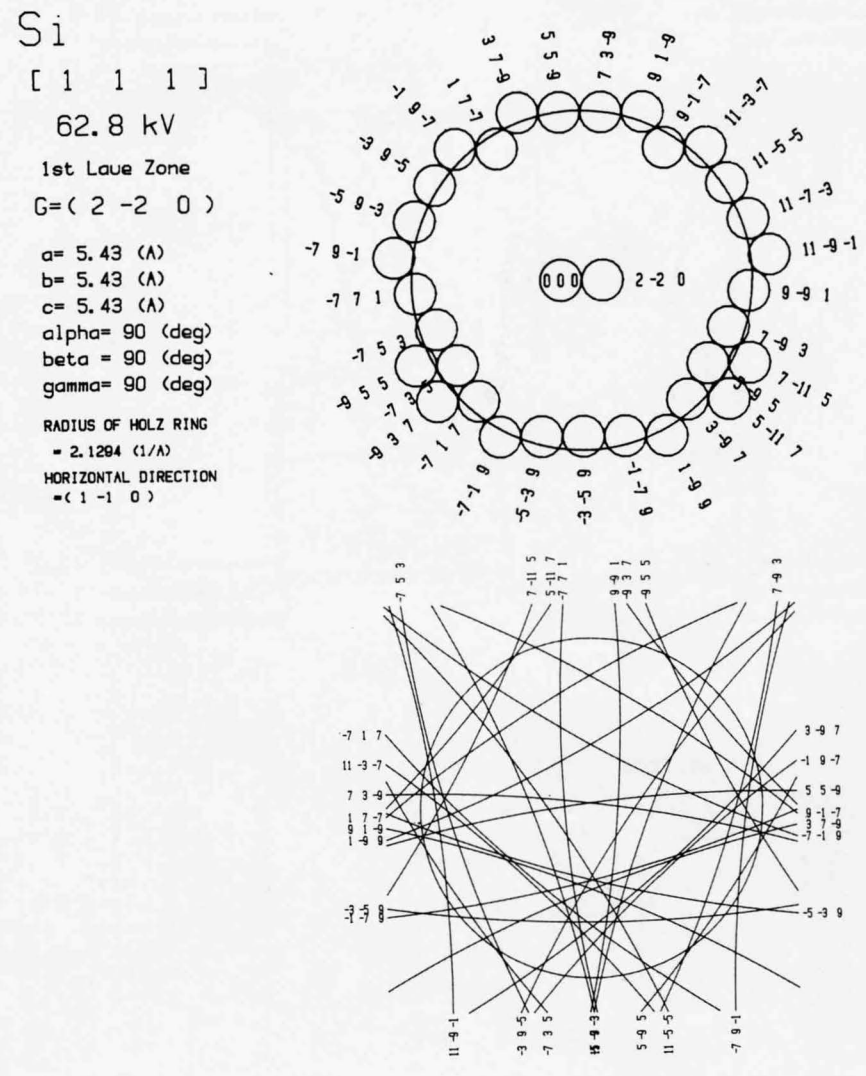

Determinations of Crystal Lattice Spacings and Accelerating Voltages

When the accelerating voltage for the incident beam is known, HOLZ-line patterns can be simulated by computation with varying lattice parameters. When the simulated patterns are brought into agreement with the pattern experimentally obtained, the lattice parameters can be determined. Conversely, when a HOLZ-line pattern obtained from a crystal with known lattice spacings is compared with the simulated patterns, the accelerating voltage can be determined. For these determinations, the use of dynamically interacting lines must be avoided. The accuracy of this method is a few parts of a thousand.

As an example, HOLZ lines were simulated for a (111) Si at accelerating voltages around 100kV. Five distances, A, B, C, D and E indicated in the photograph on this page, were measured from the simulated patterns. The curves of the accelerating voltage vs. the ratios between these distances are shown in the figure on the next page. A series of CBED patterns was taken from a (111) Si by slightly changing the accelerating voltage. The accelerating voltages for Photos (b) to (f) were identified by measuring these ratios and by using the figure, as shown in the table.

P.M. Jones, G.M. Rackham and J.W. Steeds: *Proc. R. Soc. Lond.*, **A354** (1977) 197.

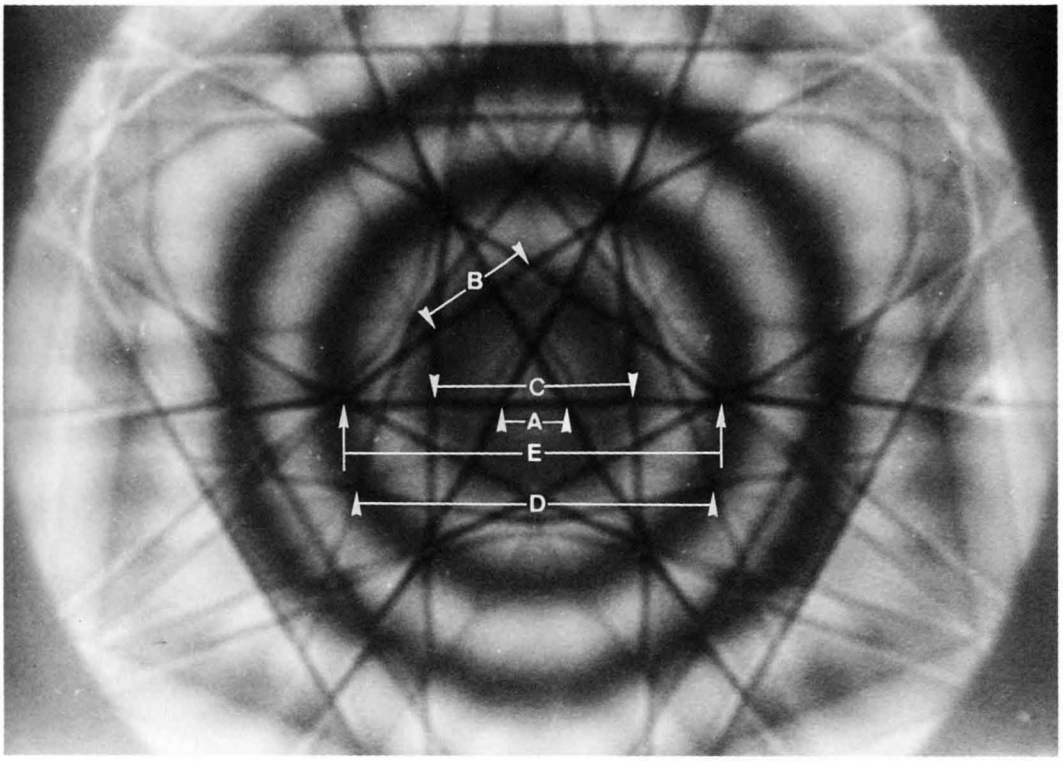

(d)

	b	c	d	e	f
D/B	6.423	4.710	3.095	2.106	1.457
D/C	3.516	2.607	1.781	1.222	0.849
D/E	1.953	1.371	0.935	0.629	0.428
A.V.	97.4kV	98.6kV	100.2kV	101.9kV	103.5kV

A.V. : Accelerating voltage

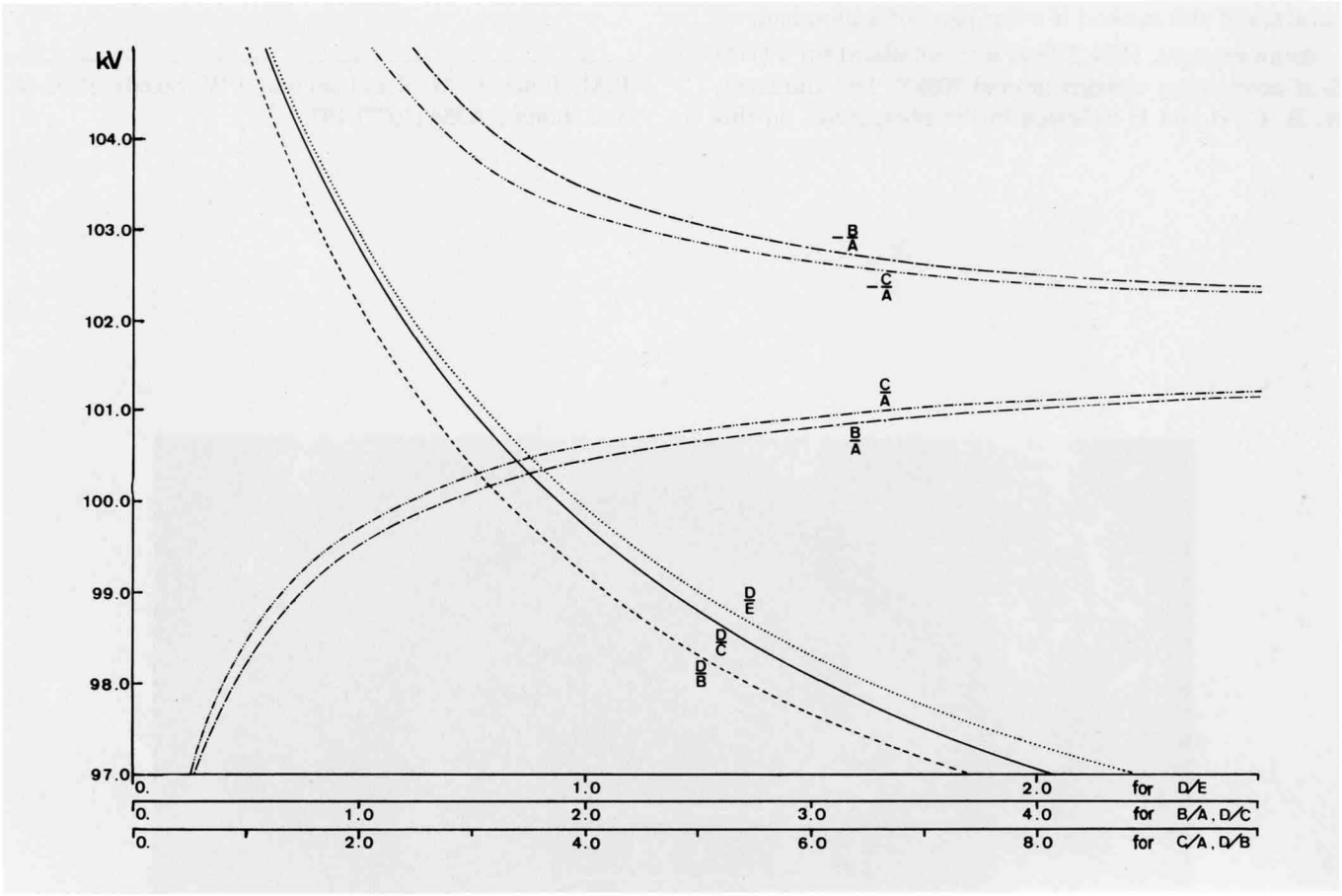

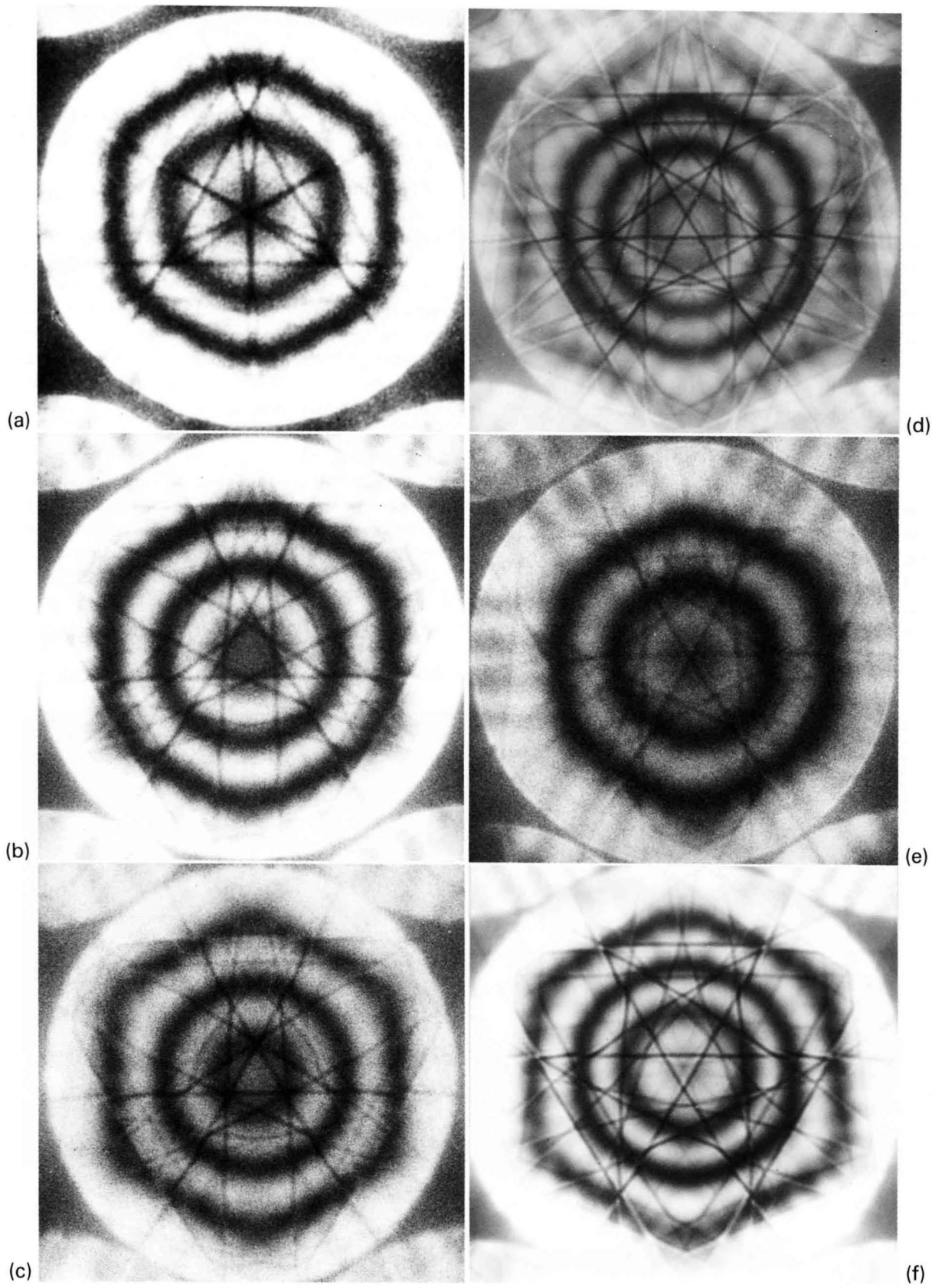

Bright-field patterns taken by varying accelerating voltage around 100kV.

Specimen-Thickness Determination

We describe here a specimen-thickness determination method which utilizes an equation derived from the two-beam dynamical theory of electron diffraction. The equation used is

$$\left(\frac{S_i}{n_i}\right)^2 = \frac{-1}{\xi_g{}^2}\left(\frac{1}{n_i}\right)^2 + \frac{1}{t^2},$$

where ξ_g is the extinction distance of an excited reflection g, t is the specimen thickness to be determined, S_i expresses the deviation of the i-th minimum from the exact Bragg position and is defined by the equation given below, and n_i is a whole number.

The data needed in advance is the lattice spacing of the reflection g and the accelerating voltage of the incident beam. It should be noted that the extinction distance of the reflection is not necessary for the determination, but obtained from the slope of the plot of

$$\left(\frac{S_i}{n_i}\right)^2 \text{ vs } \left(\frac{1}{n_i}\right)^2.$$

The distances to be measured are L_0 from the center of the diffracted beam profile to the center of the transmitted beam, and L_1, L_2, L_3 and L_4 from the center of the diffracted beam profile to each of the successive minima. These distances are indicated in the photograph, which shows the $2\bar{2}0$ intensity profile of a silicon crystal taken at an approximately two-beam condition.

S_i is given by the equation

$$S_i = \frac{\lambda}{d^2}\left(\frac{L_i}{L_0}\right),$$

where λ is the wavelength of the incident beam and d is the spacing of the reflection planes. By using the values of S_i and by setting $n_1 = 1$ and $n_{i+1} = n_i + 1$, the values of $(S_i/n_i)^2$ and $(1/n_i)^2$ are calculated. Next, by setting $n_1 = 2$ and $n_{i+1} = n_i + 1$, these two values are calculated. These calculations are repeated successively by setting $n_1 = 3$, 4.... For a value of n_1, the plot (the regression line) of $(S_i/n_i)^2$ vs. $(1/n_i)^2$ results in a straight line, where the square of the correlation coefficient r^2 takes a value nearest to unity. The specimen thickness is given by the intercept of the straight line with the $(S_i/n_i)^2$ axis. This method determines the specimen thickness, with an accuracy of better than $\pm 2\%$.

The specimen thickness was determined for the intensity profile of the photograph. The data needed beforehand and the obtained values are given in the tables. The straight line plot of $(S_i/n_i)^2$ vs. $(1/n_i)^2$ was obtained for $n_1 = 2$, and is shown in the graph. The value of the intercept of the line with the vartical axis is 8.67×10^{-7} Å^{-2}, resulting in the thickness of 1070Å.

P.M. Kelly, A. Jostsons, R.G. Blake and J.G. Napier: *phys. stat. sol., (a)* **31** (1975) 771.

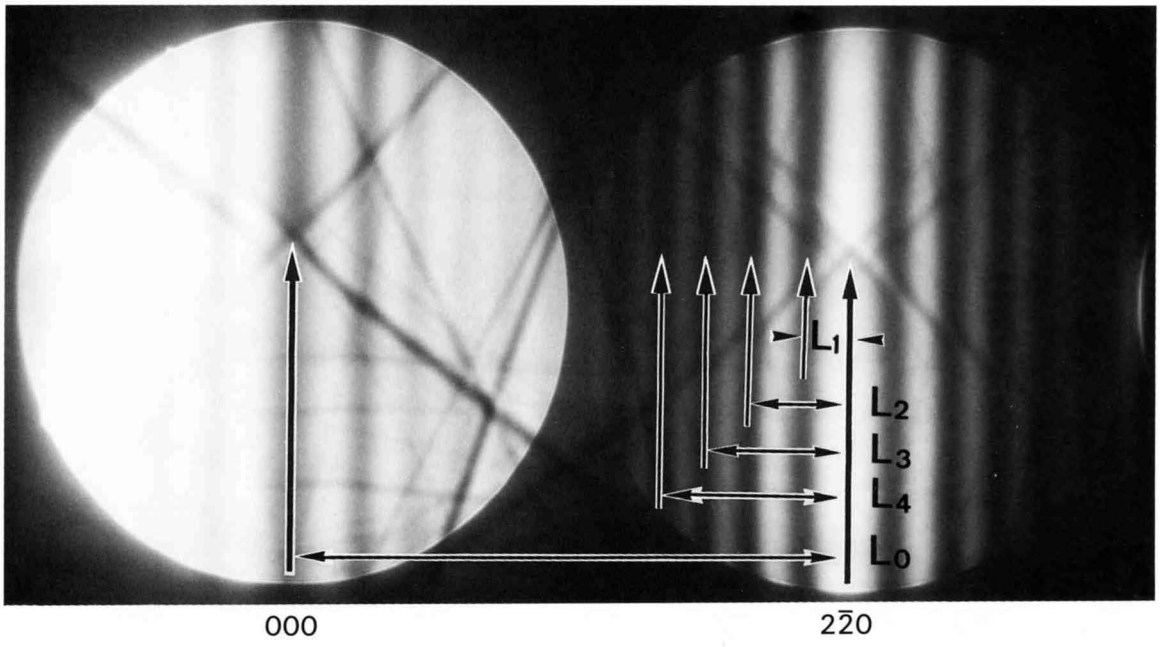

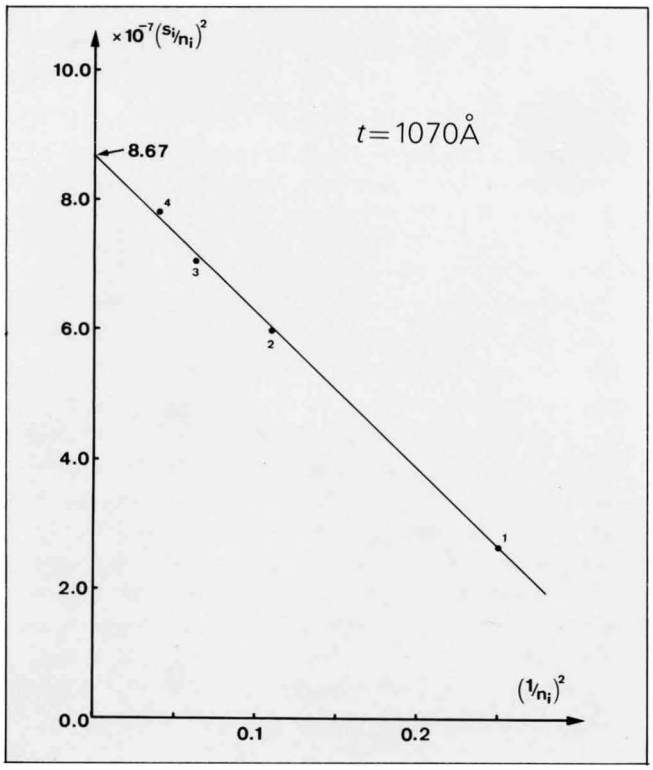

i	(L_i/L_o)	λ	d	S_i
1	7.98×10^{-2}	4.75×10^{-2}(Å)	1.92(Å)	1.03×10^{-3}
2	1.80×10^{-1}			2.32×10^{-3}
3	2.61×10^{-1}			3.36×10^{-3}
4	3.43×10^{-1}			4.42×10^{-3}

		$i=1$	$i=2$	$i=3$	$i=4$
$n_i=1$	$(1/n_i)^2$	1.00			
	$(s_i/n_i)^2$	1.06×10^{-6}			
$n_i=2$	$(1/n_i)^2$	0.250	0.250		
	$(s_i/n_i)^2$	2.65×10^{-7}	1.35×10^{-6}		
$n_i=3$	$(1/n_i)^2$	0.111	0.111	0.111	
	$(s_i/n_i)^2$	1.18×10^{-7}	5.98×10^{-7}	1.25×10^{-6}	
$n_i=4$	$(1/n_i)^2$	6.25×10^{-2}	6.25×10^{-2}	6.25×10^{-2}	6.25×10^{-2}
	$(s_i/n_i)^2$	6.63×10^{-8}	3.36×10^{-7}	7.06×10^{-7}	1.22×10^{-6}
$n_i=5$	$(1/n_i)^2$		4.00×10^{-2}	4.00×10^{-2}	4.00×10^{-2}
	$(s_i/n_i)^2$		2.15×10^{-7}	4.51×10^{-7}	7.81×10^{-7}
$n_i=6$	$(1/n_i)^2$			2.78×10^{-2}	2.78×10^{-2}
	$(s_i/n_i)^2$			3.14×10^{-7}	5.45×10^{-7}
$n_i=7$	$(1/n_i)^2$				2.04×10^{-2}
	$(s_i/n_i)^2$				3.99×10^{-7}

n_1	r^2	t(Å)
1	0.621	8.77×10^2
2	0.999	1.07×10^3
3	0.991	1.23×10^3
4	0.988	1.36×10^3

Point-Group Determination

The point group of a crystal is determined from four CBED patterns: a bright-field pattern (BP), whole pattern (WP), dark-field pattern (DP) and a pair of dark-field patterns (±DP). BP means the bright-field pattern observed in a pattern taken with the electron incidence parallel to a zone axis (ZAP). WP means the resultant of BP and all the reflected patterns surrounding BP in the ZAP, or means the ZAP itself. DP means the dark-field pattern containing the exact Bragg angle. ±DP means a pair of DPs whose reflection indices have opposite signs.

We shall explain the point-group determination procedure with a Si crystal as an example. Photo (a) shows the ZAP from a Si crystal. The BP has a threefold rotation axis and three mirror planes, or $3m_V$ symmetry. The WP has the same symmetry. Photos (b) and (c) show the $2\bar{2}0$ and $\bar{2}20$ DPs. Each of them has a mirror symmetry m_2 perpendicular to the reflection vector. This mirror symmetry is caused by a twofold rotation axis parallel to the specimen surface and distinguished by the suffix 2 from the mirror symmetry m_V originating from the mirror plane perpendicular to the surface. One of the DPs coincides with the other upon translation. This symmetry is called translational symmetry or 2_R, indicating the presence of an inversion center.

These symmetries are schematically depicted in Figs. (a), (b) and (c). The large circles correspond to diffraction disks. The intensities at the angular positions represented by the small circles are the same. That is, these circles show the symmetries of the patterns. The crosses inside the circles in DP and ±DP indicate the exact Bragg angle positions, and those outside the circles indicate the zone axis. The cross inside the circle in BP & WP depicts the zone axis.

The diffraction group giving rise to these pattern symmetries is found to be $6_R mm_R$ by consulting the symmetry tables shown in an appendix (p.153). The pattern symmetries of $6_R mm_R$ and those of $3m$, a little similar to the former, are quoted in Table (a). Table (b) shows that there are two crystal point-groups $\bar{3}m$ and $m3m$ causing the diffraction group $6_R mm_R$. To find the right point group, a ZAP has to be taken by a different incidence. Photo (d) shows $4mm$ symmetry in BP and WP. The point group giving rise to fourfold rotation symmetry is not $\bar{3}m$ but $m3m$. The point group of Si crystals is thus determined to be $m3m$.

B.F. Buxton, J. A. Eades, J.W. Steeds and G.M. Rackham: *Phil. Trans. R. Soc. London*, **281** (1976) 171.
M. Tanaka, R. Saito and H. Sekii: *Acta Cryst.*, **A39** (1983) 357.

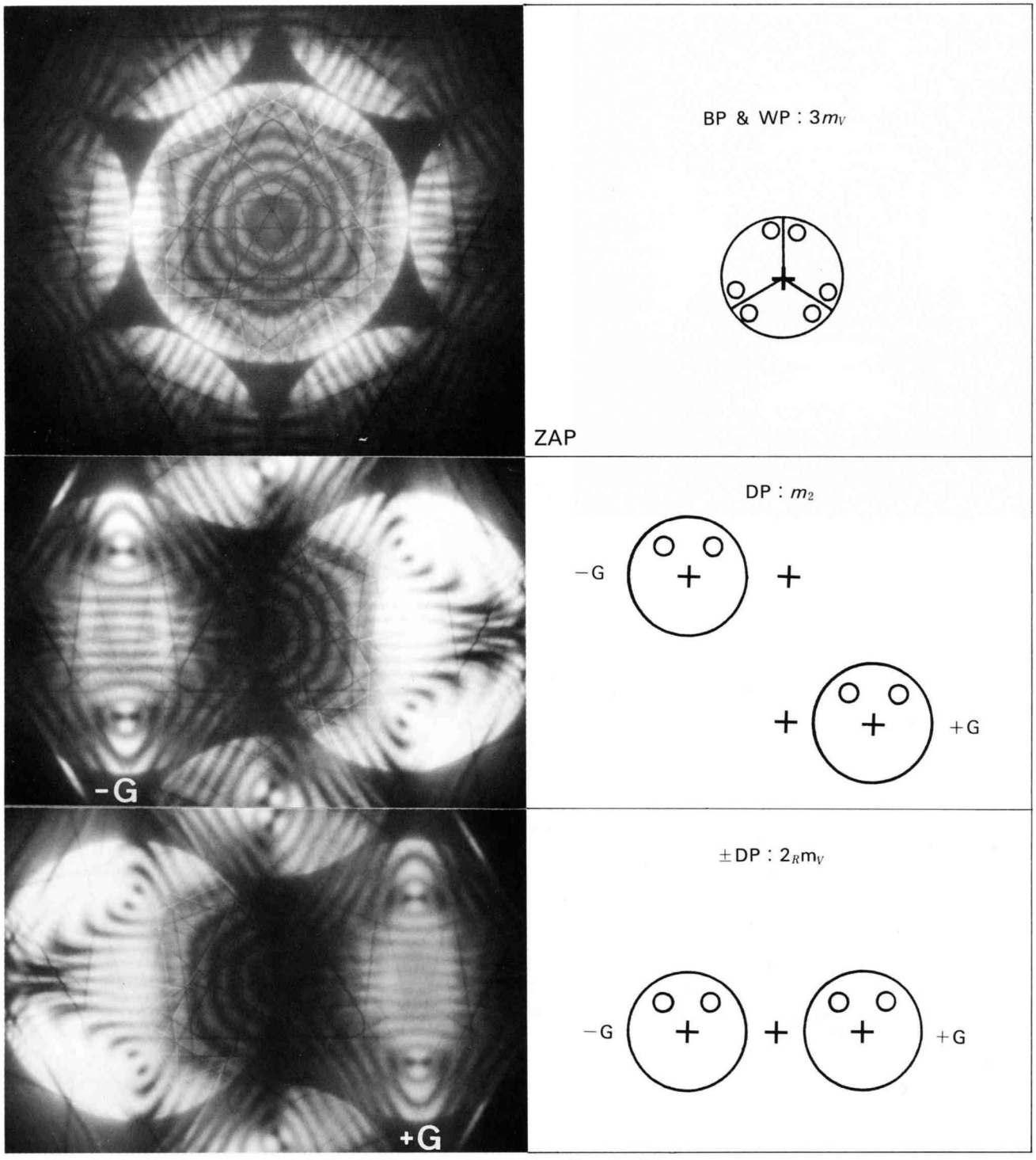

Photo (a):ZAP showing $3m_v$ symmetry in BP and WP. Photos (b) and (c): −DP and +DP showing m_2 symmetry.

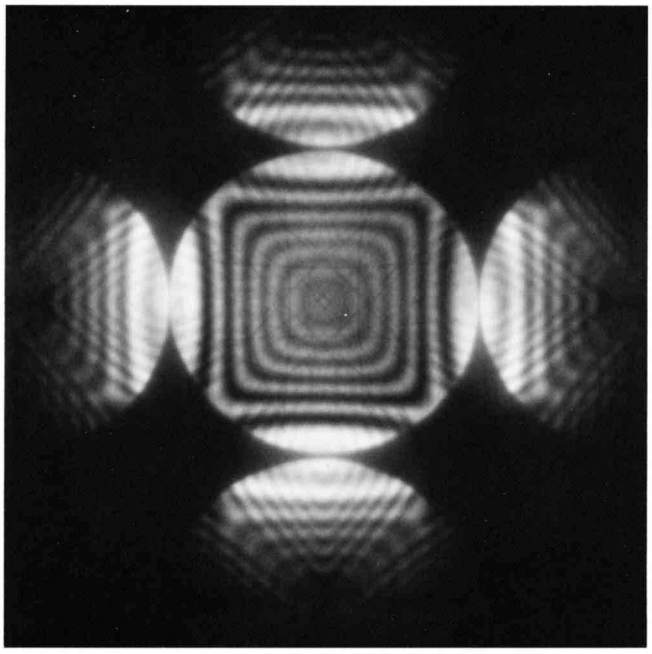

(d)

ZAP from Si crystal. BP and WP show $4mm$ symmetry.

Table (a) CBED pattern symmetries of the diffraction groups $6_R mm_R$ and $3m$.

Diffraction group	BP	WP	DP	±DP
$6_R mm_R$	$3m_r$	$3m_r$	$\begin{matrix}1\\ m_2\\ m_r\end{matrix}$	$\begin{matrix}2_R\\ 2_R m_r\\ 2_R m_R\end{matrix}$
$3m$	$3m_r$	$3m_r$	$\begin{matrix}1\\ m_r\end{matrix}$	$\begin{matrix}1\\ m_r\\ 1\end{matrix}$

Table (b) Zone axis symmetries

point group	⟨111⟩	⟨100⟩	⟨110⟩	⟨*uvo*⟩	⟨*uuw*⟩	[*uvw*]
$m3m$	$6_R mm_R$	$4mm1_R$	$2mm1_R$	$2_R mm_R$	$2_R mm_R$	2_R
point group	[0001]		⟨$11\bar{2}0$⟩		$[u\bar{u}.w]$	$[uv.w]$
$\bar{3}m$	$6_R mm_R$		21_R		$2_R mm_R$	2_R

Symmetrical many-beam excitation

In the point-group determination method described in the previous pages, it is tacitly assumed that only a reflection G is exactly excited for observing dark-field pattern symmetries. However, it is possible to excite many reflections simultaneously. A new point-group determination method has been developed, which utilizes the symmetries appearing in hexagonal six-beam, rectangular four-beam and square four-beam patterns, where these beams are simultaneously set at the Bragg conditions. We call these patterns symmetrical many-beam (SMB) CBED patterns.

The method of Buxton *et al.* finds firstly the symmetry elements with respect to a zone axis parallel to the incident beam (two-dimensional symmetry elements) in a ZAP and, secondarily, the remaining symmetry elements (three-dimensional symmetry elements), in dark-field disks. In the SMB method, plural three-dimensional symmetry elements are observed in an SMB pattern and two-dimensional symmetry elements are observed in a pair of SMB patterns. When the SMB method is utilized, most diffraction groups can be identified from an SMB pattern in a photograph.

Photos (a), (b) and (c) show CBED patterns taken from a (111) pyrite (FeS_2) specimen. The space group of FeS_2 is $P2_1/a\bar{3}$ and the diffraction group of the specimen is 6_R. The zone-axis pattern (Photo (a)) shows the threefold rotation symmetry in BP and WP. The hexagonal six-beam pattern (Photo(b)) shows no symmetry higher than 1 in the disks O, G, F and S and shows the symmetry 6_R between the disks S and S'. The same symmetry is also seen in Photo (c). The symmetry 2_R is observed between the disks G and $\bar{G}$, and the symmetry 6_R is seen between the disks F and $\bar{F}$. These results agree exactly with the theoretical results given in the table below the photographs and on an appendix (page 157). The table on the appendix shows that the diffraction group 6_R can be identified from only one hexagonal six-beam pattern, since there is no other diffraction group which gives rise to the same symmetry in the six disks. When the method of Buxton *et al.* is used, four patterns in three photographs are needed to identify the group 6_R (see the table on page 153).

Photos (d), (e) and (f) show CBED patterns taken from a (110) V_3Si specimen at an accelerating voltage of 80 kV. The space group of V_3Si is $Pm3n$ and the diffraction group of the specimen is $2mm1_R$. The zone axis pattern (Photo (d)) shows $2mm$ symmetry in BP and WP. The symmetries expected from the diffraction group $2mm1_R$, which are given in the table below the photographs and on an appendix (page 159), are observed in the rectangular four-beam pattern (Photos (e) and (f)). The diffraction group $2mm1_R$ can also be identified from one rectangular four-beam pattern.

When a pair of SMB patterns is taken, all but five of the diffraction groups are completely identified. For cases where a pair of SMB patterns is needed, however, the use of an SMB pattern and a ZAP is recommended, since two-dimensional symmetries are found easily in the ZAP.

M. Tanaka, R. Saito and H. Sekii: *Acta Cryst.*, **A39** (1983) 357.

FeS_2 [111] $P2_1/a\bar{3}$ Hexagonal six-beam excitation

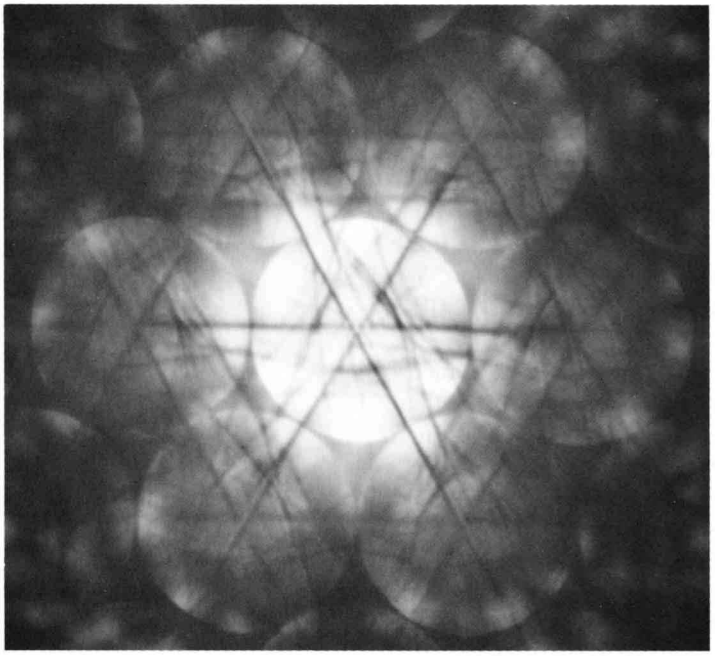

(a)

(c)

(b)

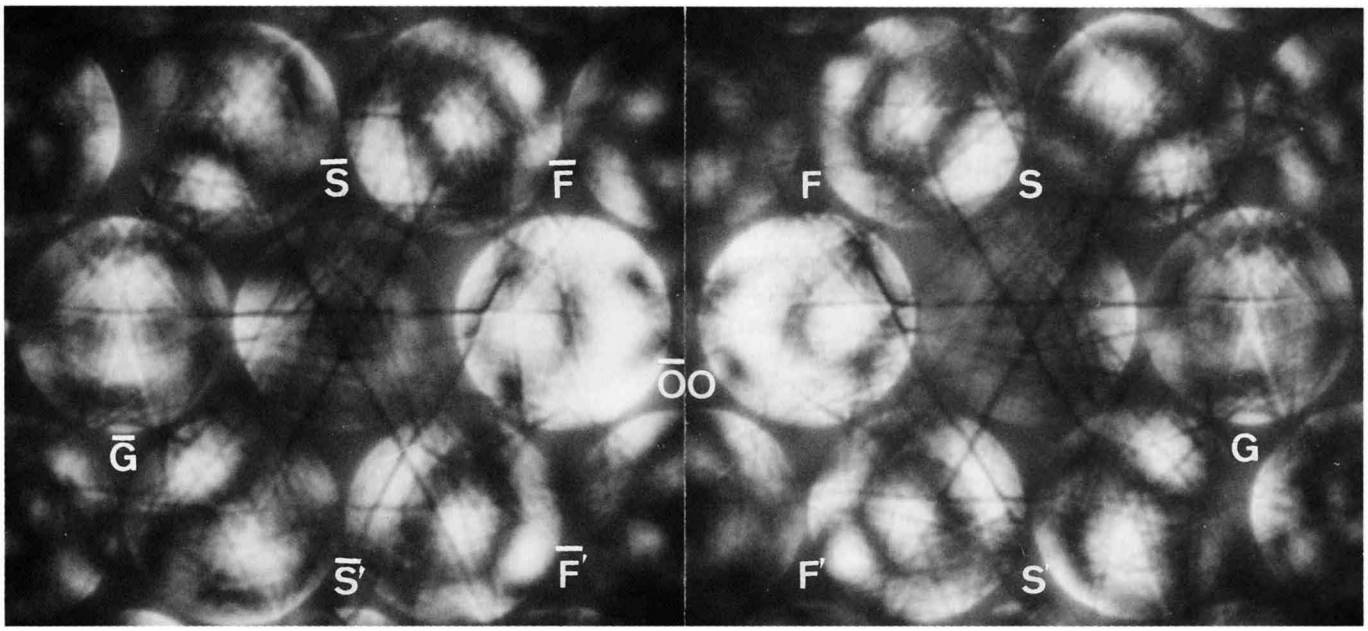

6_R								
BP	WP		G	O	F	S	FF′	SS′
3	3		1	1	1	1	1	6_R
			±G	±O	±F	±S	F′F̄	S′S
			2_R	1	6_R	1	1	1

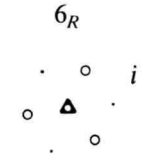

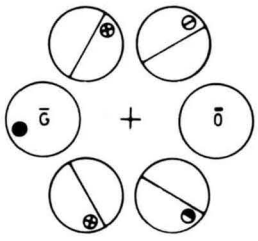

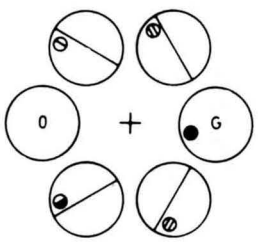

V_3Si [110] $P4_2/m\bar{3}2/n$ Rectangular four-beam excitation, 80kV

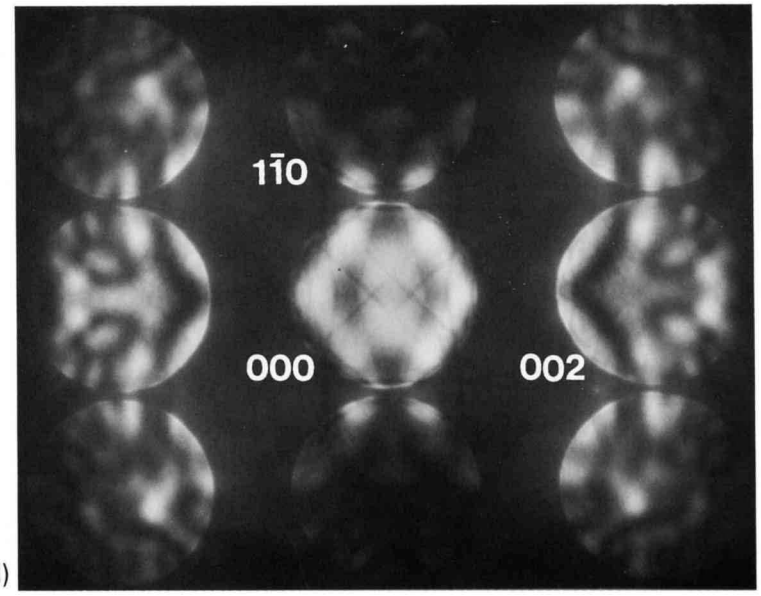

(d)

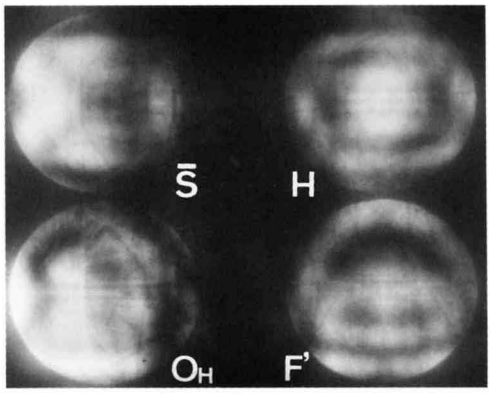

(e)

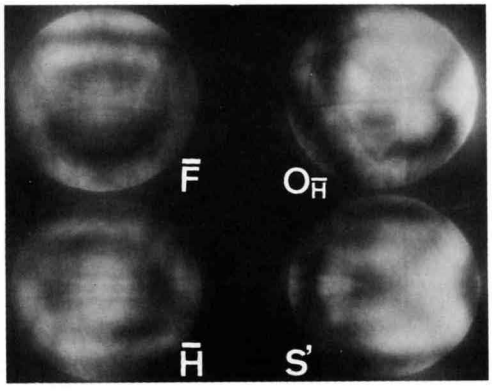

(f)

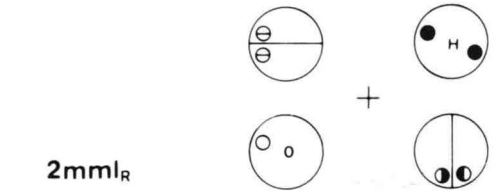

2mml$_R$

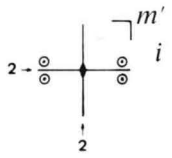

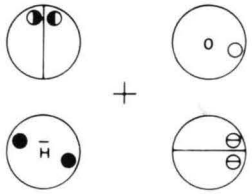

$2mm\,1_R$								
BP	WP	O	H	F'	$\bar{S}$	$\bar{S}S'$	$\bar{F}F'$	$H\bar{H}$
$2mm$	$2mm$	1	1_R	m_2	m_2	$2m_R$	$2m_R$	21_R

Space-Group Determination

When a crystal has a screw axis or glide planes, forbidden reflections occur in the approximation of kinematical diffraction. When dynamical diffraction takes place, such reflections are allowed to have finite intensity by so-called "Umweganregung". However, the extinction of intensity is still caused for certain directions of the incident beam by the dynamical diffraction effect. This extinction appears as dark lines in CBED disks, and is called dynamic extinction lines or Gjønnes-Moodie (GM) lines after their study.

Figure (a) illustrates the dynamic extinction. The $h00$ (h = odd) reflections are kinematically forbidden owing to an a-glide plane perpendicular to the b-axis and/or a 2_1 screw axis in the a-direction. Let us consider an Umweganregung path "a" in the 0-th Laue zone for the 100 forbidden reflection. The path "b" is geometrically equivalent to the path "a" with respect to the glide plane and the 2_1 screw axis. When the excitation error of these two paths are the same—the Laue point of the incident beam lies in the ($0k0$) plane passing through the origin—the wave passing through the path "a" and that through the path "b" have the same amplitude and opposite signs. Then these two waves are superposed on the 100 disk and cancel out each other, resulting in the dark line A in the forbidden reflections, as shown in Fig. (b). In the path "c", the reflections are arranged in the reversed order compared to those in the path "b". When the 100 reflection is exactly excited, the two paths "a" and "c" have the same excitation error. The waves passing through these paths have the same amplitude and opposite signs, and cancel out each other on the 100 disk, resulting in the dark line B in this disk, as shown in Fig. (b).

The dynamic extinction effect is analogous to the interference phenomenon in the Michelson interferometer. That is, the incident beam is split into two beams by Bragg reflections in a crystal. These beams follow different Umweganregung paths, in which they suffer a relative phase shift of π when reflected by crystal planes, and then are superposed on a kinematically forbidden reflection to cancel out each other.

Table (a) shows GM line rules for glide planes and 2_1 screw axis. It reveals that A_2 and B_2 GM lines are produced by glide planes and 2_1 screw axis, and that A_3 GM line is caused by glide planes and B_3 GM line by 2_1 screw axis. Tables of dynamic extinction in which expected GM lines are listed for various incident-beam directions of all the space groups are given in an appendix (pp.162 ~ 172).

Photos (a) and (b) respectively show CBED patterns obtained from thin and thick areas of FeS_2 with [010] incidence. In (a), only broad fringes due to two-dimensional (0-th Laue zone) interaction are observed. A_2 GM lines are seen in the odd-order forbidden reflection disks and B_2 GM line in the exactly excited first-order reflection disk. In (b), fine lines due to three-dimensional interaction can be observed. The fine lines are symmetric about A_2 and B_2 GM lines. This fact means the presence of A_3 and B_3 GM lines. Then, the patterns reveal that both an a-glide plane and a 2_1 screw axis exist.

When the table for the space group $P2_1/a\bar{3}$ of FeS_2 is referred to, it is seen that an A_3 GM line due to the glide plane and a B_3 GM line due to the 2_1 screw axis should be separately observed in the $\bar{1}10$ and 001 disks with 110 incidence (Table (b)). Photo (c) shows a [110] ZAP of FeS_2. A_2 lines are seen in both the $\bar{1}10$ and 001 disks. Since the fine lines are symmetric and asymmetric about the A_2 lines in the $\bar{1}10$ and 001 disks, respectively, the A_3 GM line should be present in the $\bar{1}10$ disk but not in the 001 disk, revealing the presence of the glide plane parallel to the (001) and the 2_1 screw axis in the [001]. To confirm these results, two CBED patterns were taken at the $\bar{1}10$ and 001 Bragg settings (Photos (d) and (e)). The fine lines are symmetric with repsect to the A_2 line in the $\bar{1}10$ disk (Photo (d)), and are symmetric with respect to the B_2 line in the 001 disk (Photo (e)). This result confirms again that the glide plane is parallel to the (001) and that the 2_1 screw axis is in the [001].

The tables given in an appendix (pp.162 ~ 172) are applicable to the cases in which the projection of the Laue point is present at the midpoint of the line connecting the transmitted beam and the forbidden reflection. In rectangular many-beam patterns, the GM line rules are modified. As an example, we shall see a modification in rectangular four-beam patterns from FeS_2. In Photo (f), the 100, 013 and 113 reflections are set at Bragg conditions. B_2 and B_3 GM lines are seen in the 100 reflection, indicating the presence of a 2_1 screw axis in the [100]. The GM line rule given in the column of the [$hk0$] incidence for the space group $P2_1/a\bar{3}$ is still applicable to this reflection, since crystal rotation about a screw axis gives rise to no effect on the GM lines due to the screw axis.

Only a B_2 line is seen in the 013 disk, although it is somewhat obscured by fine HOLZ lines. This result contradicts the GM line rule, which requires the appearance of A_2 and A_3 lines together with a B_2 line. The A_2 and A_3 lines appear only when the incident beam lies in a glide plane. In the present case, this condition is not satisfied. On the other hand, the B_2 line is still present, since two Umweganregung paths, "a" and "c" shown in Fig. (a), are kept set at the identical diffraction condition.

When the 200, 013 and 213 reflections are set at the Bragg conditions (Photo (g)), B_2 and B_3 lines no longer appear in the 100 disk. The B_2 line still appears in the 013 disk, since this reflection is exactly excited.

J. Gjønnes and A.F. Moodie: *Acta. Cryst.*, **19** (1965) 65.

M. Tanaka, H. Sekii and T. Nagasawa: *Acta. Cryst.*, **A39** (1983) 825.

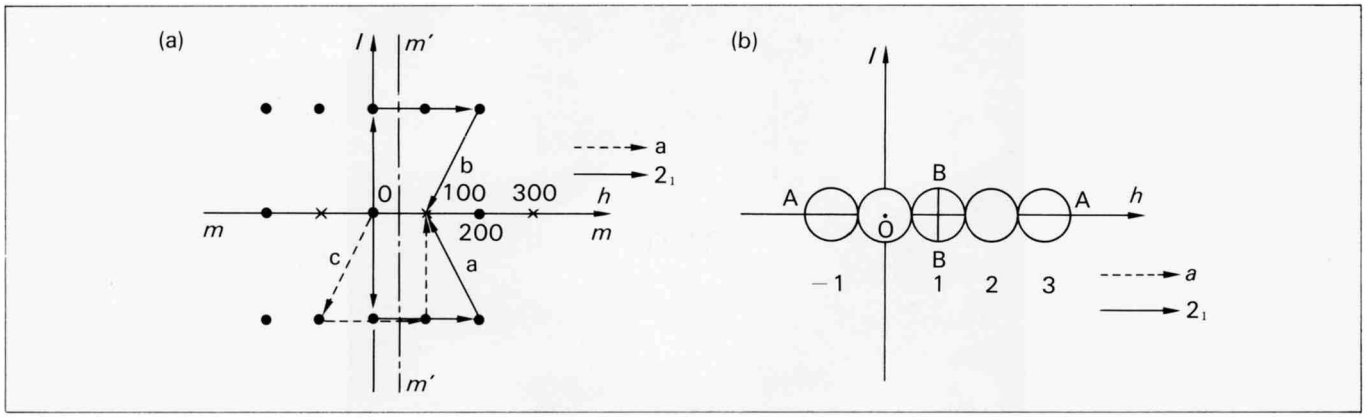

Illustration of the production of GM lines. (a) Umweganregung paths a, b and c. (b) *A* and *B* GM lines in forbidden refrections.

Table (a) Dynamic extinction rules for symmetry elements of a plane-parallel specimen.

Symmetry elements of plane-parallel specimen	Orientation to specimen surface	GM lines	
		Two dimensional (0-th Laue zone) interaction	Three dimensional (HOLZ) interaction
Glide planes	perpendicular : g	A_2 and B_2	A_3
	parallel : g'	——	Intersection of A_3 and B_3
Twofold screw axis	perpendicular : 2_1	——	——
	parallel : $2_1'$	A_2 and B_2	B_3

Table (b)

Space group	Incident beam direction			
	[010] (cyclic)		[*hk*0] (cyclic)	
205 $Pa\bar{3}$ $P2_1/a\bar{3}$	$h00$	A_2B_2	$00l$	A_2B_2
	a_3, 2_{11}	A_3B_3	2_1	B_3
	$00l$		$\bar{k}h0$	A_2B_2
	2_{13}	B_3	a	A_3

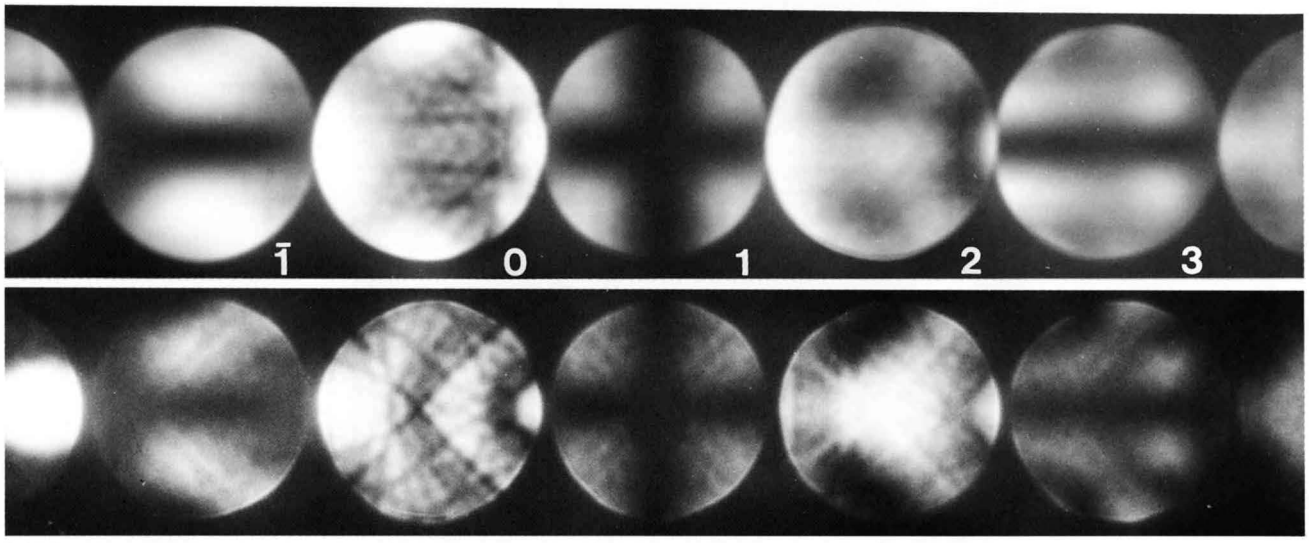

CBED patterns obtained from (a) thin and (b) thick areas of a (010) FeS_2. (a) A_2 and B_2 GM lines are seen. (b) Not only A_2 and B_2 but also A_3 and B_3 GM lines are seen.

FeS_2 [110]

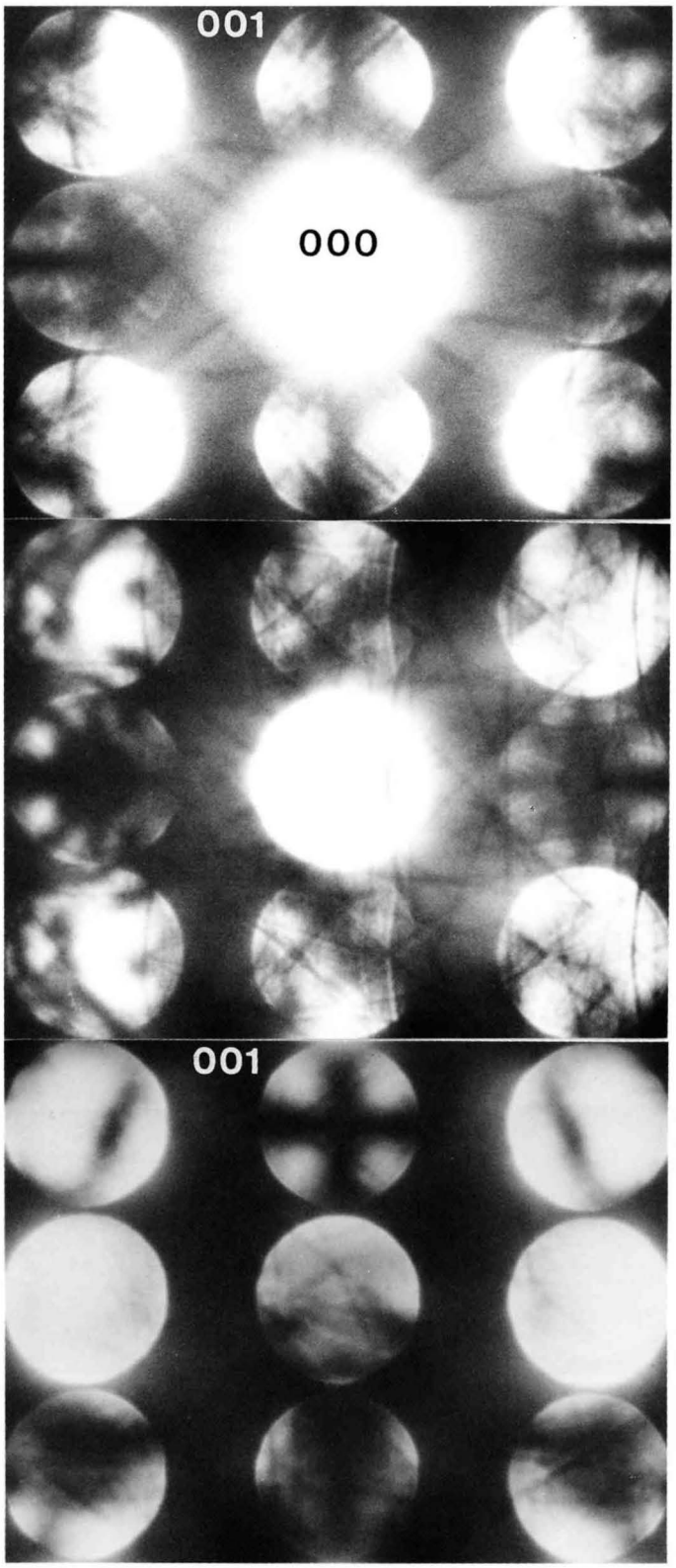

GM lines taken from a (110) FeS_2. (c) ZAP showing A_2 and A_3 GM lines in $\pm\bar{1}10$ disks, and A_2 GM lines in the ± 001 disks. (d) the $\bar{1}10$ disk exactly excited, showing A_2, B_2 and A_3 GM lines. (e) the 001 disk exactly excited, showing A_2, B_2 and B_3 GM lines.

FeS_2 [03$\bar{1}$] GM-lines in rectangular four-beam excitation

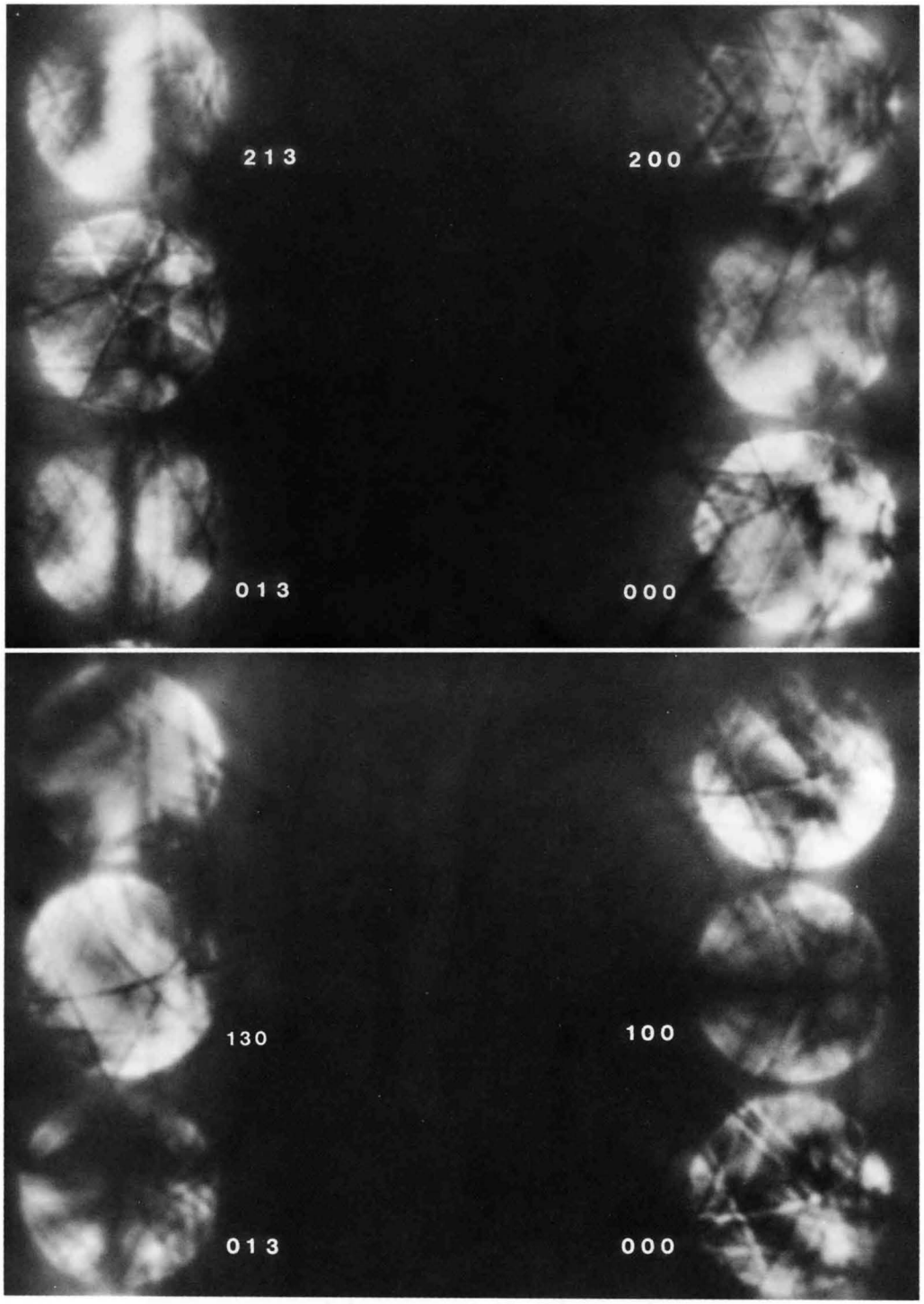

(f)

(g)

Example : $ErRh_4B_4$

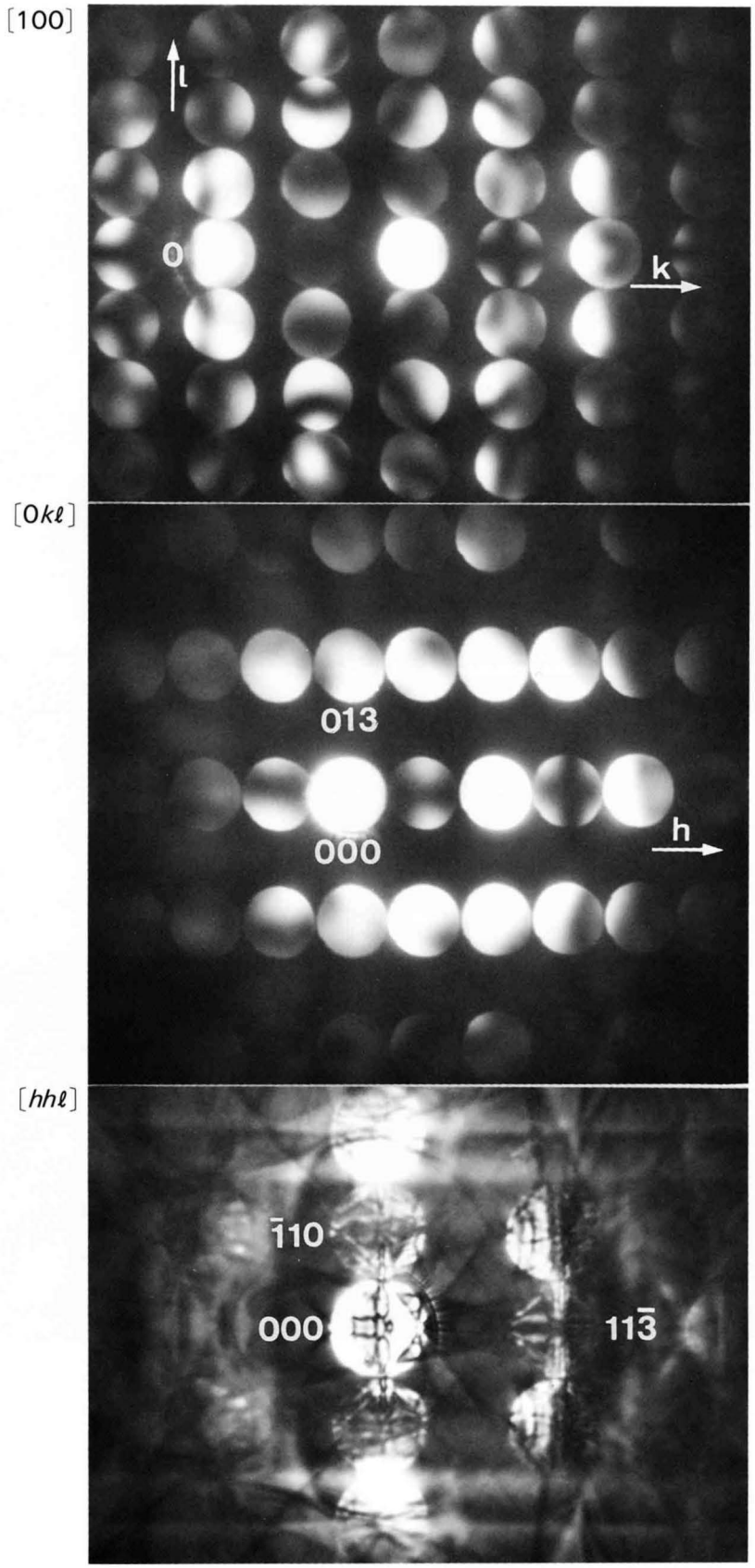

Four space-groups belonging to point-group $4/mmm$

Incident beam direction / Space group		[100]		[$h0\ell$]		[$hh\ell$]	
129	$P4/nmm$ $P4/n2_1/m2/m$	0k0 $n, 2_{12}$	A_2 B_2 A_3 B_3	$0k0$ 2_1	A_2 B_3 B_3		
130	$P4/ncc$ $P4/n2_1/c2/c$	0k0 $n, 2_{12}$ 00ℓ c_{12}	A_2 B_2 A_3 B_3 A_3	$h0\ell_0$ c_1 $0k0$ 2_1	A_2 B_2 A_3 A_2 B_2 B_3	$hh\ell_0$ c_2	A_2 B_2 A_3
137	$P4_2/nmc$ $P4_2/n2_1/m2/c$	0k0 $n, 2_{12}$	A_2 B_2 A_3 B_3	$0k0$ 2_1	A_2 B_2 B_3	$hh\ell_0$ c	A_2 B_2 A_3
138	$P4_2/ncm$ $P4_2/n2_1/c2/m$	0k0 $n, 2_{12}$ 00ℓ c_2	A_2 B_2 A_3 B_3 A_3	$h0\ell_0$ c $0k0$ 2_1	A_2 B_2 A_3 A_2 B_2 B_3		

We shall explain the space-group determination procedure with a magnetic superconductor $ErRh_4B_4$ as an example. The room temperature phase of $ErRh_4B_4$ belongs to the tetragonal crystal system and has lattice spacings $a=0.5292$ nm and $c=0.7374$ nm.

Three possible space groups, $P4_2/n$, $P\bar{4}m2$ and $P4_2/nmc$, have been proposed until now. We have determined the point group to be $4/mmm$, although we have omitted to describe this point-group determination procedure. Photo (a) on the opposite page shows the CBED pattern taken with [100] incidence at the 030 Bragg setting. A_2 and B_2 GM lines are seen in the 030 disk. Three-dimensional GM lines are not observed, since HOLZ reflections are weak. When we consult the column of [100] incidence in the table of an appendix (pp.168, 169), we find four space groups compatible with the experiment — No. 129, No. 130, No. 137 and No. 138 as shown in the table on this page. Photo (b) shows a CBED pattern taken with a [0kl] incidence at the 300 Bragg setting. A_2 and B_2 GM lines are seen in the 300 disk. However, no A GM line is seen in the 013 disk. When consulting the column of [0kl] incidence in the tables, two space groups, No. 129 and No. 137, are found to remain as possible space groups. Lastly, the CBED pattern taken with an [hhl] incidence is examined (Photo (c)). In the $11\bar{3}$ disk, an A_3 GM line is seen. When an A_3 GM line is observed, an A_2 GM line should also be observed. However, an A_2 GM line is obscure in the photograph, presumably owing to a weak interaction between the 0-th Laue-zone reflections.

When the last column of the table is referred to, it is seen that the space group No. 137 only produces an A_3 GM line. As a result, the space group $P4_2/nmc$ — one of the expected groups — is determined to be the right space group.

Application Data

LACBED Pattern I

Si [111] $F4_1/d\bar{3}2/m$

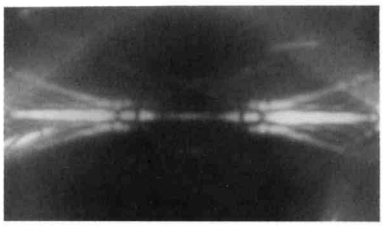

$6\bar{6}0$

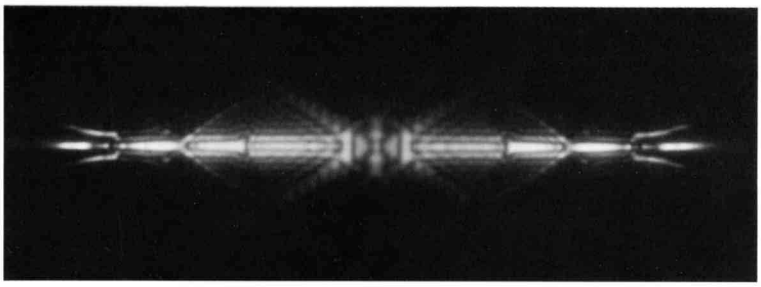

$4\bar{4}0$

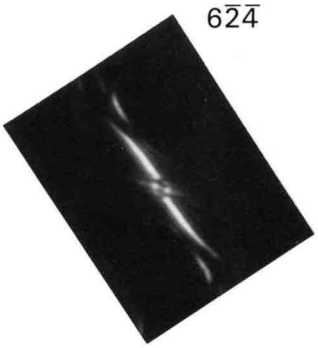

$6\bar{2}\bar{4}$

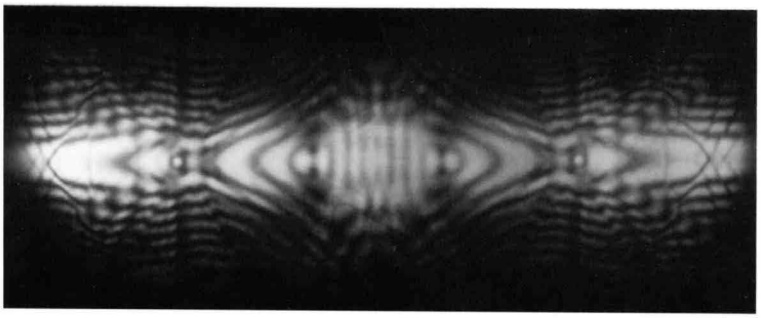

$2\bar{2}0$

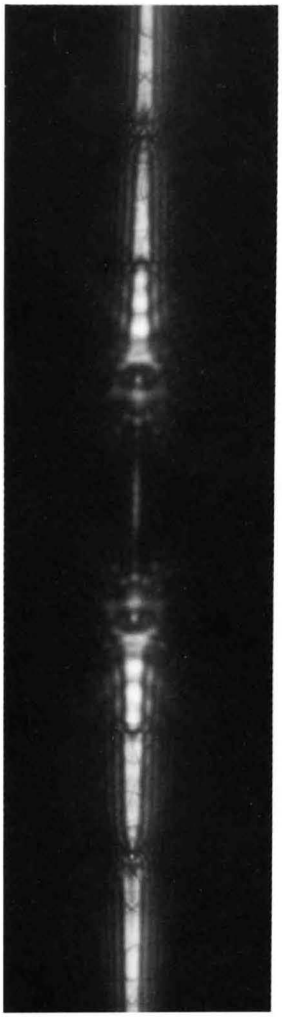

$22\bar{4}$

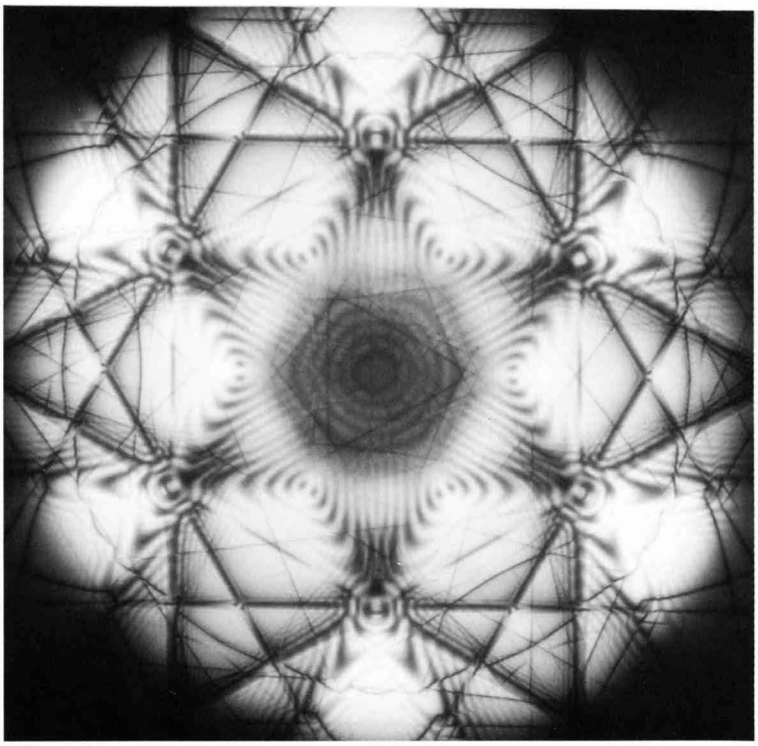

000

Si [110] BR method

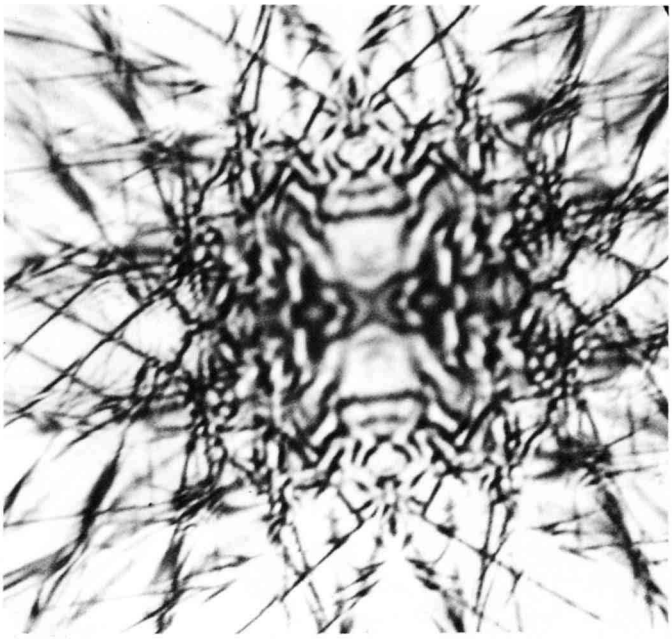

000

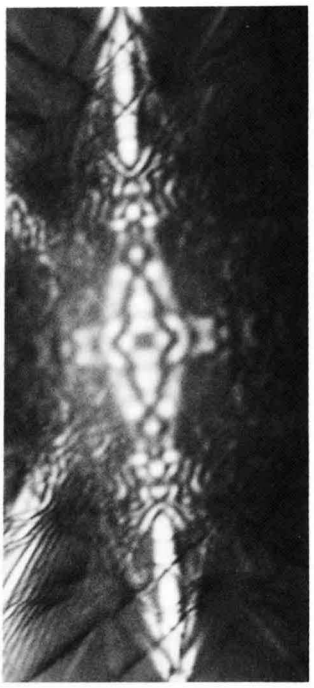

002

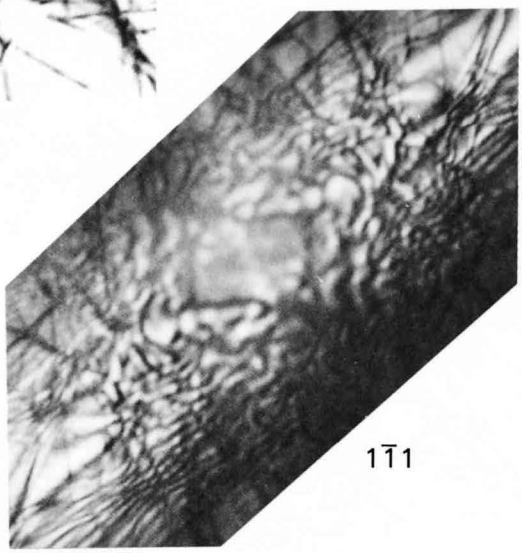

$1\bar{1}1$

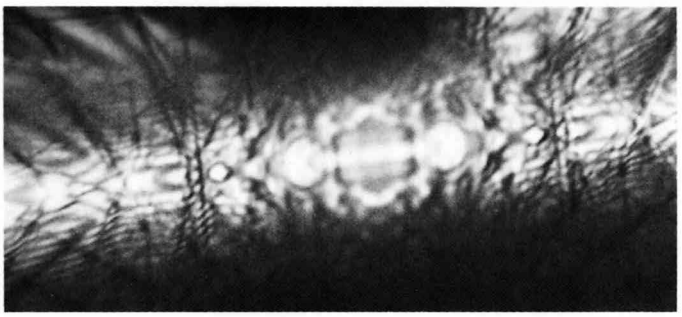

$2\bar{2}0$

Si [110]

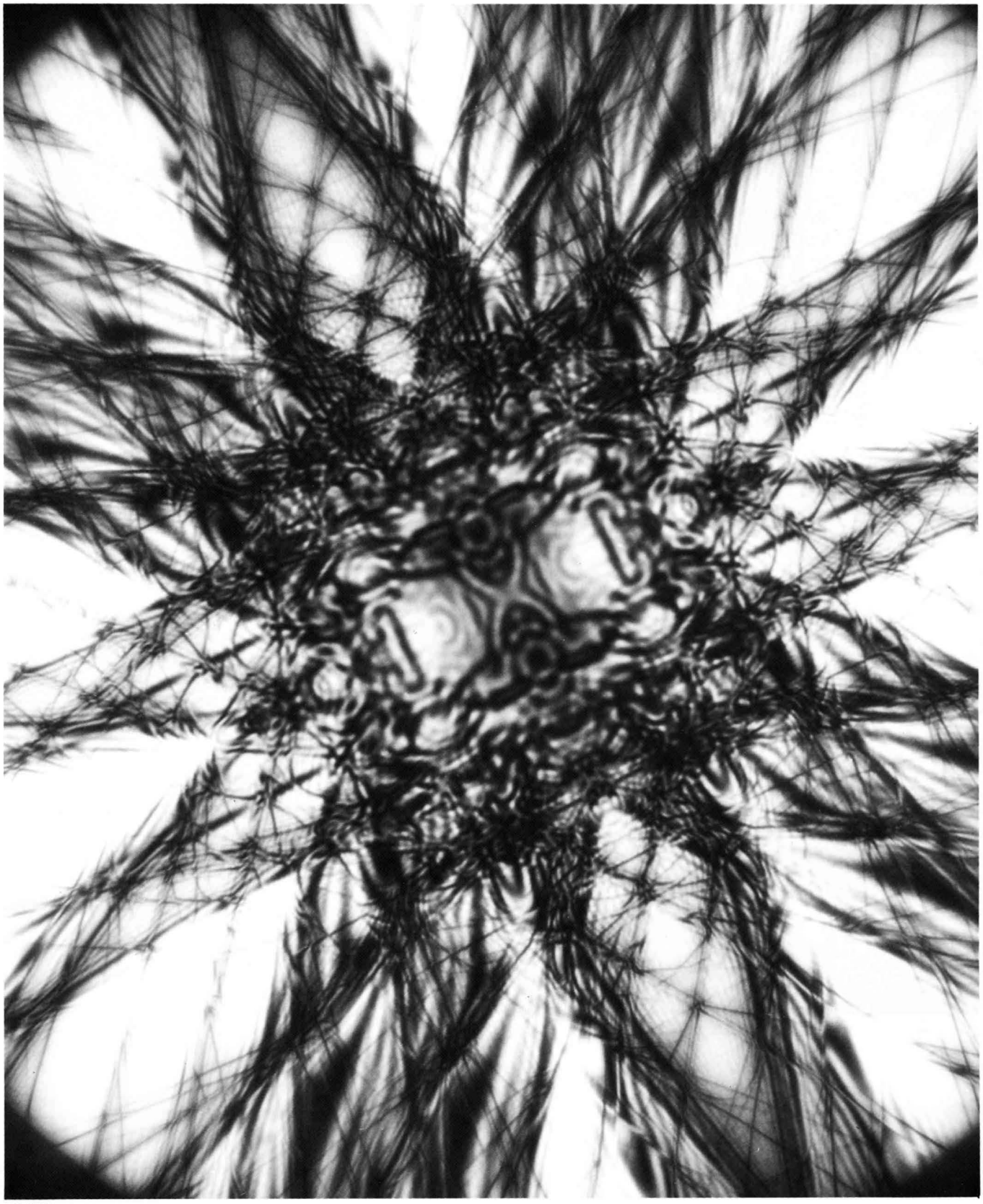

000

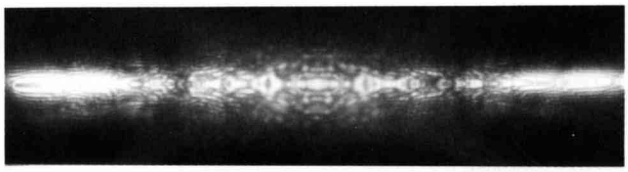

004

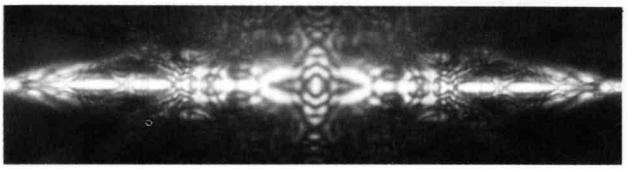

002

000

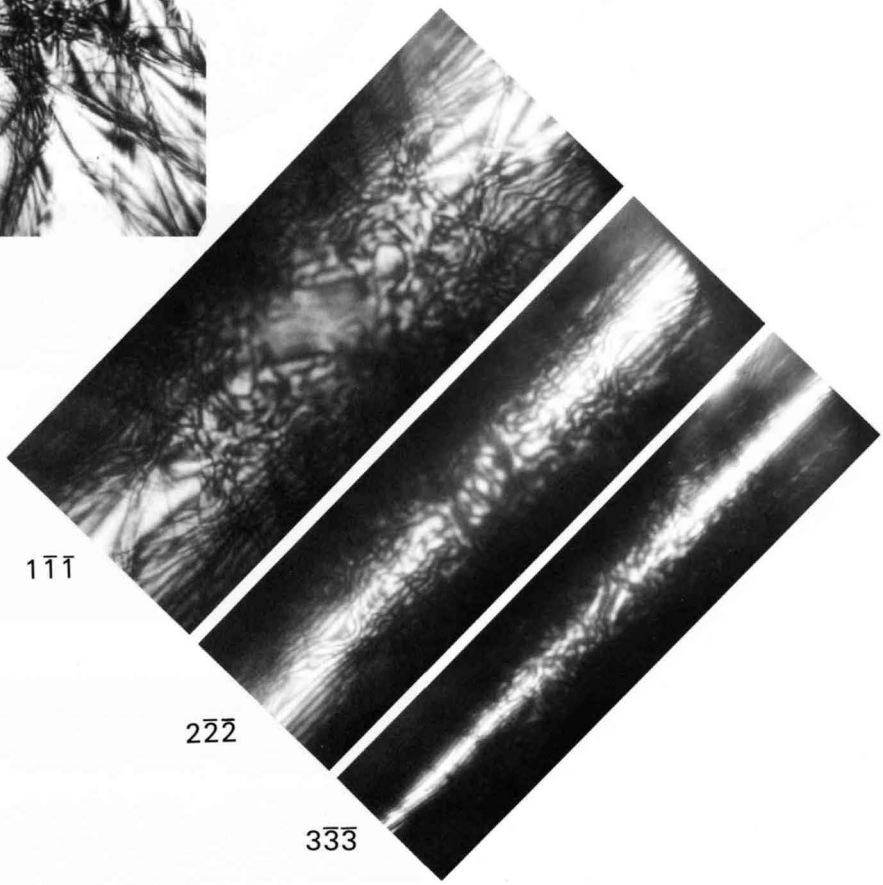

$1\bar{1}\bar{1}$

$2\bar{2}\bar{2}$

$3\bar{3}\bar{3}$

Si [100]

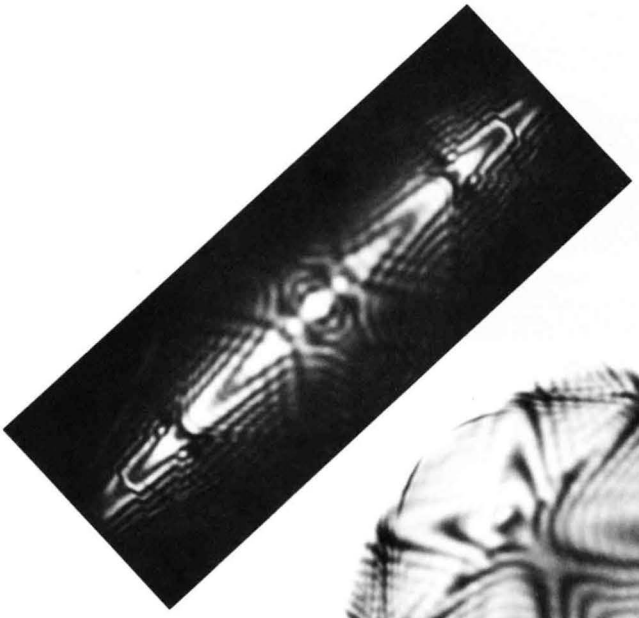

004

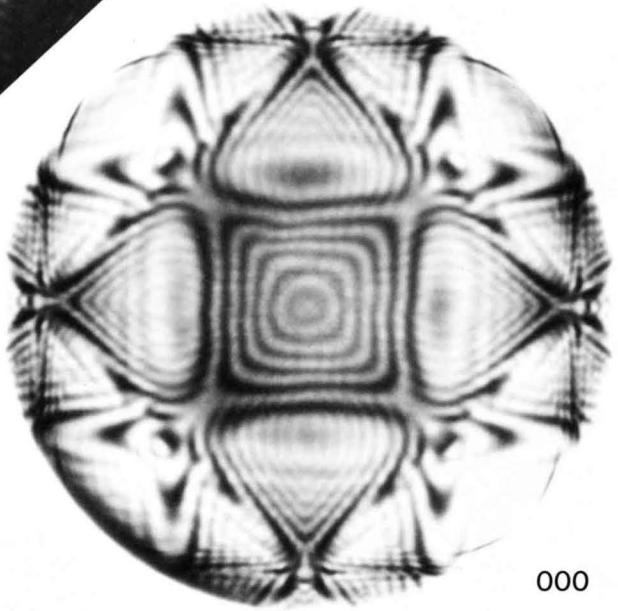

000

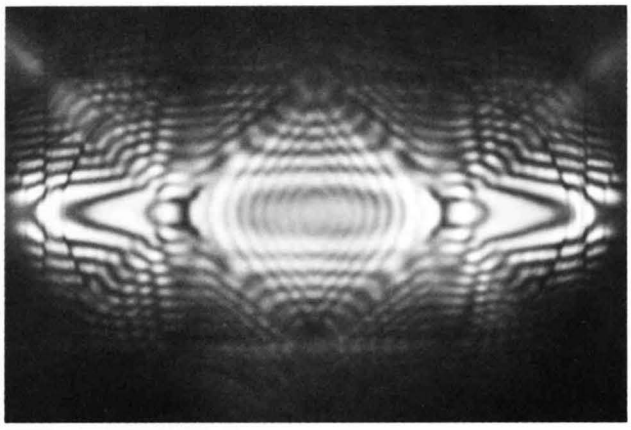

$02\bar{2}$

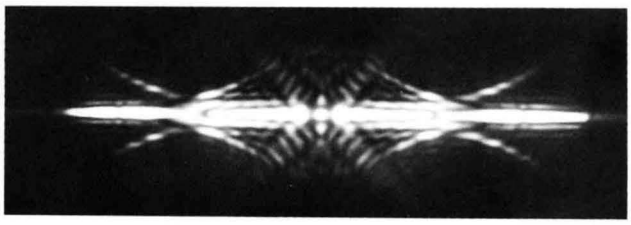

$04\bar{4}$

Si [100] BR method

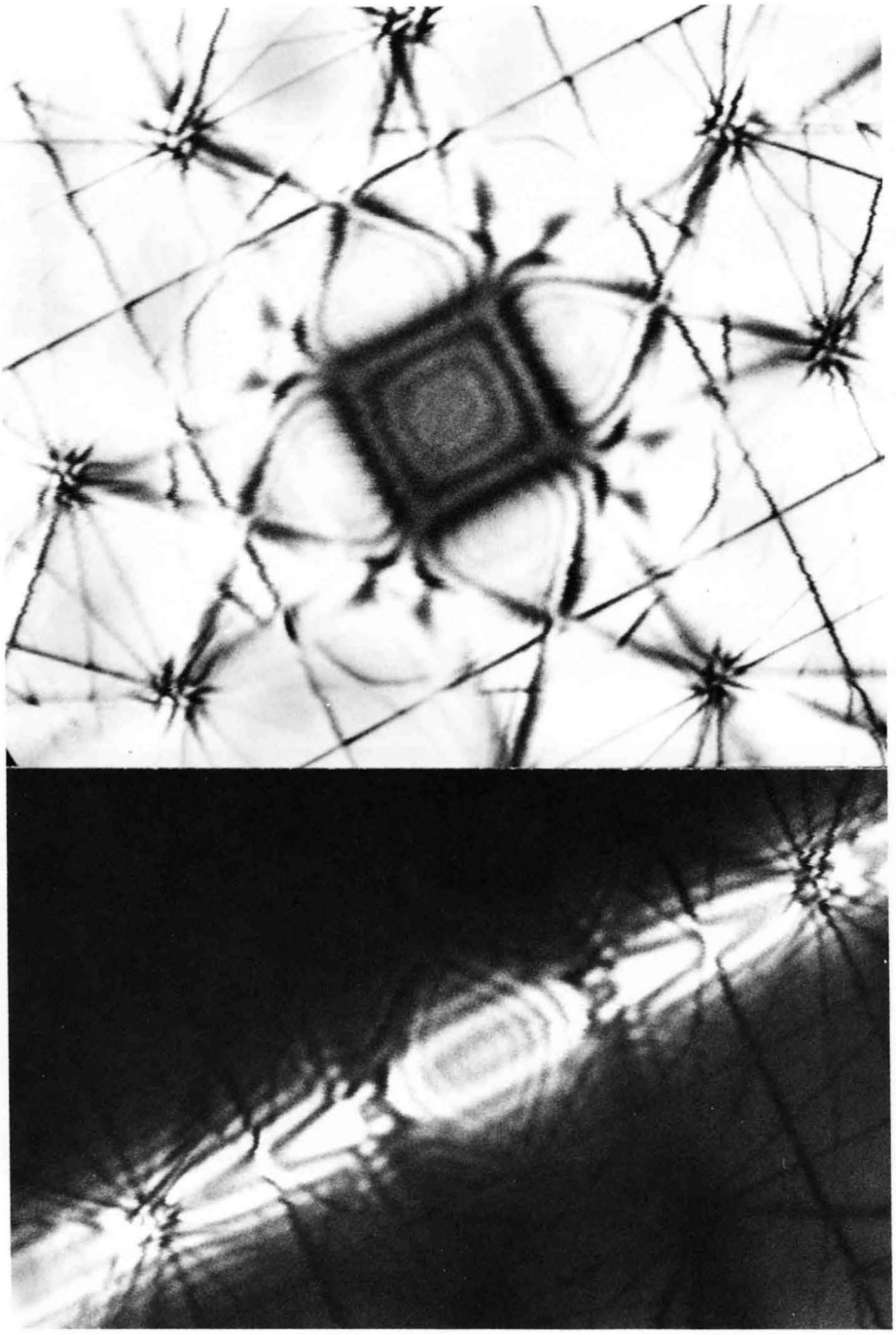

Ge [111] $F4_1/d\bar{3}2/m$

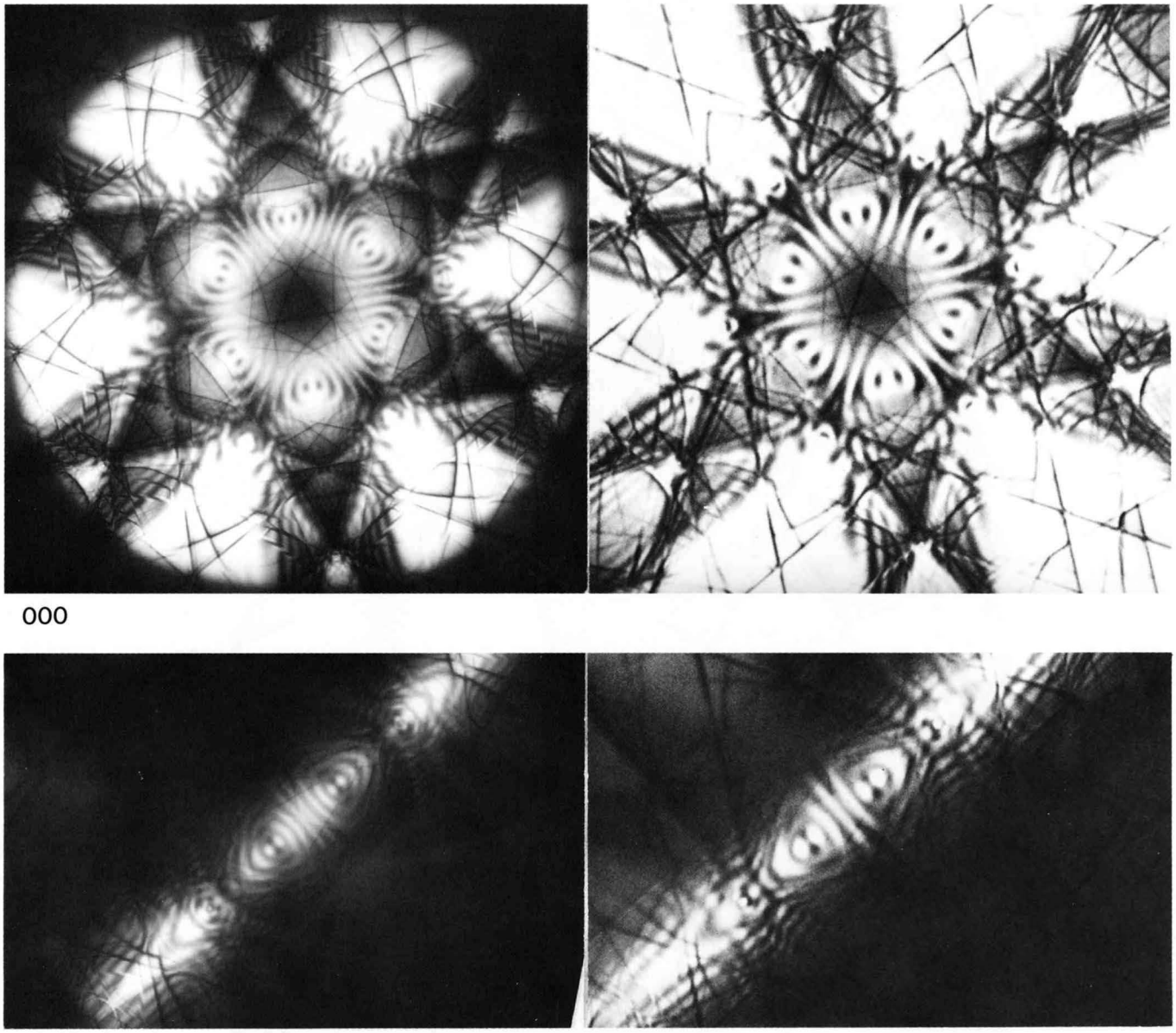

000

$2\bar{2}0$ CTEM BR method

Ge [100]

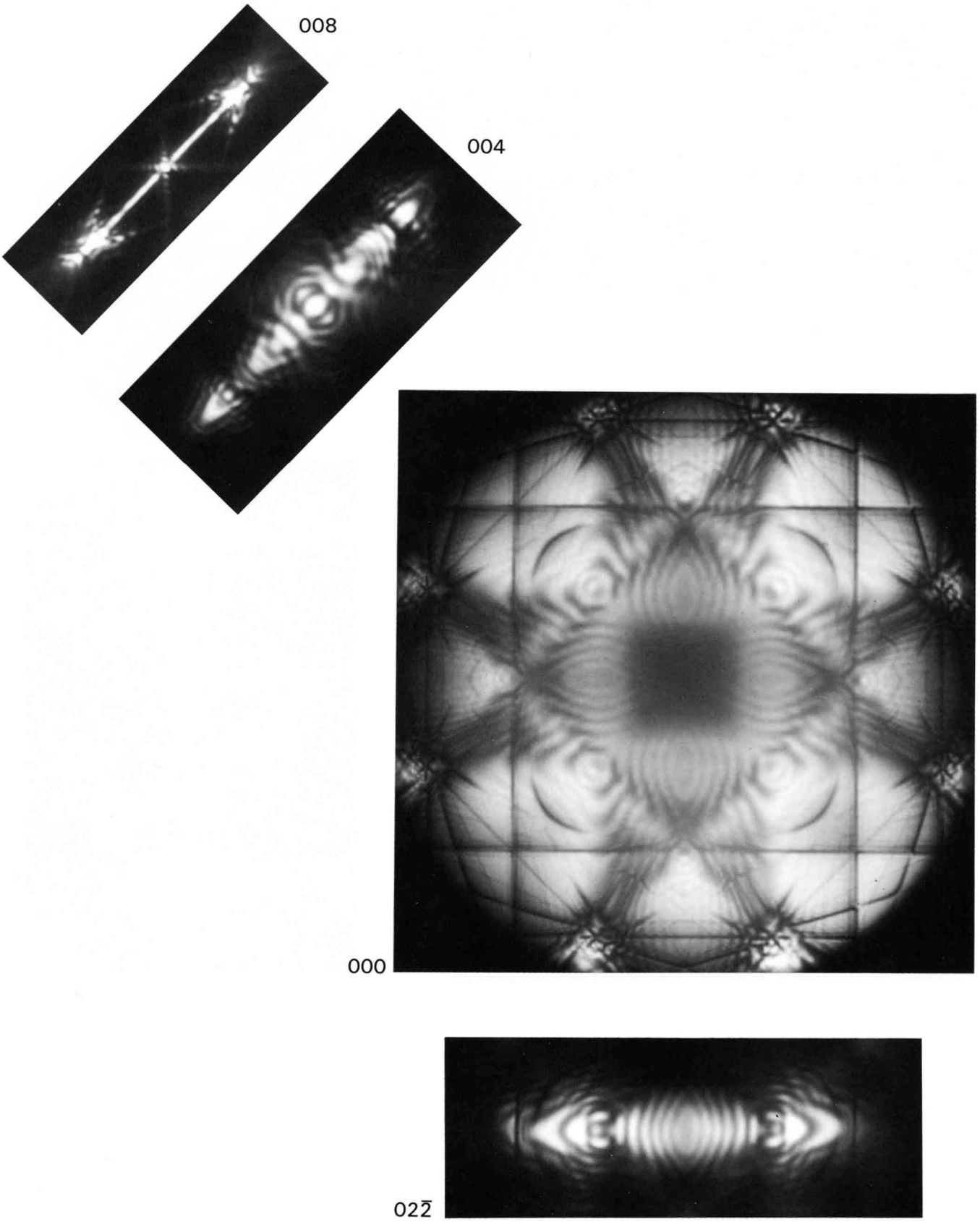

Ge [110]

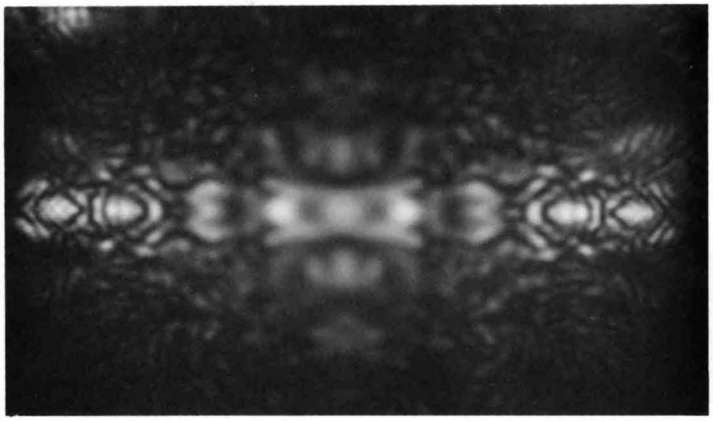

002

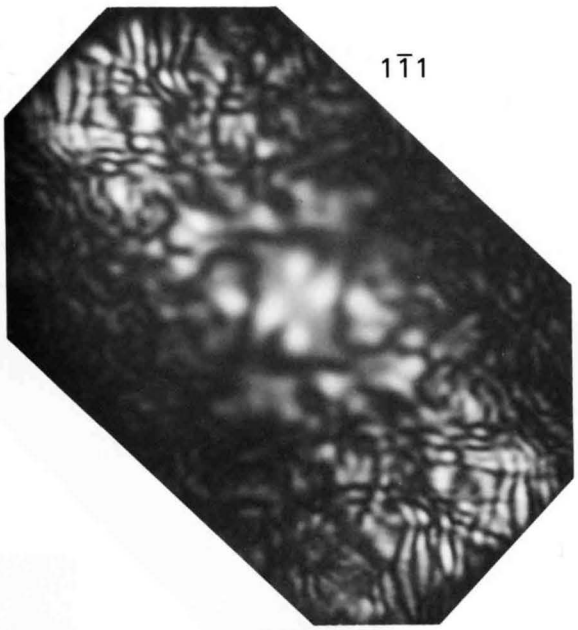

$1\bar{1}1$

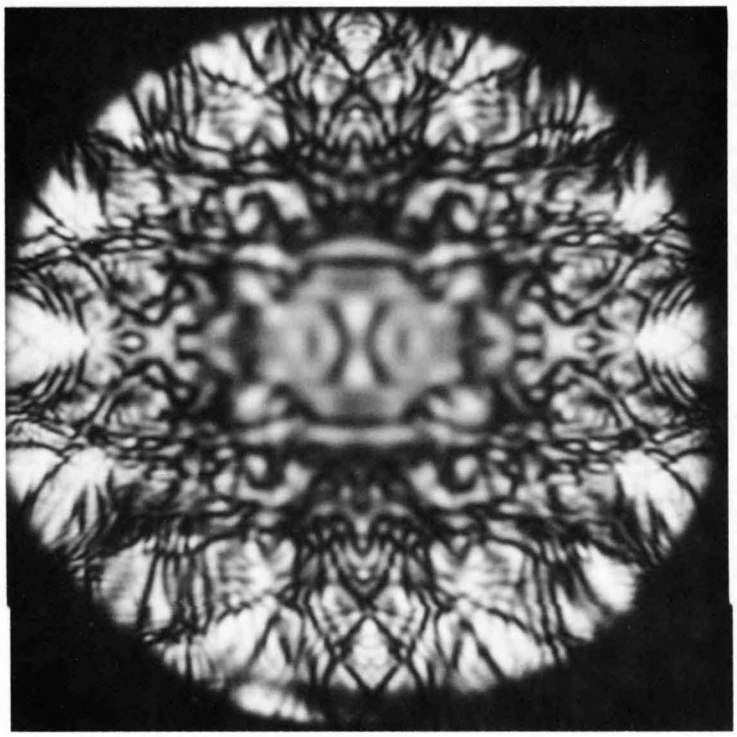

000

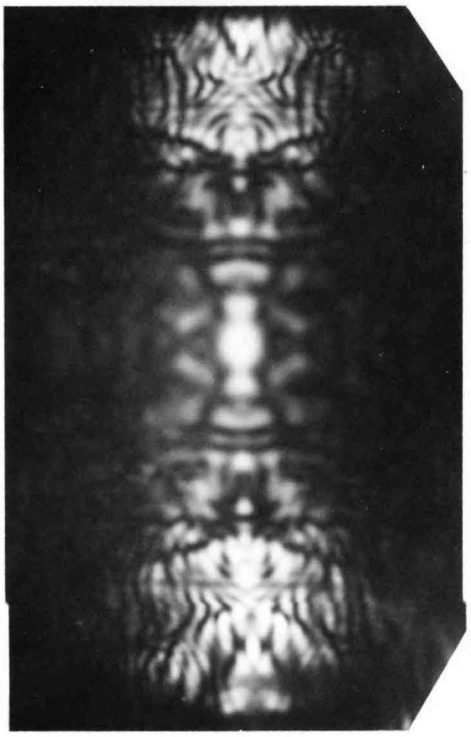

$2\bar{2}0$

Ge [110] BR method

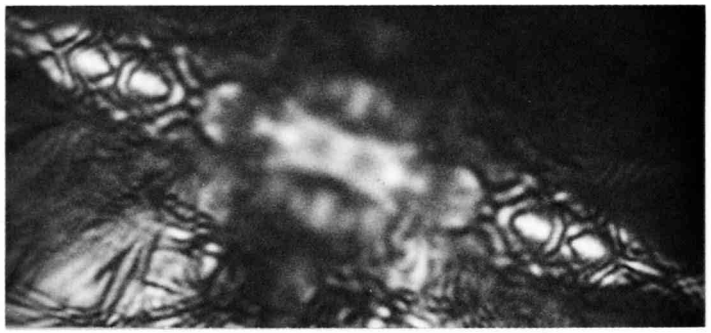

002

000

$2\bar{2}0$

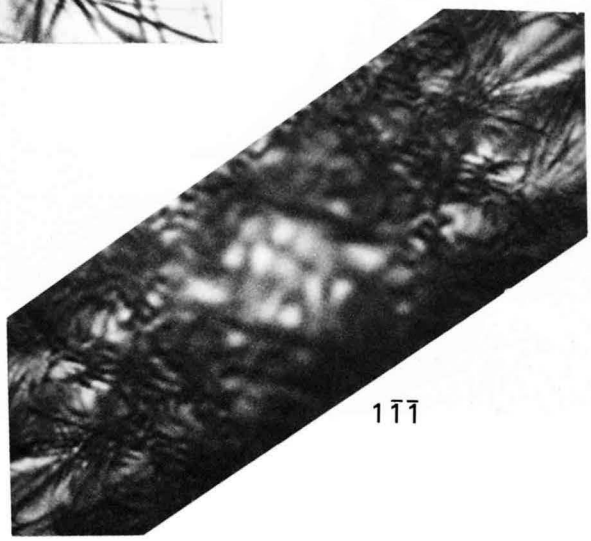

$1\bar{1}\bar{1}$

Signal Processing, BR method

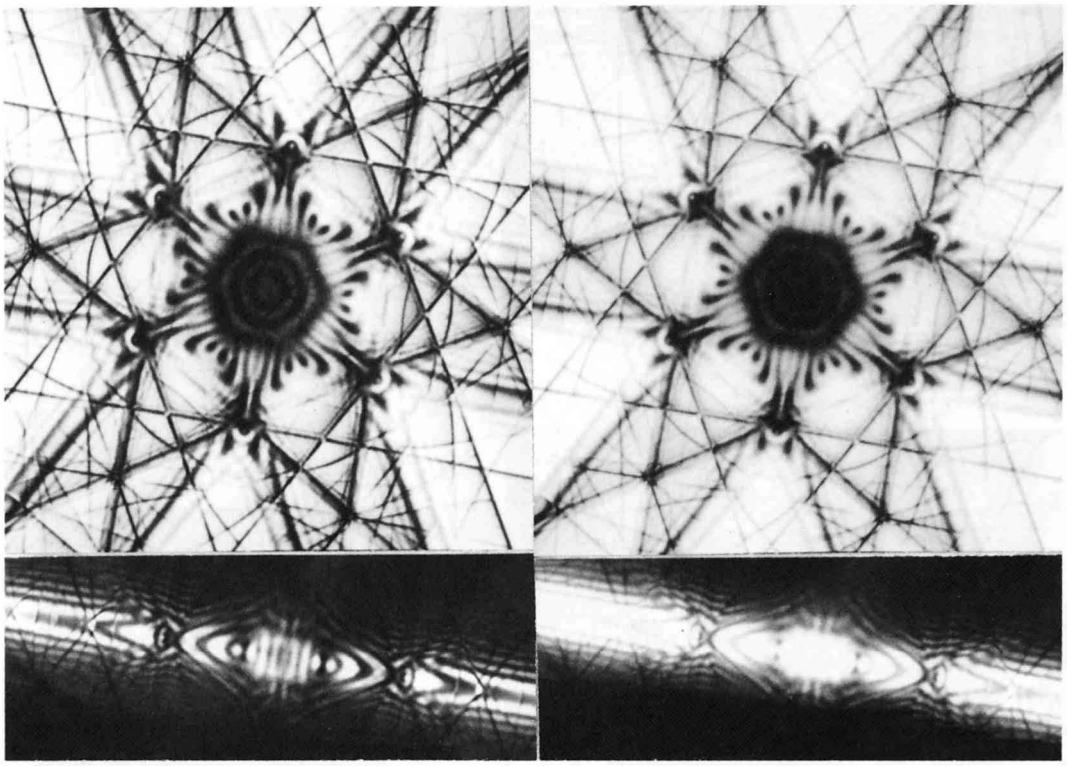

Si [111]

000

$2\bar{2}0$

With signal processing. Without signal processing.

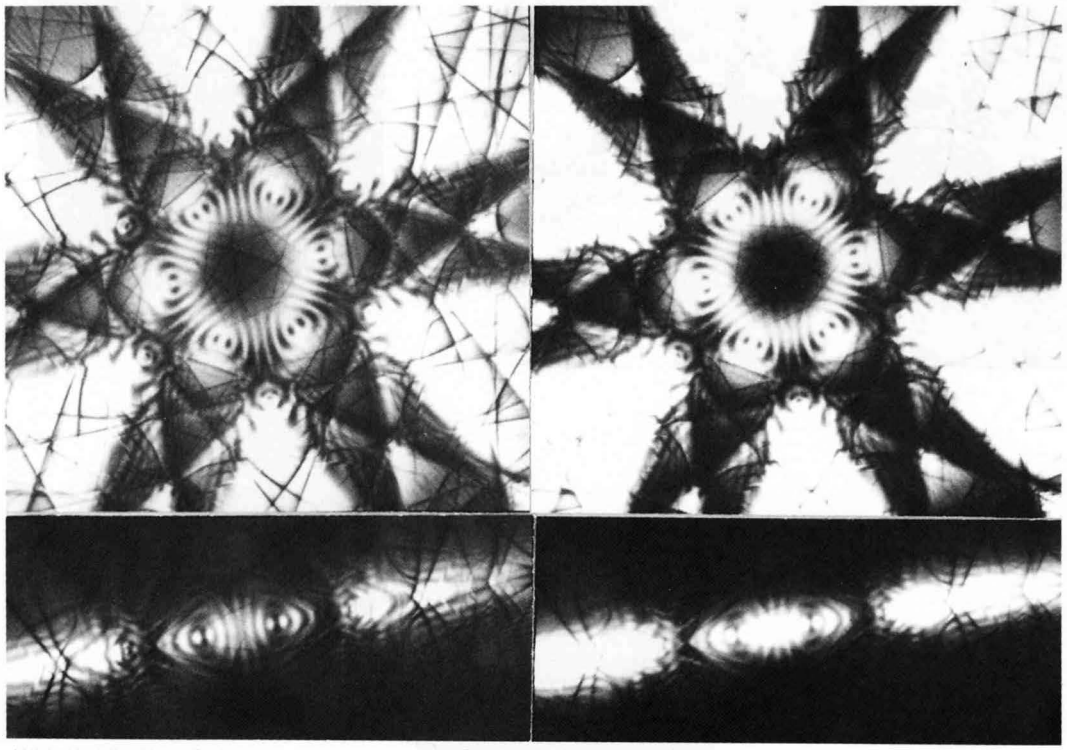

Ge [111]

000

$2\bar{2}0$

With signal processing. Without signal processing.

MnSi [111] $P2_13$ 80kV

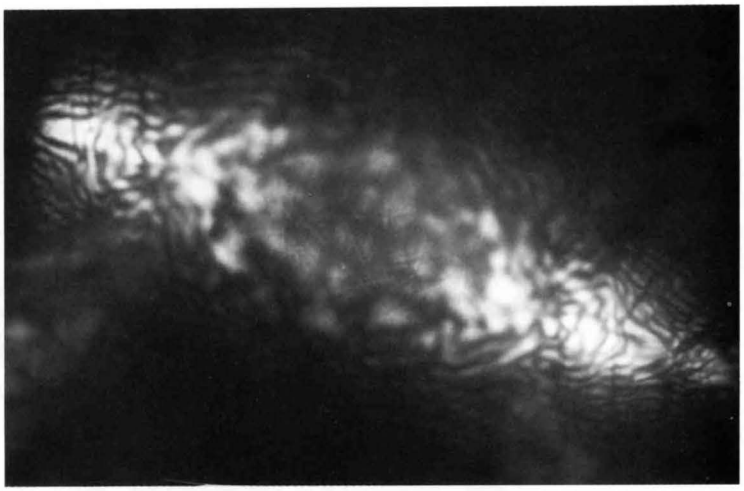

$\bar{1}\bar{1}2$

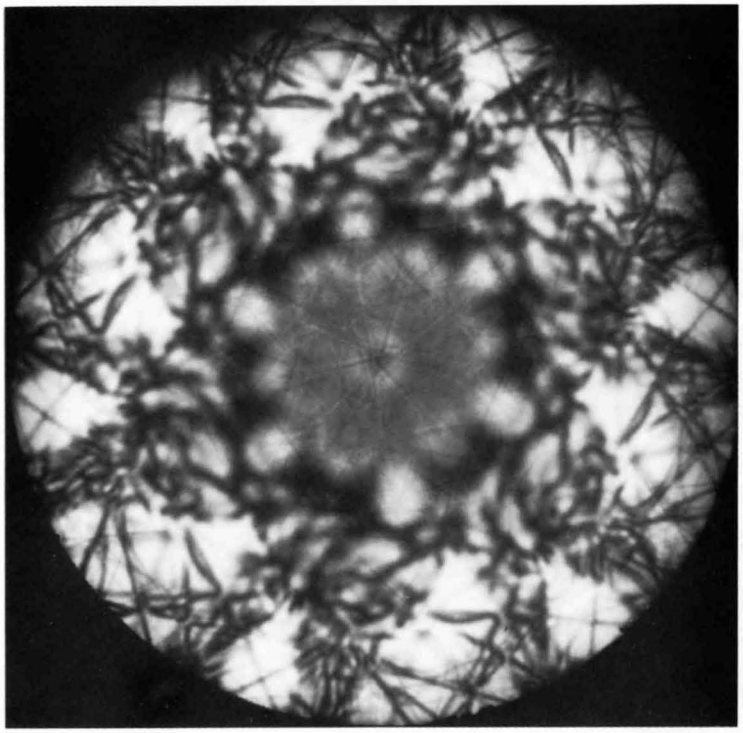

000

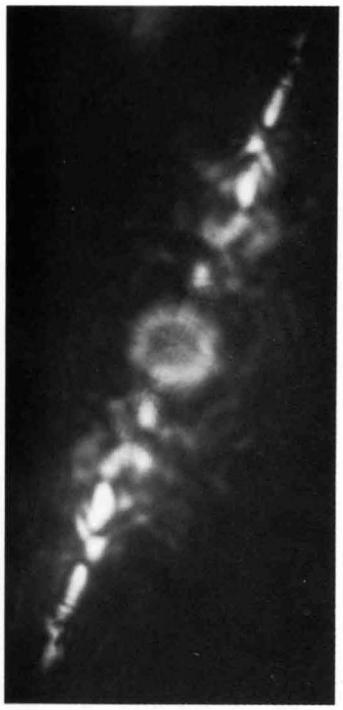

$2\bar{2}0$

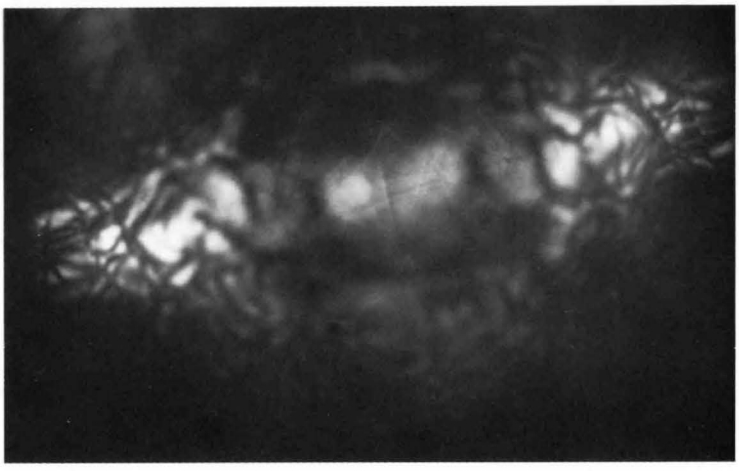

$10\bar{1}$

MnSi [110]

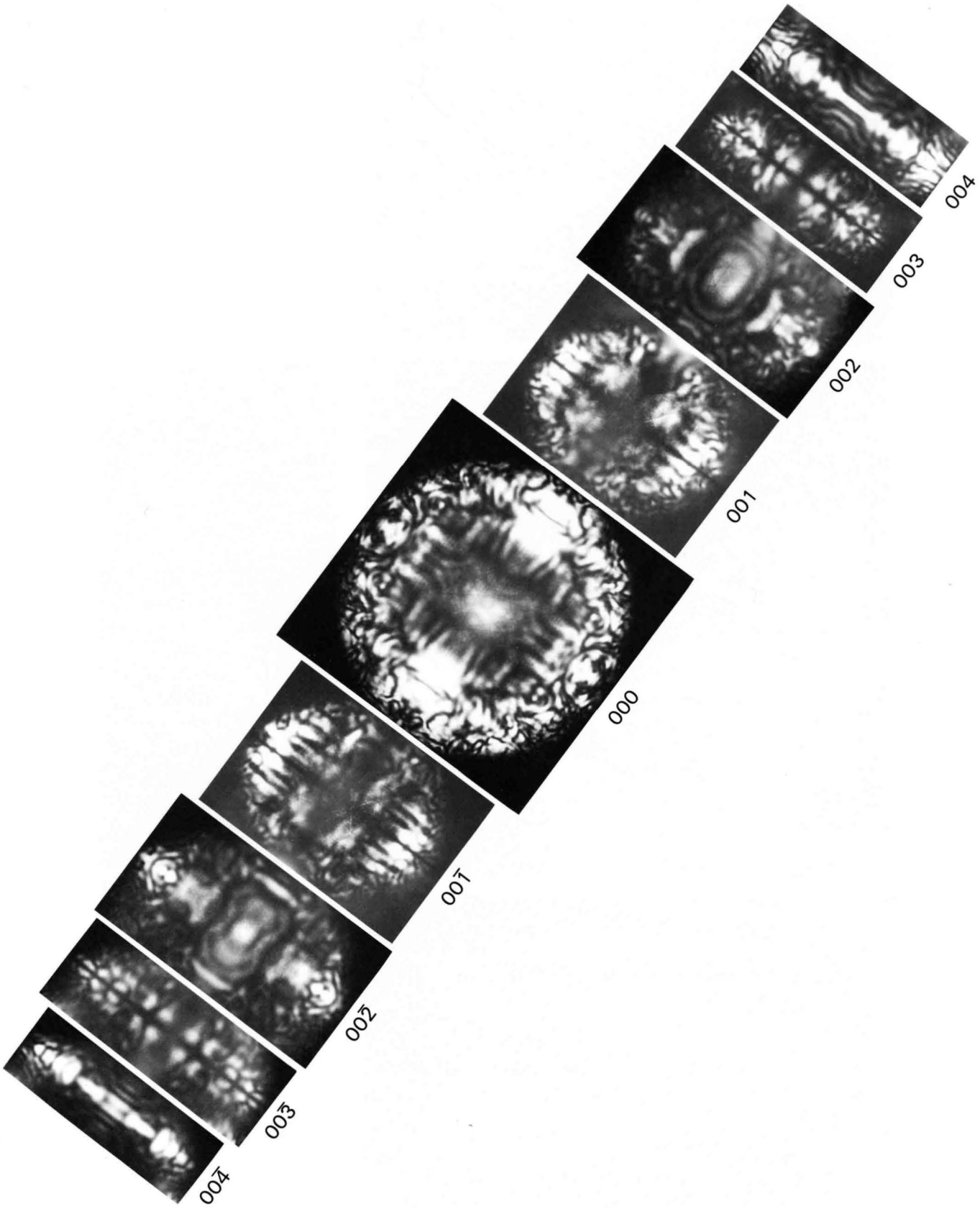

MnSi [100] 80kV

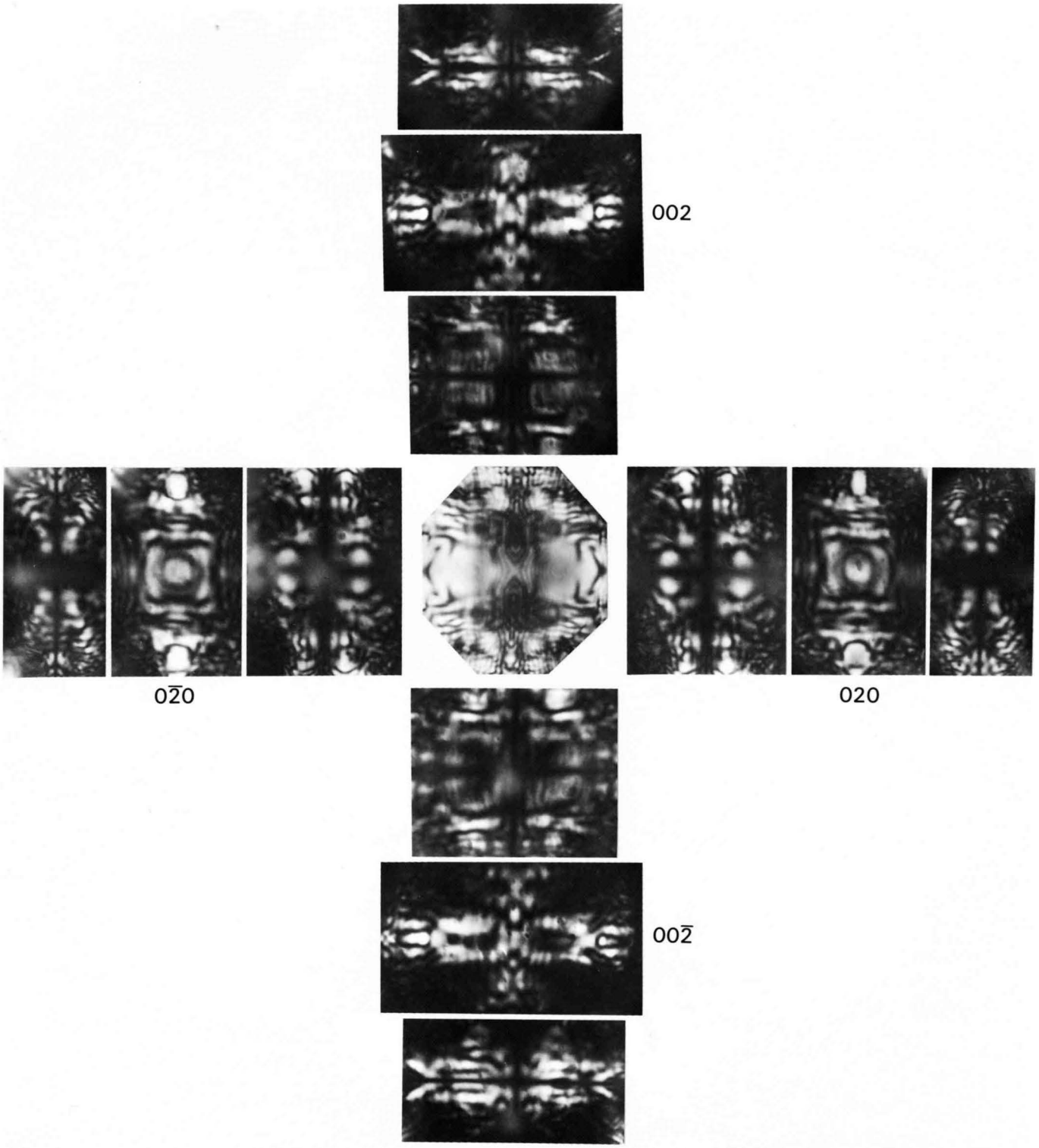

$MgAl_2O_4$ [100] $F4_1/d\bar{3}2/m$

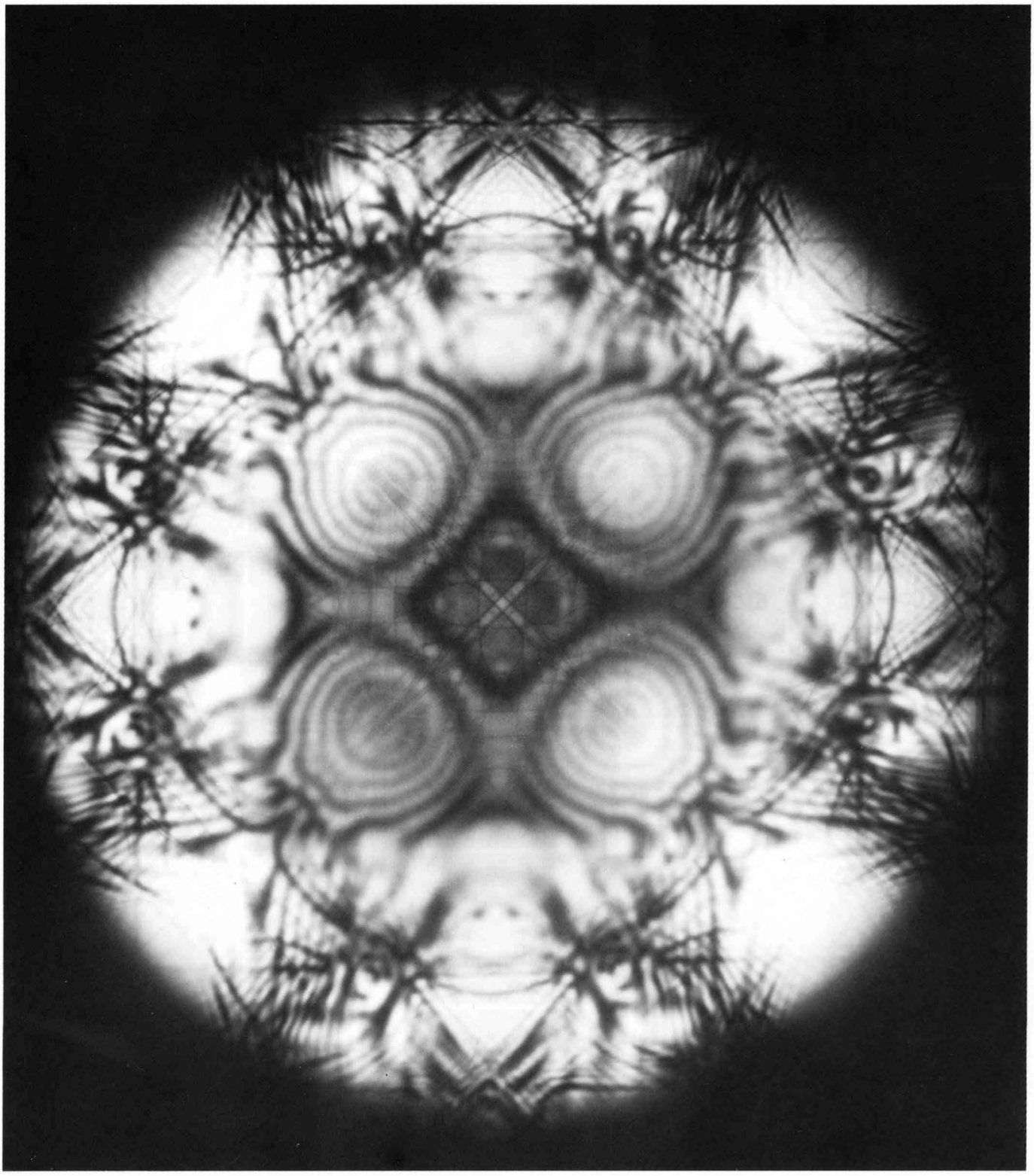

000

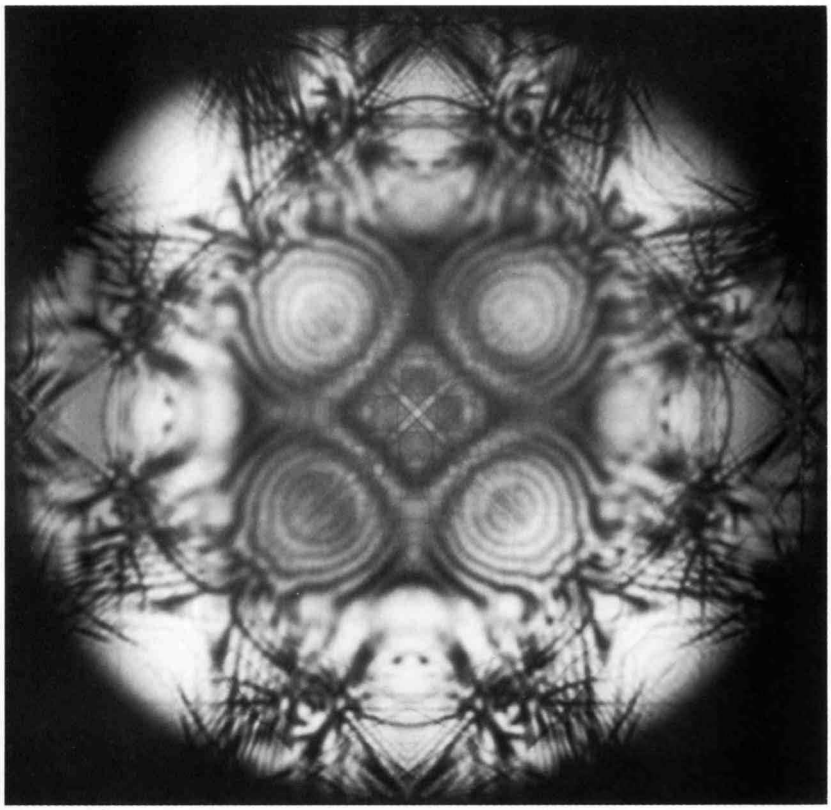

000

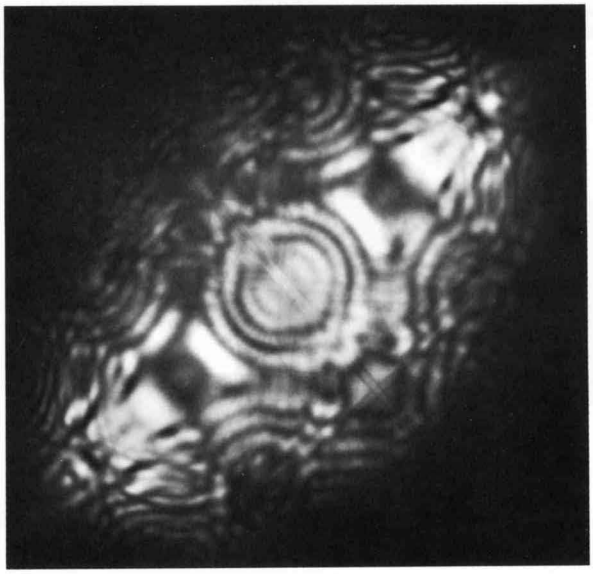

040

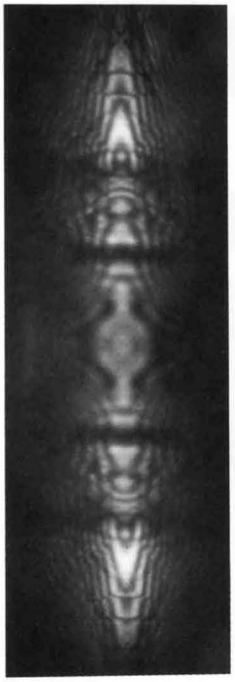

$02\bar{2}$

GaAs [110] $F\bar{4}3m$

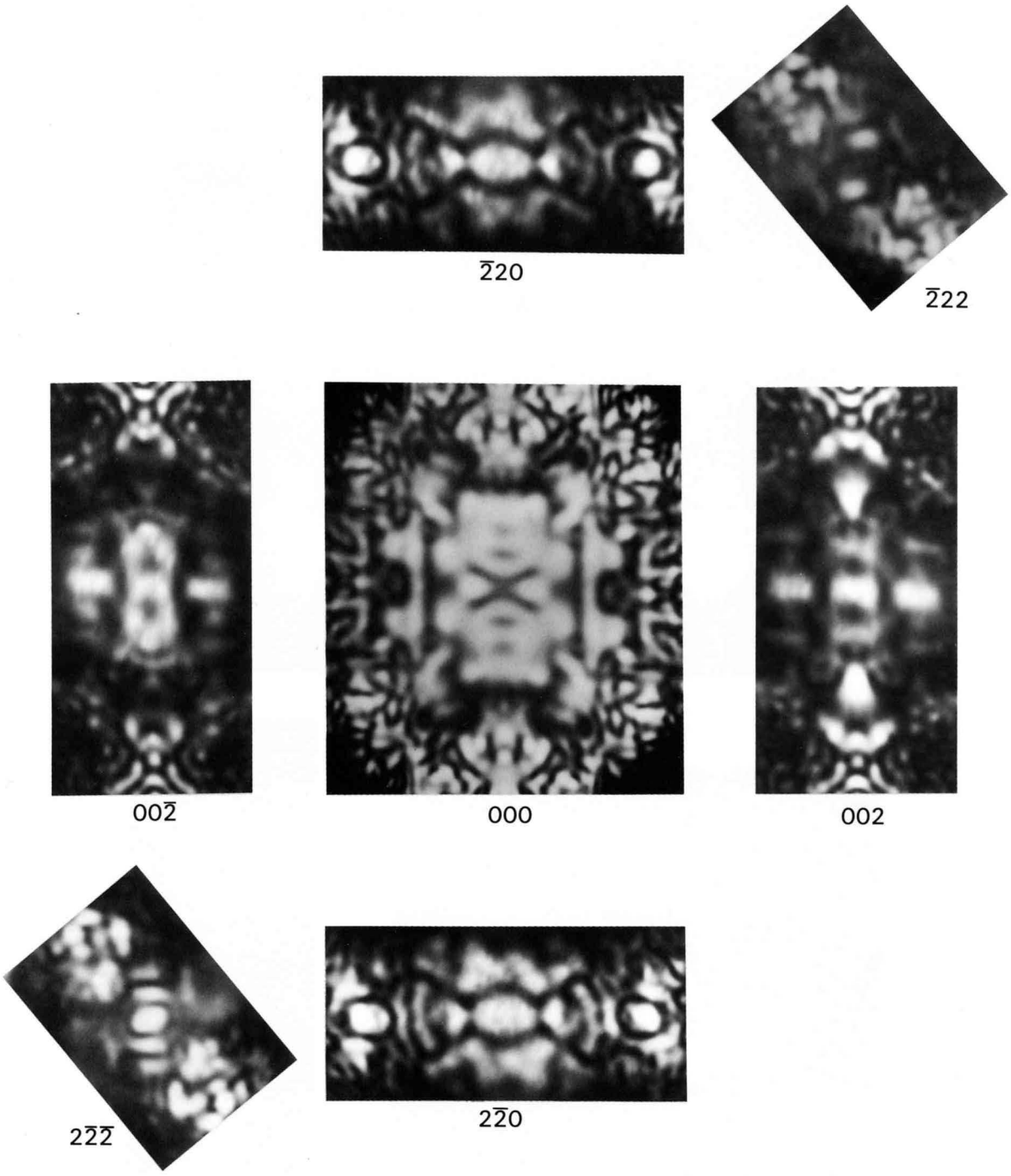

FeS_2 [100] $P2_1/a\bar{3}$

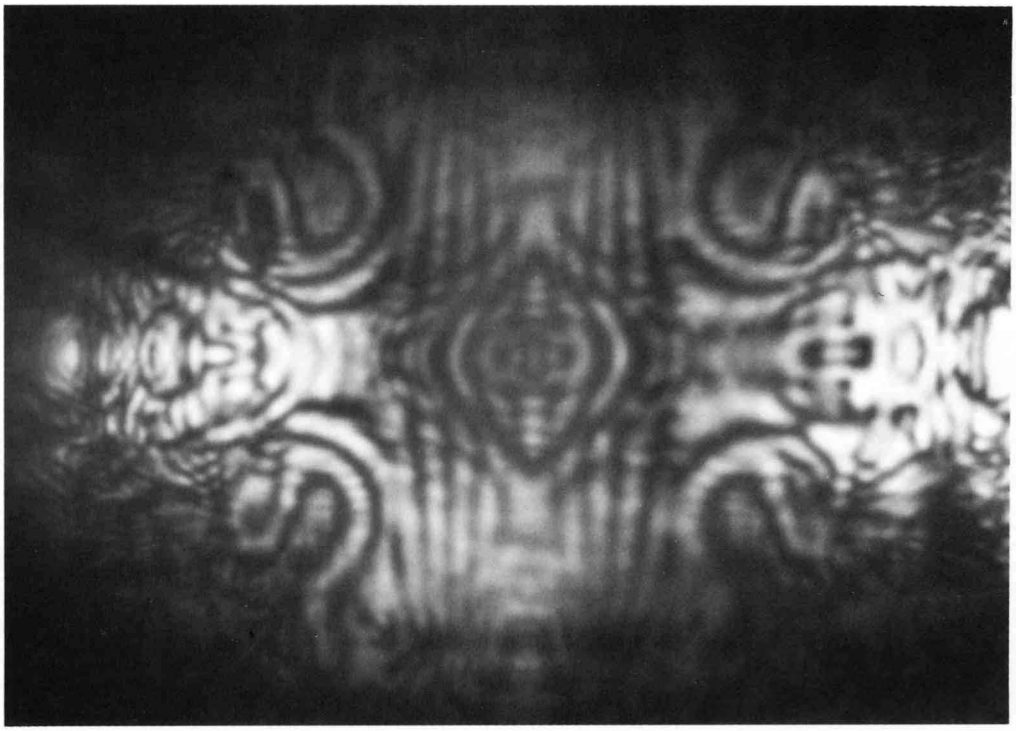

000

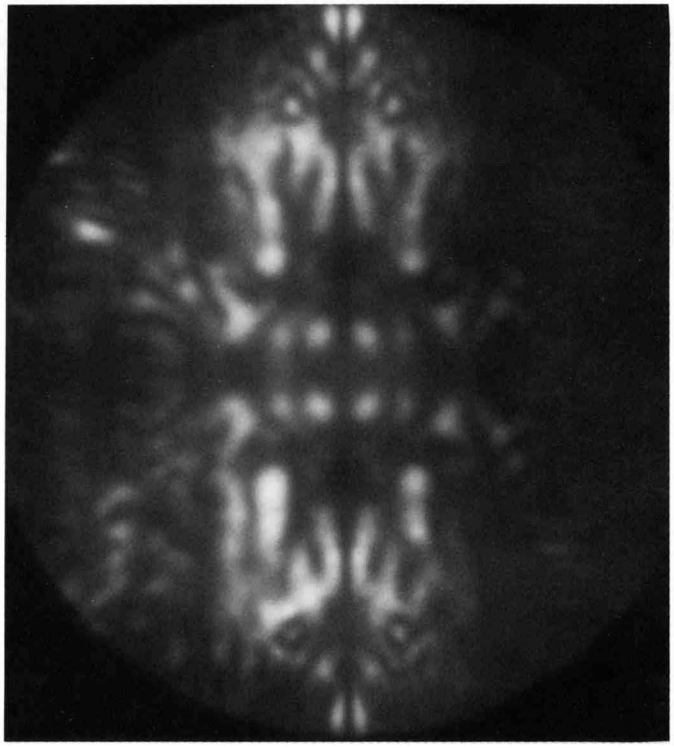

001

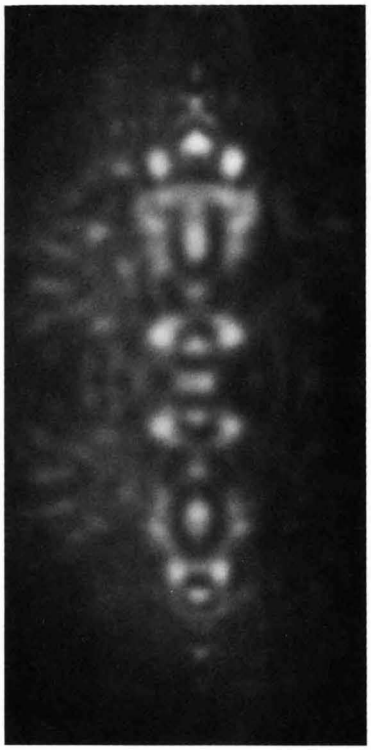

002

6H-SiC [0001] $P6_3mc$

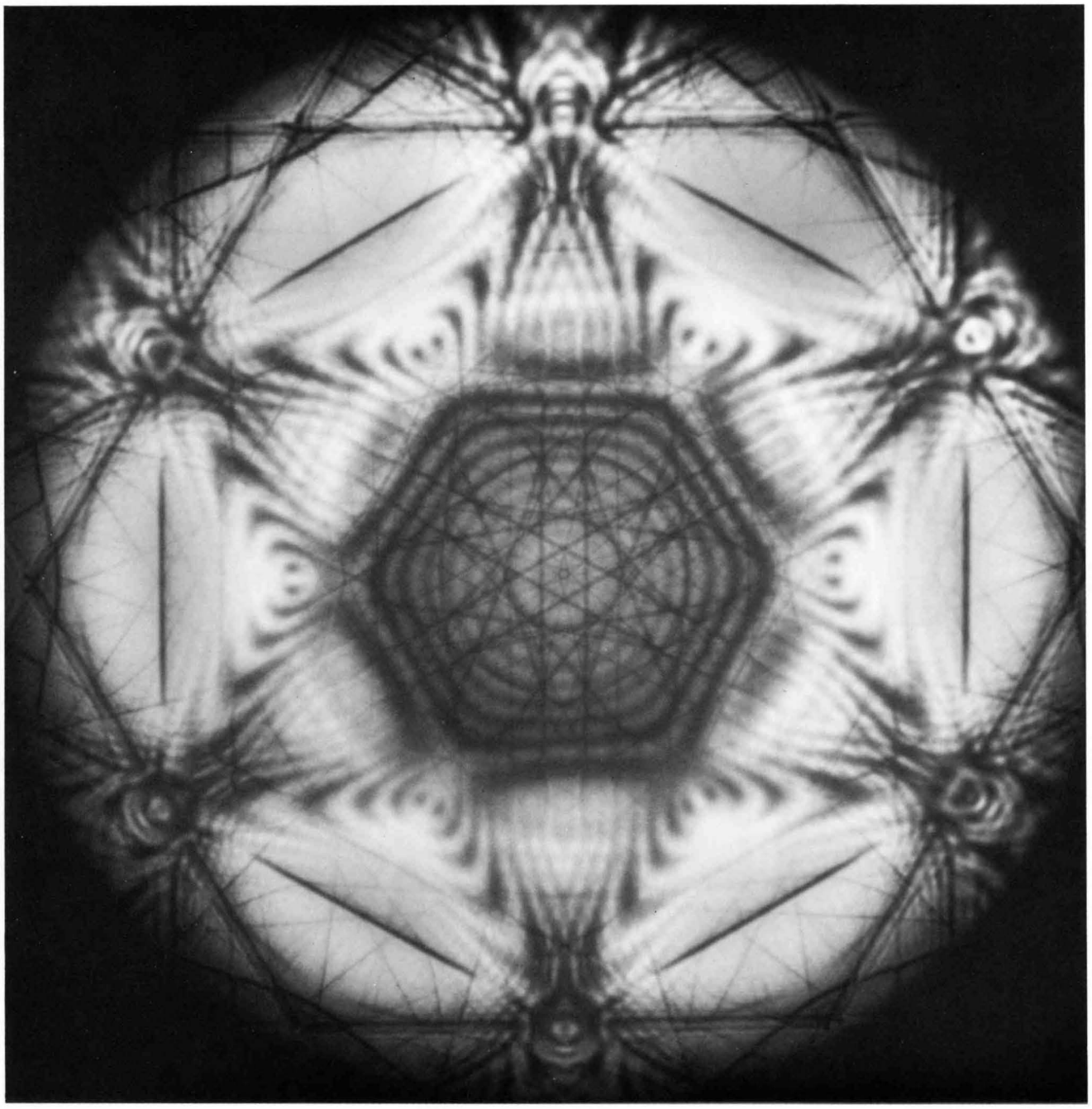

000

CdS $[\bar{2}110]$ $P6_3mc$ **80kV**

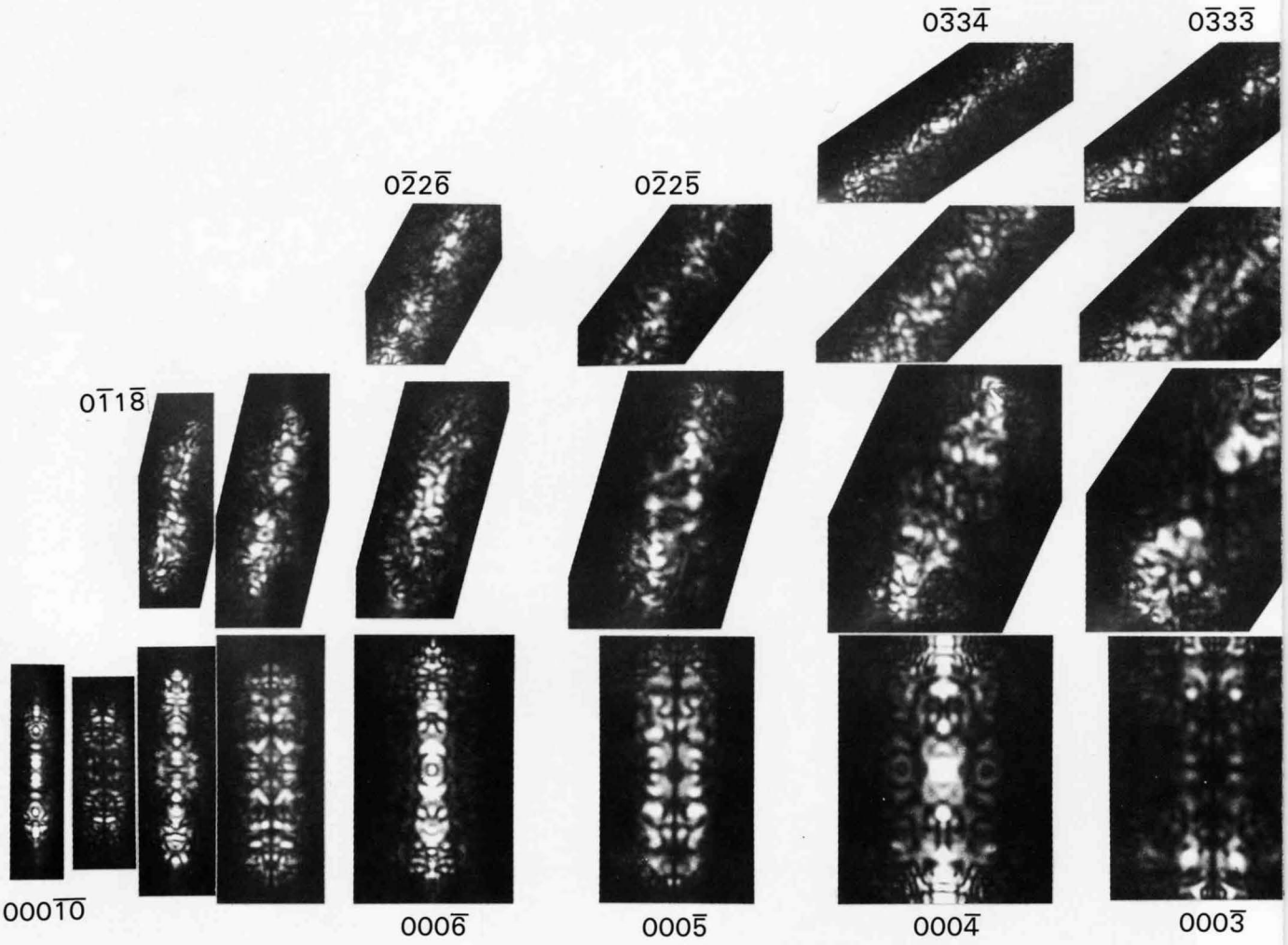

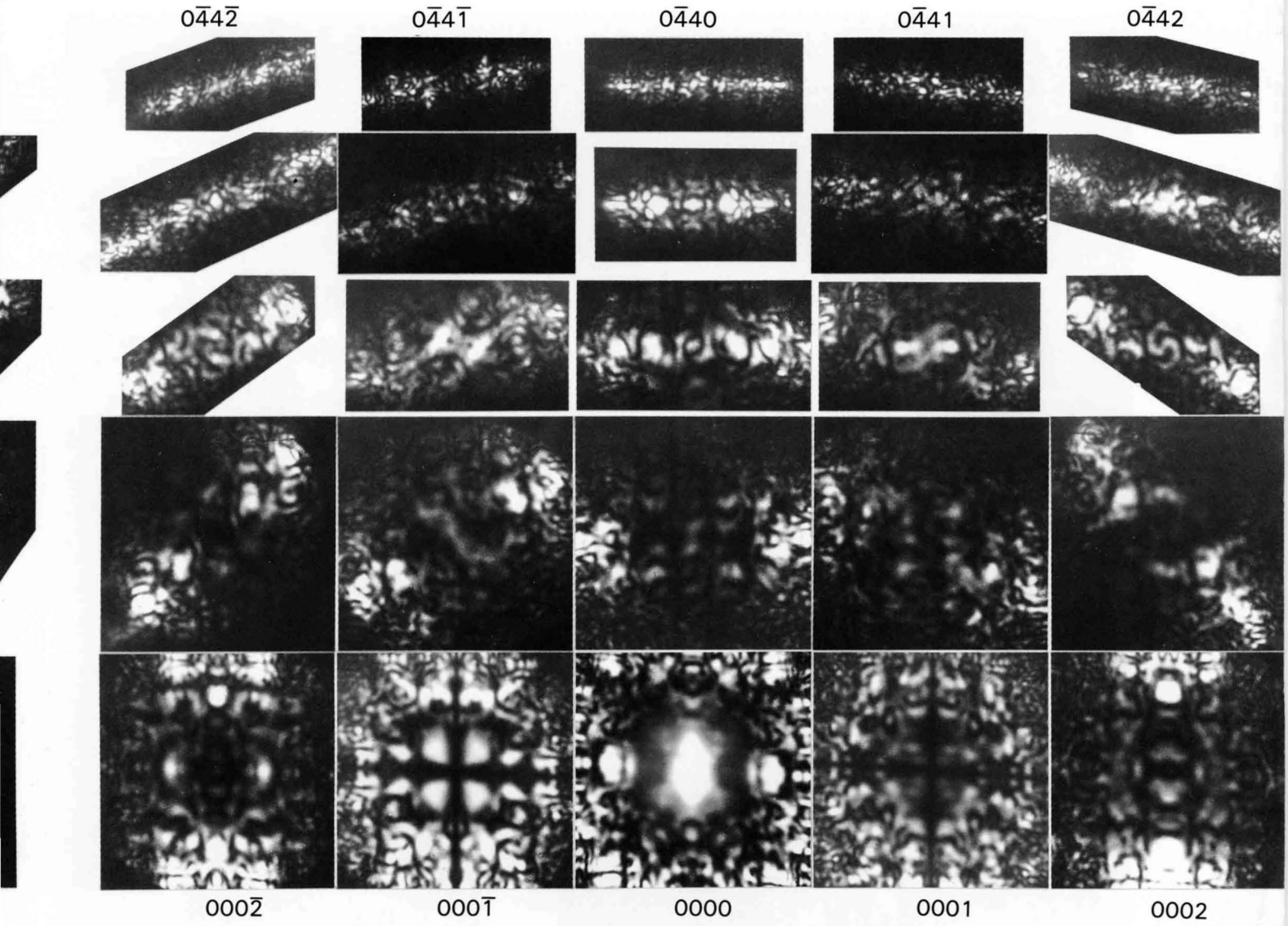
0$\bar{4}4\bar{2}$
0$\bar{4}4\bar{1}$
0$\bar{4}40$
0$\bar{4}41$
0$\bar{4}42$
000$\bar{2}$
000$\bar{1}$
0000
0001
0002

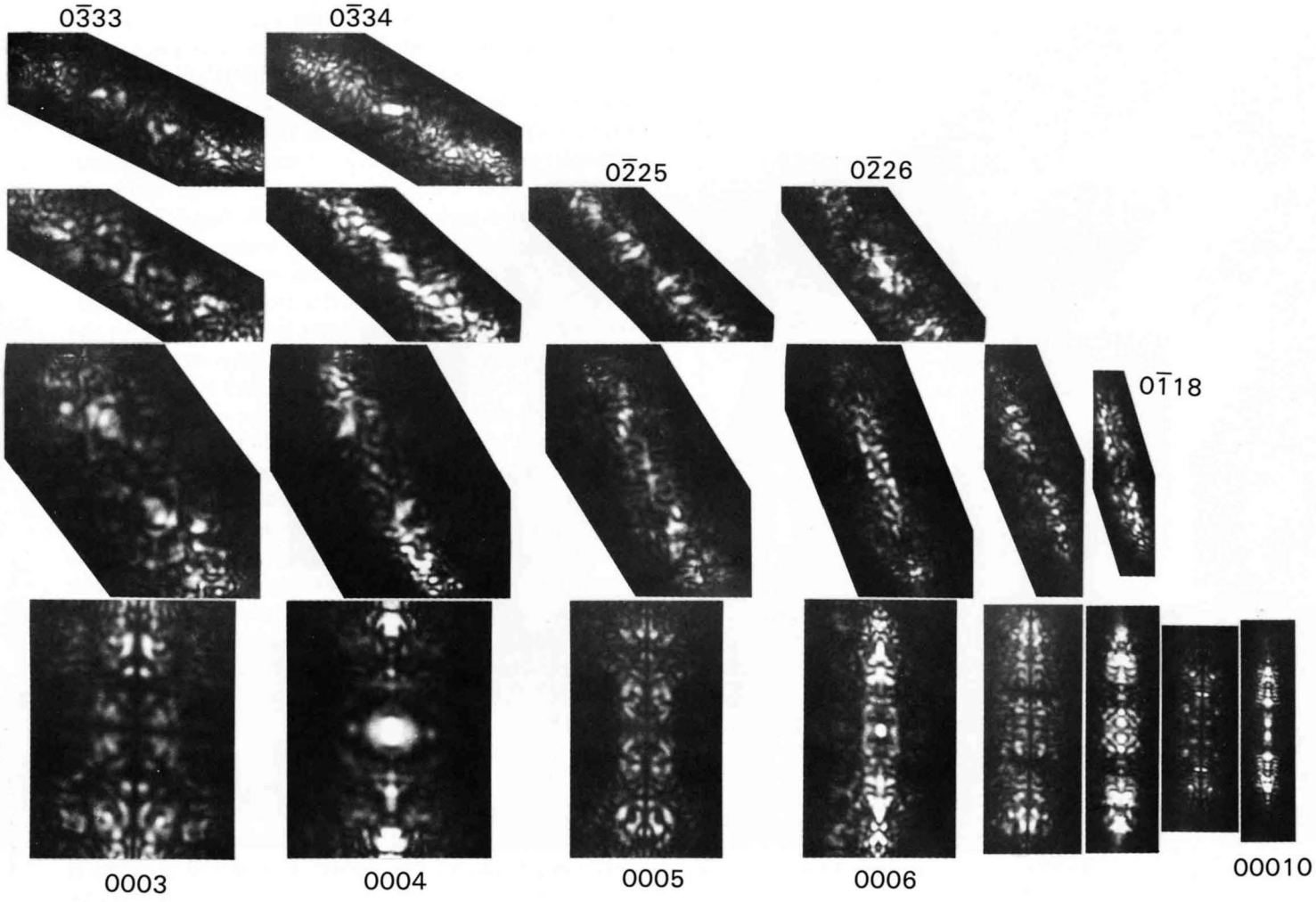
0$\bar{3}$33
0$\bar{3}$34
0$\bar{2}$25
0$\bar{2}$26
0$\bar{1}$18
0003
0004
0005
0006
00010

LACBED Patterns II

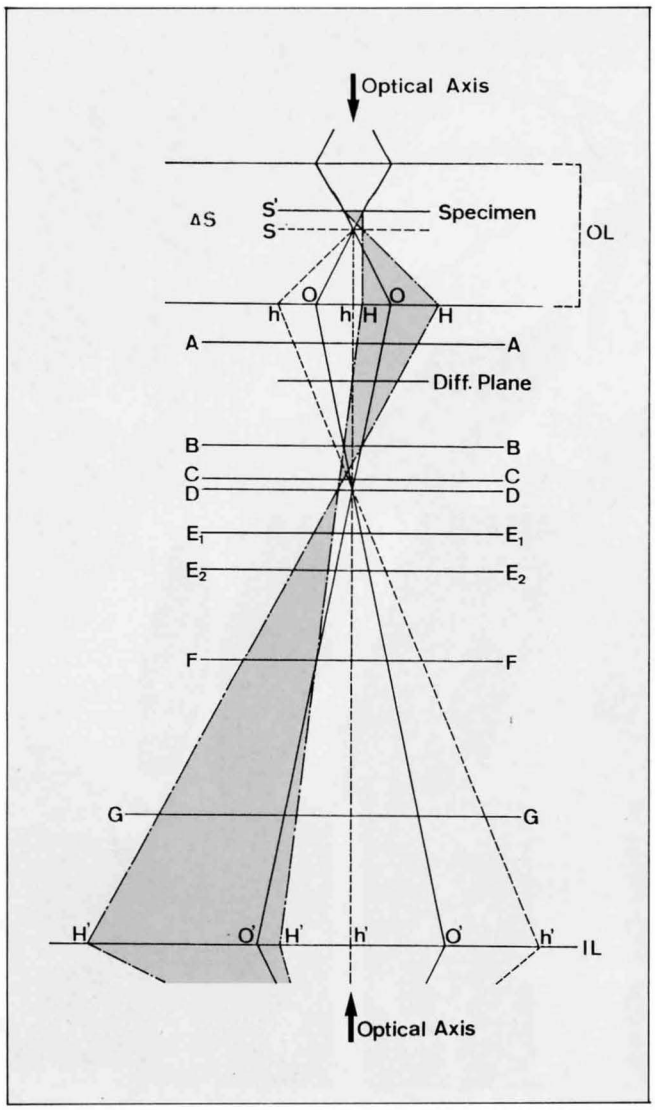

LACBED by CTEM

Photos (A) to (G) show a series of CBED patterns obtained from a specimen placed at S' with $\Delta S \simeq 30\mu$m, by varying the focus position of the intermediate lens successively from A to G in the ray path. Photo (A) shows the pattern at plane A above the back focal plane (the diffraction plane). The disks are seen overlapped in accordance with the ray paths OO' and HH'. No spherical aberration effect is observed, since this pattern is formed near the diffraction plane. Photo (B) shows the image on plane B, exhibiting the circle of least confusion. Photo (C) shows the image at plane C. Image disks are separated from each other. The inner or first-order image disks are seen compressed radially owing to a spherical aberration effect. A harmful aberration effect due to coma is seen in the outer diffraction disks. Photo (D) shows the image on a plane just below plane D or the Gaussian image plane of the object (specimen) position S. The sense of spherical aberration and coma effects is opposite to that in Photo (C). In these two photos, it is difficult to see the intensity distribution in the disks because of a strong aberration effect and insufficient magnification. As the plane focussed by the intermediate lens is lowered, the details of the intensity distribution become clear as shown in Photo (E_2), although the strong aberration effect is still present. Photo (F) shows the image at plane F lower than the plane in Photo (E_2). Bright- and dark-field LACBED patterns (or images) are simultaneously obtained. The patterns are seen slightly stretched outwards owing to the spherical aberration effect. When the focussed plane is further lowered to plane G, the diffraction disks are overlapped again as shown in Photo (G), in accordance with the ray path.

When a position in the specimen placed at a defocussed plane S' of a convergent beam is defined, the incident-beam angle against the optical axis at the position is determined uniquely. In other words, there is one-to-one correspondence between the position in the specimen and incident-beam angle. Hence, both the microscopic image and the diffraction pattern obtained from a parallel-sided specimen area without bending give the same pattern. That is, the intensity change with the incident-beam angle in the diffraction pattern corresponds to that with the specimen position in the microscopic image. It should be noted that the image is subjected to a severe spherical aberration effect, and requires a high magnification for revealing the intensity distribution because the illuminated specimen area is very small ($\lesssim 10$ nm). The role of the specimen position and incident-beam angle are interchanged continuously between the image and the diffraction pattern. Therefore, when we examine a parallel-sided specimen area without bending and can ignore the spherical aberration effect, we can utilize the defocussed images formed at plane F for the symmetry determination of crystals.

Si [111] 80kV

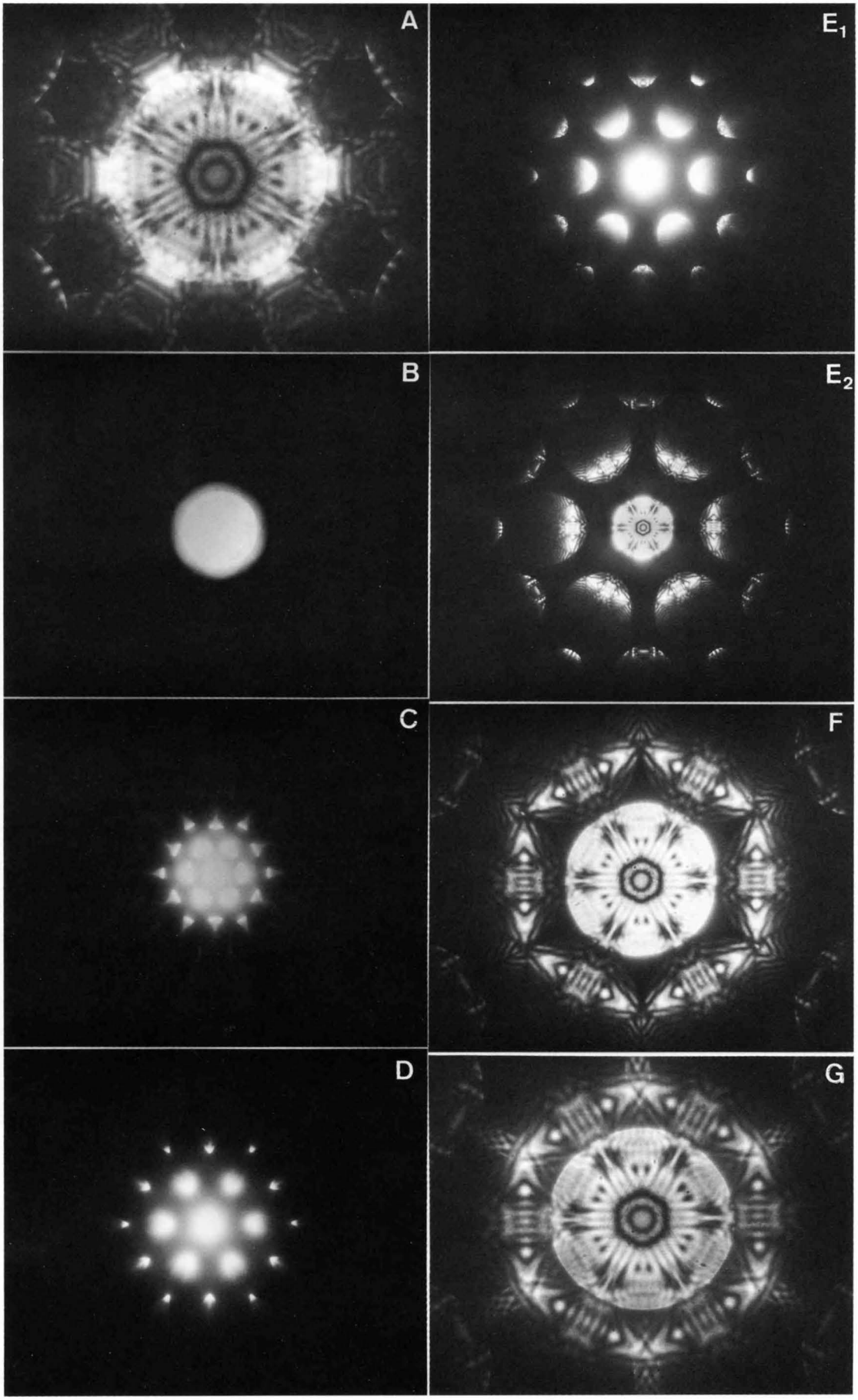

Si [111] 60kV

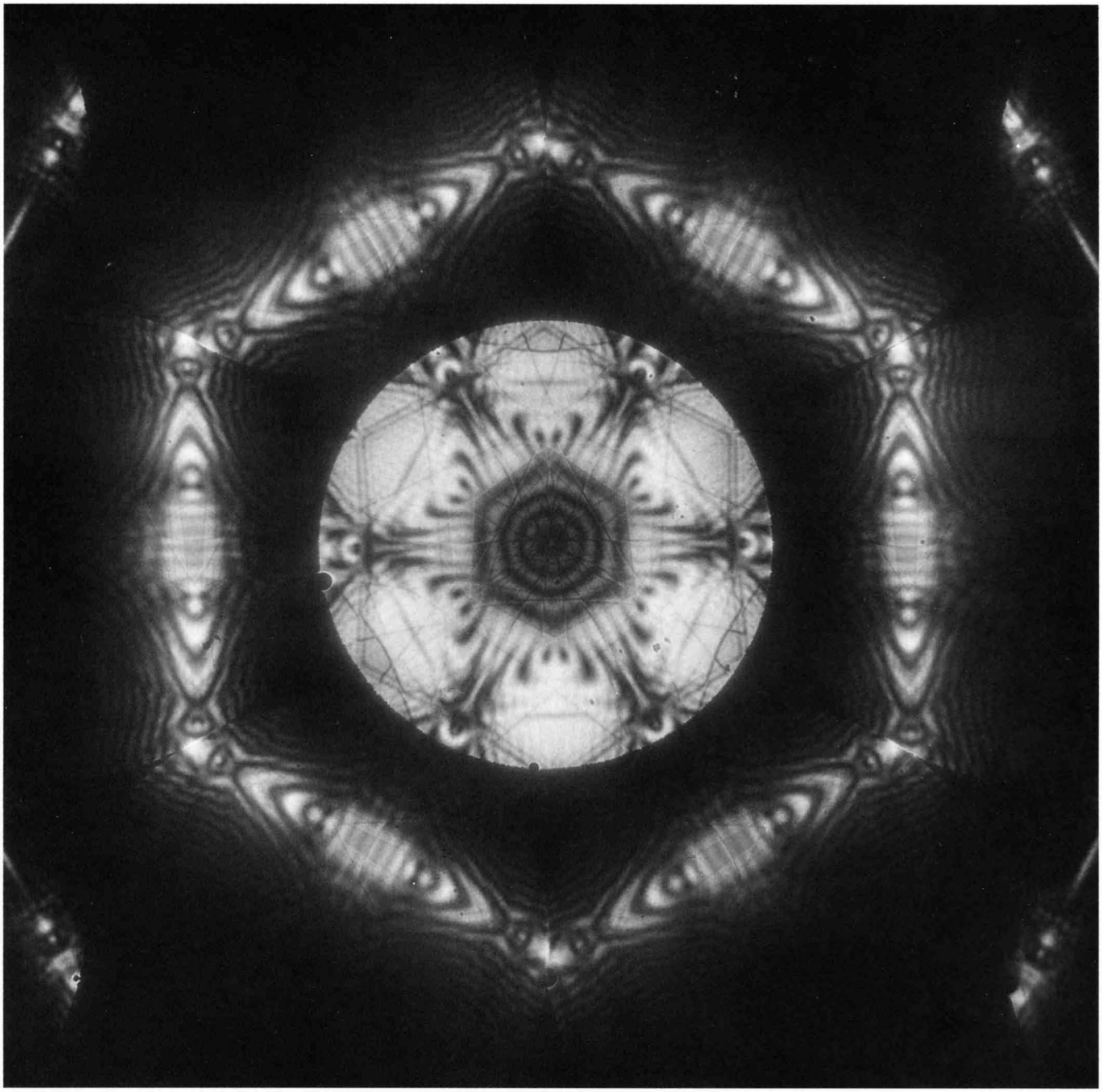

When the amount of defocus ΔS increases, the bright- and dark-field disks are separated from each other at a plane A above the diffraction plane. This photograph, taken at a plane above the diffraction plane by setting $\Delta S \simeq 100\mu$m, shows no practical distortion. To obtain a pattern without distortion, a parallel sided and perfect specimen area more than 1μm in diameter is needed.

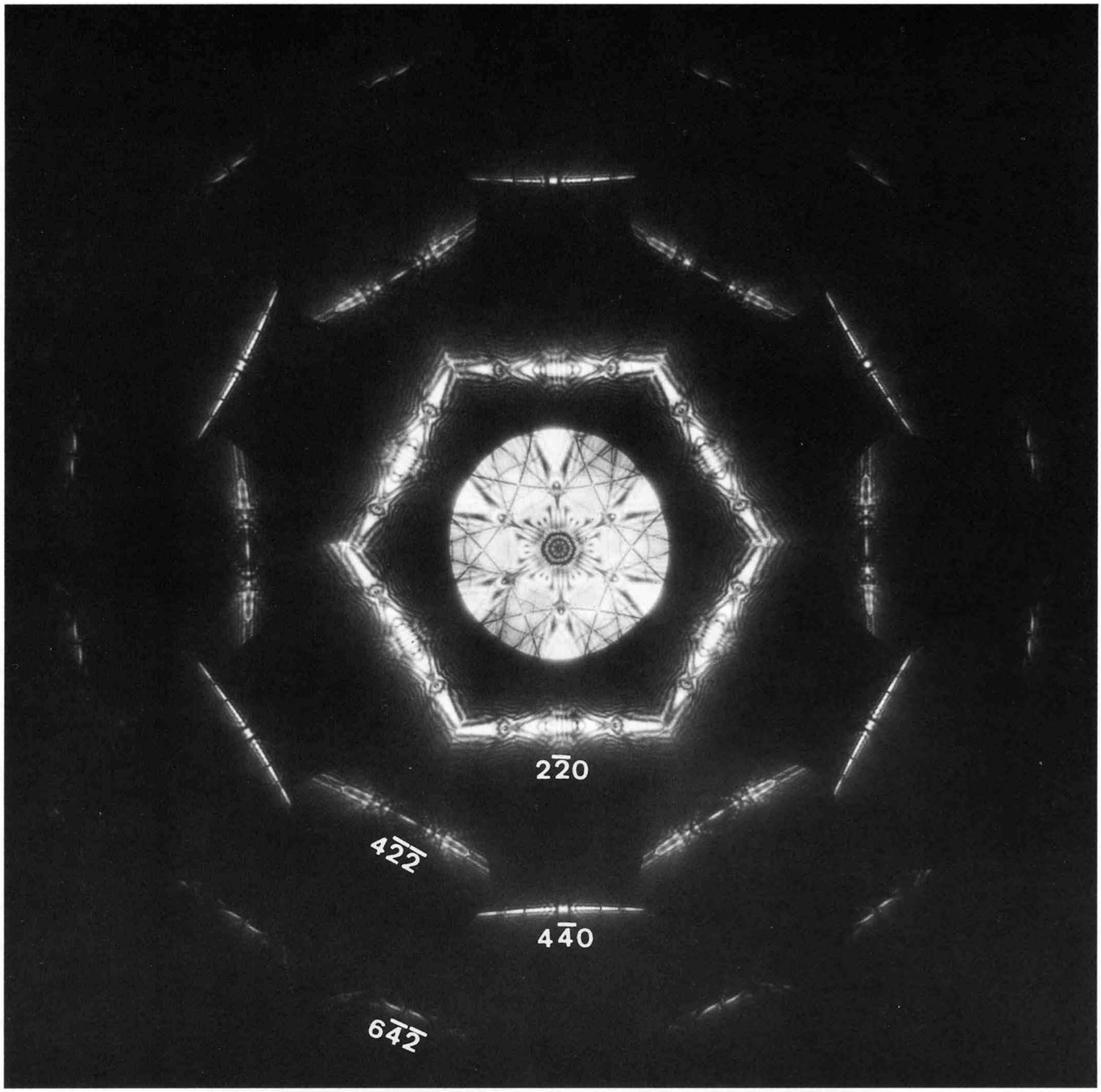

When the convergent angle of the incident beam is increased, dark-field symmetries of a high-order reflections can be seen. This photograph was taken below plane D by setting $\Delta S \simeq 60\mu$m. The symmetry 2*mm* due to the interaction between the 0-th Laue-zone relfections is seen in the $4\bar{2}\bar{2}$ and $4\bar{4}0$ disks. The symmetry 1_R due also to two-dimensional interaction is seen in the $6\bar{4}\bar{2}$ disk.

Si [111] Off-zone-axis patterns 60kV

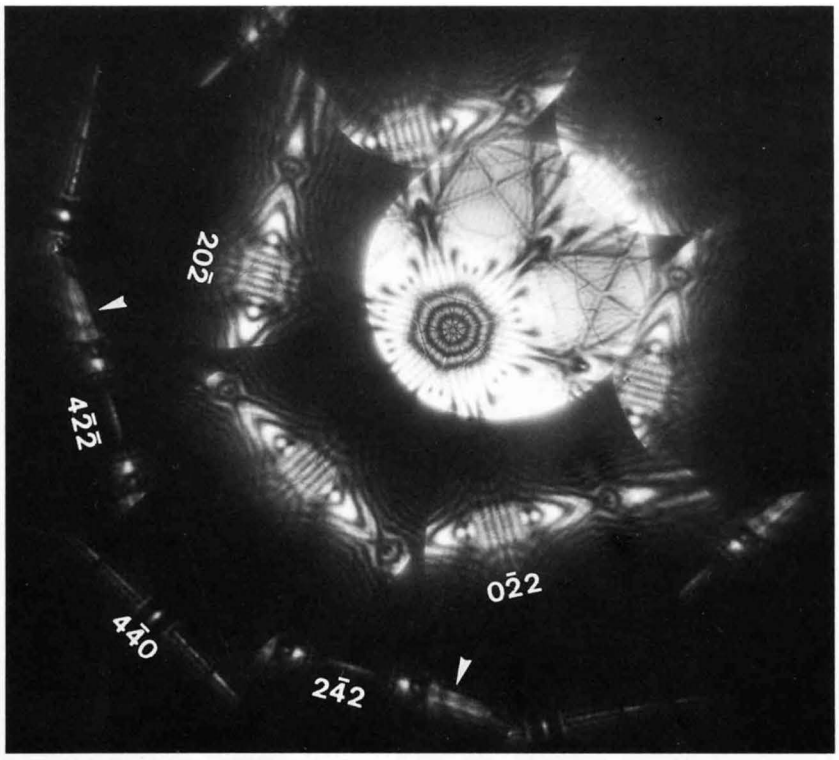

(a)

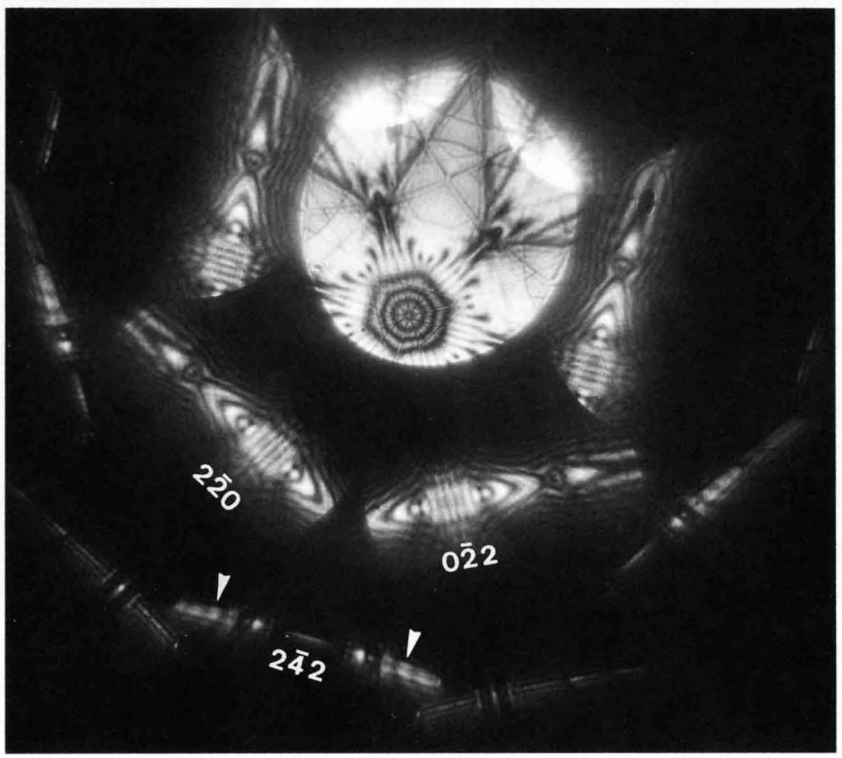

(b)

(a) Hexagonal six-beam LACBED pattern.
This pattern corresponds to the second setting of the specimen symmetry $6_R mm_R$ (see page 157). The symmetry m_2 due to HOLZ interaction is observed in the $0\bar{2}2$, $20\bar{2}$ and $4\bar{4}0$ disks. The symmetry 6_R (indicated by arrows) due also to 'HOLZ' interaction, is seen between the $42\bar{2}$ and $2\bar{4}2$ disks, indicating the presence of an inversion center.

(b) Off-zone-axis many-beam LACBED pattern, obtained with the incident beam tilted in the $1\bar{2}1$ direction. The symmetries m_2 and m_V due to HOLZ interaction are seen in the $2\bar{2}0$ and $0\bar{2}2$ disks and $2\bar{4}2$ disk, respectively.

GM lines

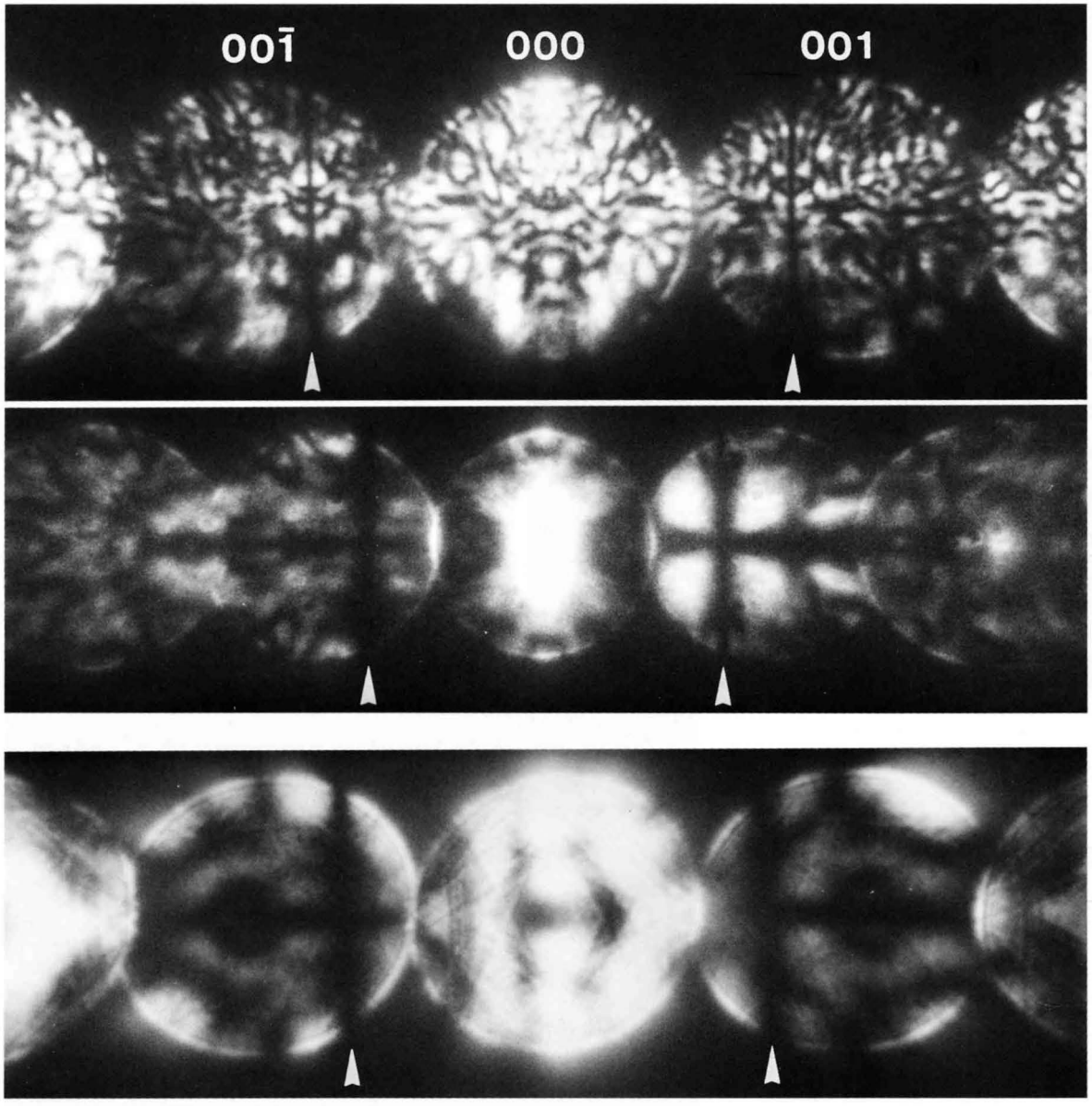

Many-beam LACBED patterns obtained by zone-axis incidences. Photo (a) was obtained from a (100) CdS having a non-centrosymmetric space-group of $P6_3mc$, by tilting ~5° around the 001 axis. B_2 GM lines are simultaneously observed in the 001 and 00$\bar{1}$ disks. The lacking of the symmetry 2_R or an inversion center is seen between the disk pair.

Photo (b) was obtained from a (100) CdS with the zone-axis incidence. The 001 and 00$\bar{1}$ disks show A_2 and B_2 GM lines simultaneously and the lack of an inversion center.

Photo (c) was obtained from a (100)FeS_2 having a centrosymmetric space-group of $P2_1/a\bar{3}$. A_2, A_3, B_2 and B_3 GM lines are seen in the 001 and 00$\bar{1}$ disks.

Hollow-Cone Beam (HCB) Patterns

Si [111]

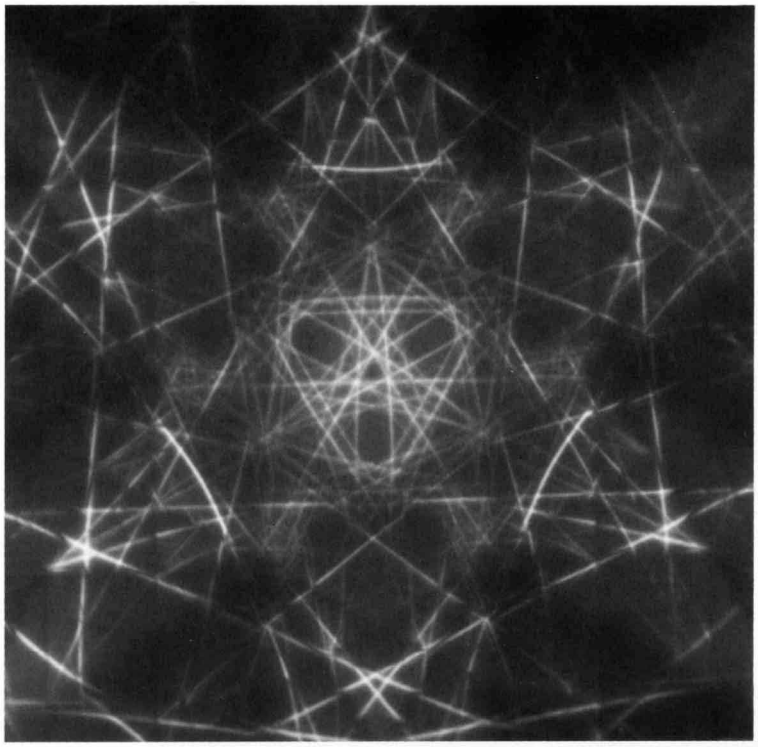

(a)

HCB-FOLZ pattern obtained by setting the incident beam in the direction of FOLZ reflection ring.

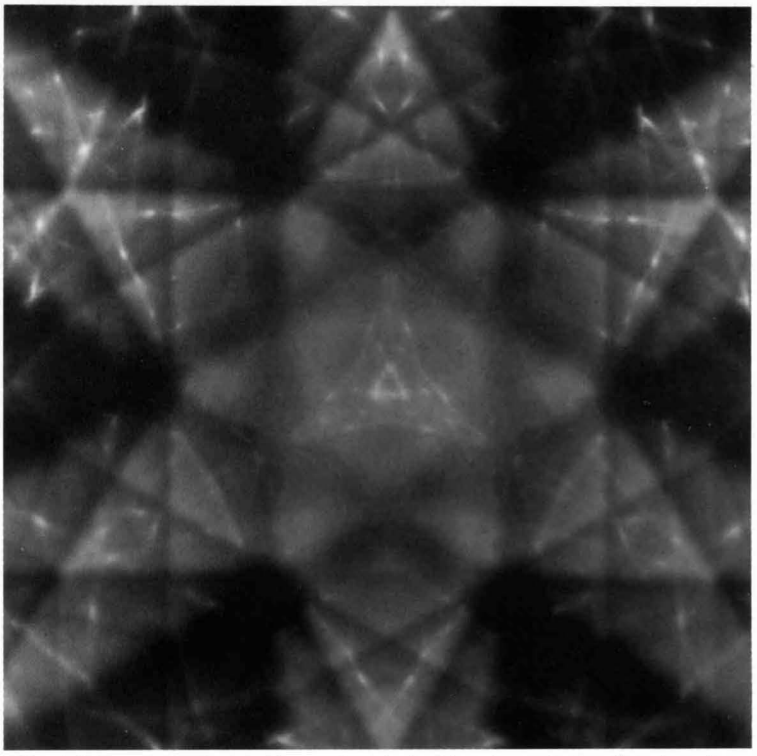

(b)

HCB-SOLZ pattern obtained by setting the incident beam in the direction of SOLZ reflection ring.

Si [111]

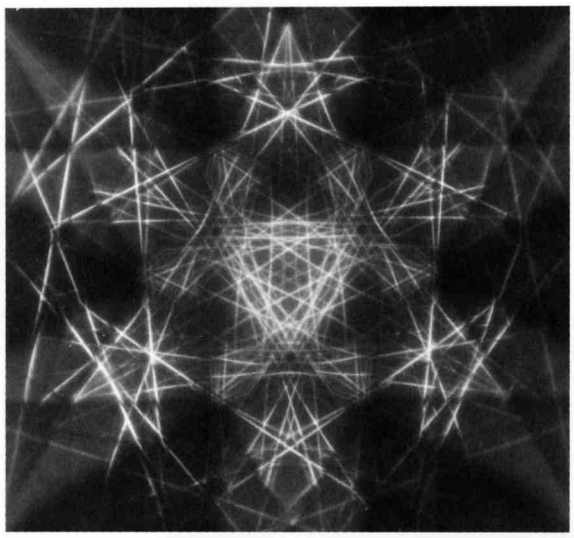

(a) **80kV**

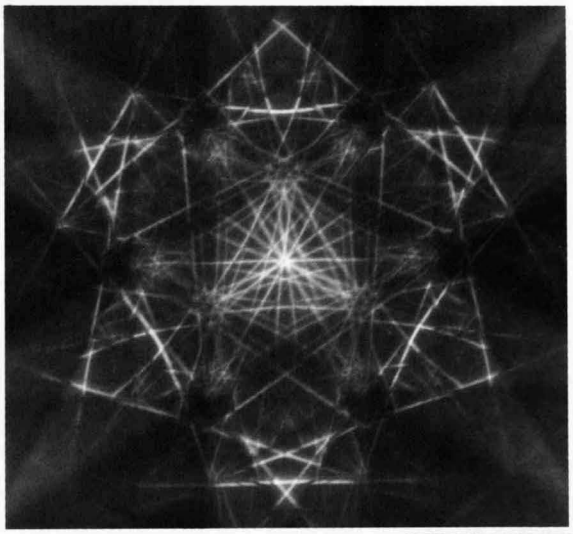

(b) **60kV**

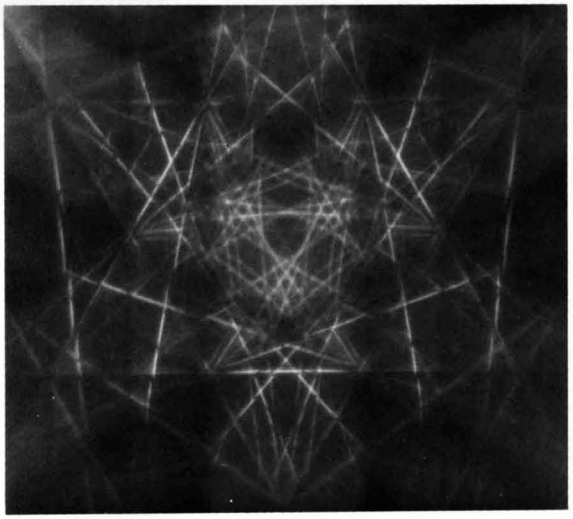

(c) **40kV**

HCB-FOLZ patterns.

Si [100]

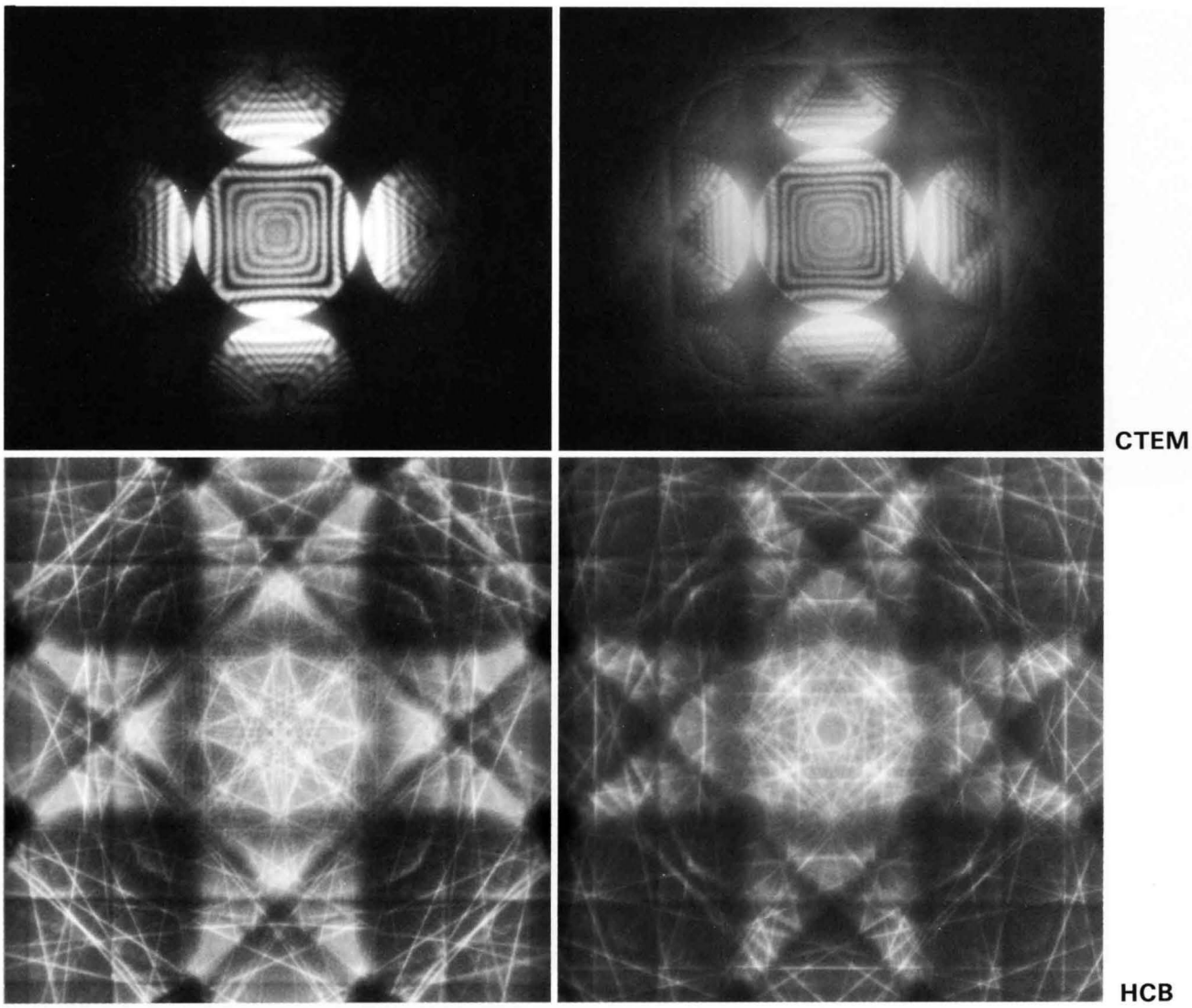

Fine FOLZ lines buried in broad and high-contrasted fringes in ordinary CBED patterns are clearly elucidated in HCB-FOLZ patterns.

Ge [111]

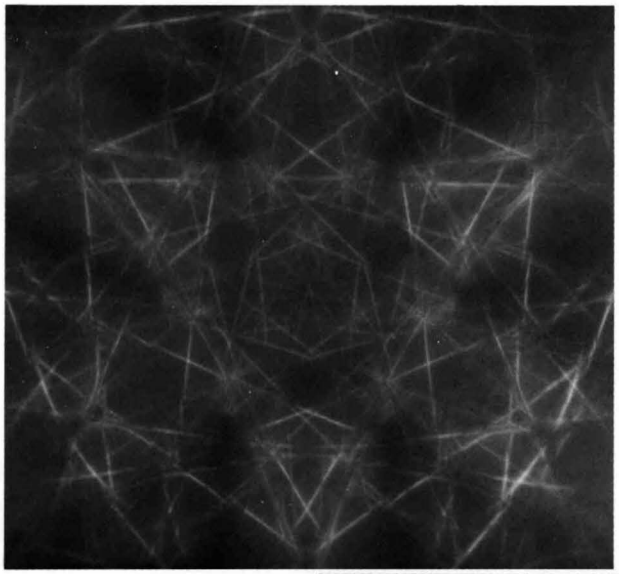

(a) 100kV

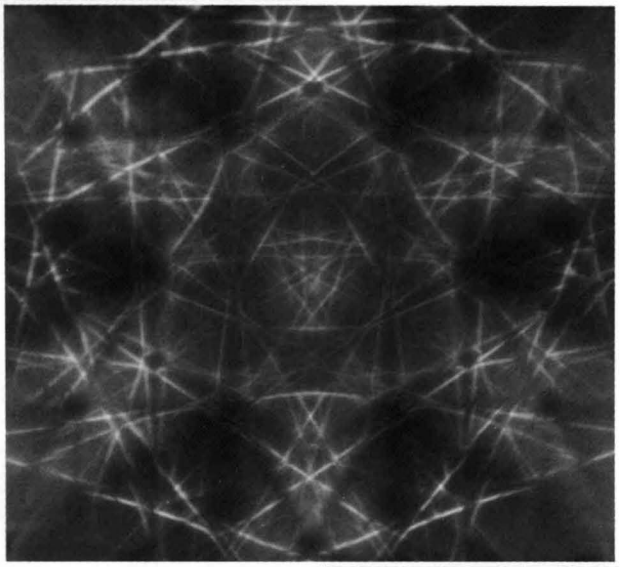

(b) 80kV

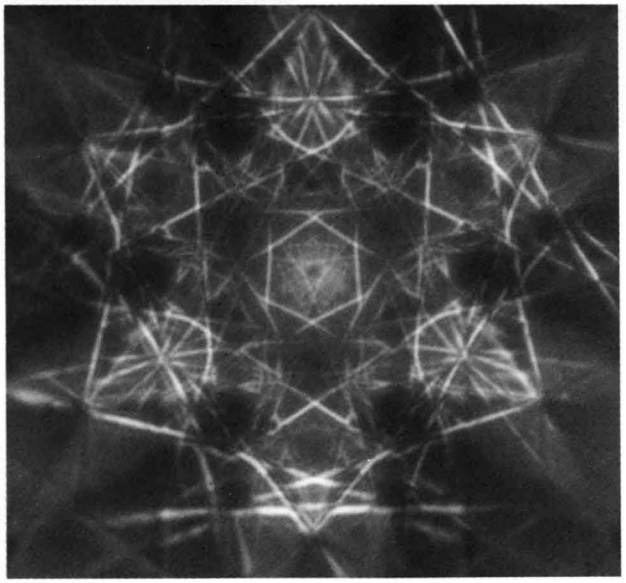

(c) 60kV

HCB-FOLZ patterns.

$MgAl_2O_4$ [100]

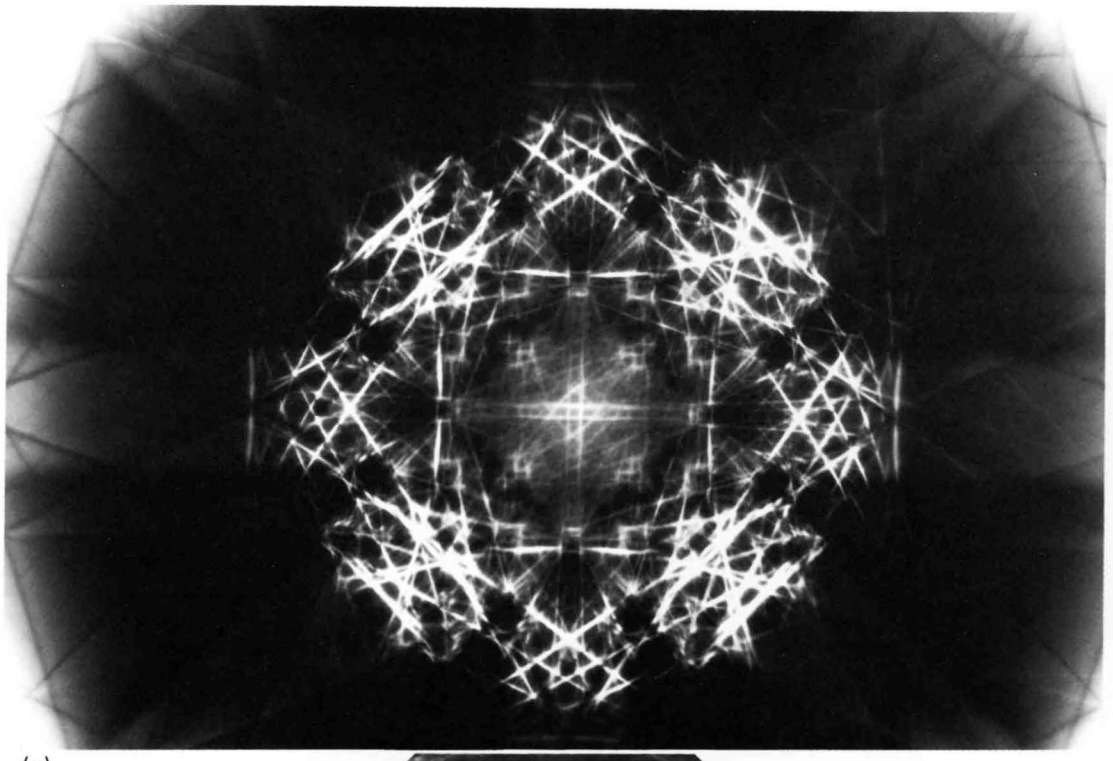

(a)

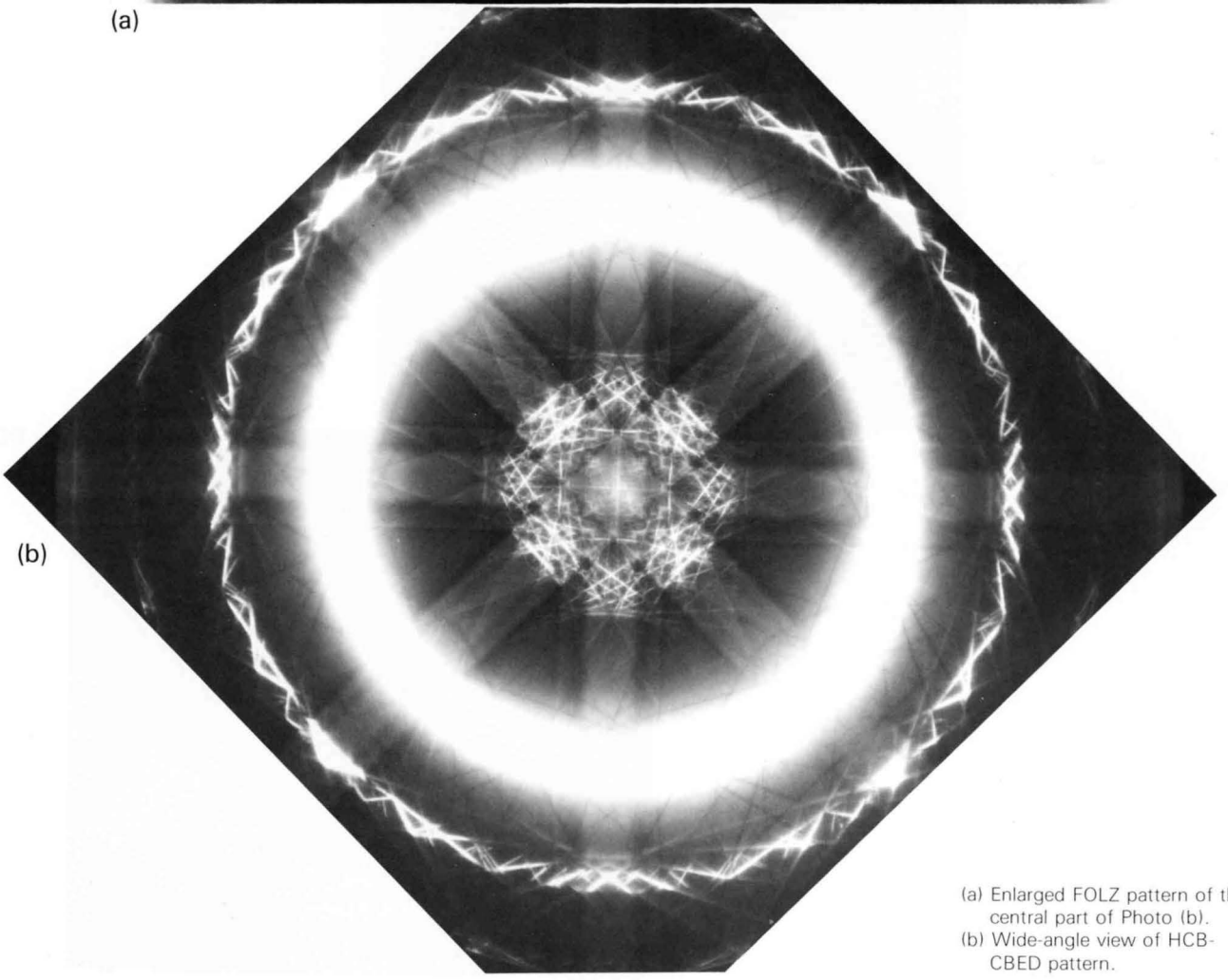

(b)

(a) Enlarged FOLZ pattern of the central part of Photo (b).
(b) Wide-angle view of HCB-CBED pattern.

MnSi [111] 80kV

CTEM

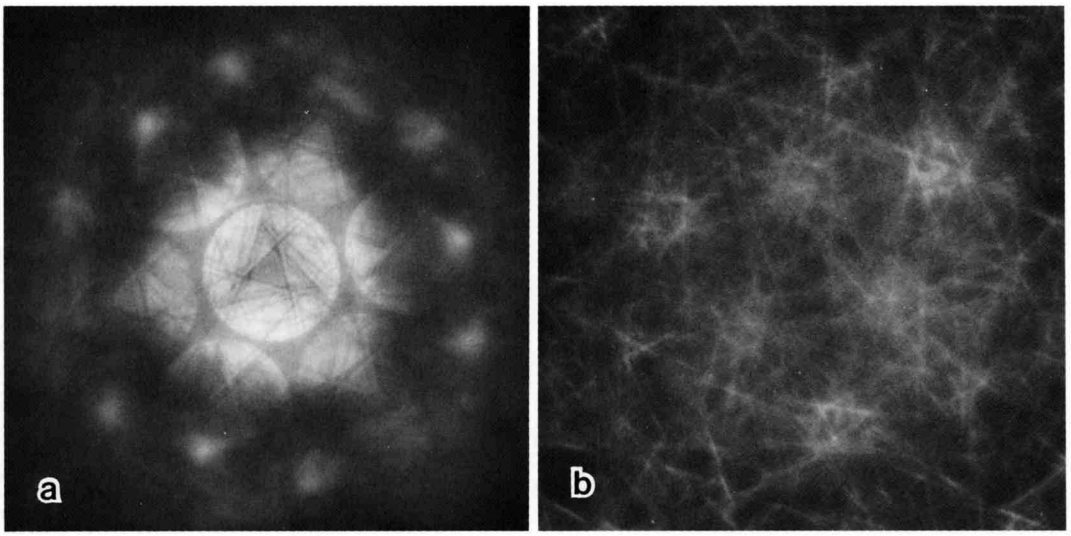

HCB

(a) Ordinary ZAP.
(b) HCB-FOLZ pattern.

Si [111] Small-angle HCB 80kV

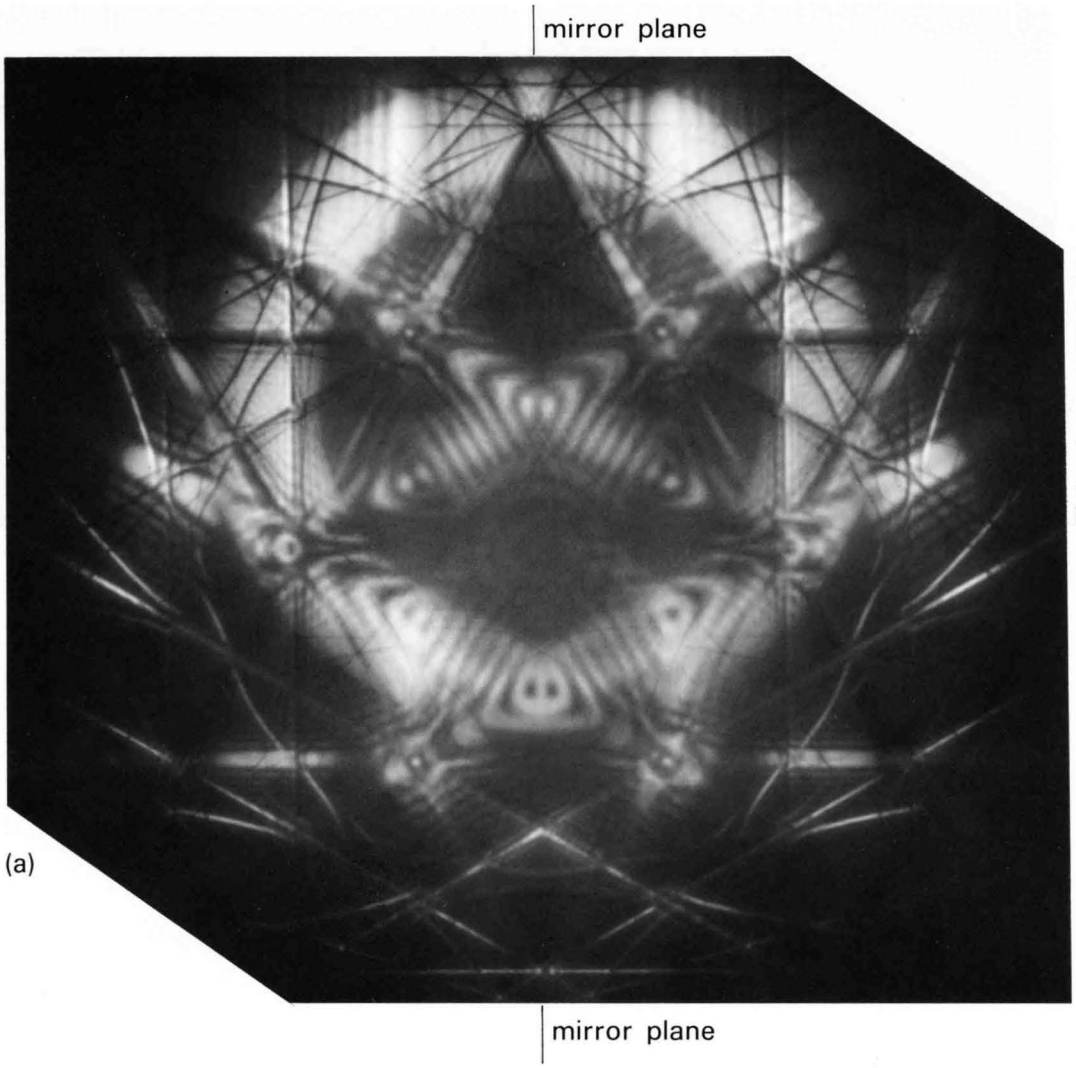

Tilt direction of the HCB is in the [$1\bar{2}1$].

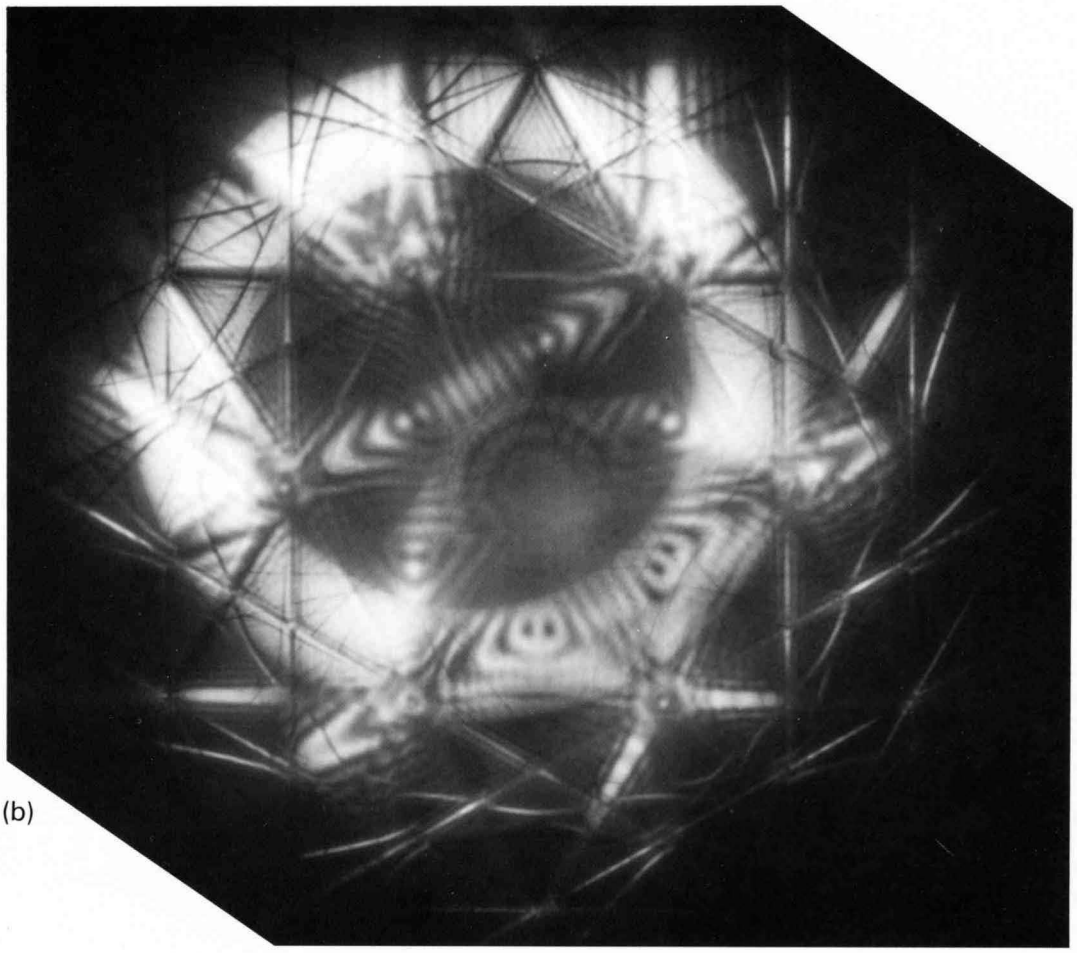

(b)

Tilt direction of the HCB in (b) is different by 30° from (a)

Field Emission Gun (FEG)

Si [110] 20kV

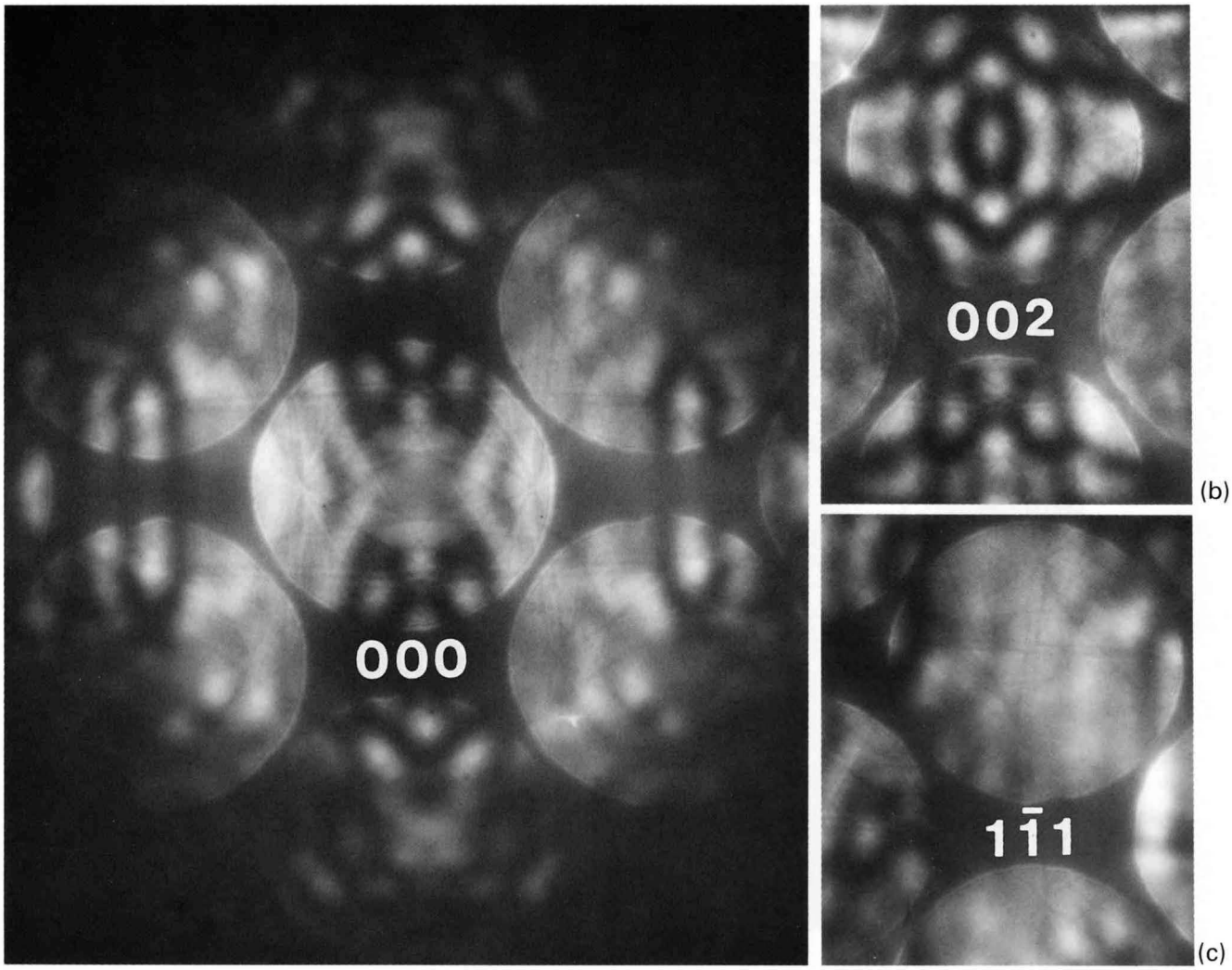

Three dimensional symmetries due to HOLZ lines are clearly seen, which can not be seen in CBED patterns taken at higher accelerating voltages. HOLZ lines exhibit 2*mm* symmetry in BP and WP, 2*mm* in the 002 DP, and 1_w in the 1$\bar{1}$1 DP.

Ge [110]

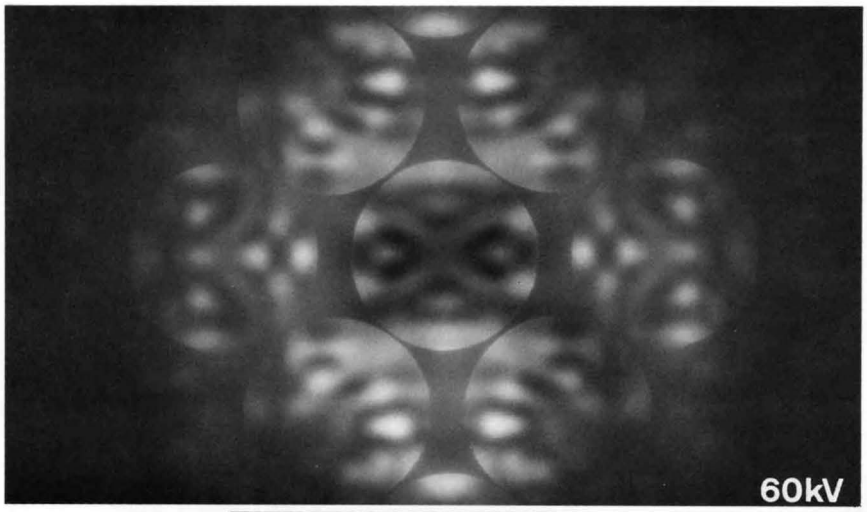

(a)

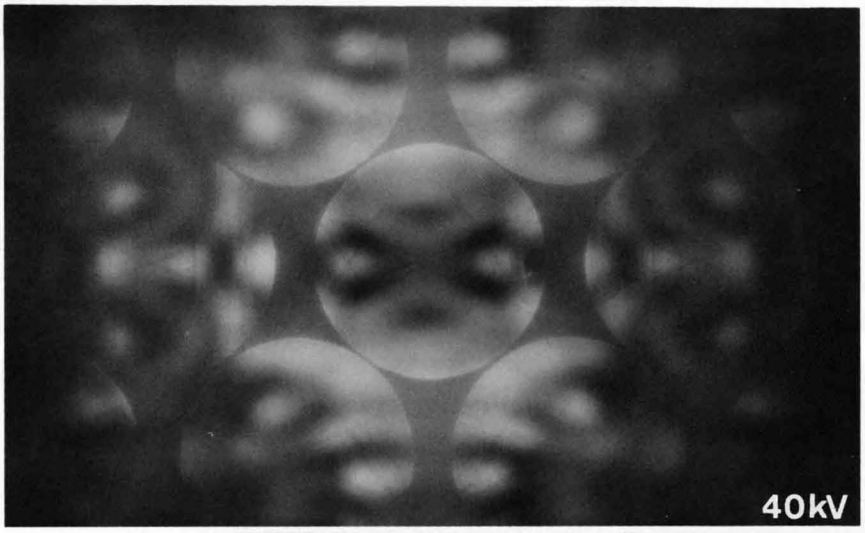

(b)

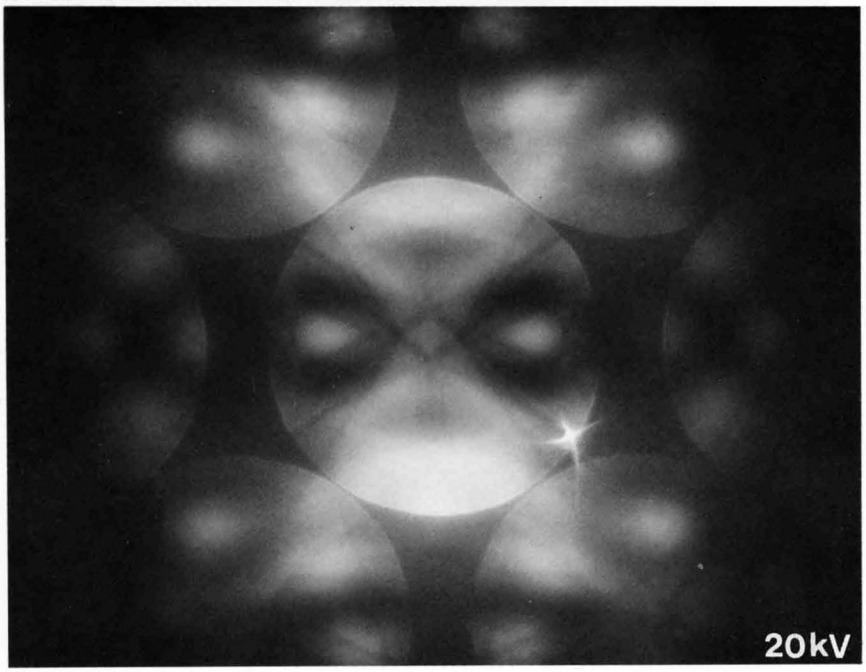

(c)

Note that three-dimensional symmetry becomes clear as the accelerating voltage is lowered.

Ge [111] 80kV

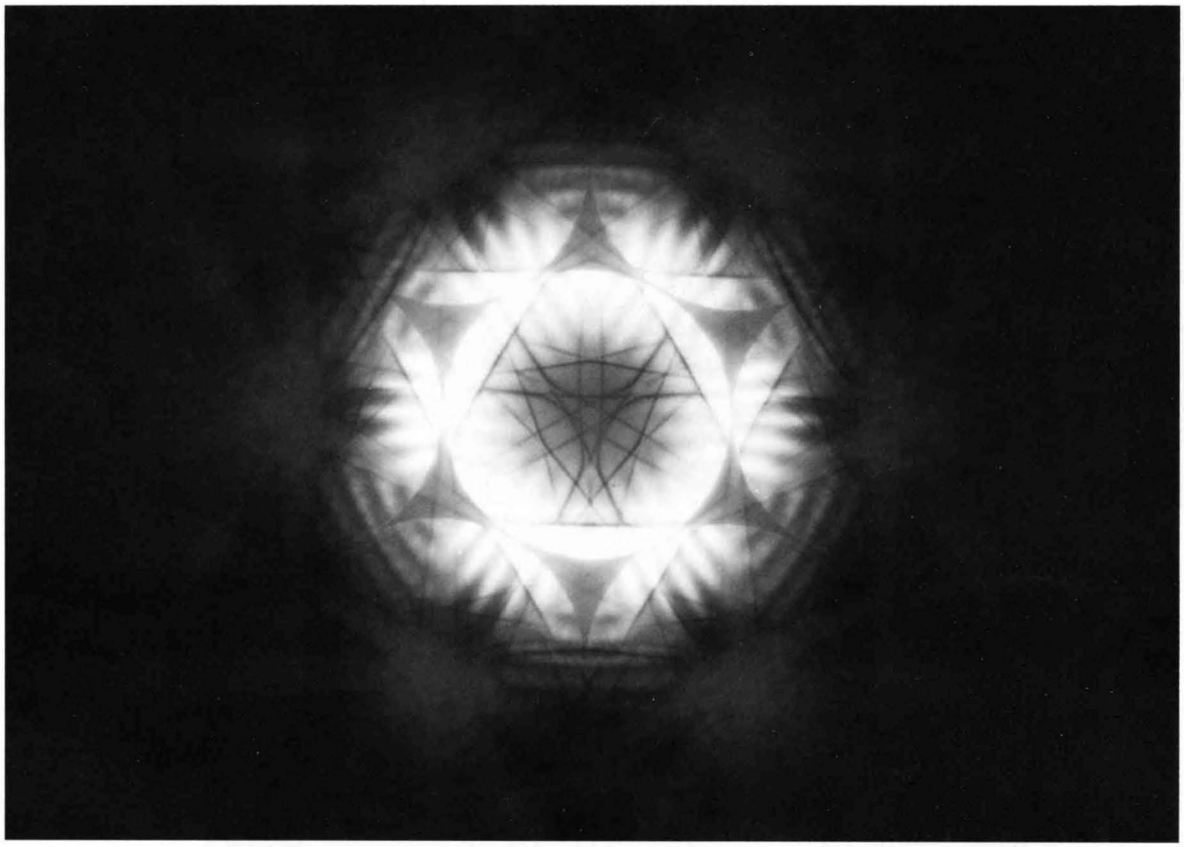

(a)

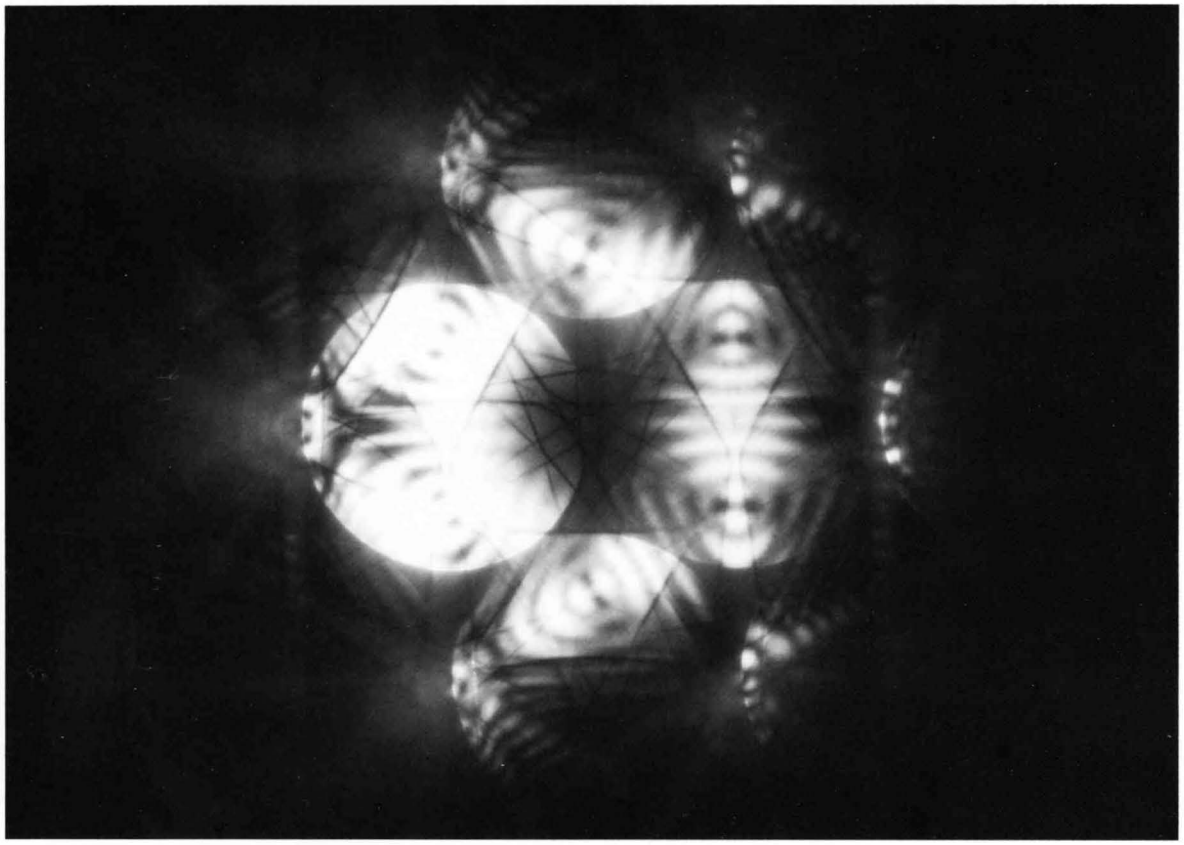

(b)

Ge [111] 60kV

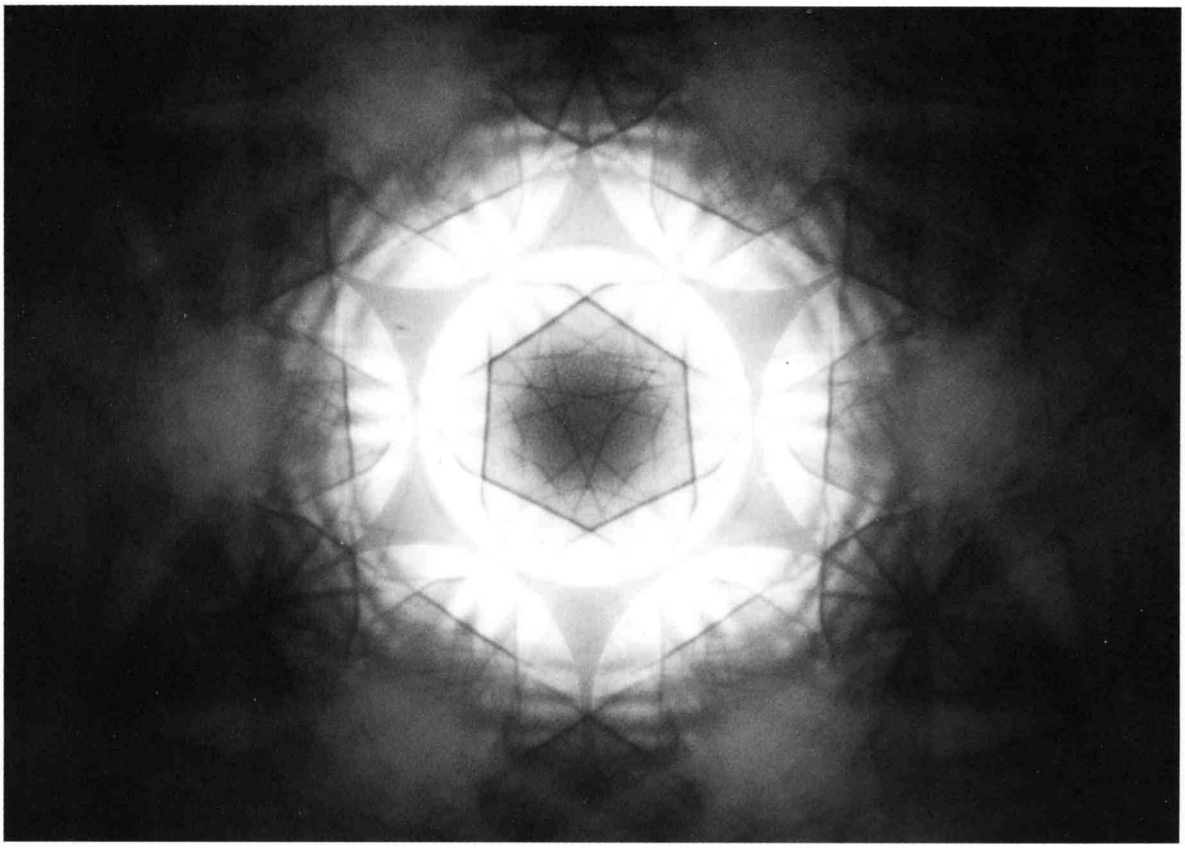

(a)

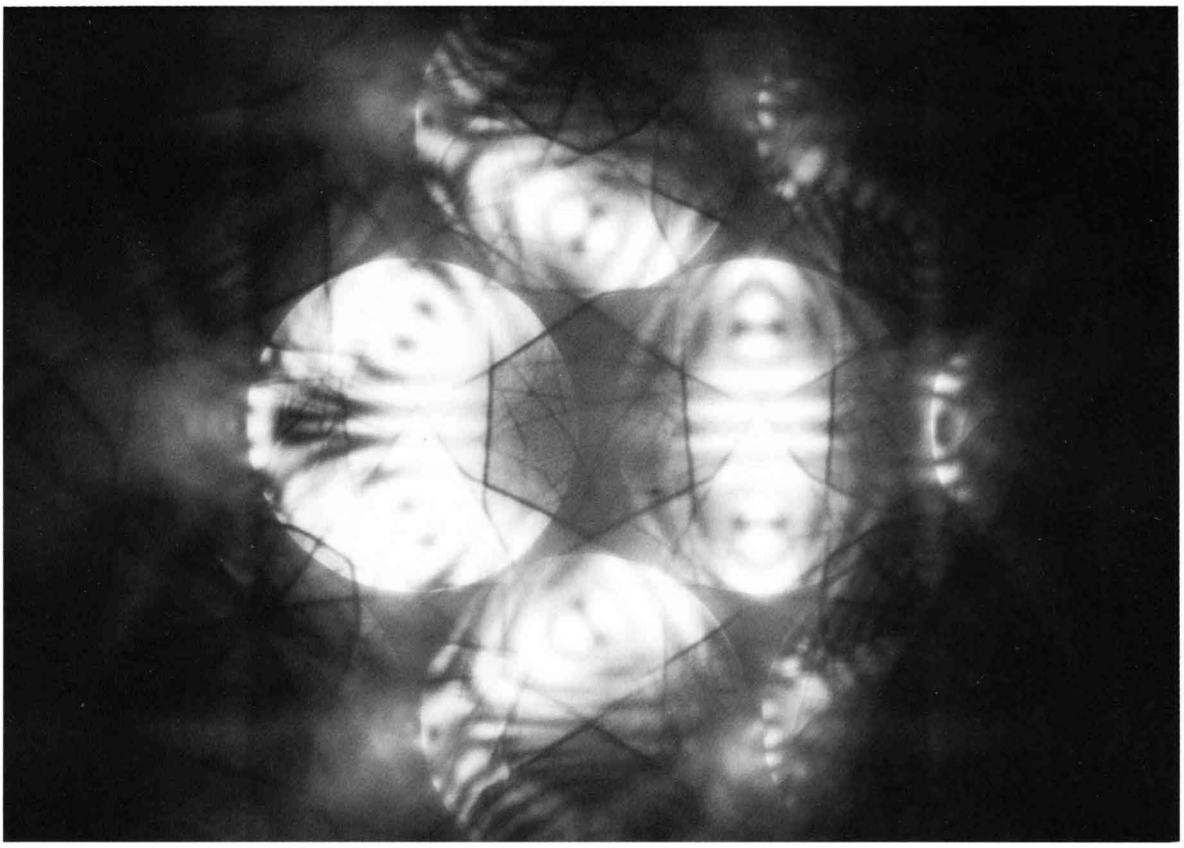

(b)

Ge [111] 40kV

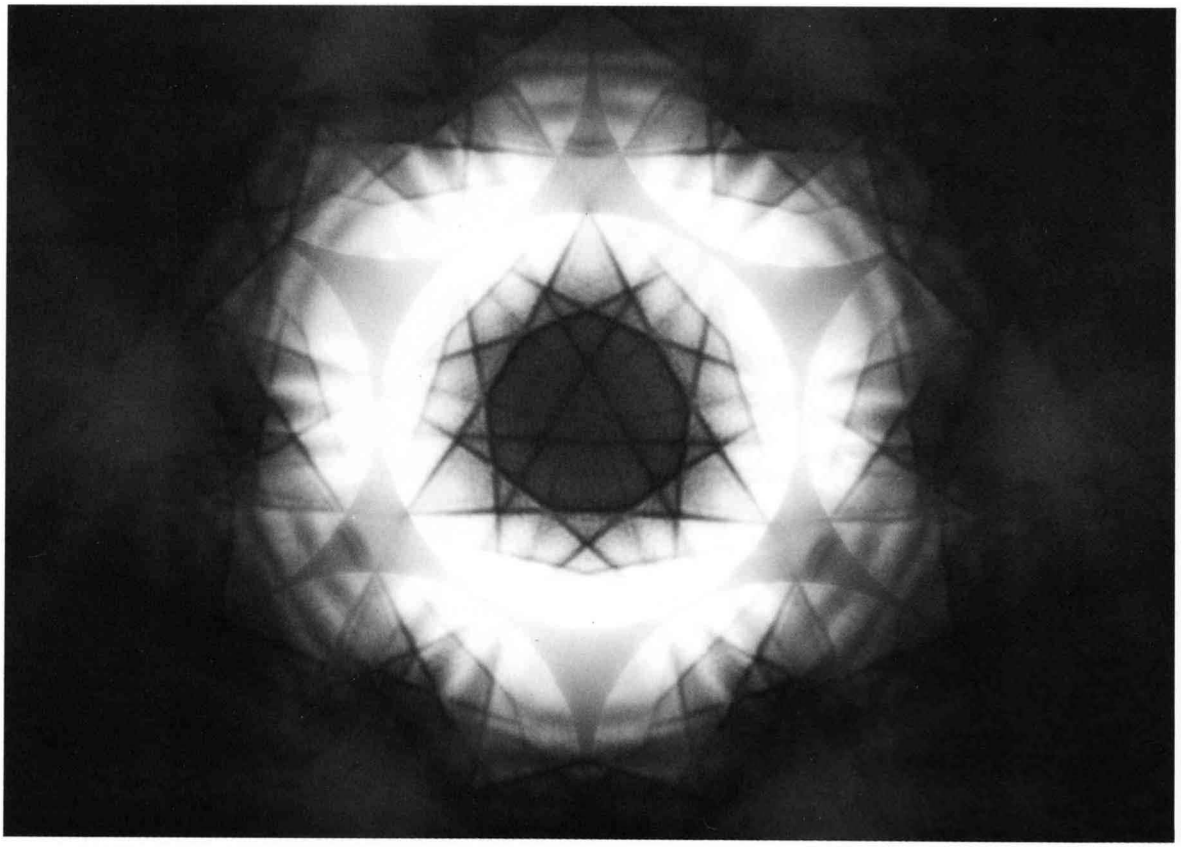

(a)

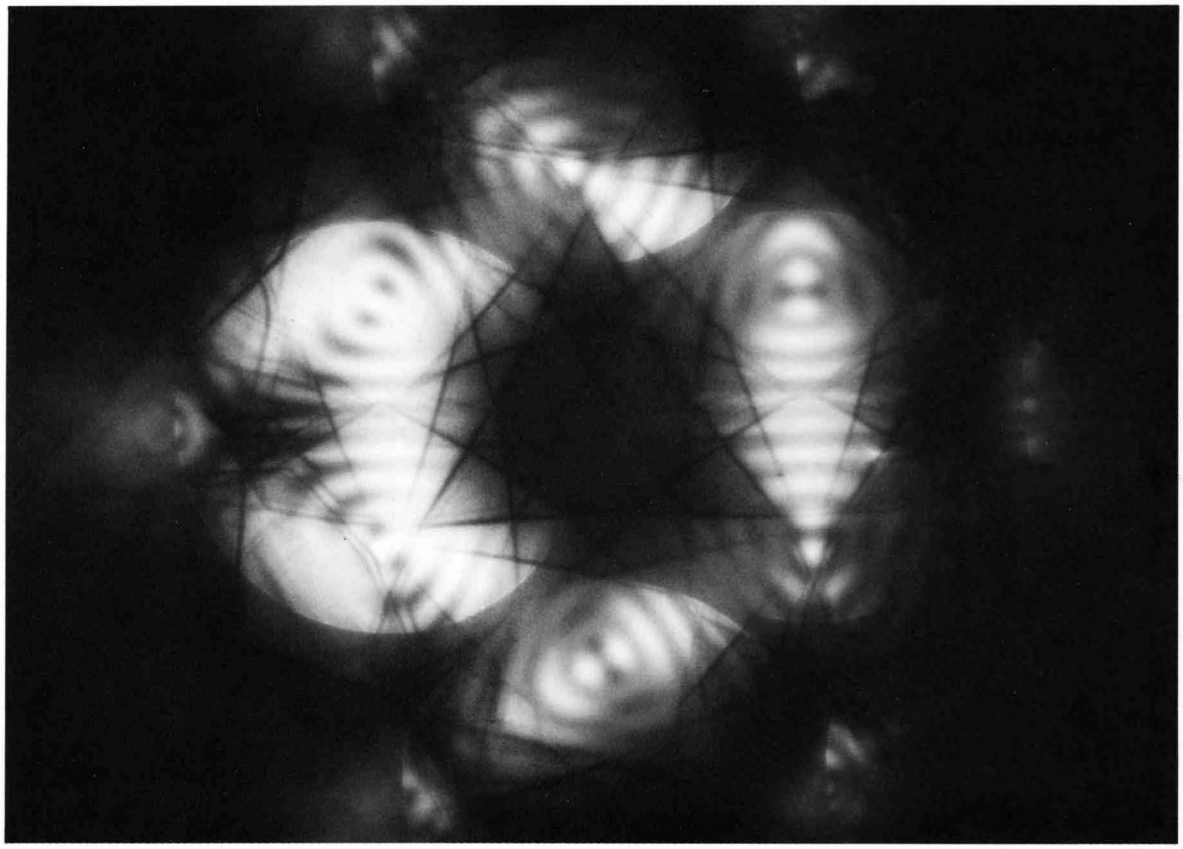

(b)

Ge [111] 20kV

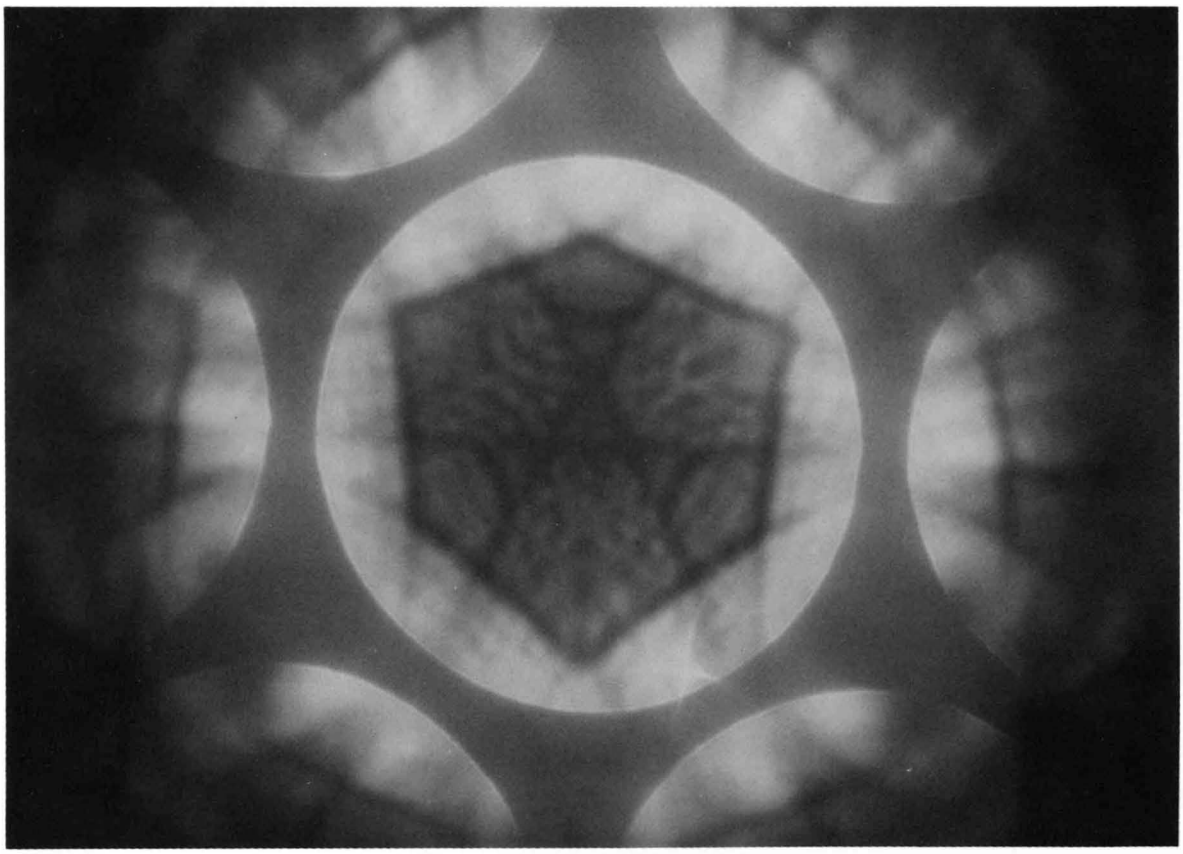

(a)

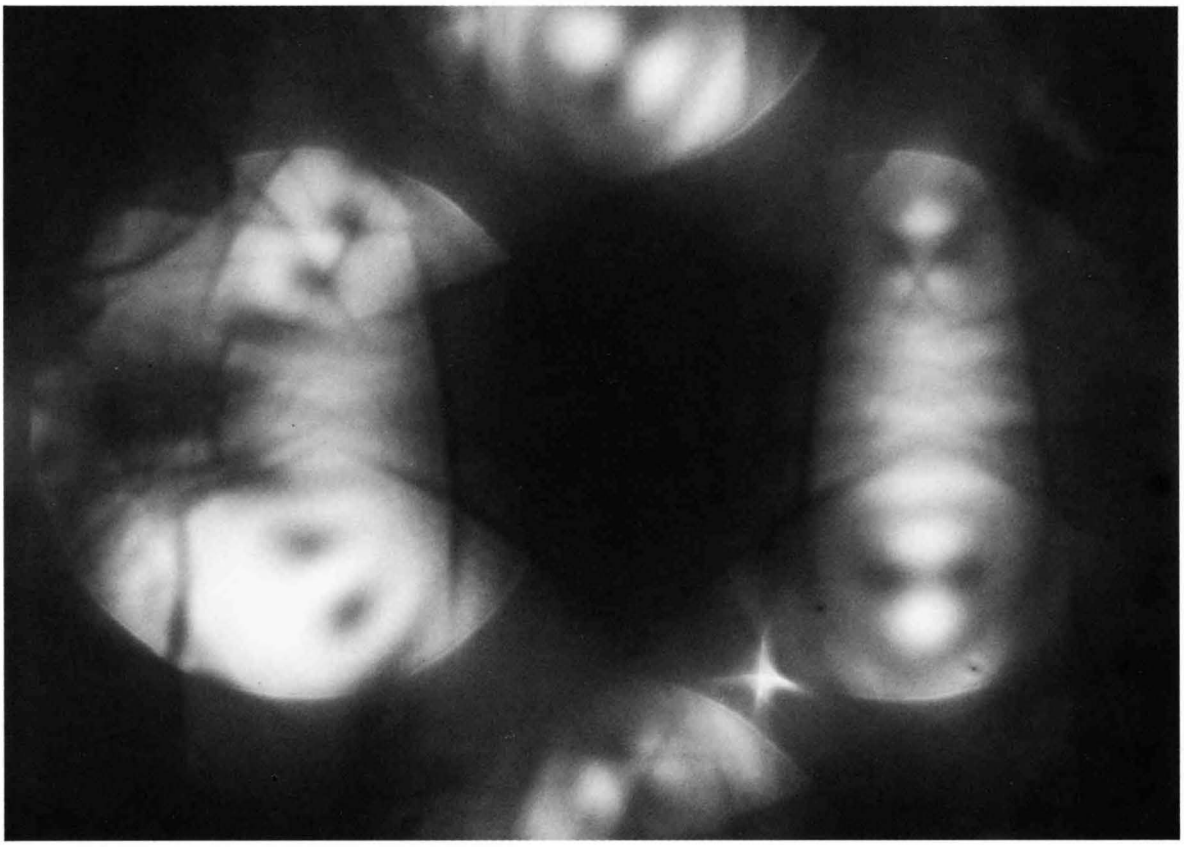

(b)

Simulation of HOLZ Lines

$MgAl_2O_4$ [001]

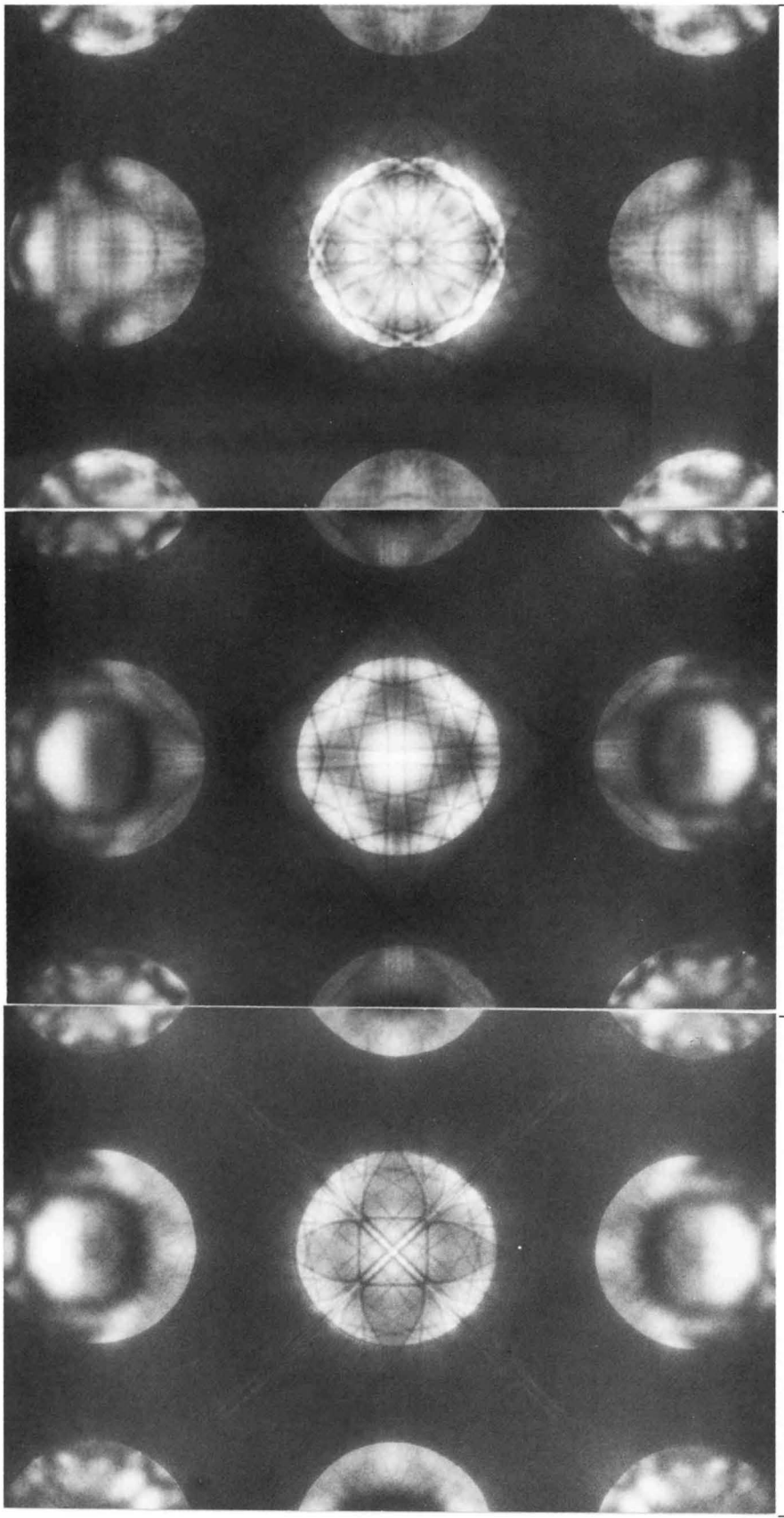

61.2kV

83.8kV

102.0kV

Spinel

[0 0 1]

61.2 kV

1st Laue Zone

G=(0 0 0)

a= 8.09 (A)
b= 8.09 (A)
c= 8.09 (A)
alpha= 90 (deg)
beta = 90 (deg)
gamma= 90 (deg)

RADIUS OF HOLZ RING
= 2.2628 (1/A)
HORIZONTAL DIRECTION
=(2 -2 0)

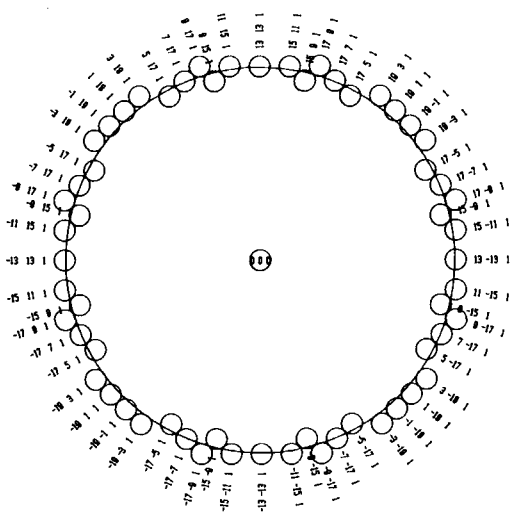

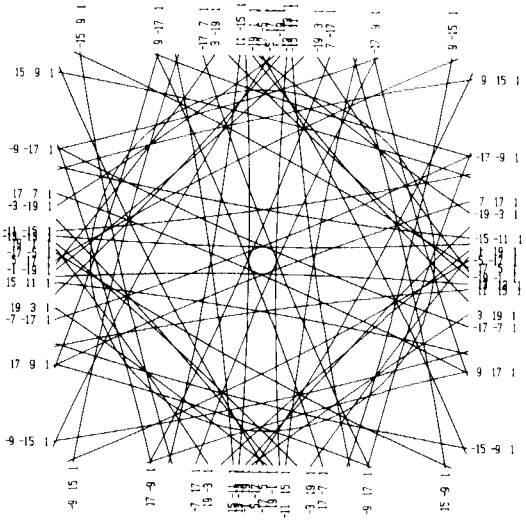

Spinel

[0 0 1]

83.8 kV

1st Laue Zone

G=(0 0 0)

a= 8.09 (A)
b= 8.09 (A)
c= 8.09 (A)
alpha= 90 (deg)
beta = 90 (deg)
gamma= 90 (deg)

RADIUS OF HOLZ RING
= 2.461 (1/A)
HORIZONTAL DIRECTION
=(2 -2 0)

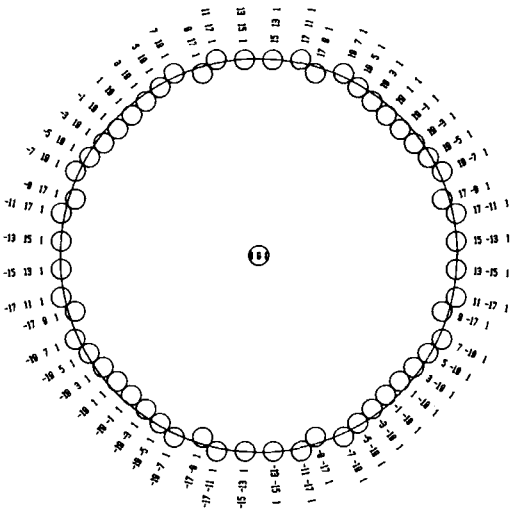

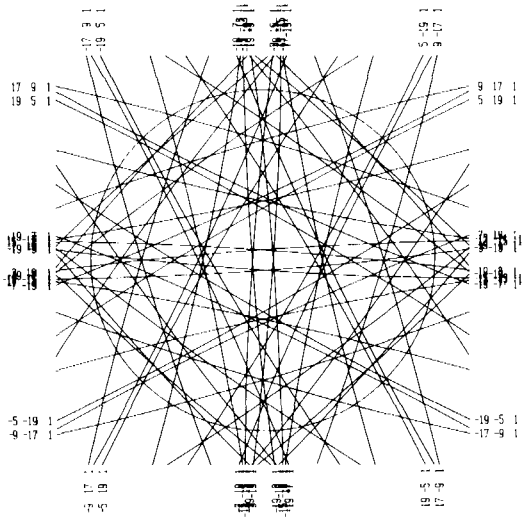

Spinel

[0 0 1]

102 kV

1st Laue Zone

G=(0 0 0)

a= 8.09 (A)
b= 8.09 (A)
c= 8.09 (A)
alpha= 90 (deg)
beta = 90 (deg)
gamma= 90 (deg)

RADIUS OF HOLZ RING
= 2.5959 (1/A)
HORIZONTAL DIRECTION
=(2 -2 0)

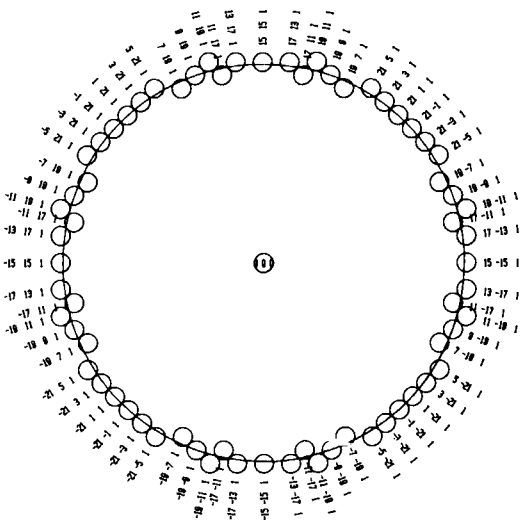

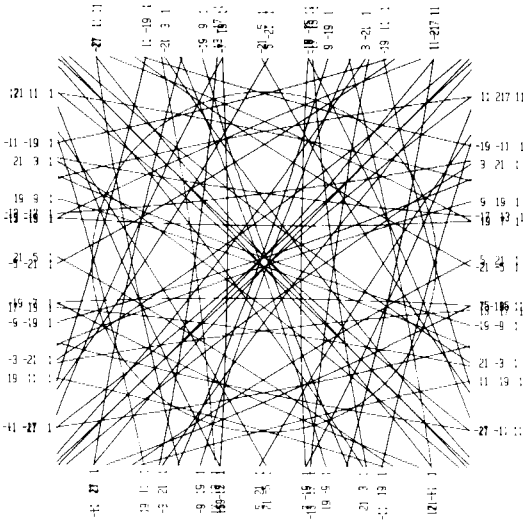

Dynamic Extinction Lines (GM Lines)

MnSi $P2_13$ 2_1 screw axis, B_2-B_3 line

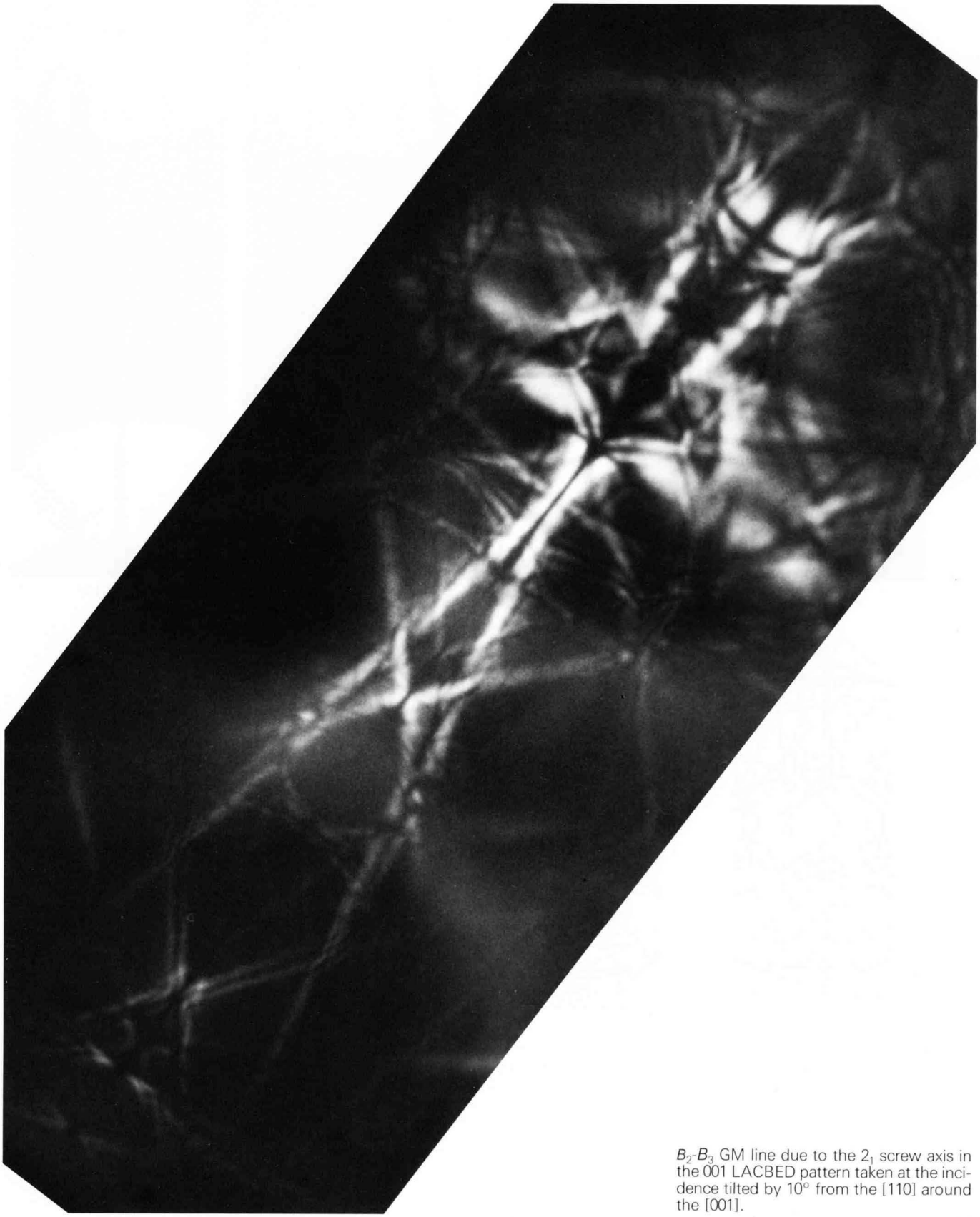

B_2-B_3 GM line due to the 2_1 screw axis in the 001 LACBED pattern taken at the incidence tilted by 10° from the [110] around the [001].

$MgAl_2O_4$ [001] $F4_1/d\bar{3}2/m$ d-glide plane, A_3 lines

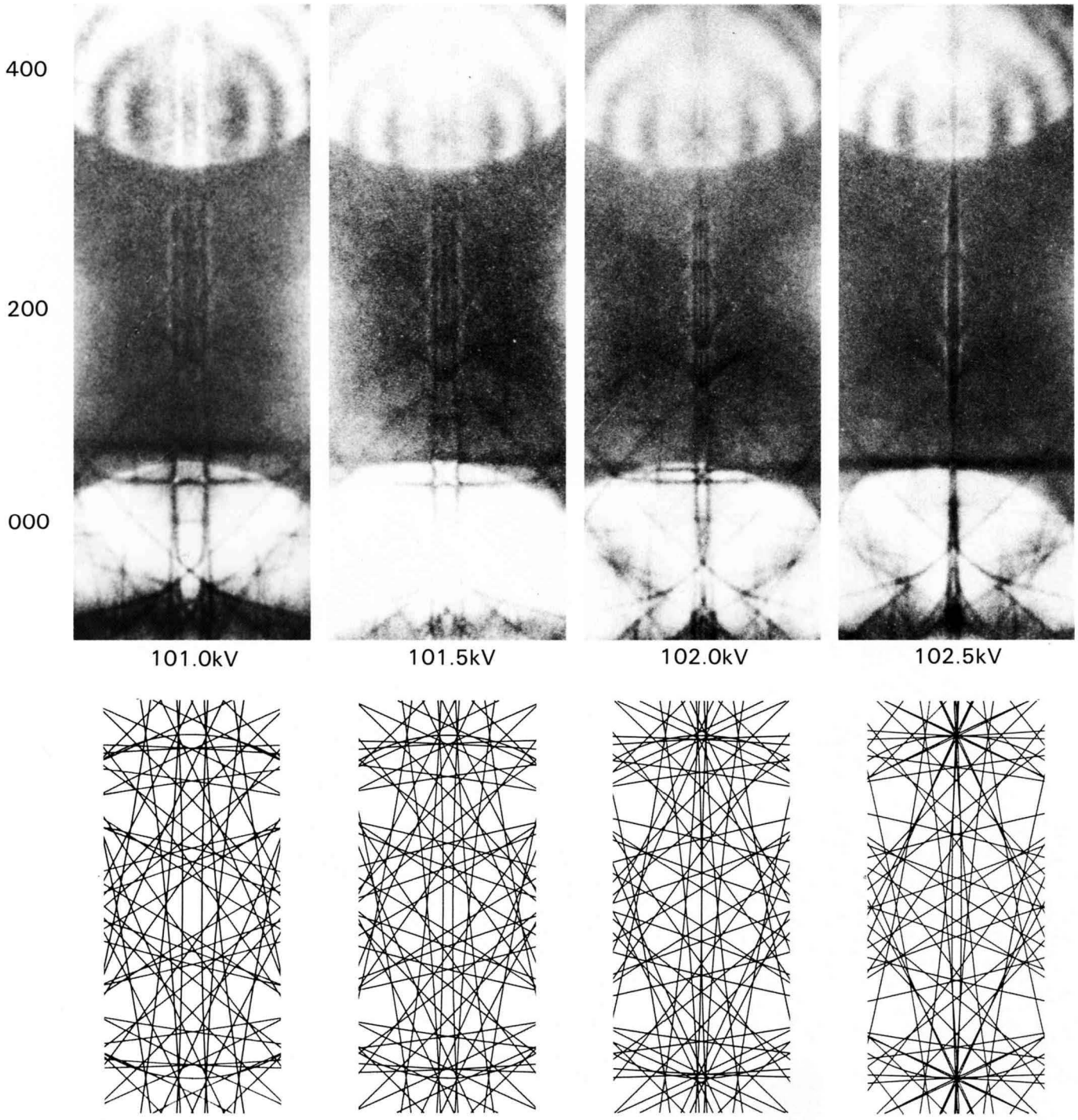

A_3 GM lines due to the d-glide plane in the 200 disks taken at varying accelerating voltages and HOLZ-line simulations. Note that HOLZ lines—the appearance of GM lines—vary quite sensitively with the change of the accelerating voltage.

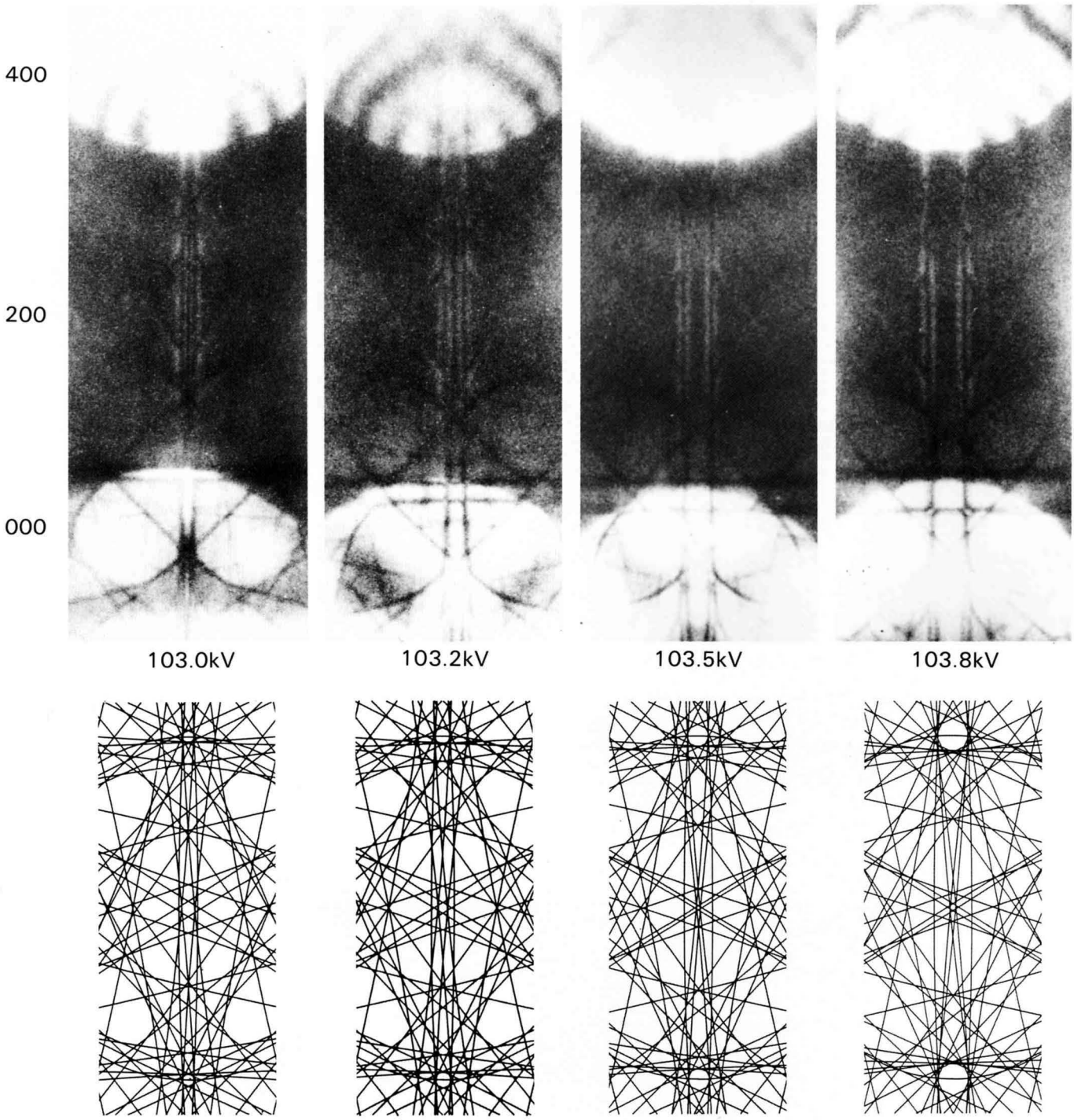
400
200
000
103.0kV
103.2kV
103.5kV
103.8kV

Si [001] $F4_1/d\bar{3}2/m$ d-glide plane, A_3 lines

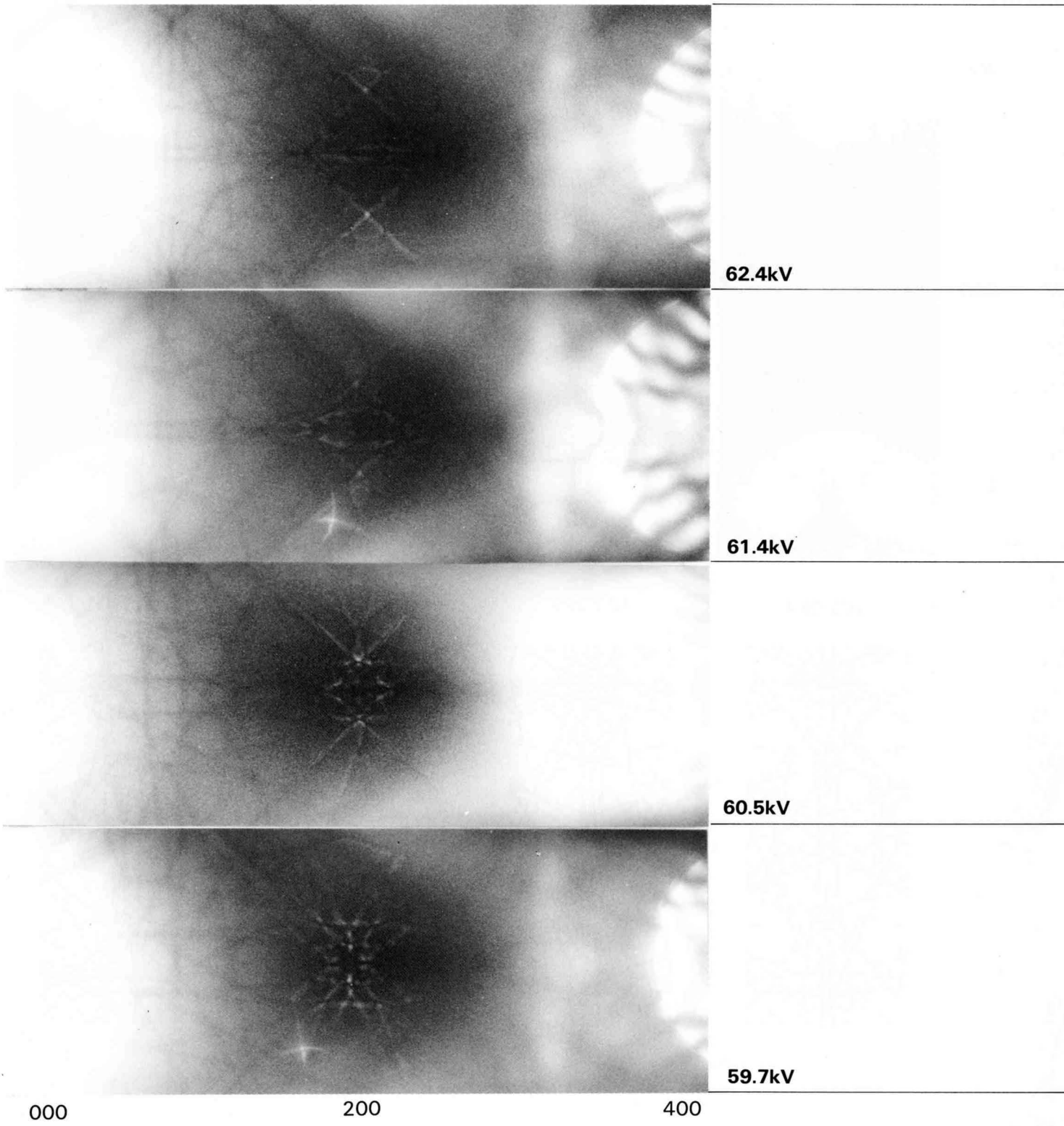

A_3 GM lines due to the d-glide plane in the 200 reflections taken at varying accelerating voltages. These photographs were needed exposures of 1 minute using FEG, because HOLZ lines in the 200 disks were very weak.

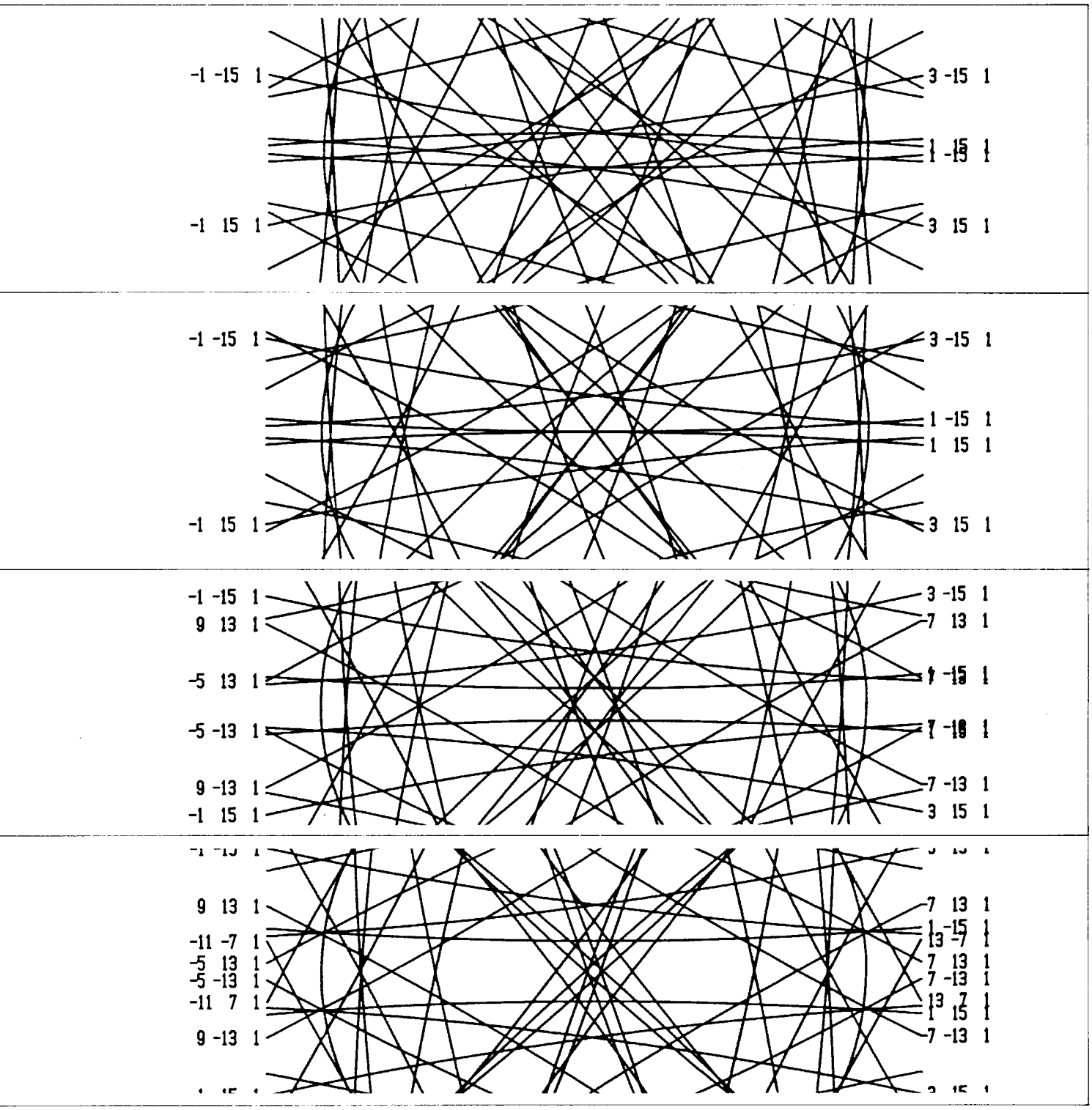

Simulation of HOLZ lines in the 200 reflections.

Y_2O_3 [110] $I2_1/a\bar{3}$ *a*-glide plane

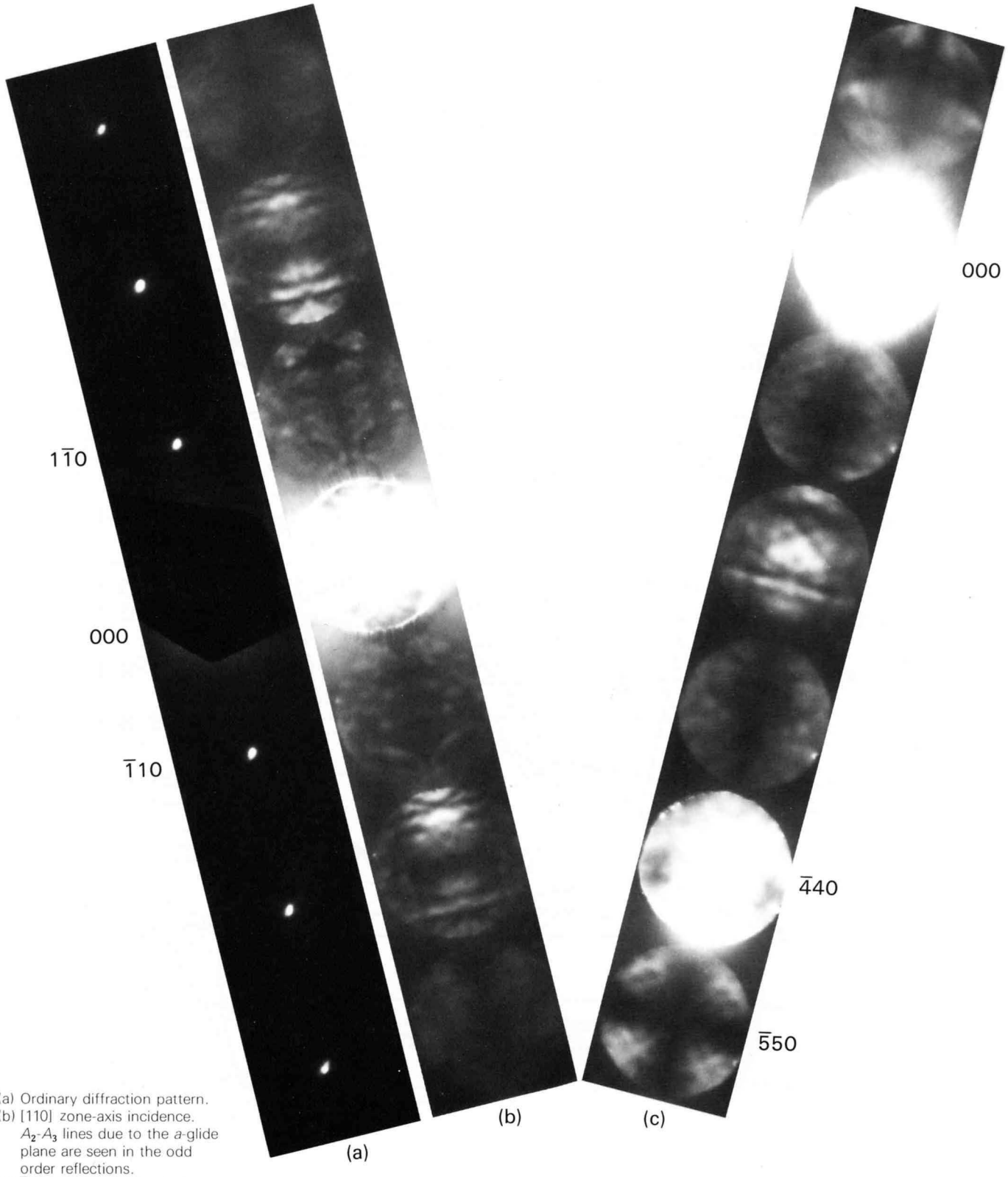

(a) Ordinary diffraction pattern.
(b) [110] zone-axis incidence. A_2-A_3 lines due to the *a*-glide plane are seen in the odd order reflections.
(c) $\bar{5}$50 reflection is exactly excited. A_2-A_3 and B_2 lines due to the *a*-glide plane are seen in the $\bar{5}$50 refrection.

$La_2Ti_2O_7$ [100] $P2_1$ 2_1 screw axis

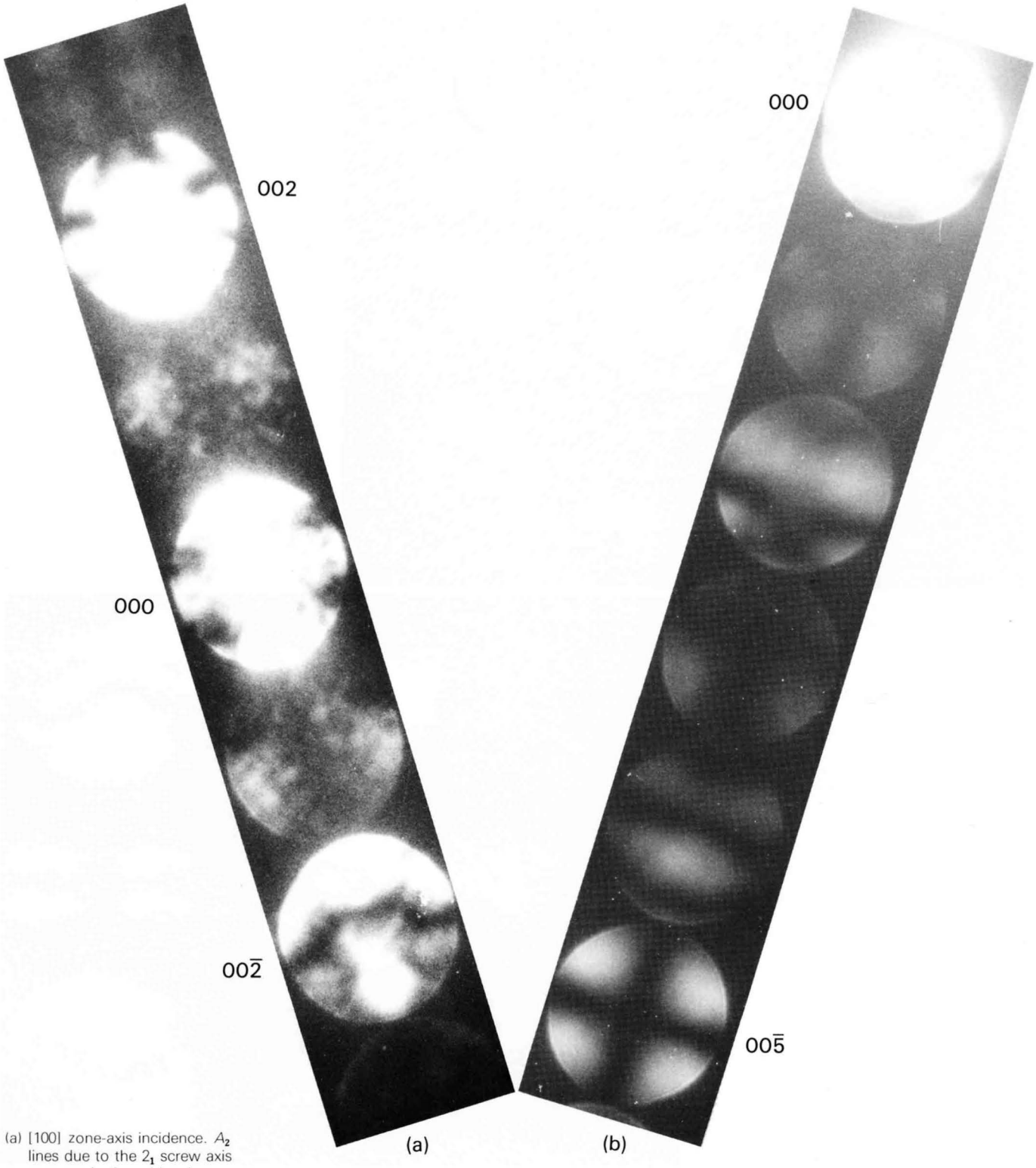

(a) [100] zone-axis incidence. A_2 lines due to the 2_1 screw axis are seen in the odd order reflections.
(b) 00$\bar{5}$ reflection is exactly excited. A_2 and B_2 lines due to the 2_1 screw axis are seen in the 00$\bar{5}$ reflection.

V_3Si [11$\bar{2}$] $P4_2/m\bar{3}2/n$ *n*-glide plane

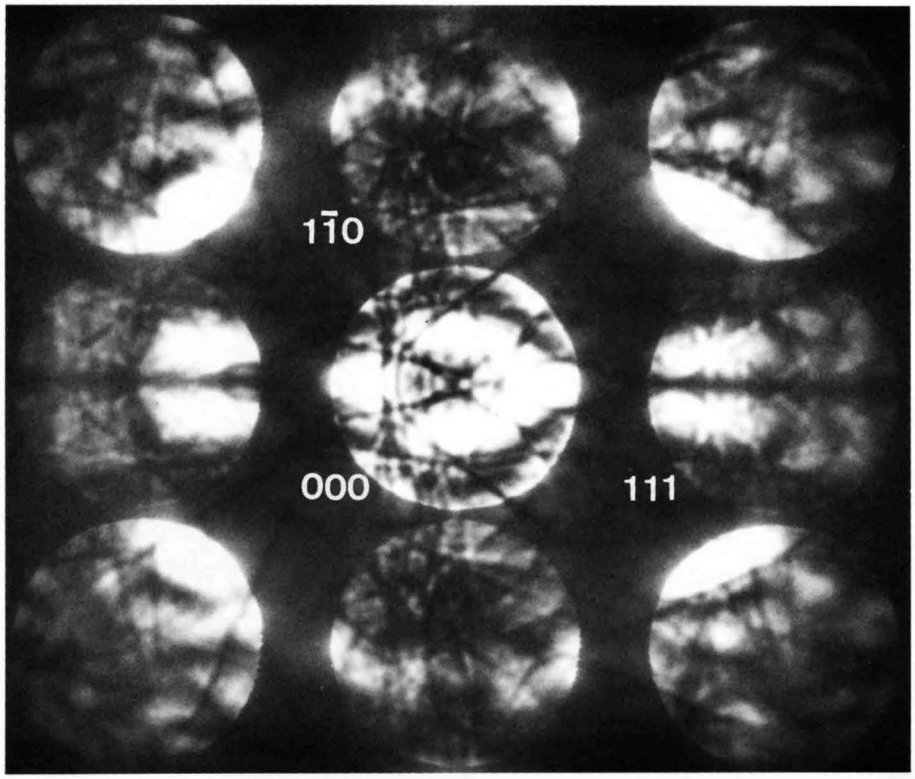

A_2-A_3 lines due to the *n*-glide plane are seen in the 111 and $\bar{1}\bar{1}\bar{1}$ disks.

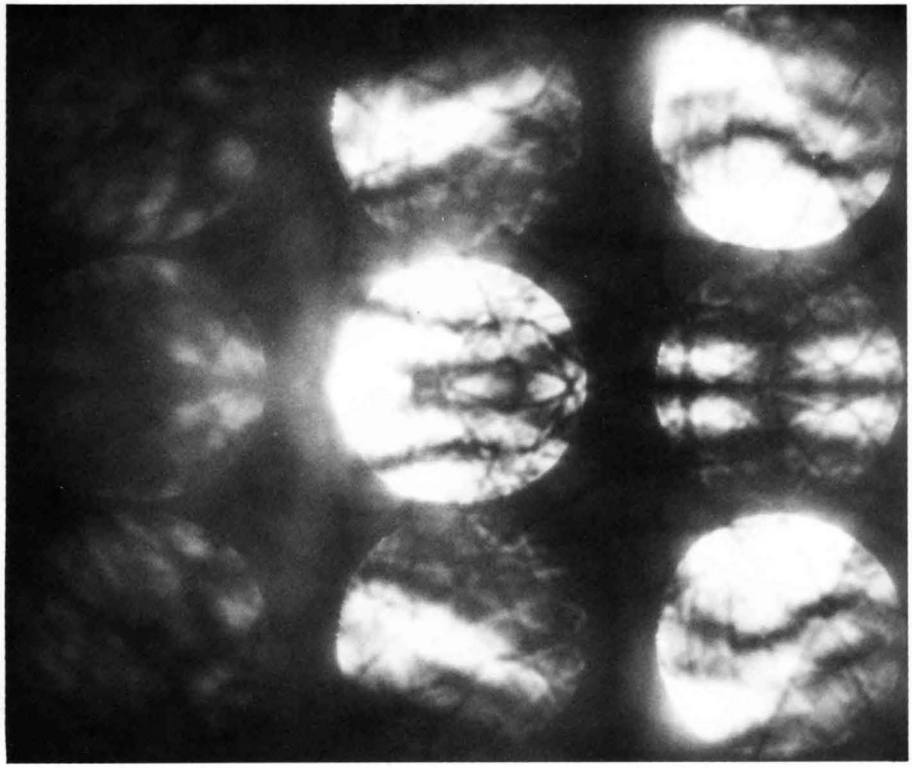

111 reflection is exactly excited. A_2-A_3 and B_2 lines due to the *n*-glide plane are seen in the 111 disk.

Materials Science (1) II-VI and III-V Semiconductors

Lattice parameters

ZnS	$a = 0.5409$nm
GaAs	$a = 0.5654$nm
InP	$a = 0.5869$nm
InAs	$a = 0.6036$nm
InSb	$a = 0.6478$nm

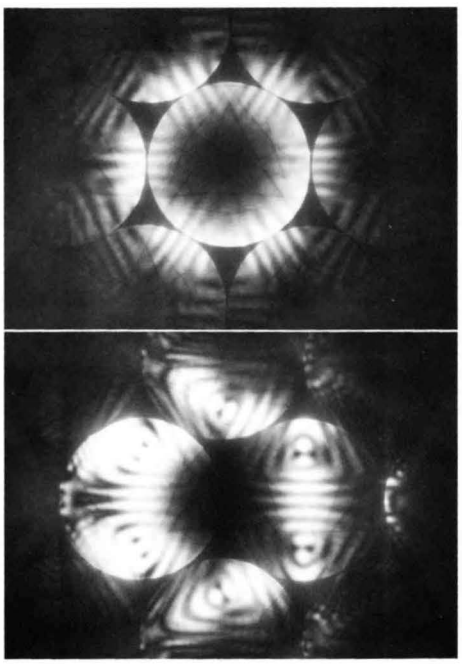

ZnS [111]

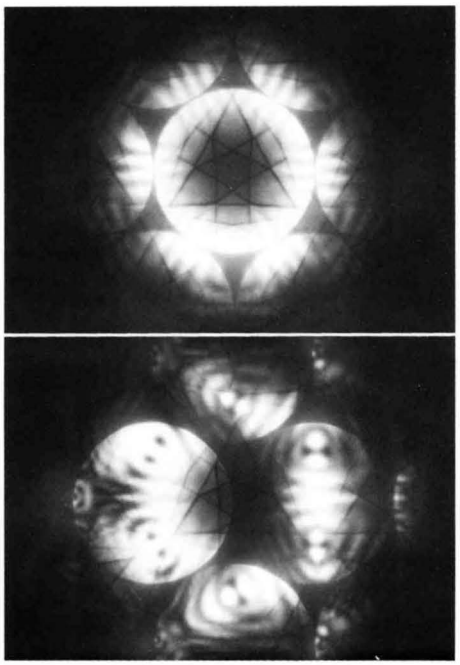

GaAs [111]

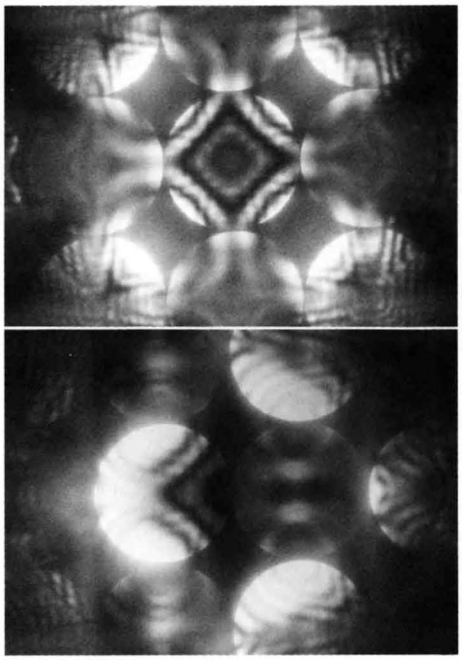

ZnS [001]

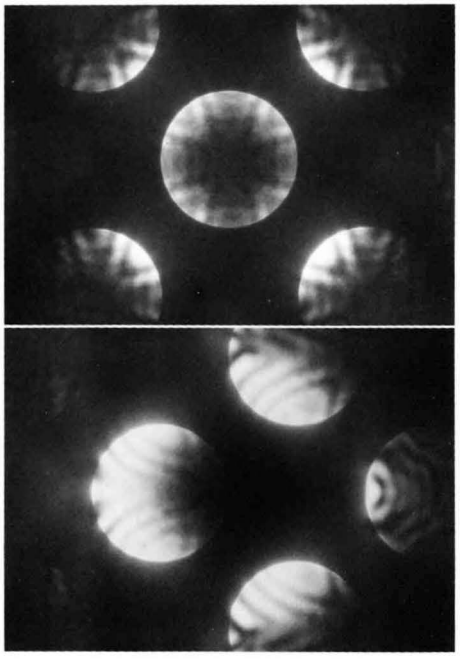

GaAs [001]

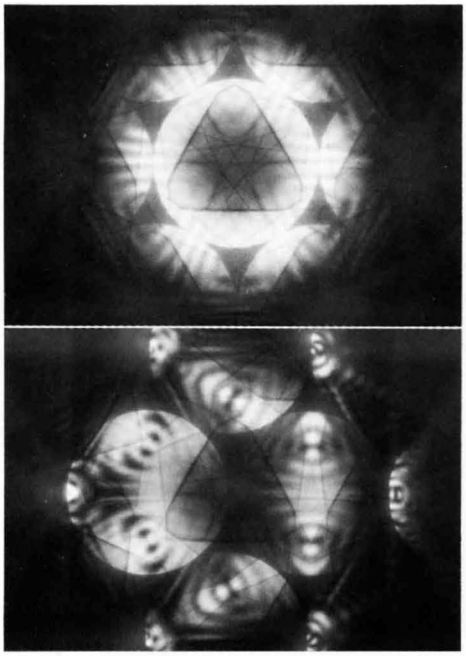

InP [111]

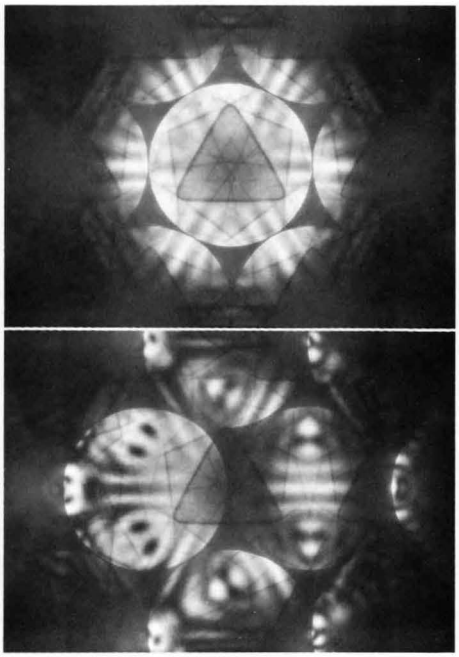

InAs [111]

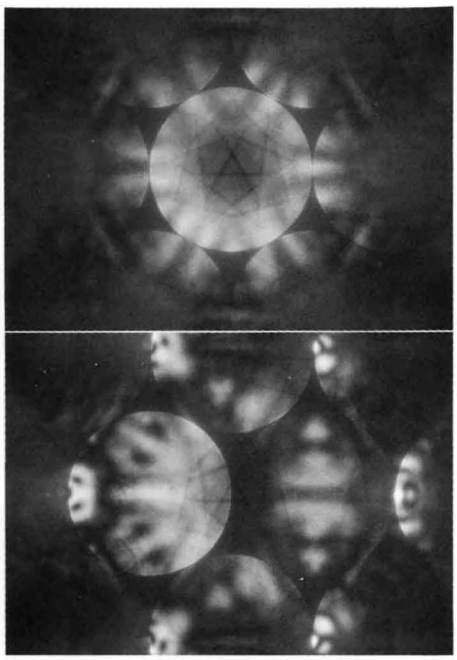

InSb [111]

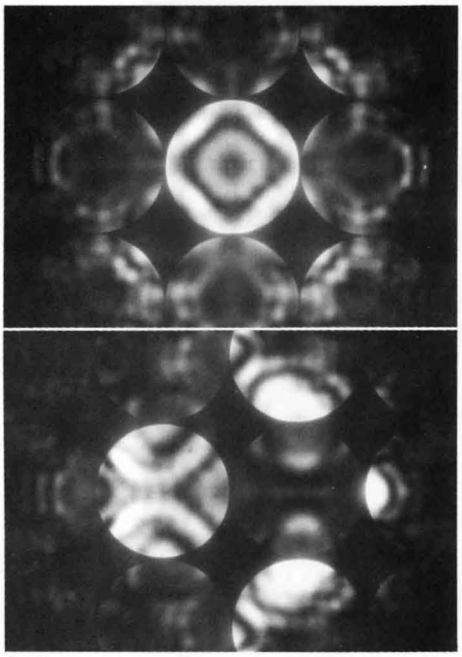

InP [001]

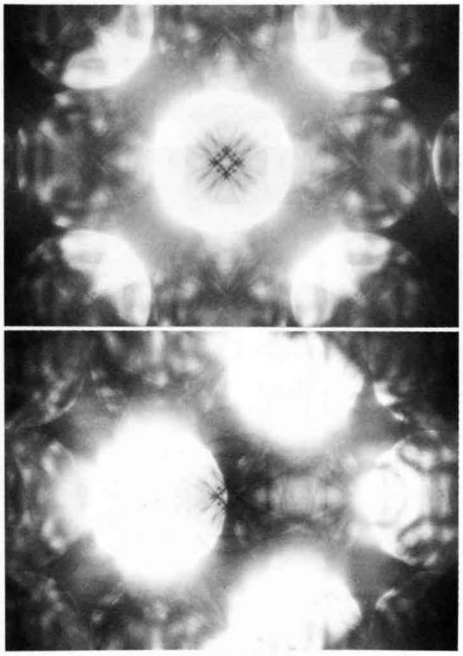

InAs [001]

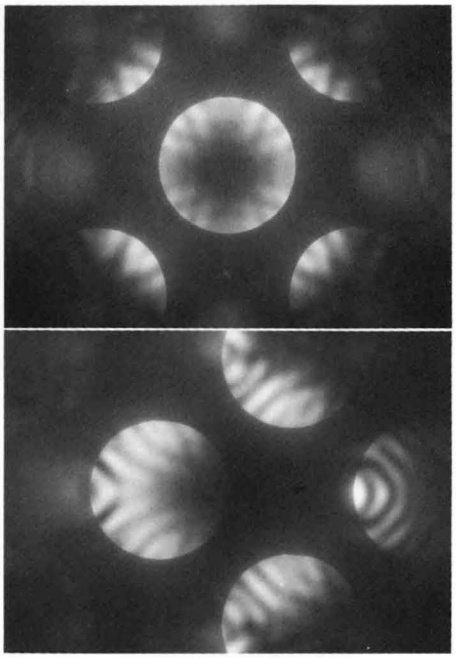

InSb [001]

ZnS [111] 80kV

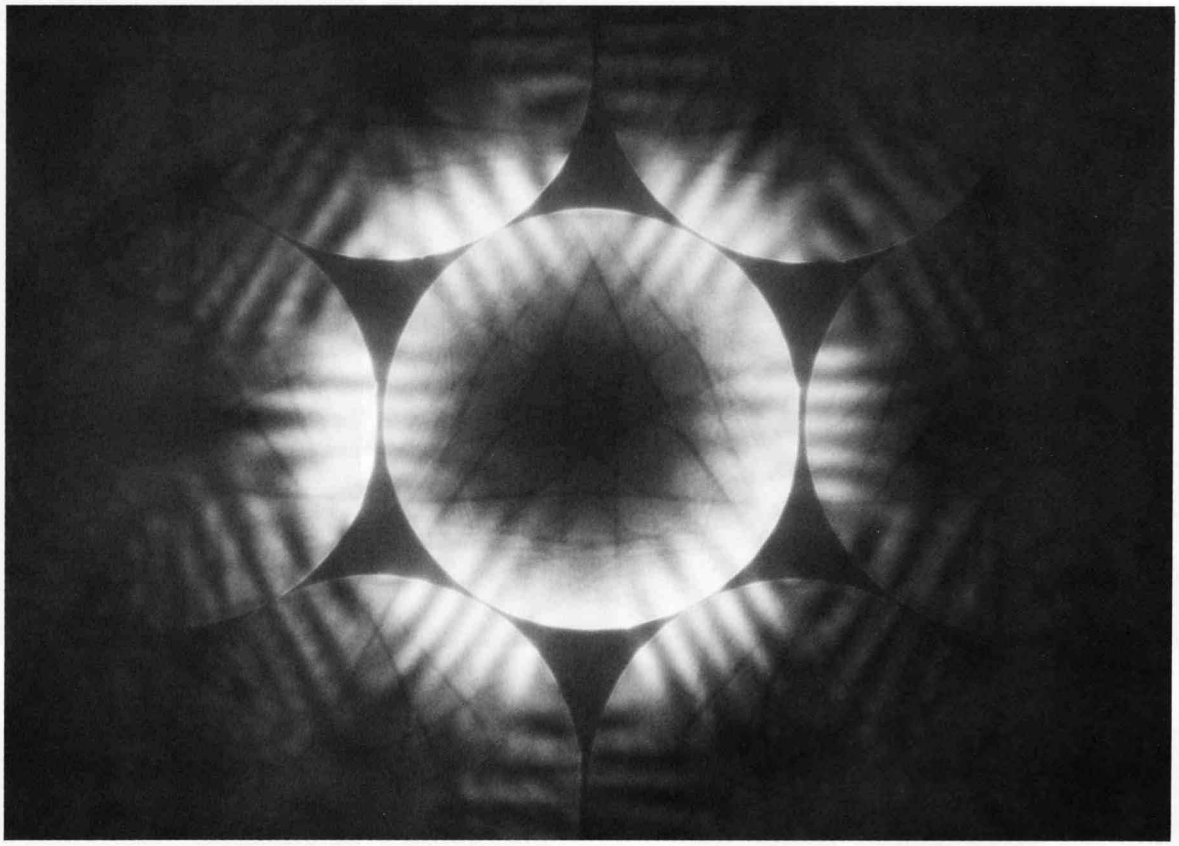

(a)

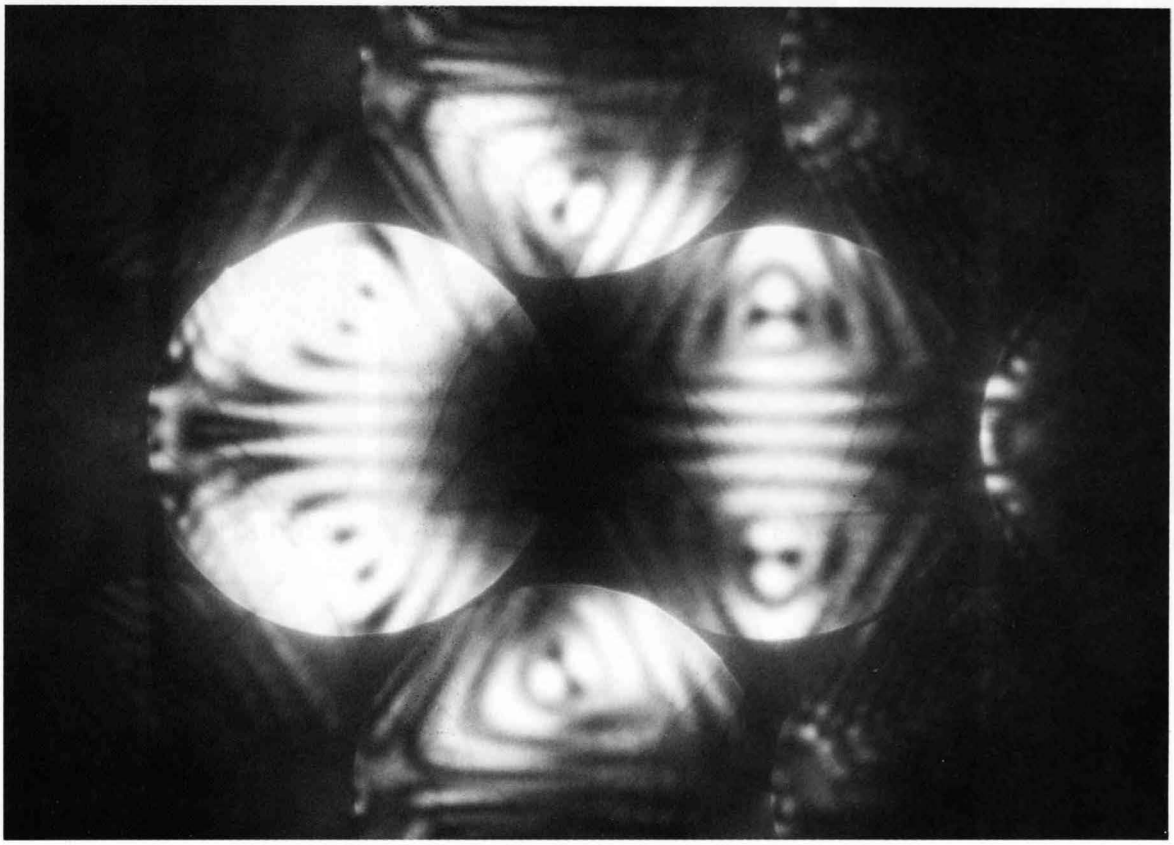

(b)

ZnS [001] 80kV

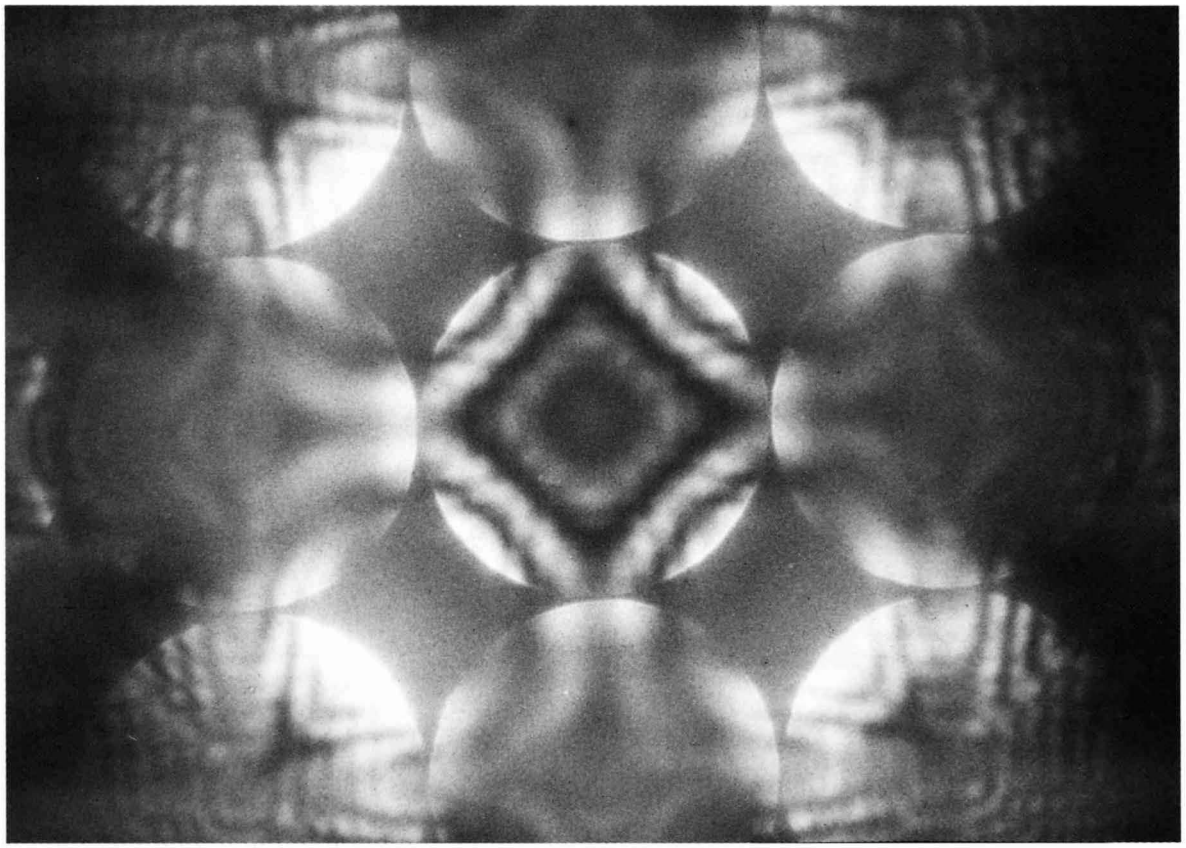

(a)

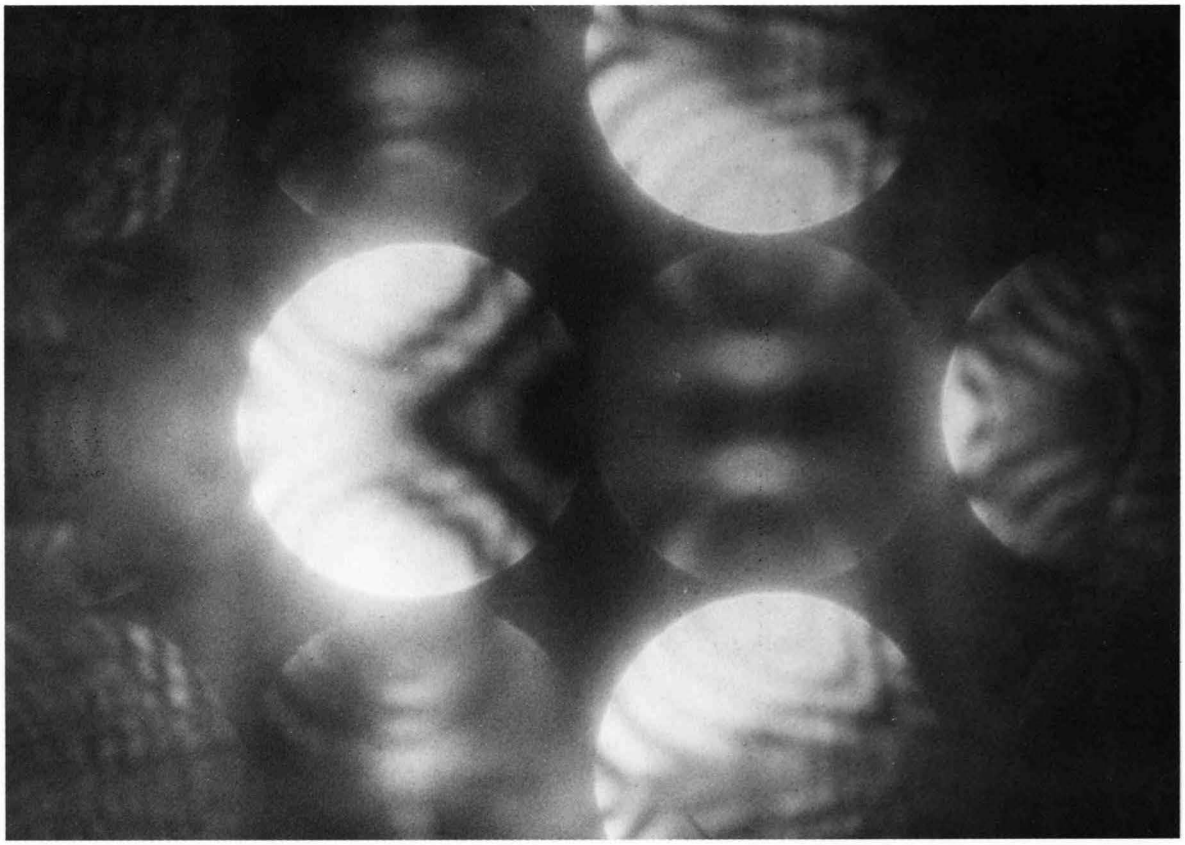

(b)

GaAs [111] 80kV

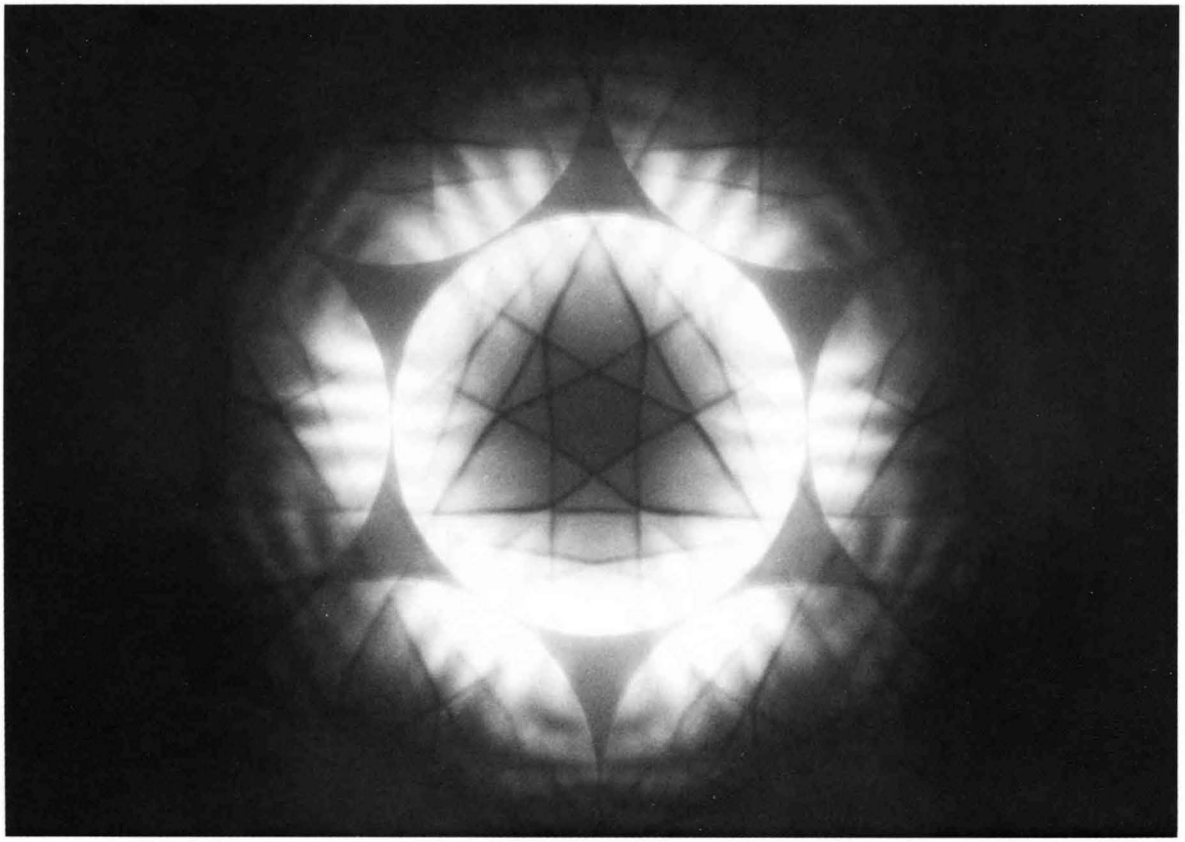

(a)

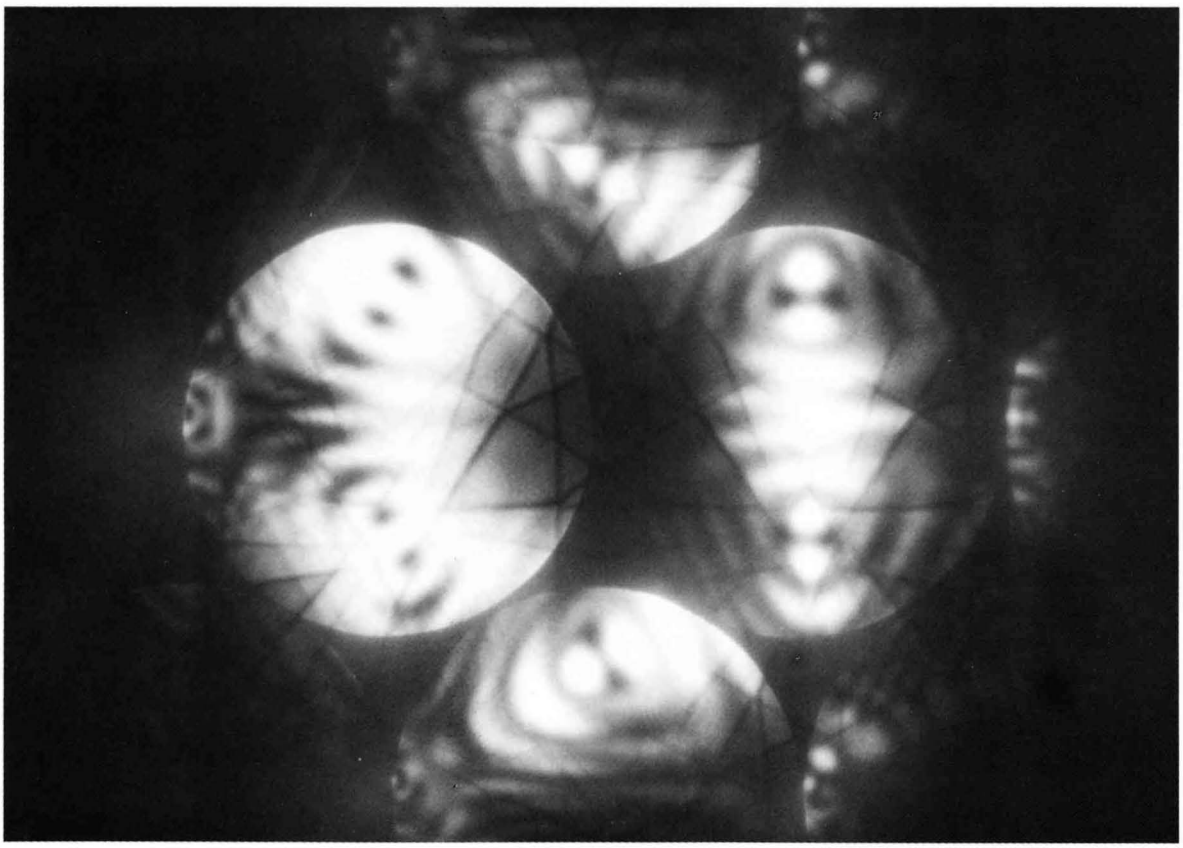

(b)

GaAs [001] 80kV

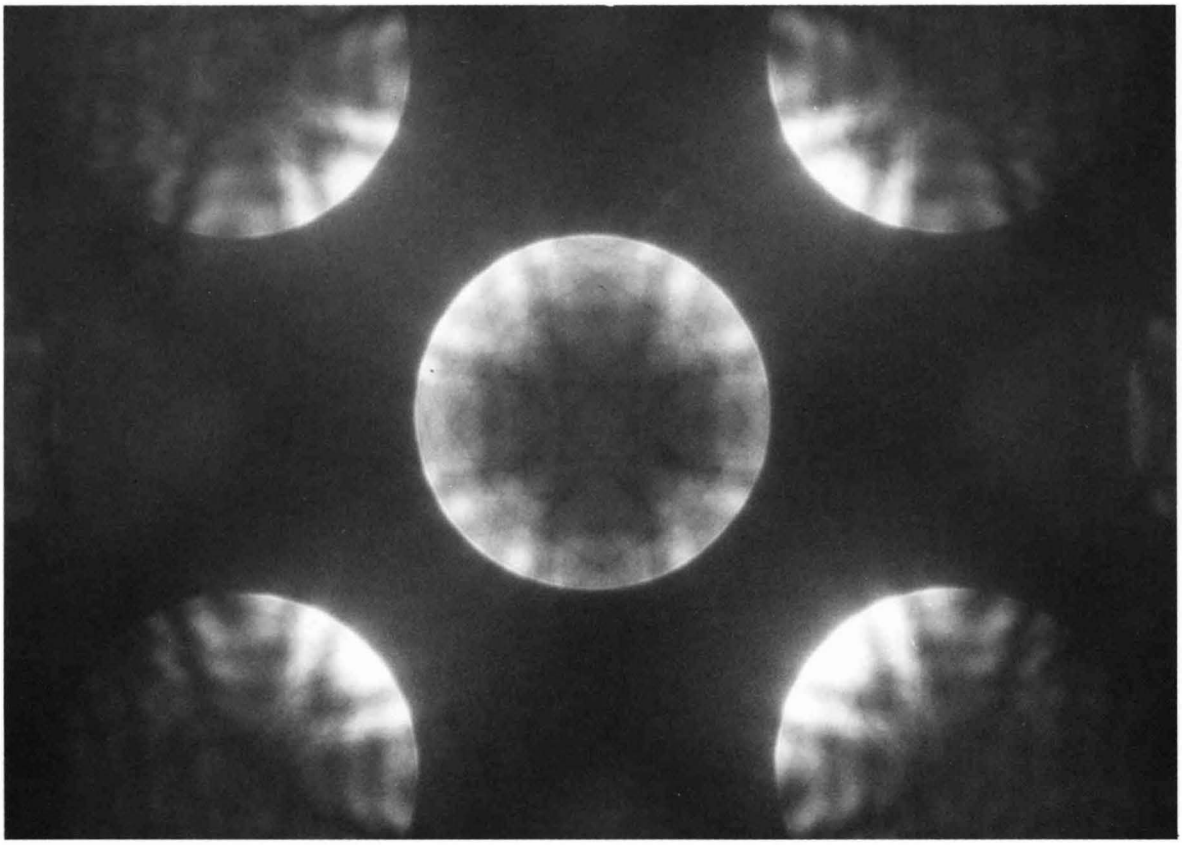

(a)

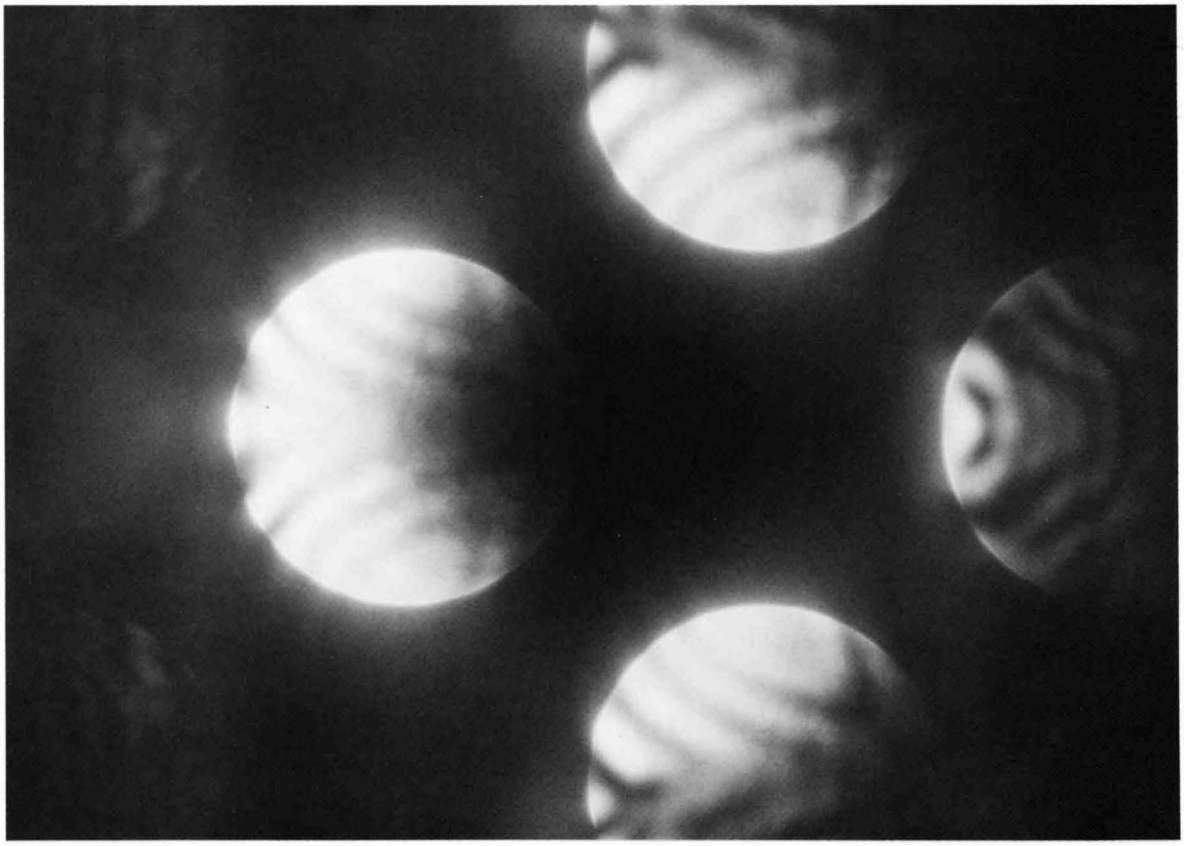

(b)

InP [111] 80kV

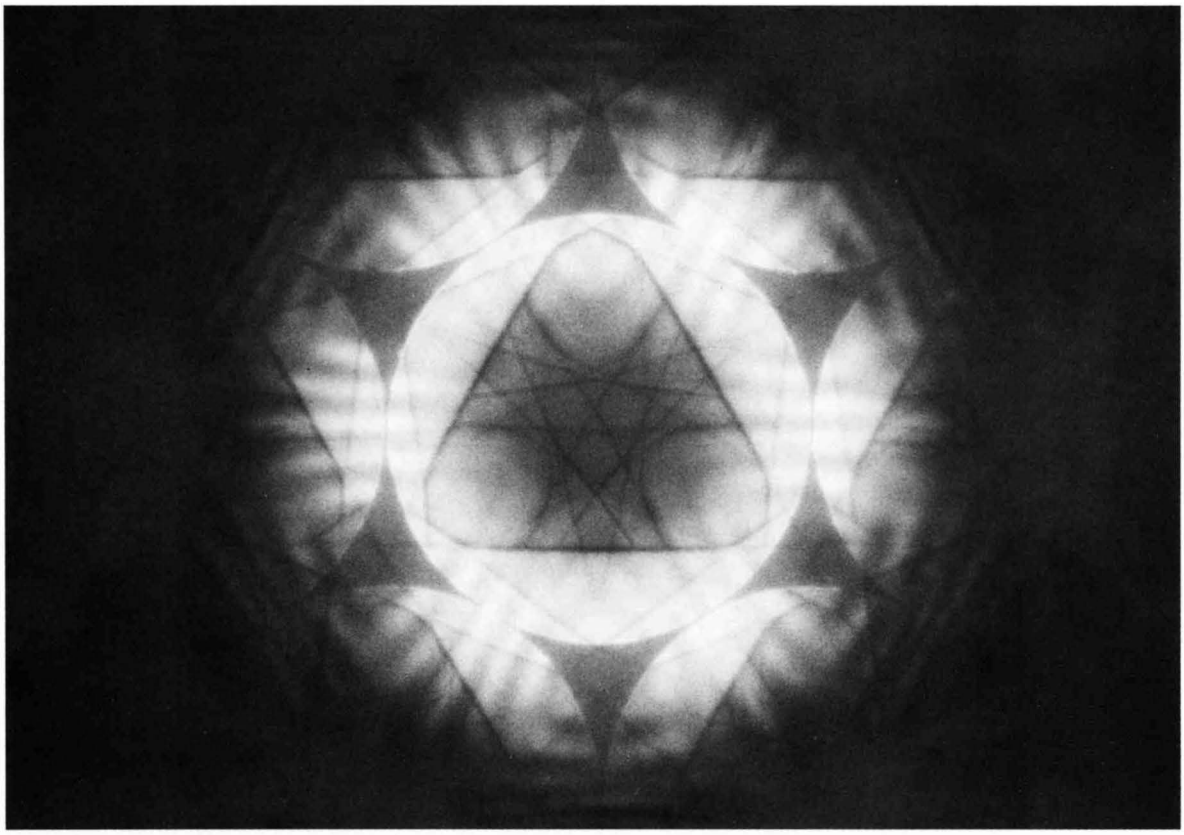

(a)

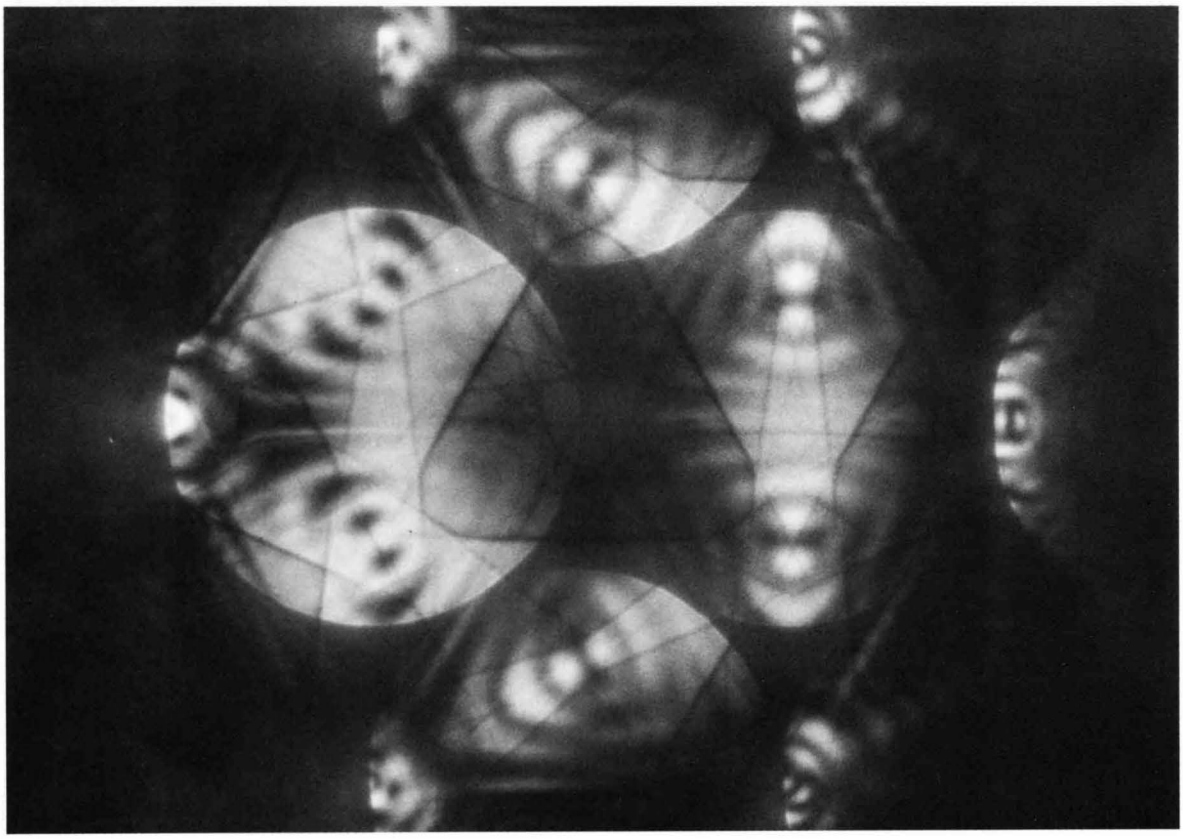

(b)

InP [001] 80kV

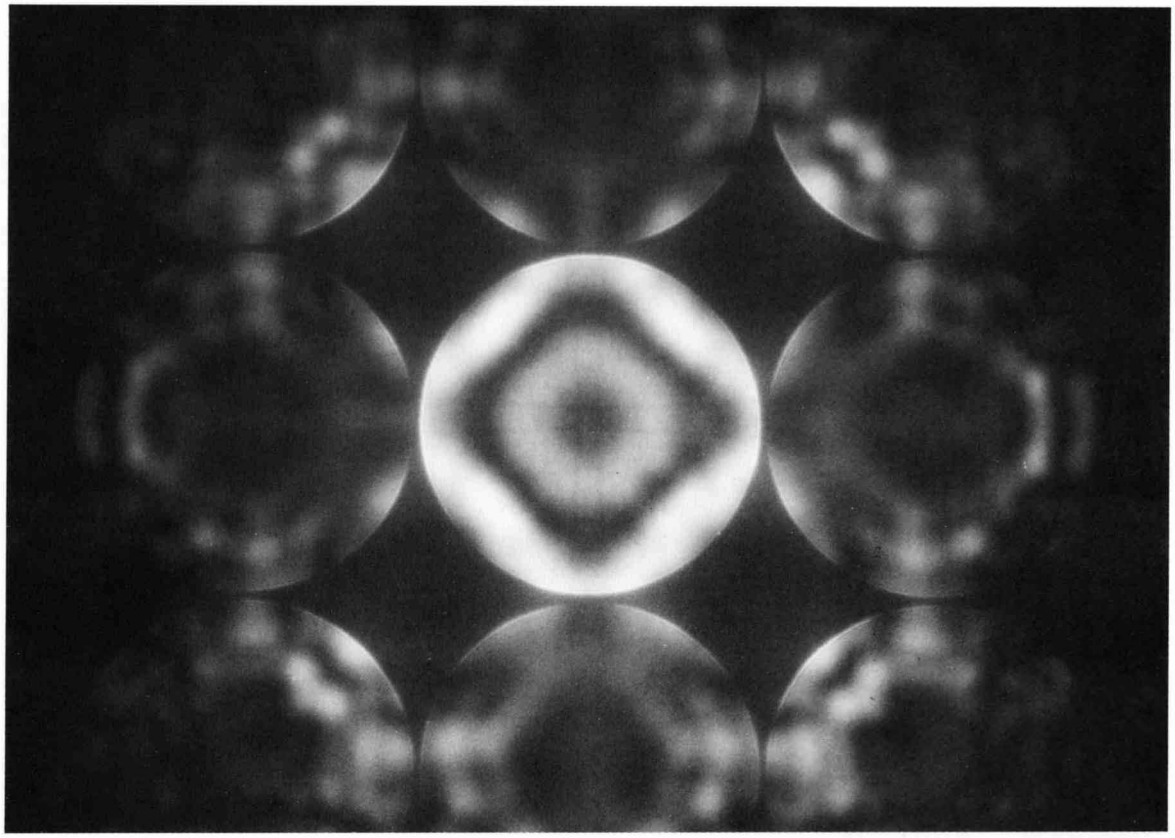

(a)

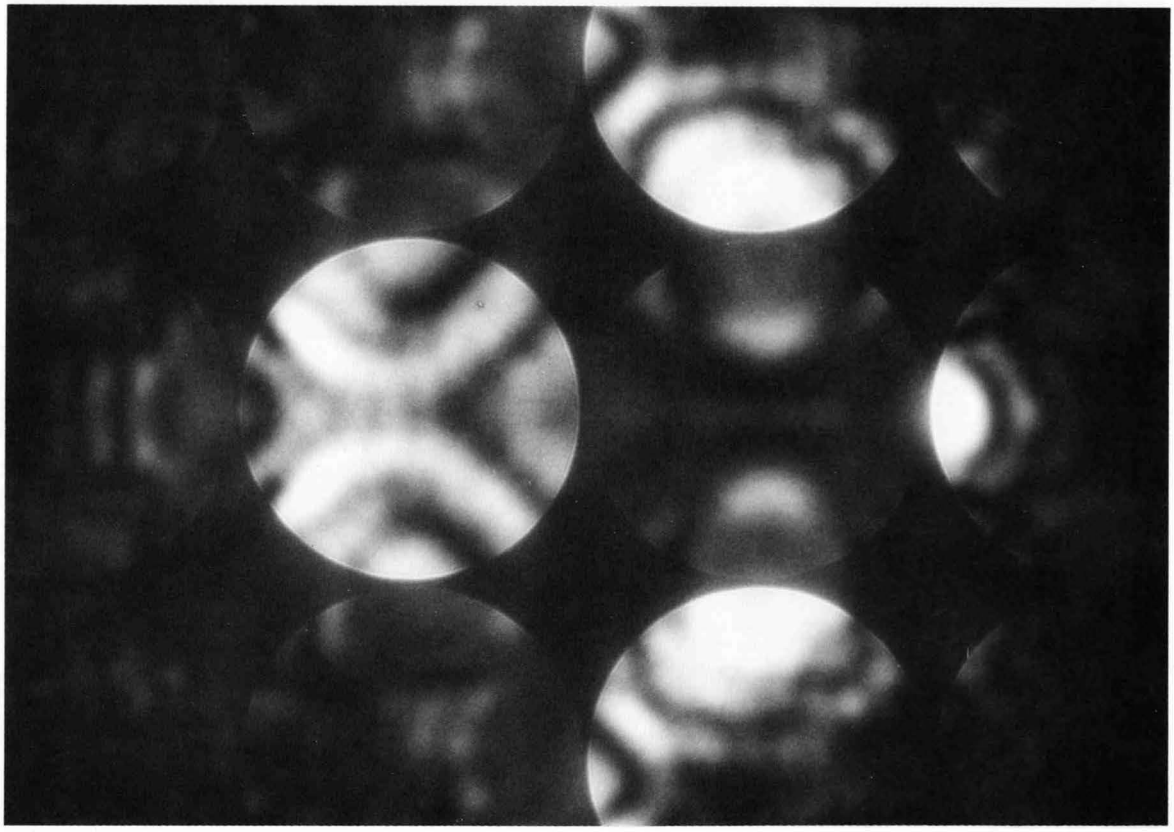

(b)

InAs [111] 80kV

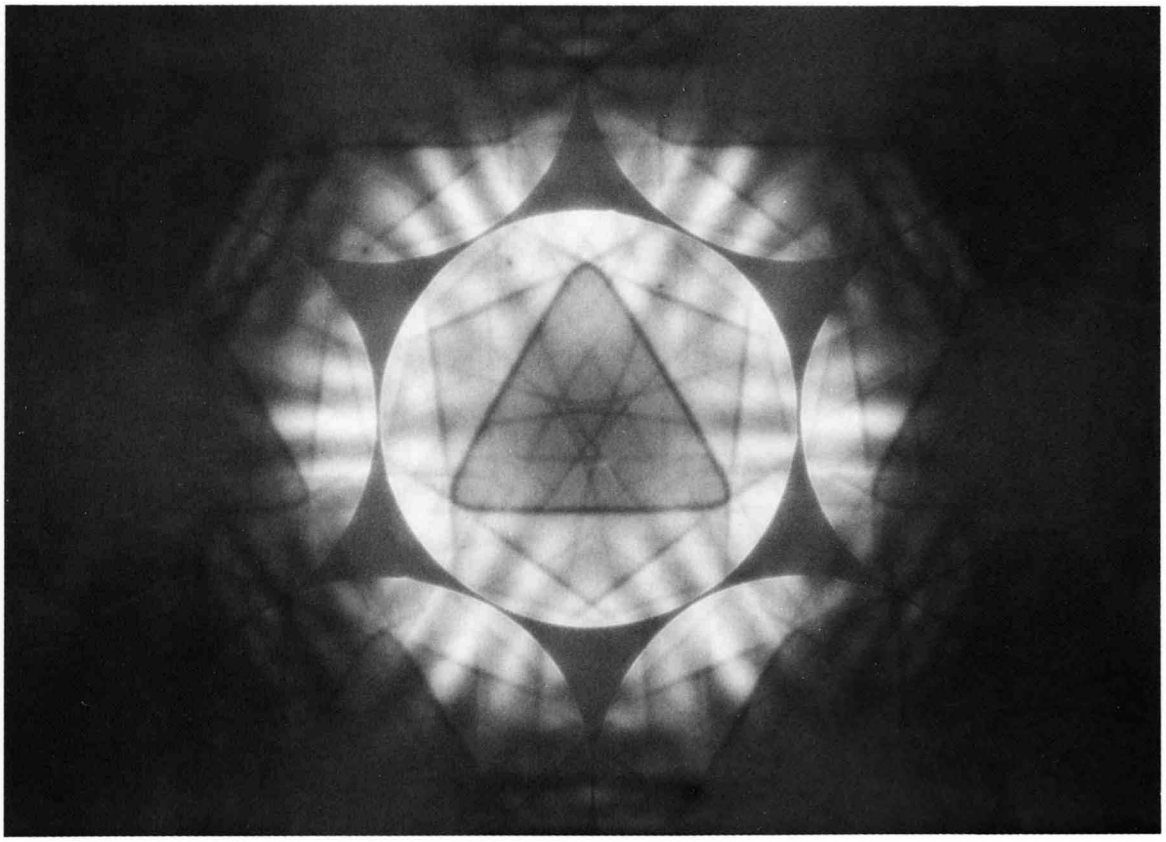

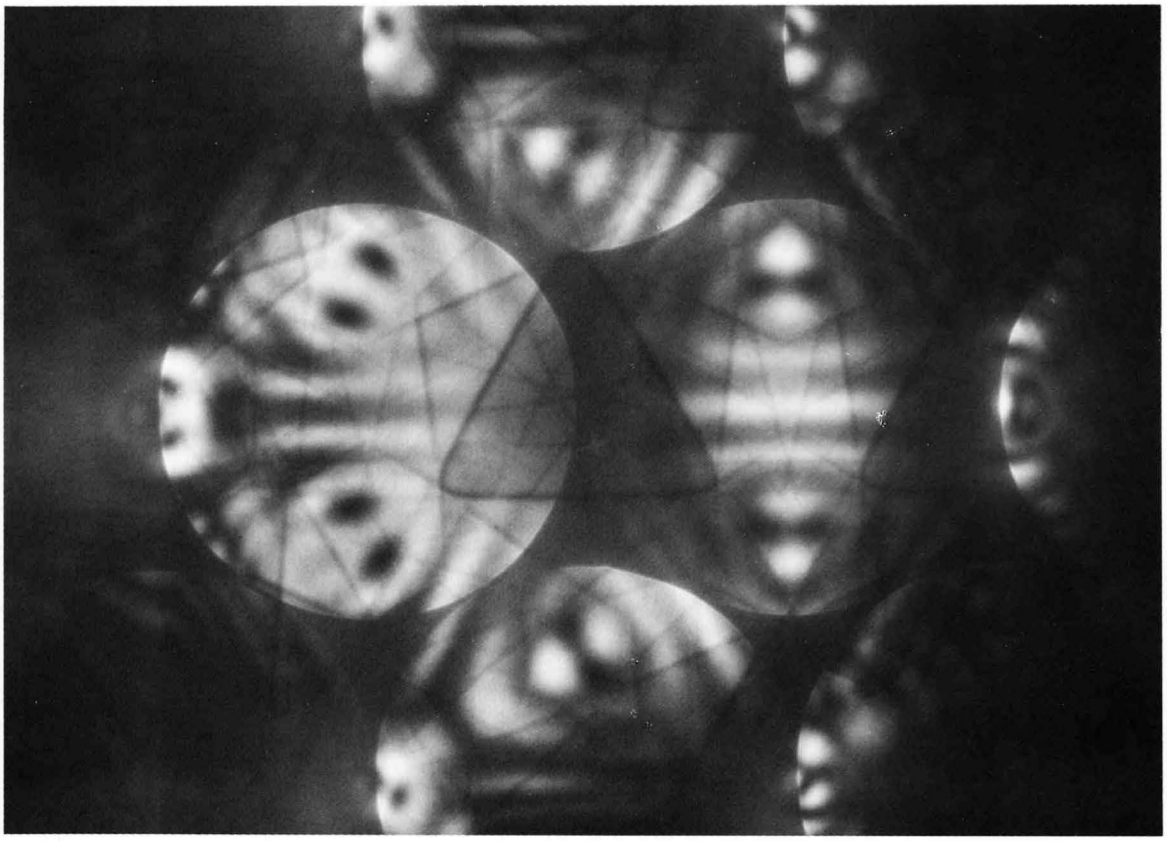

InAs [001] 80kV

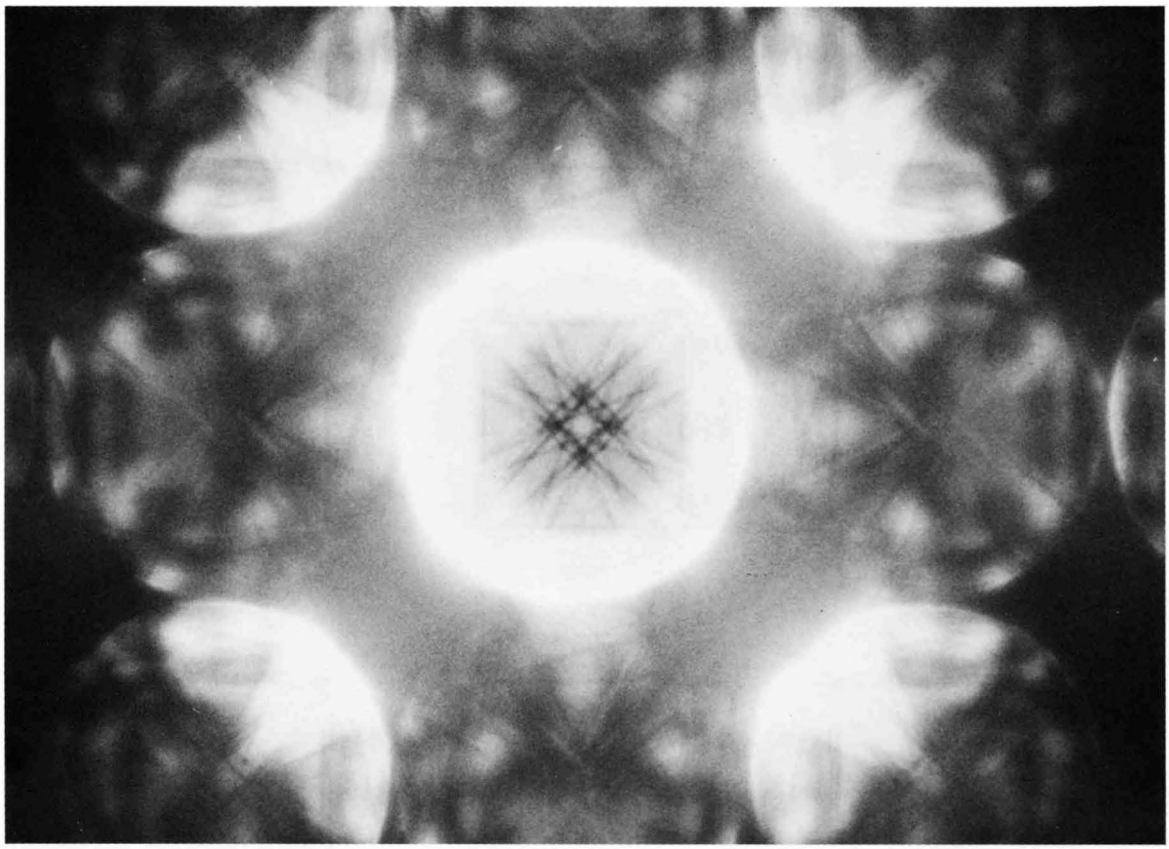

(a)

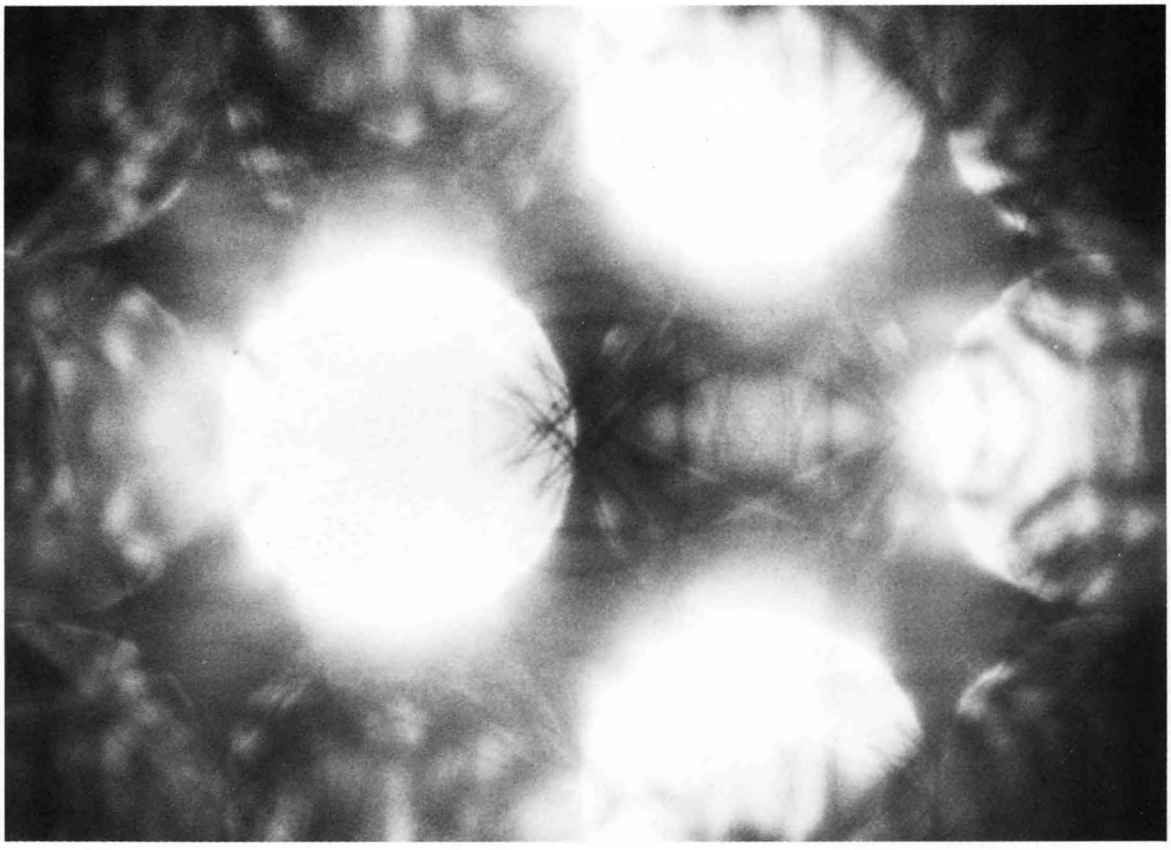

(b)

InSb [111] 80kV

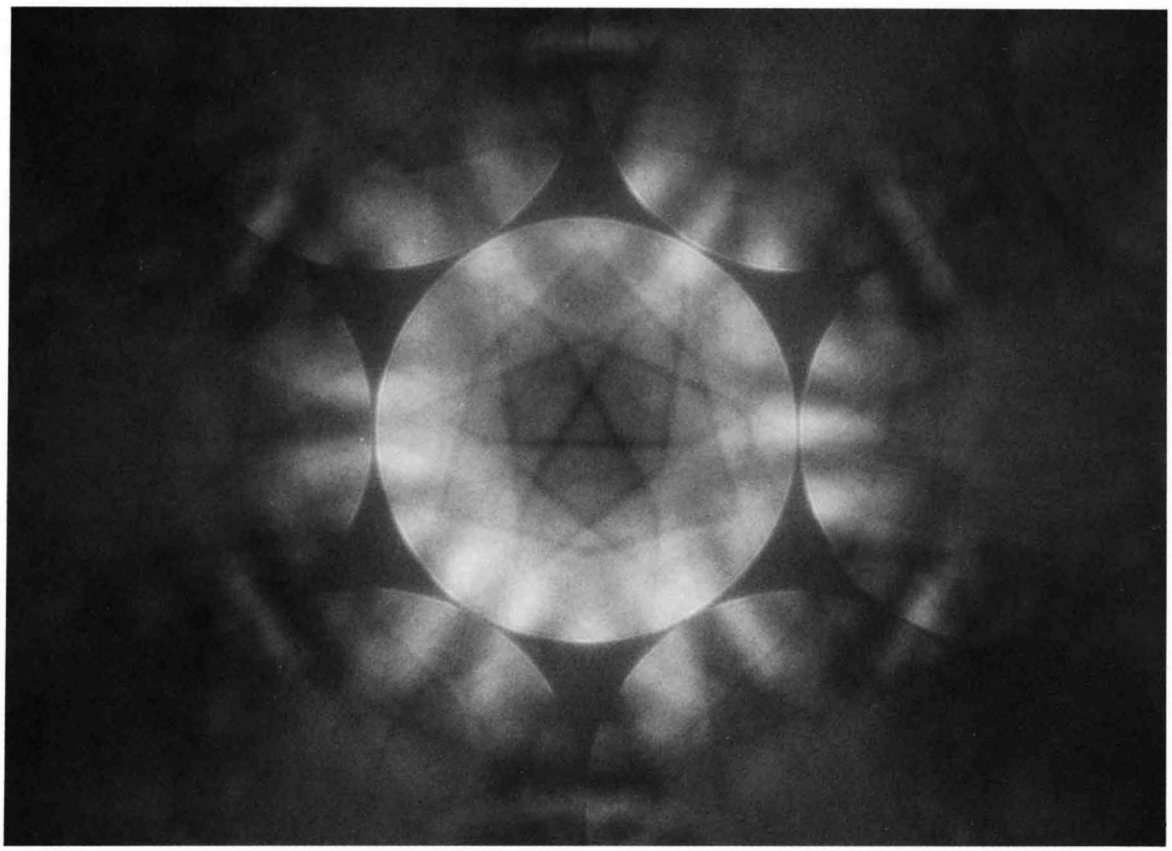

(a)

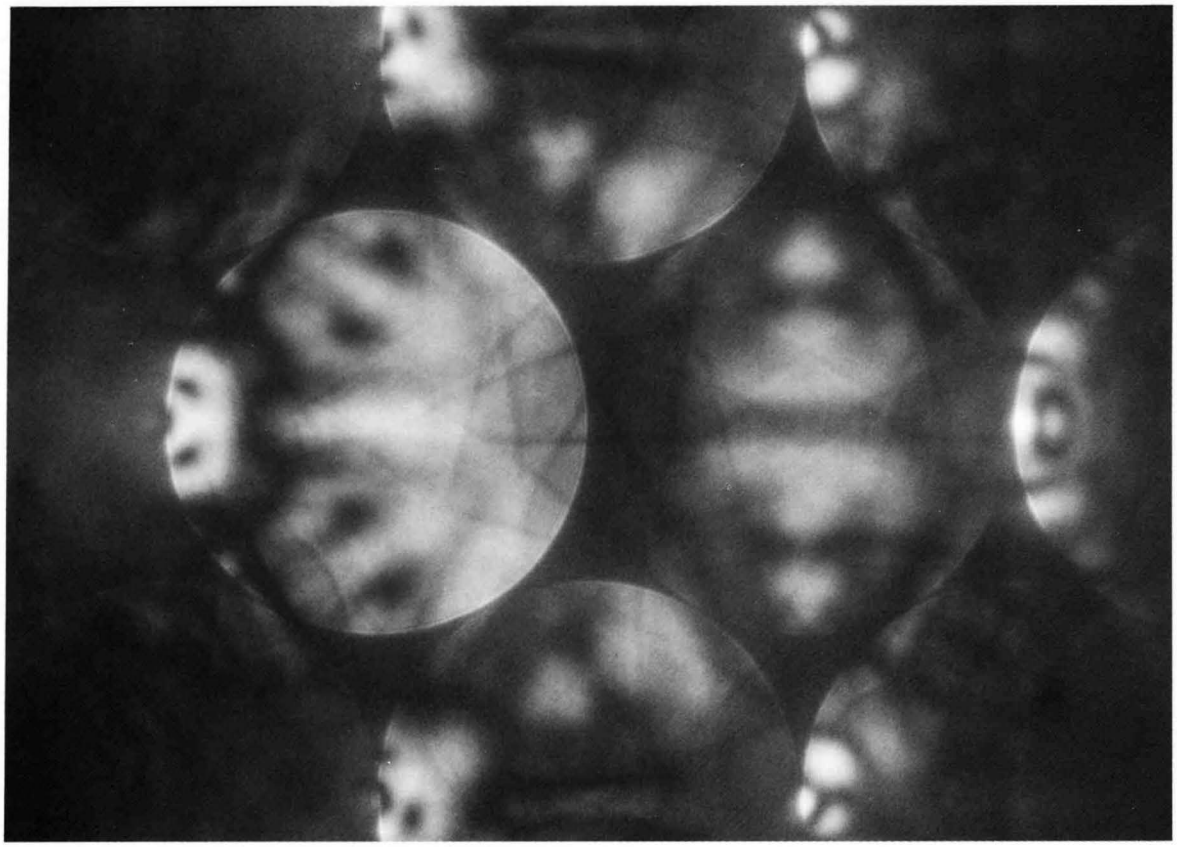

(b)

InSb [001] 80kV

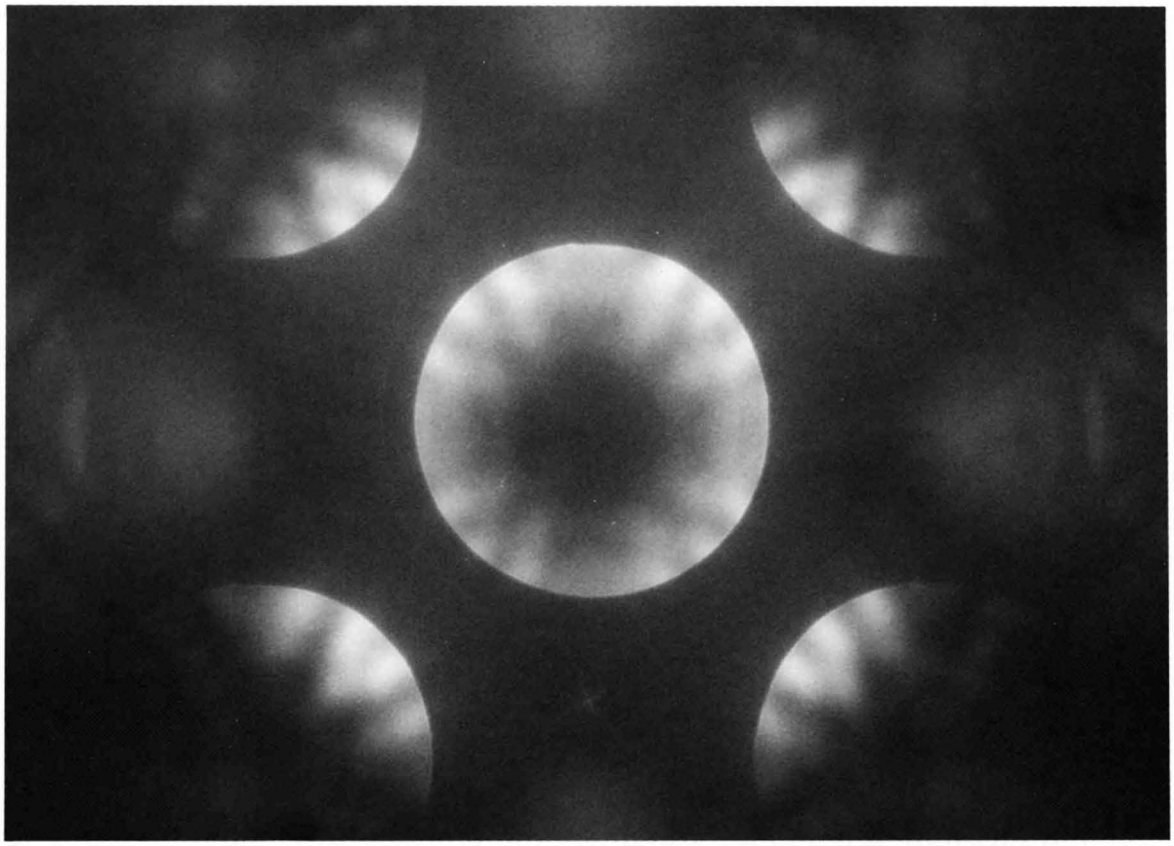

(a)

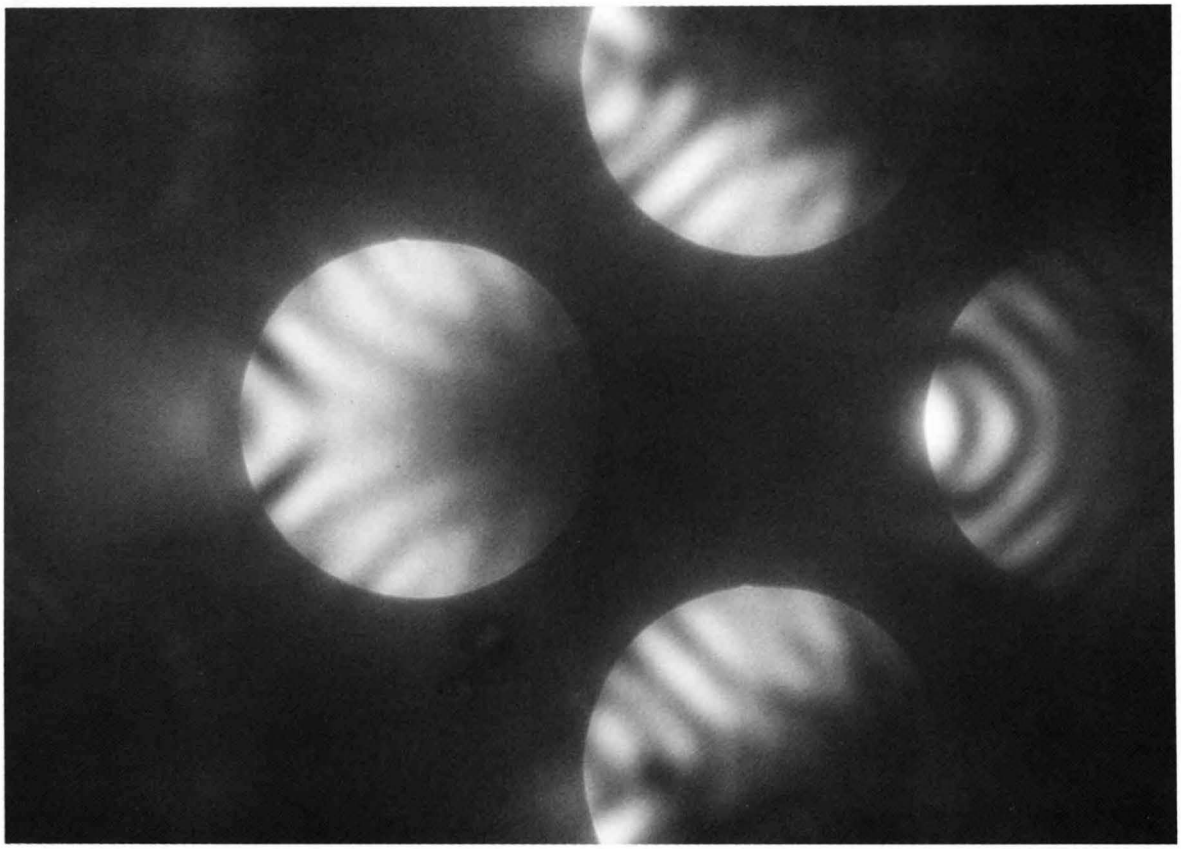

(b)

Materials Science (2) Polytypes and Stacking Faults

SiC [0001]

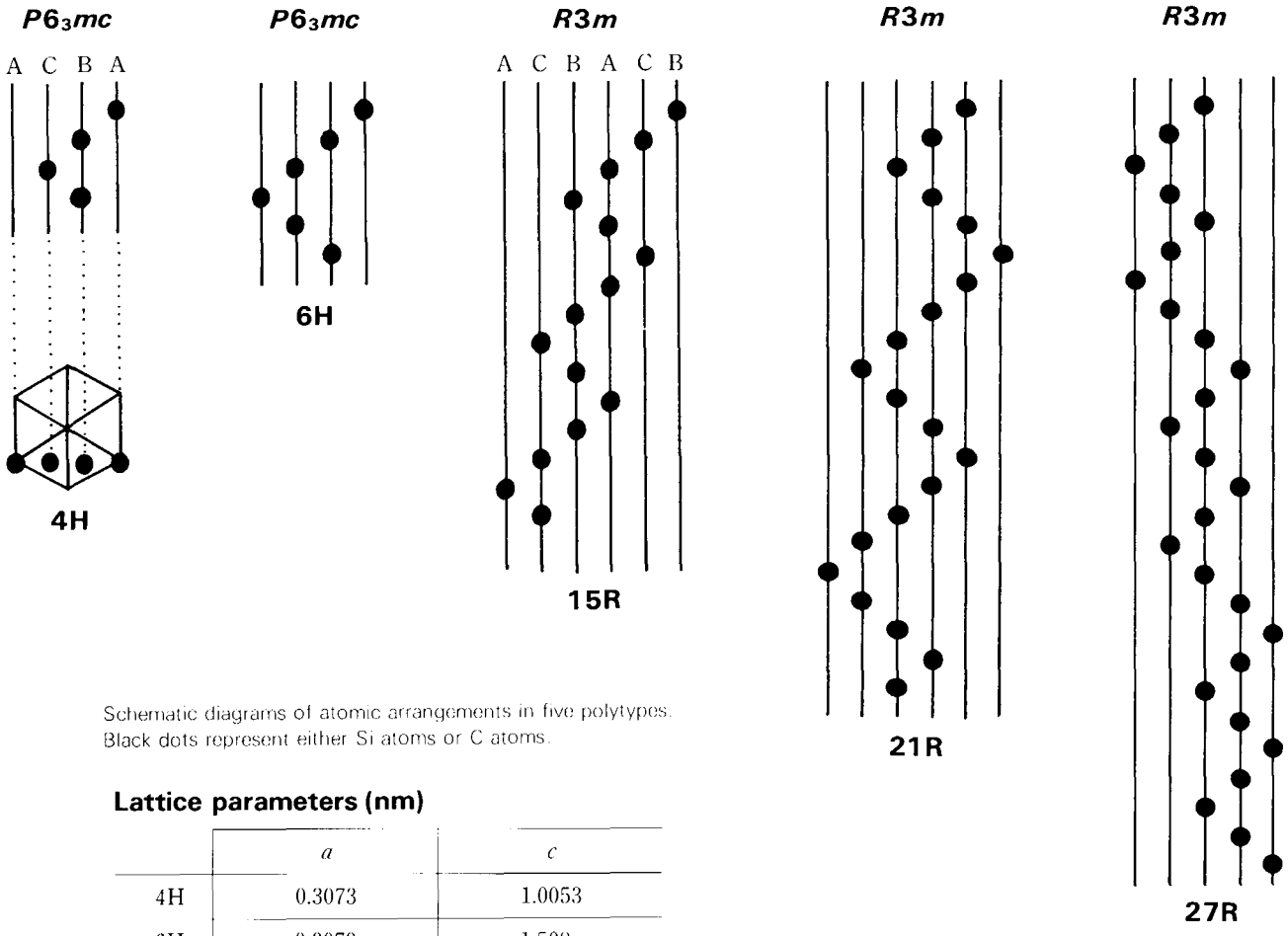

Schematic diagrams of atomic arrangements in five polytypes. Black dots represent either Si atoms or C atoms.

Lattice parameters (nm)

	a	*c*
4H	0.3073	1.0053
6H	0.3073	1.508
15R	0.3073	3.770
21R	0.3073	5.278
27R	0.3079	6.7996

Symmetry table for the five polytypes.

	Space Group	Point Group	Diffraction Group	BP	WP	DP	+DP
4H 6H	$P6_3mc$	$6mm$	$6mm$	$6m_V m_V$	$6m_V m_V$	$\begin{cases} 1 \\ m_V \end{cases}$	2 $2m_V(m_V)$
15R 21R 27R	$R3m$	$3m$	$3m$	$3m_V$	$3m_V$	$\begin{cases} 1 \\ m_V \end{cases}$	$\begin{cases} 1 \\ m_V \\ 1 \end{cases}$

SiC 4H $P6_3mc$

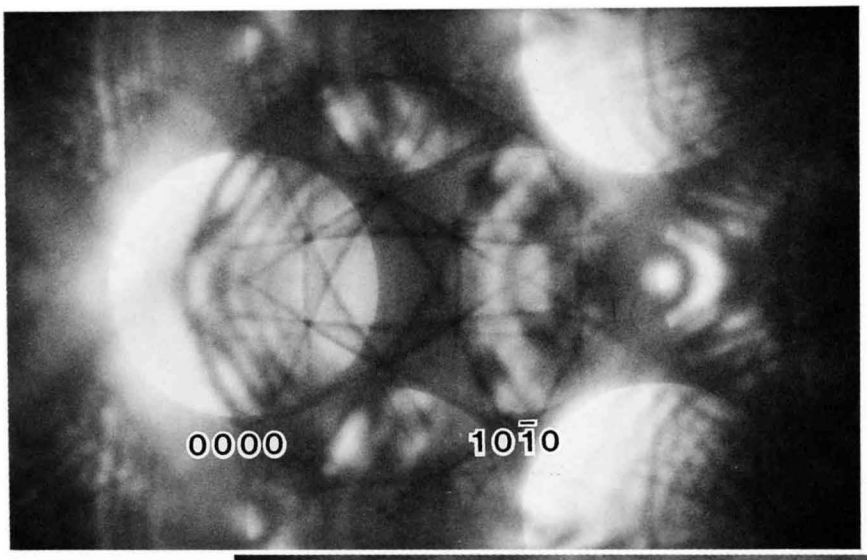

(a)

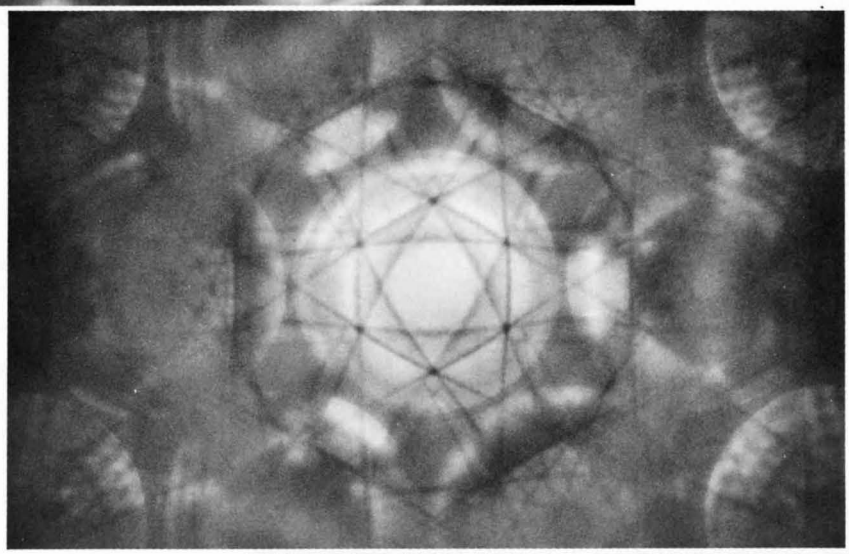

(b)

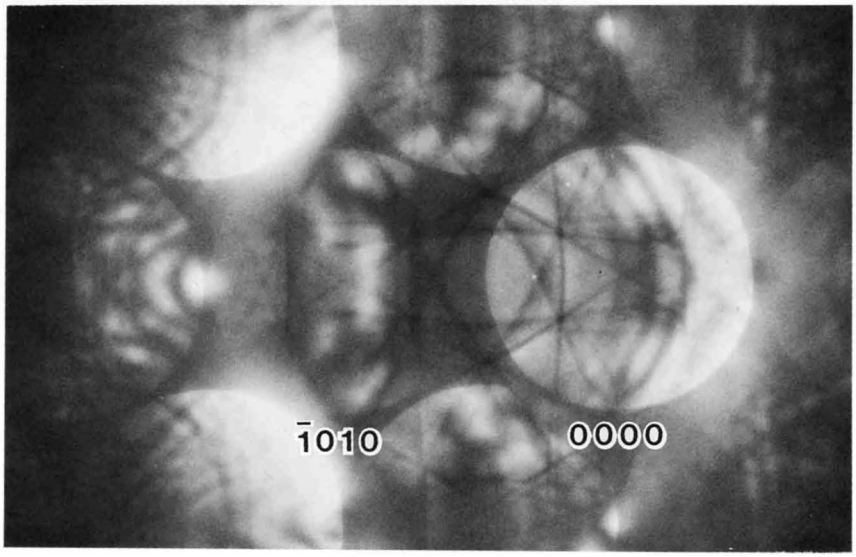

(c)

SiC 6H 200kV

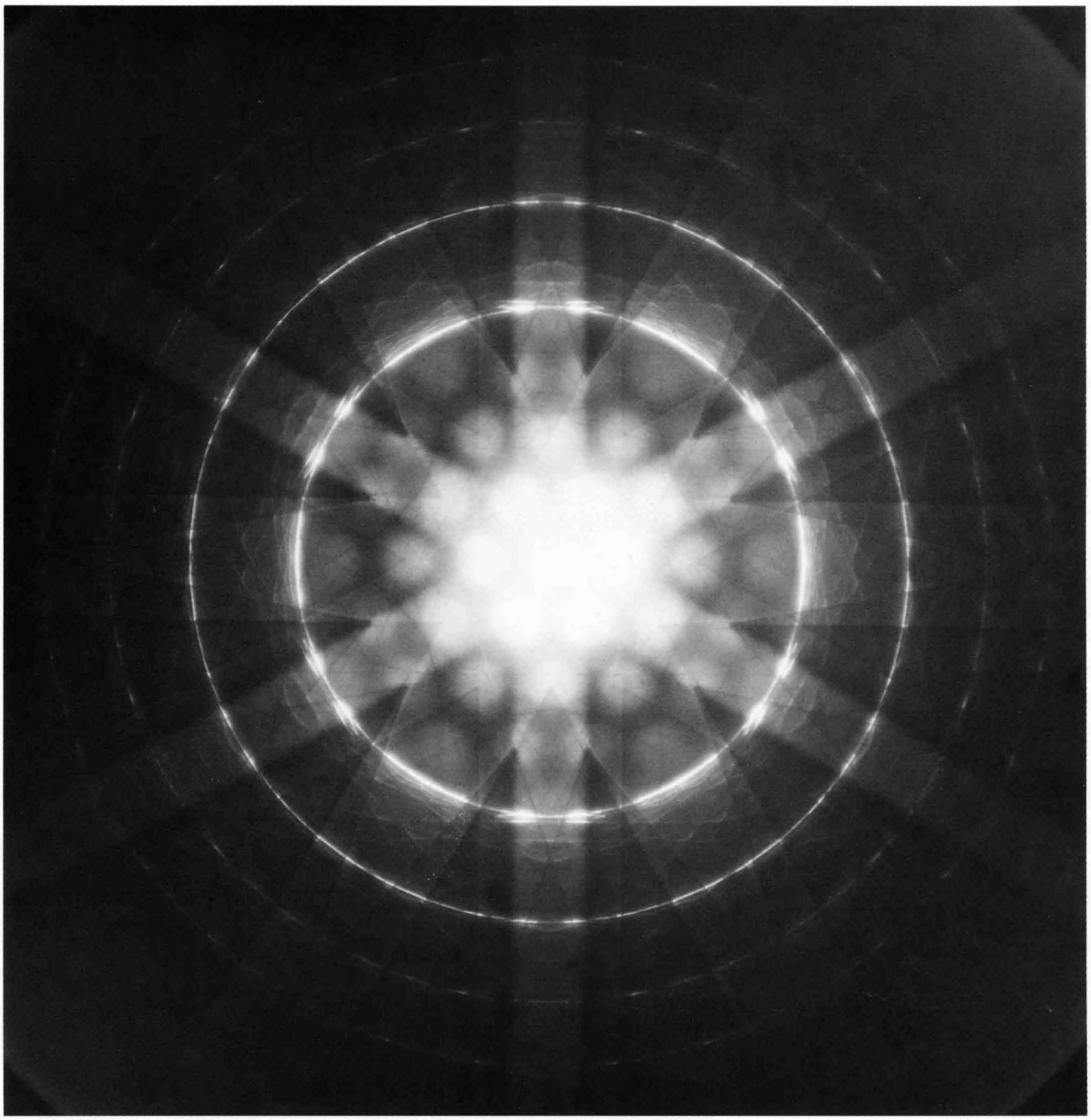

SiC 6H $P6_3mc$ 200kV

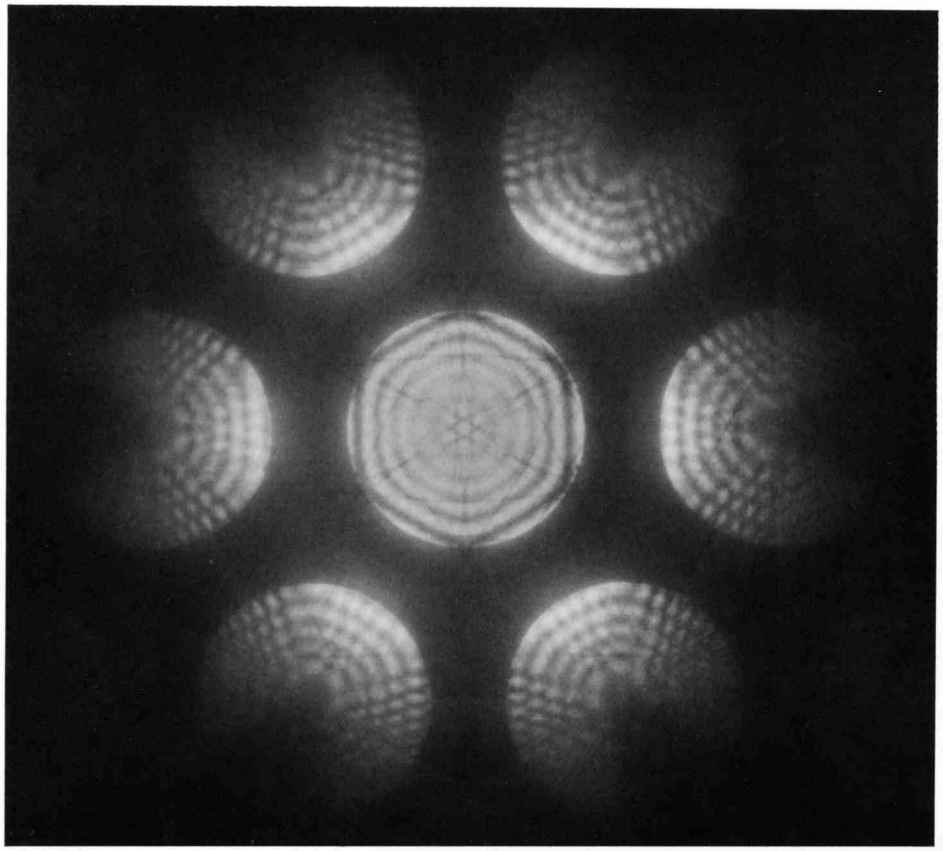

(a)

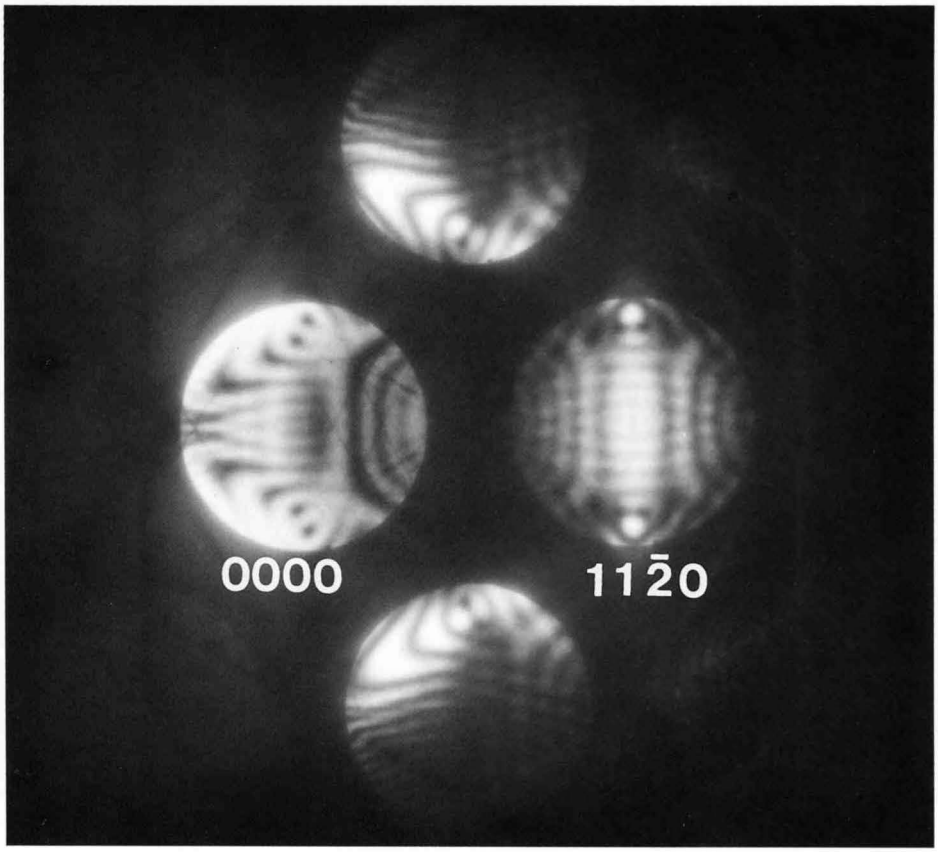

(b)

SiC 6H

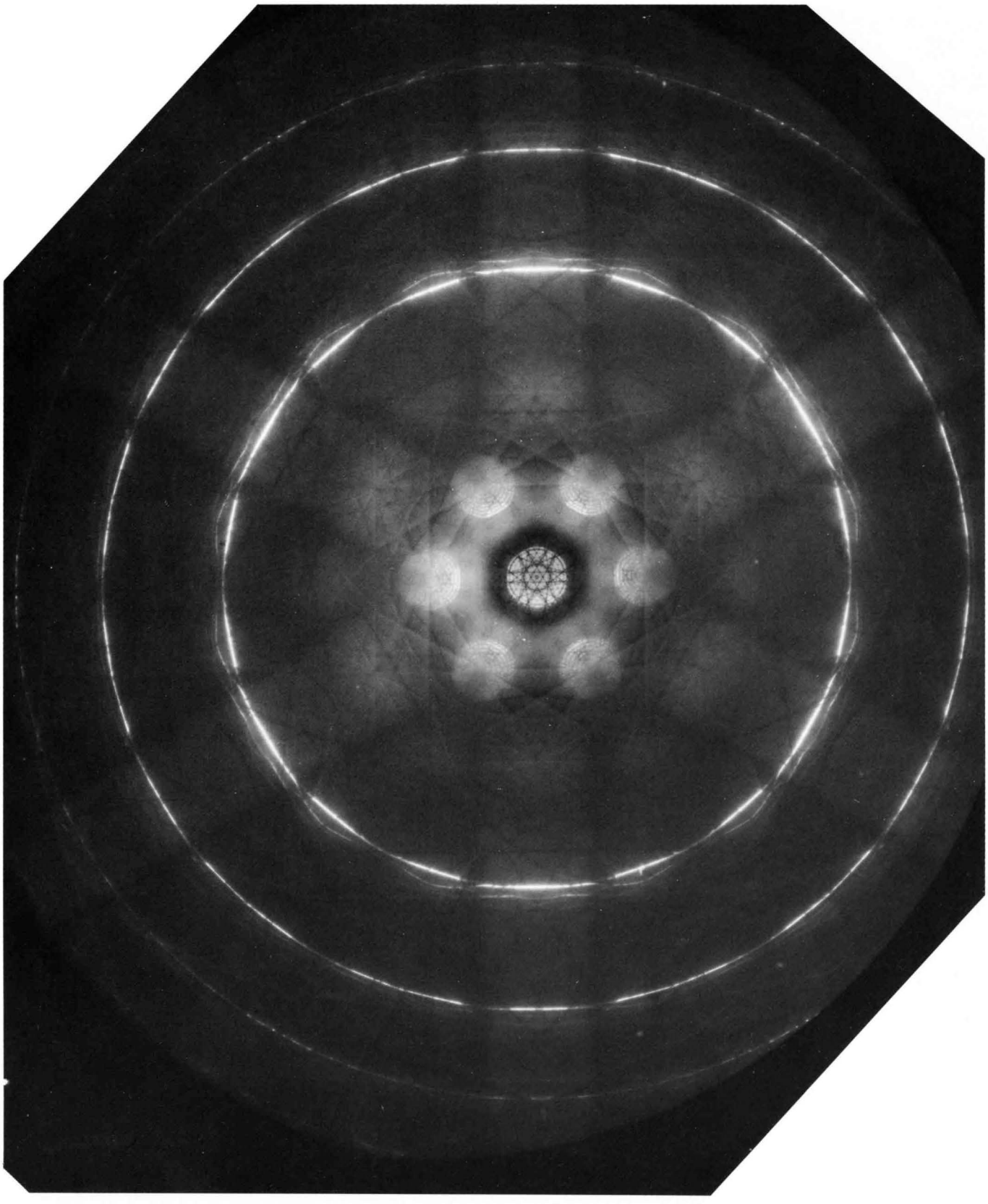

SiC 6H $P6_3mc$

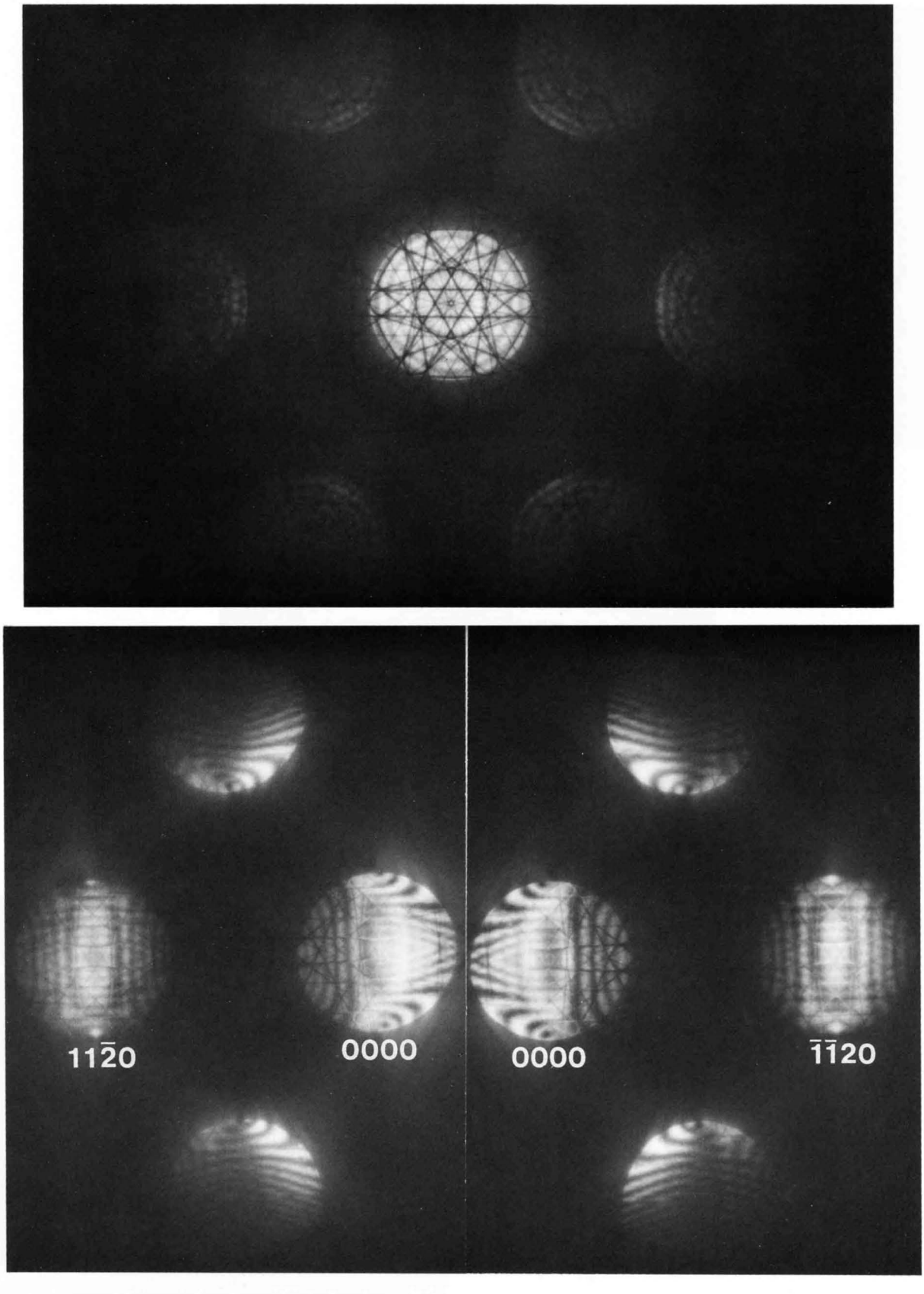

SiC 15R *R*3*m*

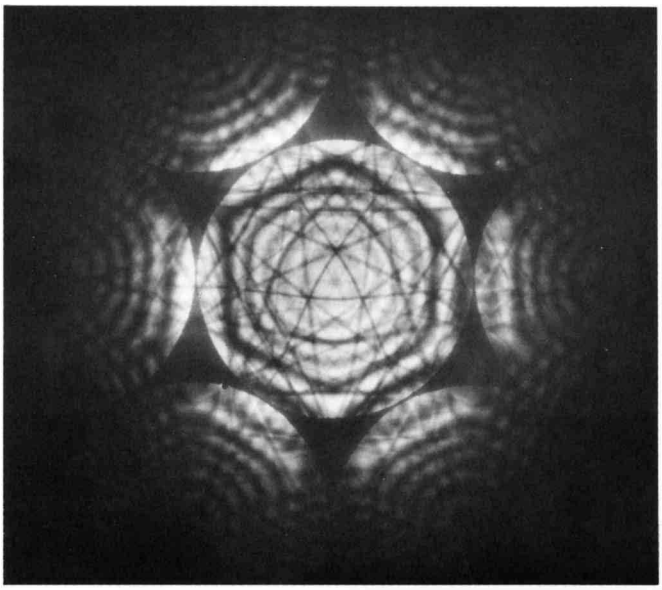

(a)

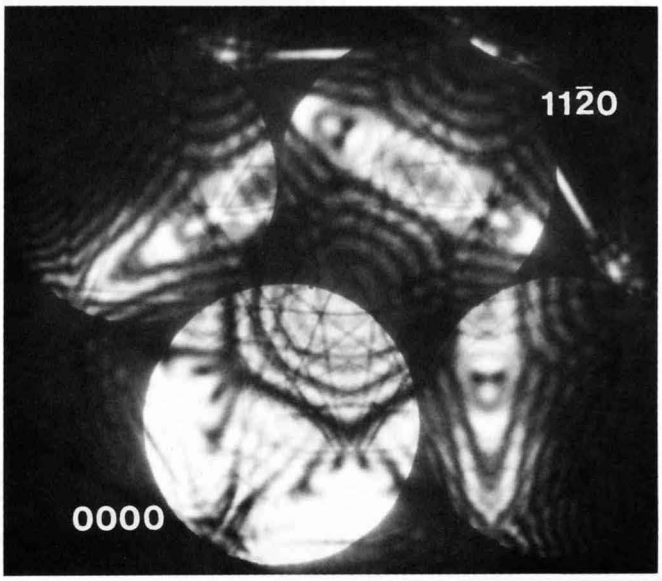

(b)

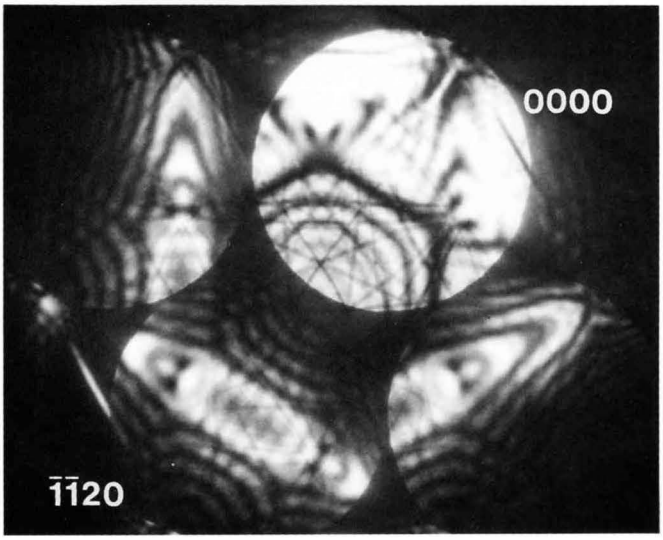

(c)

SiC 21R *R3m*

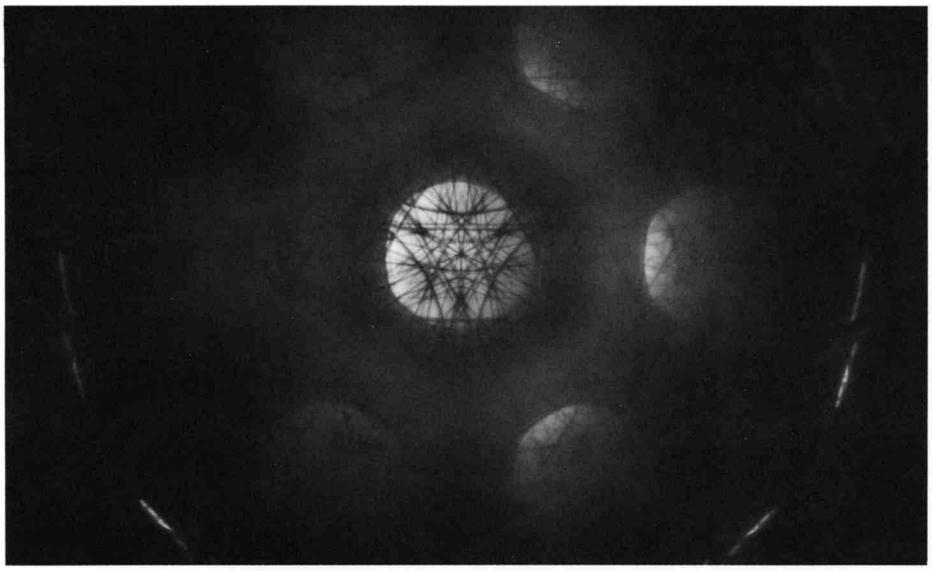

(a)

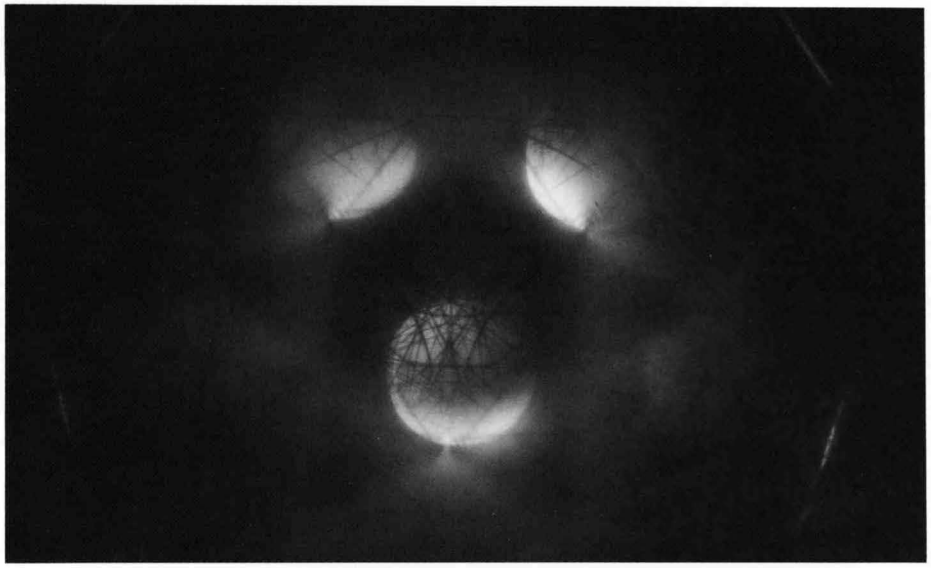

(b)

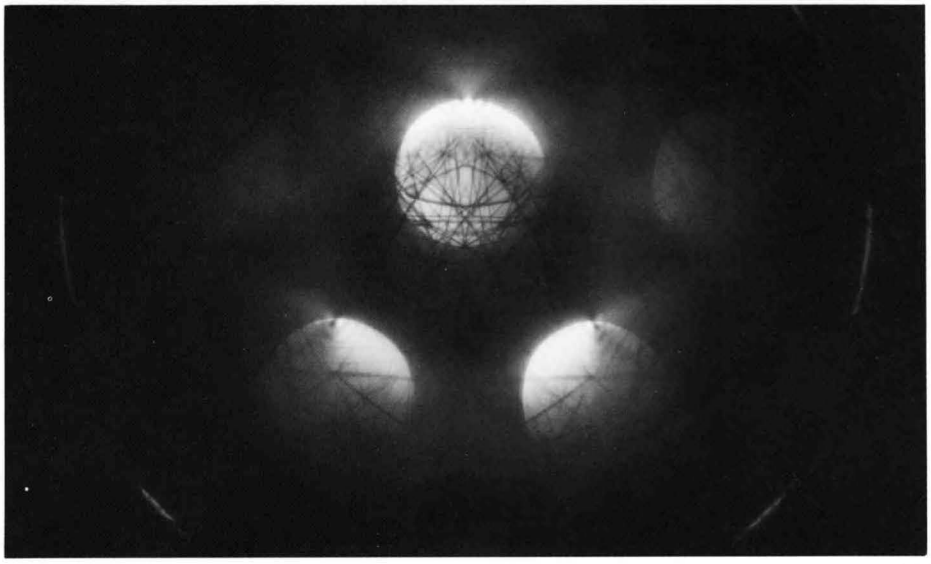

(c)

SiC 27R *R*3*m* perfect crystal

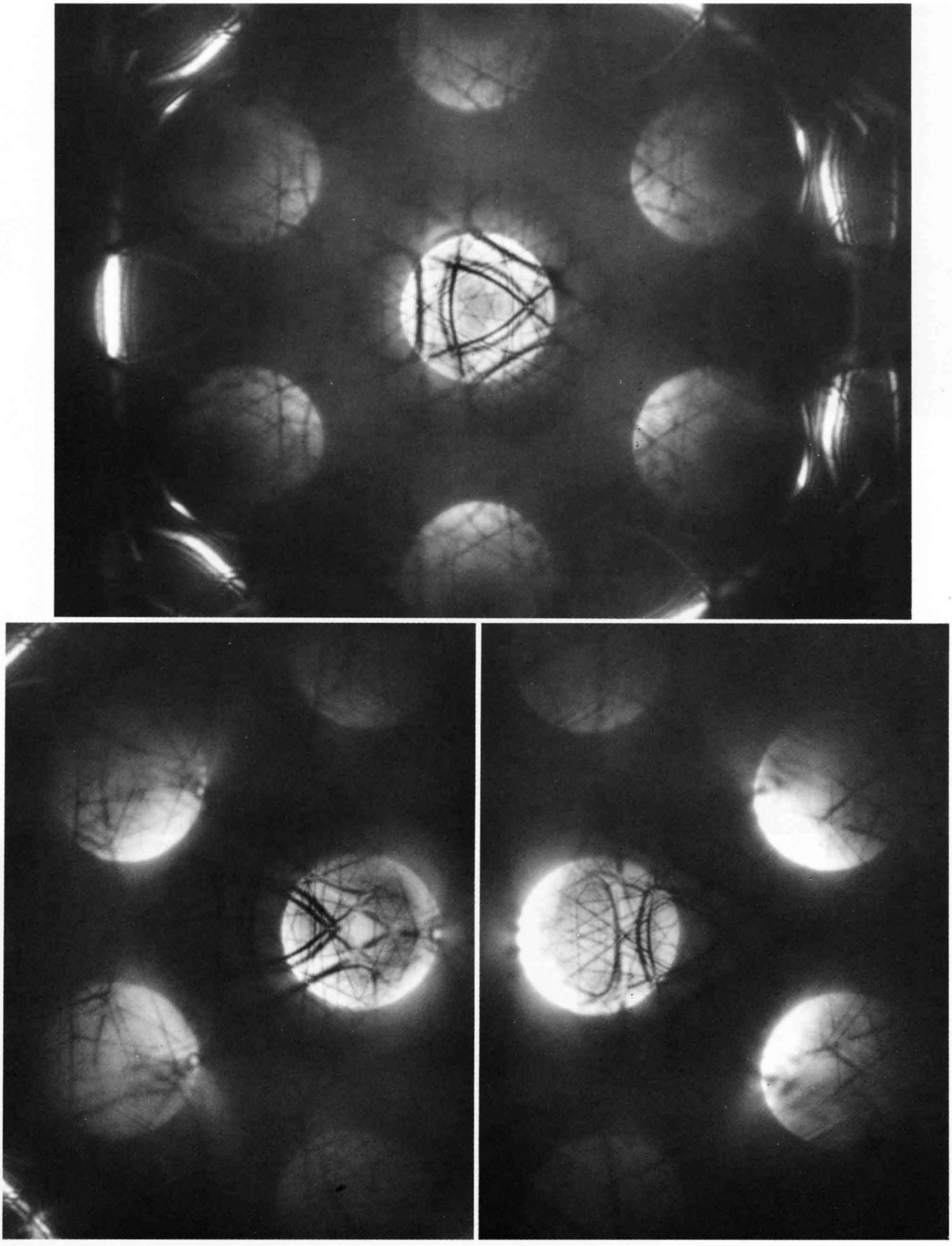

SiC 27R stacking fault

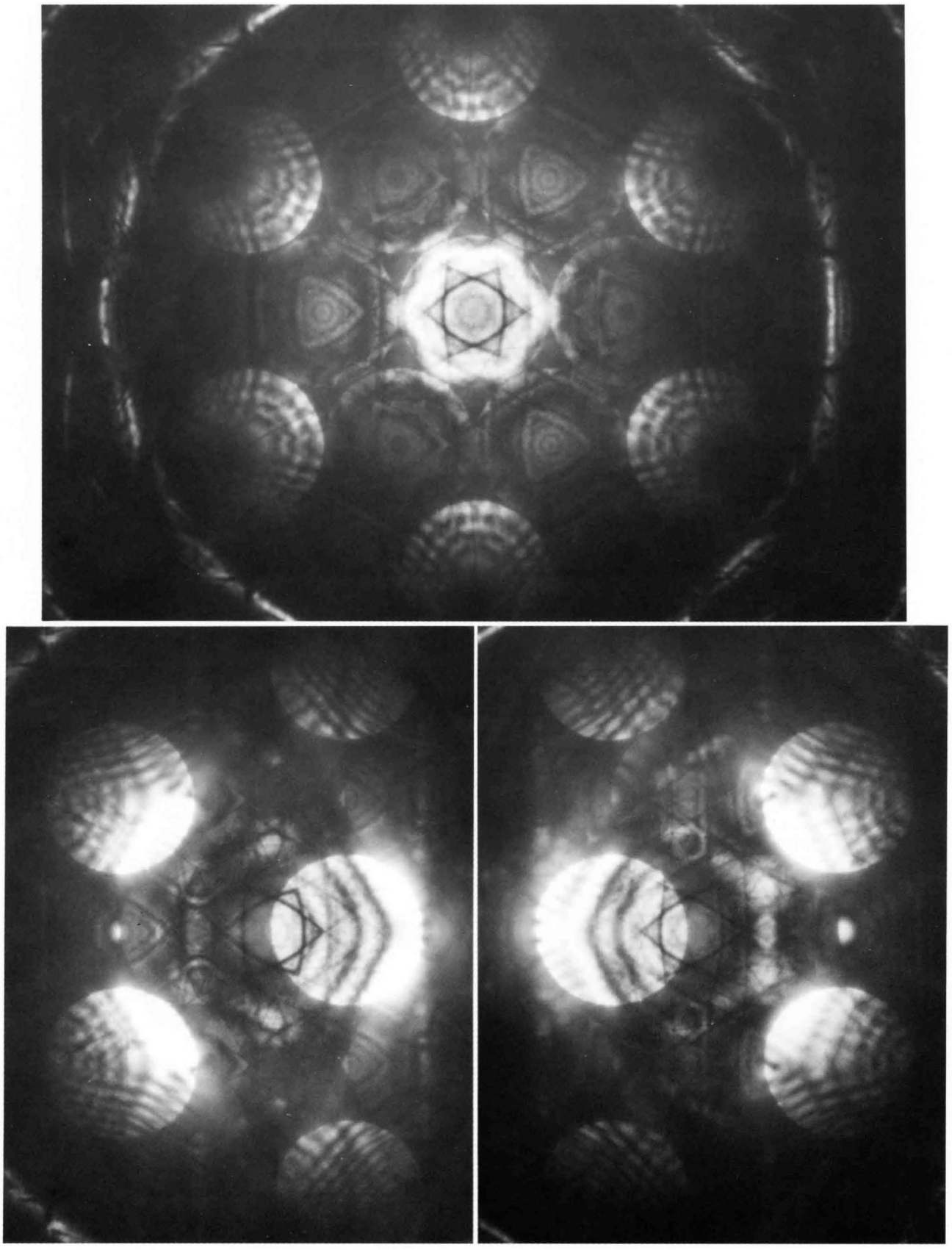

TaS_2 [0001]

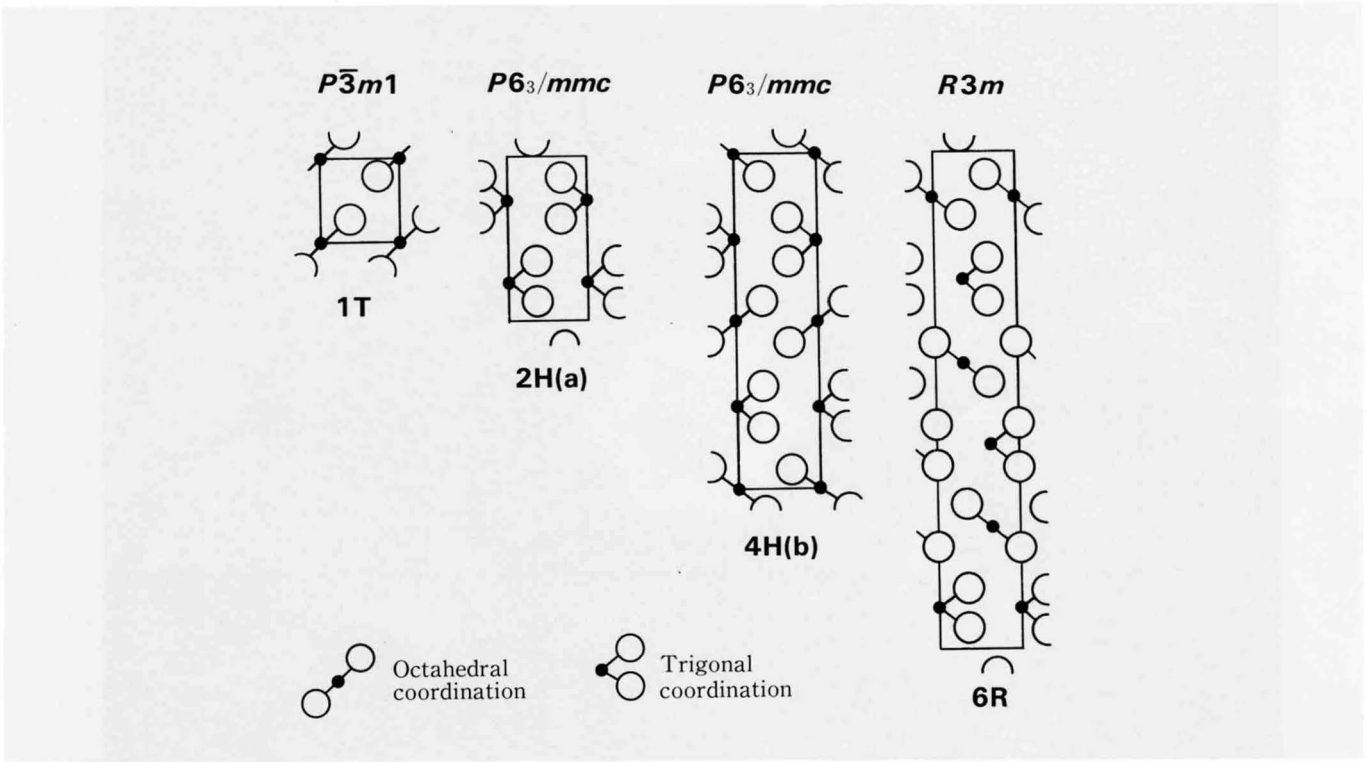

Schematic diagrams of atomic arrangements in four polytypes. The black dots and white circles represent Ta and S atoms, respectively.

Lattice parameters (nm)

	a	*c*
1T	0.3346	0.586 1.758 for NC phase
2H	0.3320	1.210
4Hb	0.3315	2.362
6R	0.3335	3.585

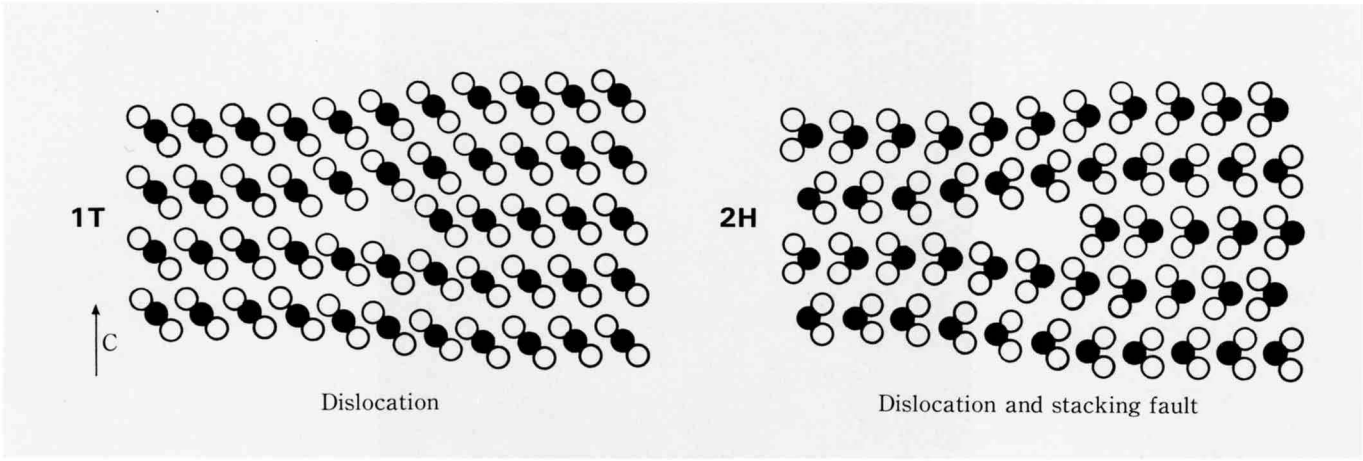

When a dislocation is introduced, 1T polytype cannot form a stacking fault, but 2H polytype can.

Symmetry table for the four polytypes.

	Space Group	Point Group	Diffraction Group	BP	WP	DP	±DP	Conditions limiting possible reflections
1T	$P\bar{3}m1$	$\bar{3}m$	$6_R mm_R$	$3m_V$	$3m_V$	$\begin{cases} 1 \\ m_2 \\ m_V \end{cases}$	2_R $2_R m_{V'}(m_2)$ $2_R m_R(m_V)$	No conditions
2H 4Hb	$P6_3/mmc$	$6/mmm$	$6mm1_R$	$6m_V m_{V'}$	$6m_V m_{V'}$	$\begin{cases} 2 \\ 2m_V m_2 \end{cases}$	21_R $21_R m_{V'}(m_V)$	$hkil$: if $h-k=3n$ then $l=2n$
6R	$R3m$	$3m$	$3m$	$3m_V$	$3m_V$	$\begin{cases} 1 \\ m_V \end{cases}$	$\begin{cases} 1 \\ m_V \end{cases}$ 1	$hkil$:$-h+k+l=3n$ $hh\bar{2}hl$:$(l=3n)$ $h\bar{h}0l$:$(h+l=3n)$

M. Tanaka, R. Saito and D. Watanabe: *Acta Cryst.*, **A34** (1978) S11.

TaS_2 1T Nearly commensulate phase

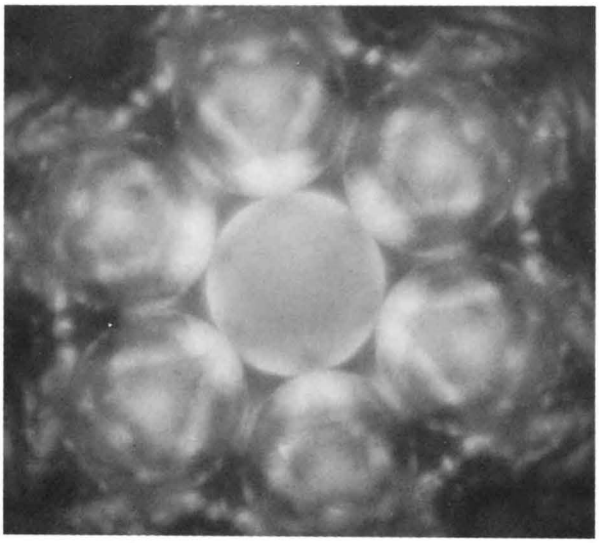

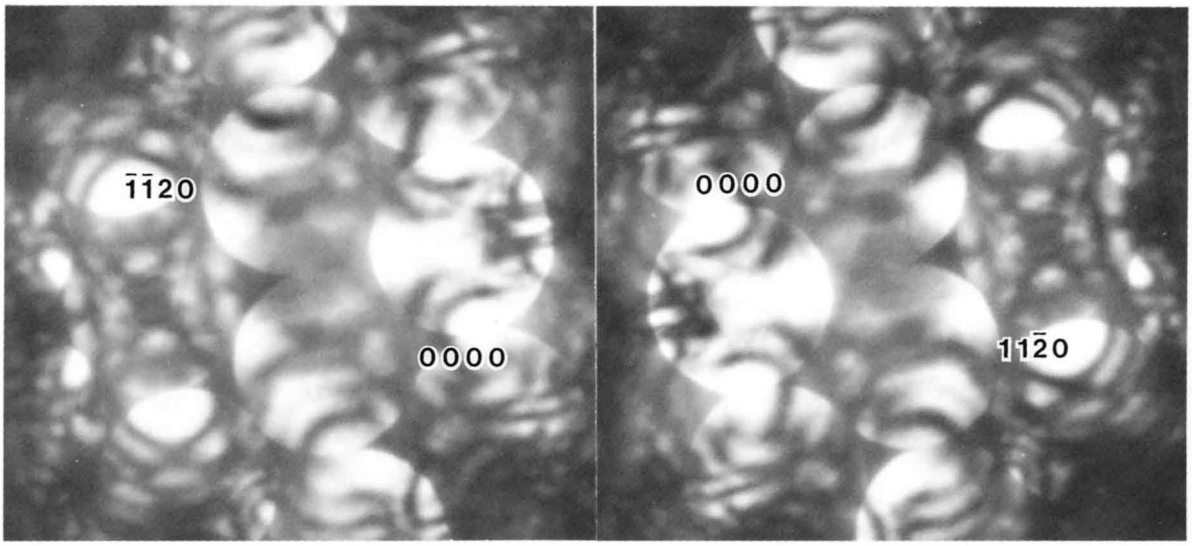

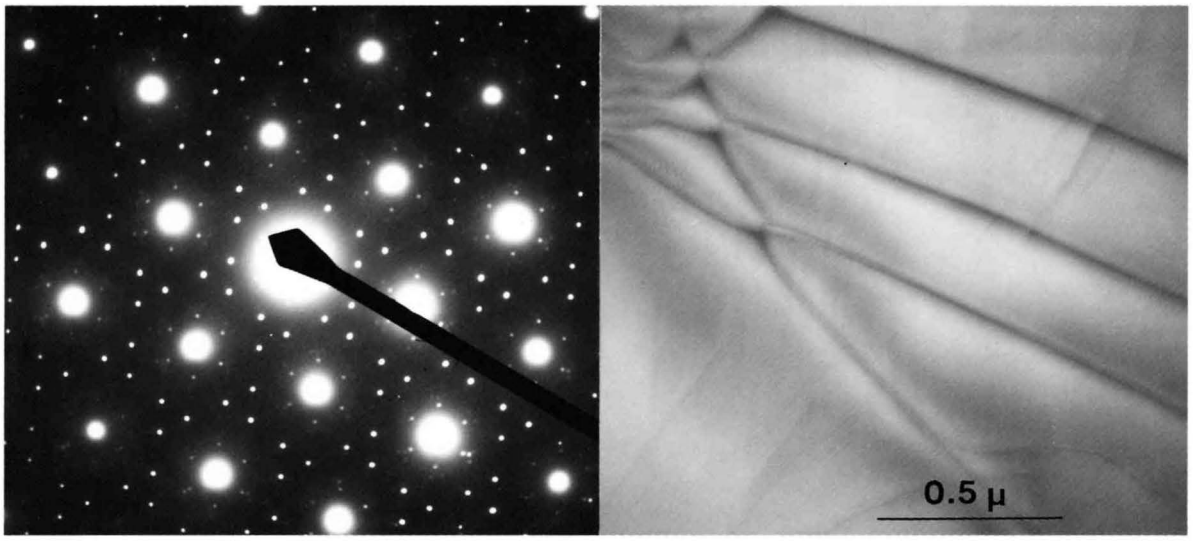

TaS_2 4Hb $P6_3/mmc$

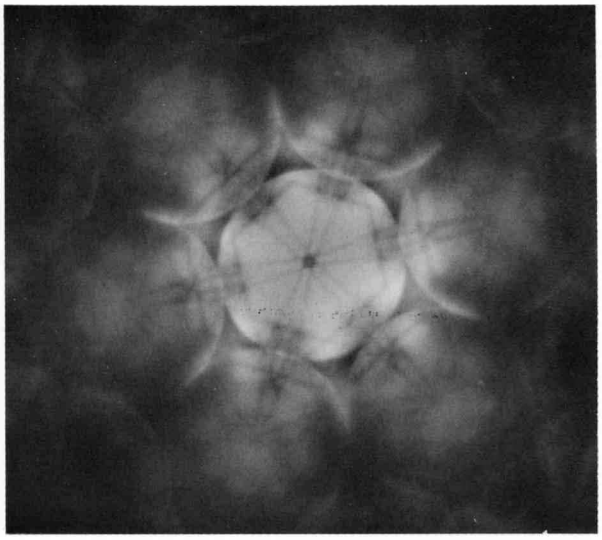

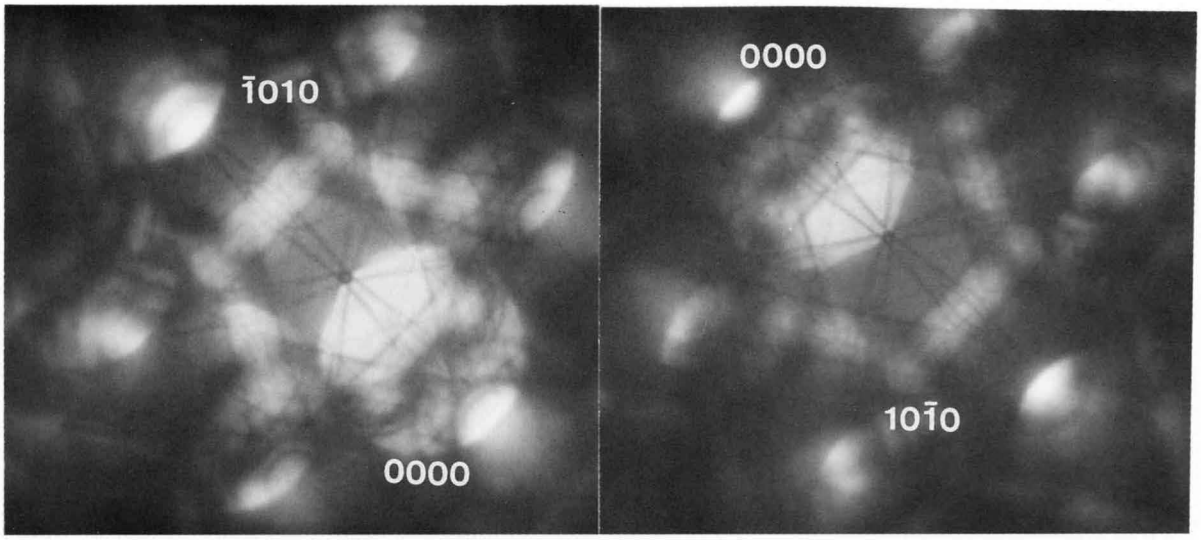

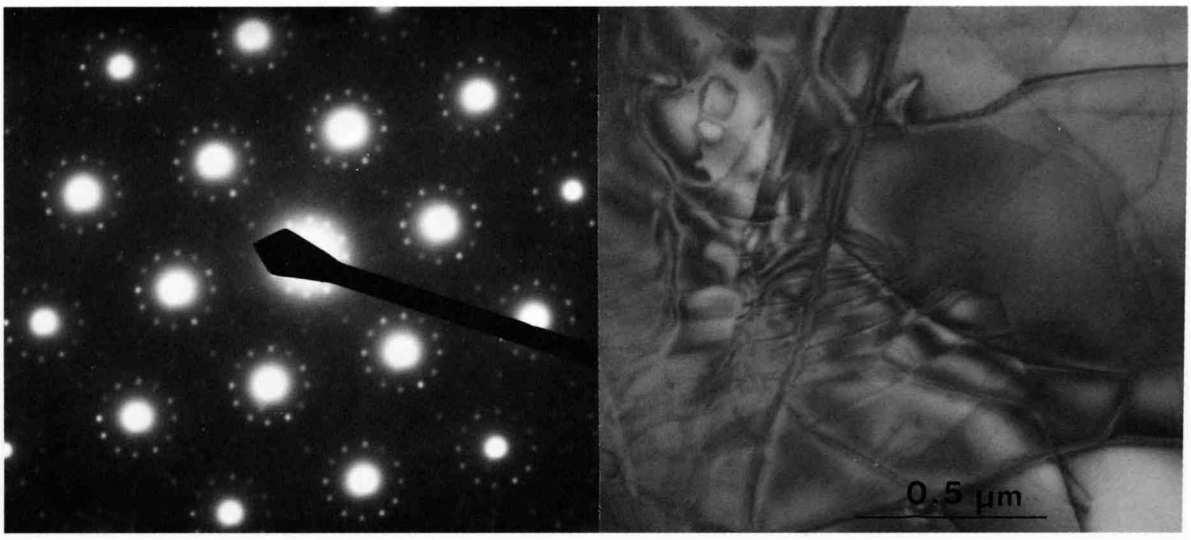

TaS_2 2H $P6_3/mmc$ perfect crystal

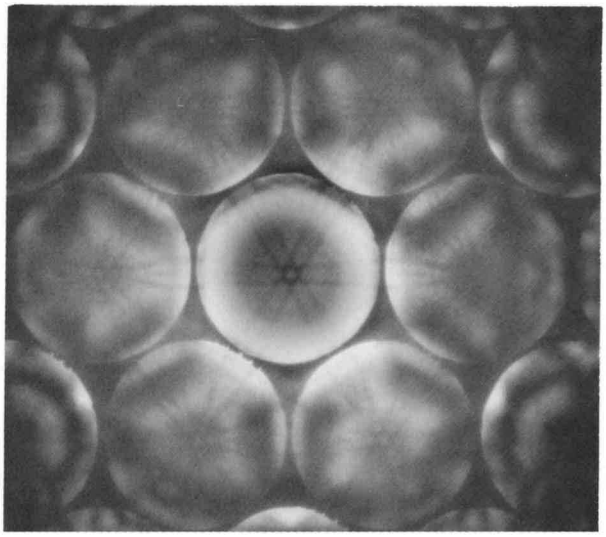

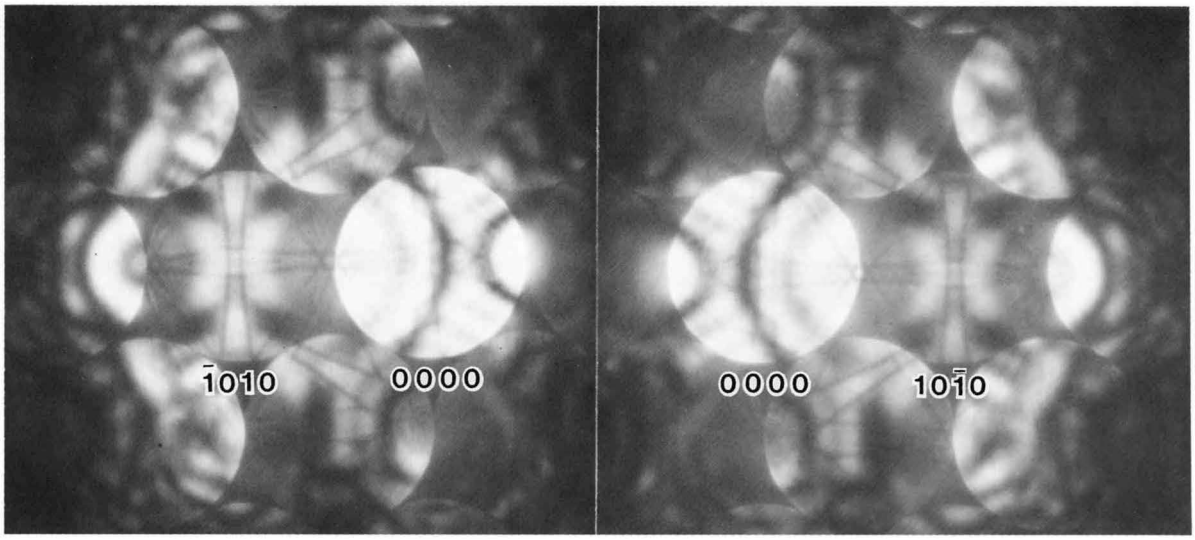

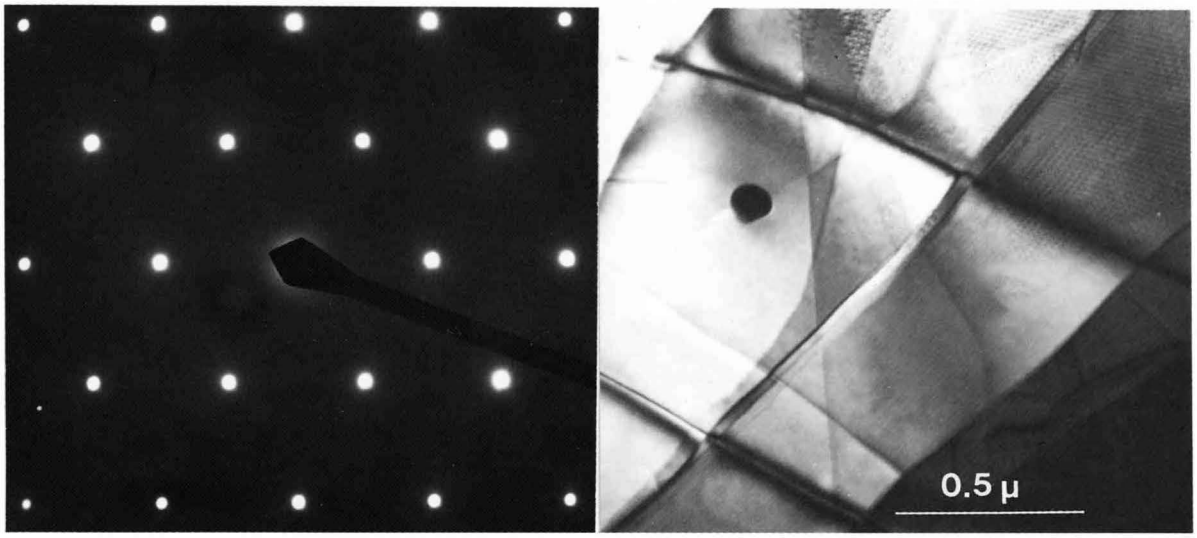

TaS_2 2H stacking fault

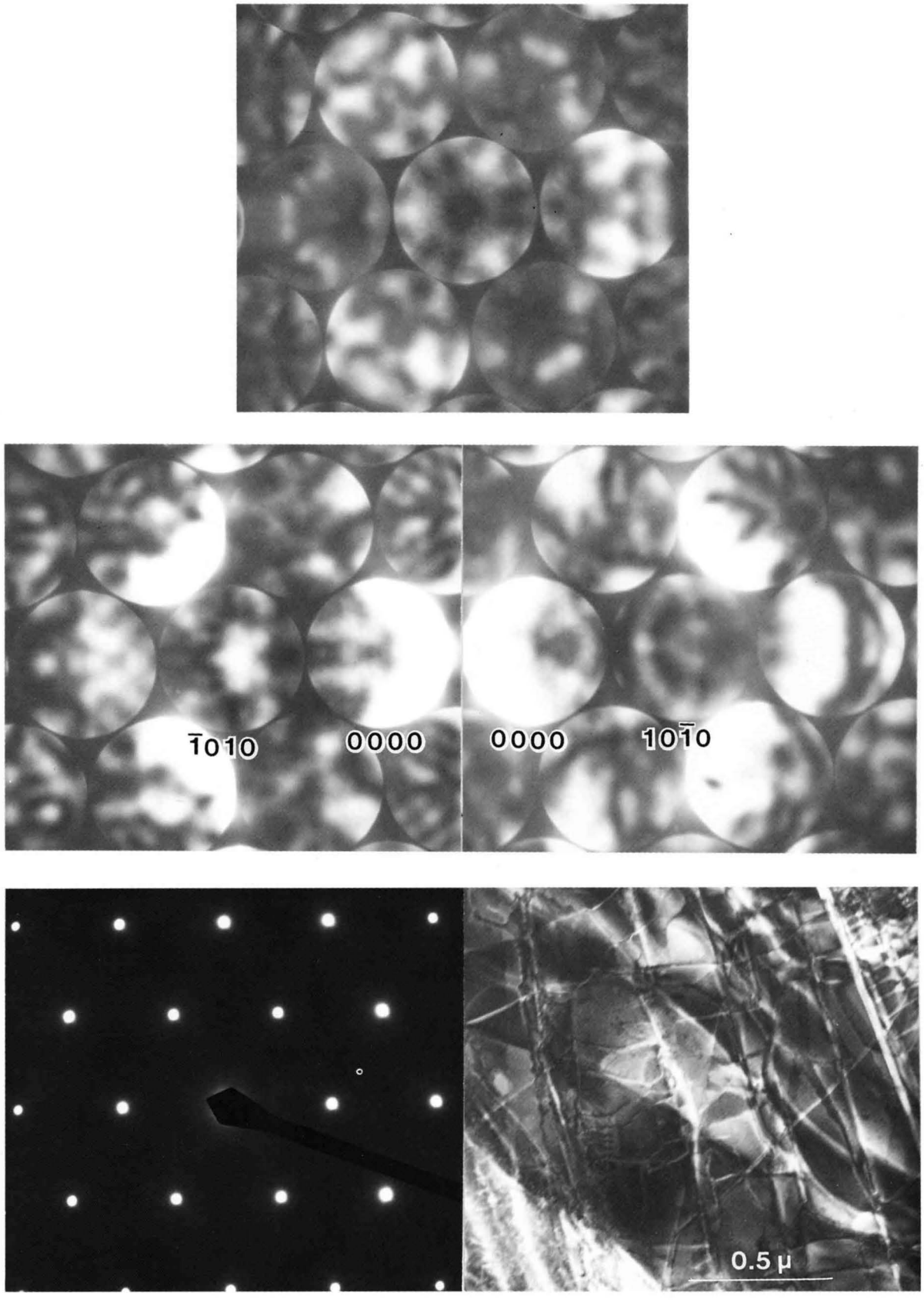

TaS_2 6R *R*3*m* perfect crystal

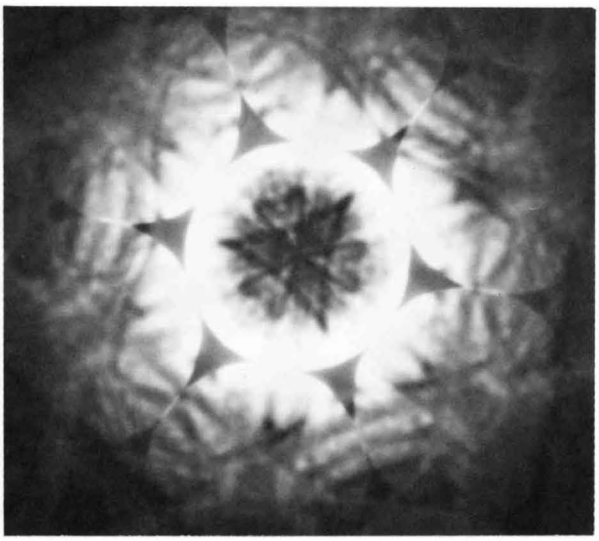

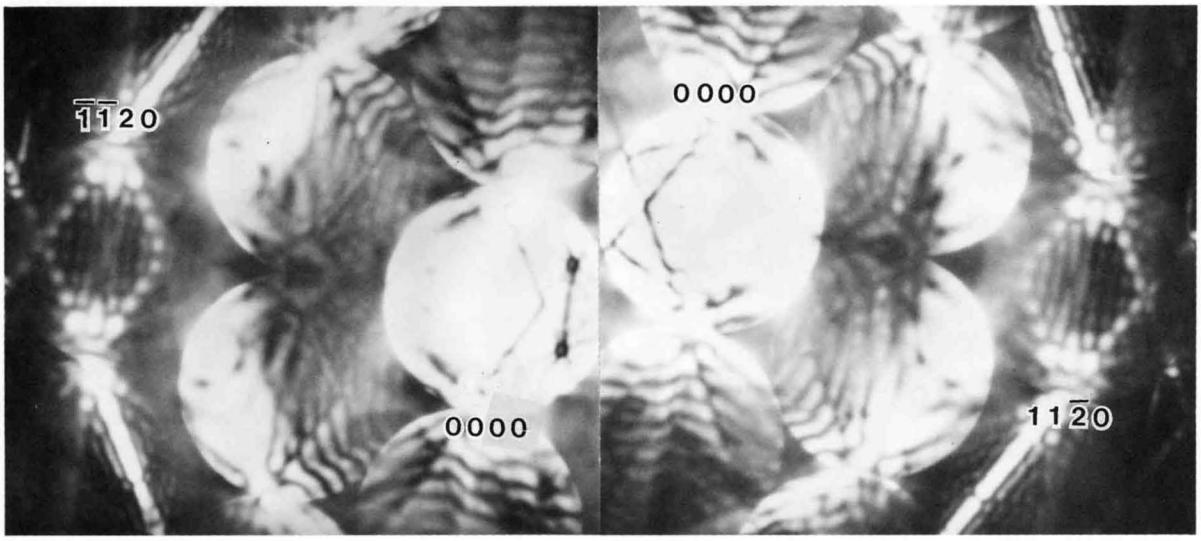

TaS_2 6R stacking fault

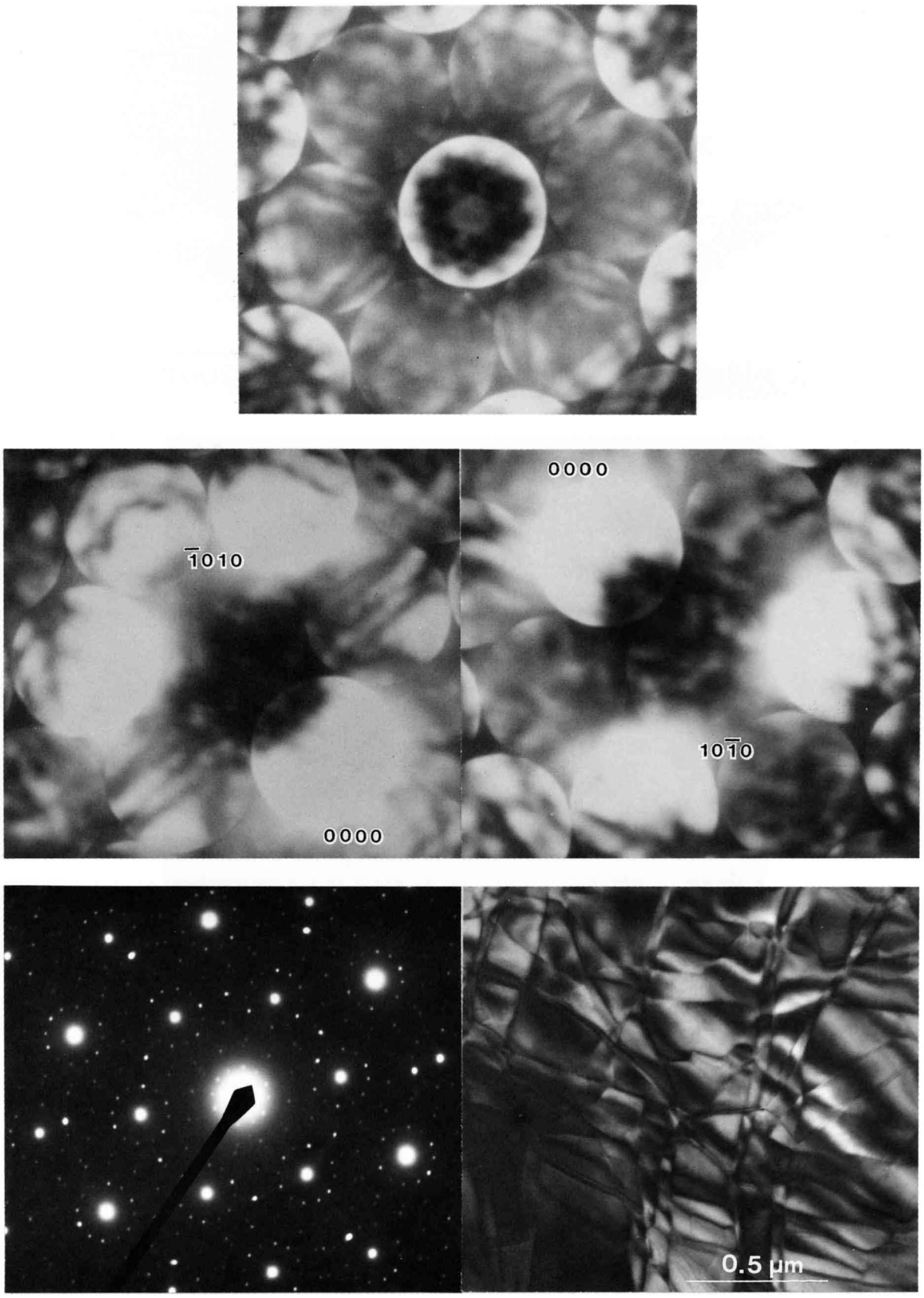

Si misorientation

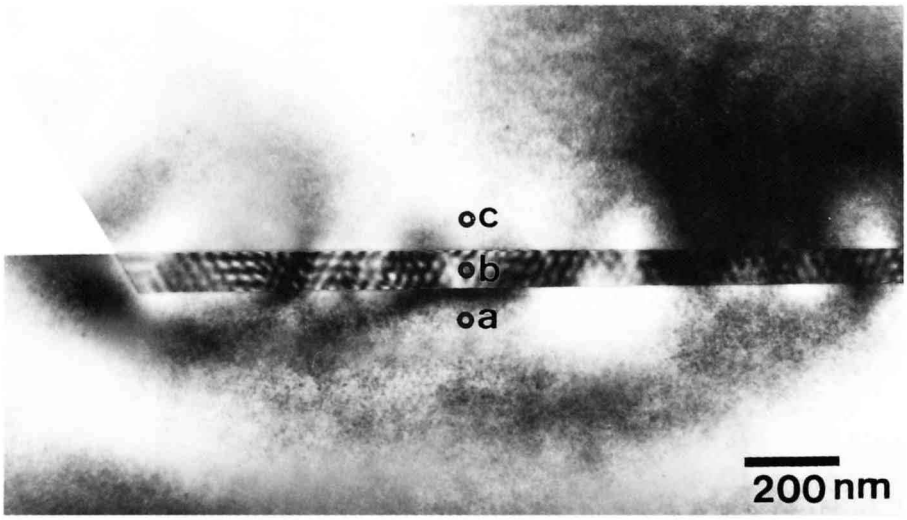

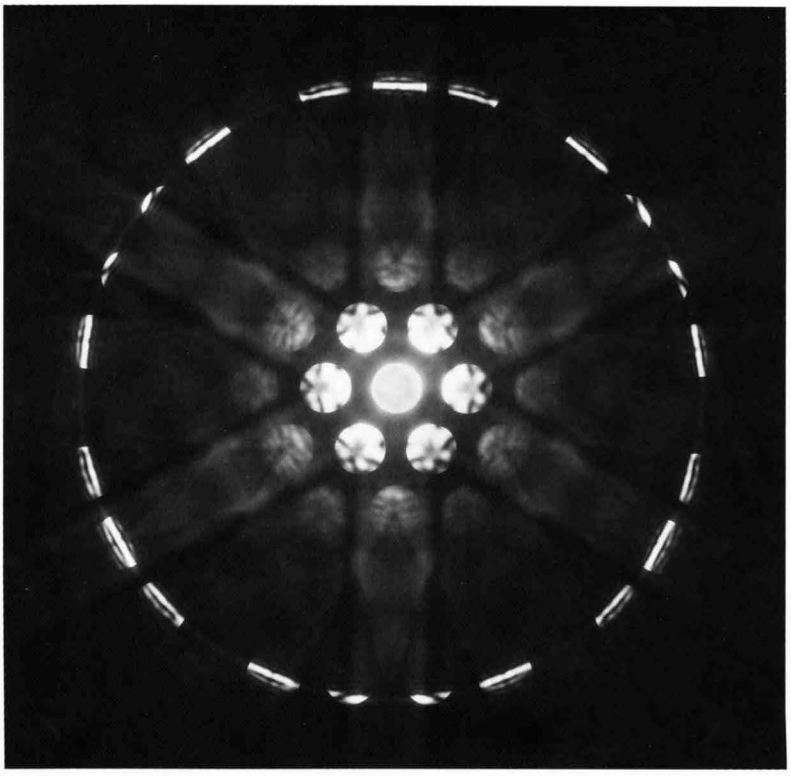

(a)

CBED pattern (a) was taken from the area "a" in the electron micrograph at the exact [111] zone-axis incidence. Patterns (b) and (c) were taken only by shifting the specimen area from "a" to "b" and "c", respectively. Two crystals are overlapped at the area "b" with a certain misorientation. These crystals were found to have a misorientation of 0.8° from the CBED patterns.

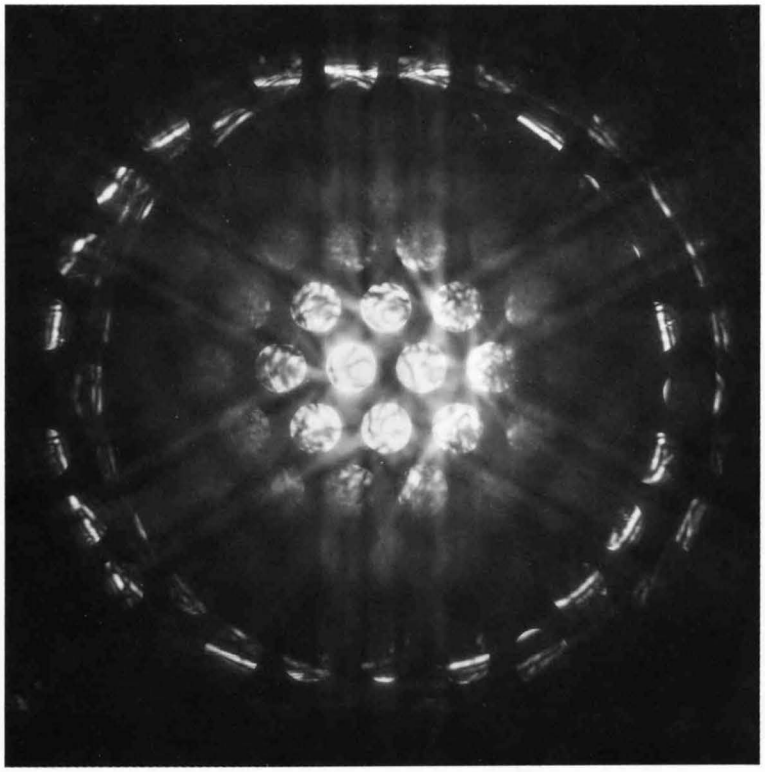

(b)

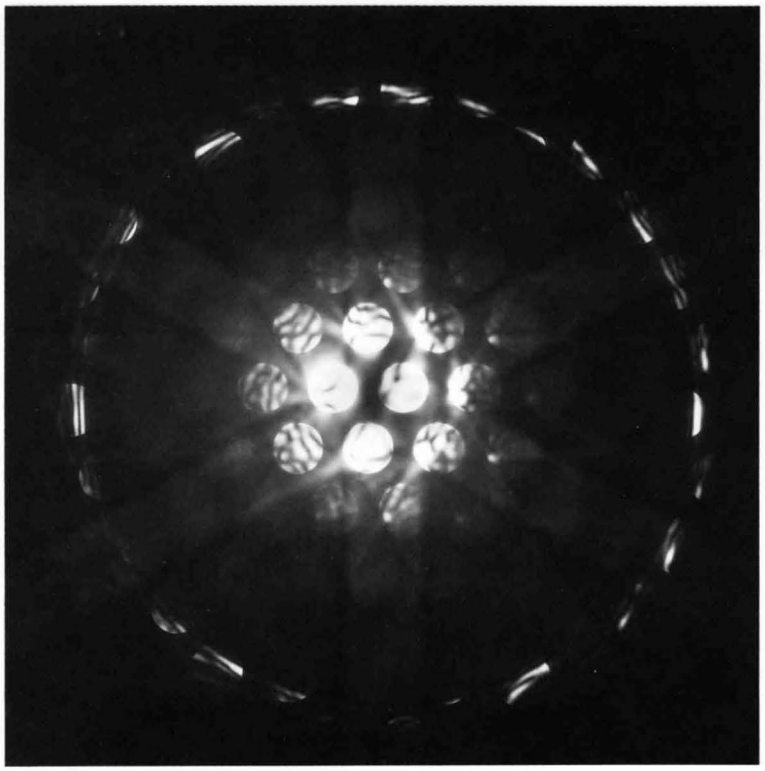

(c)

Materials Science (3) Handedness

Te [36, 9, 16] 80kV

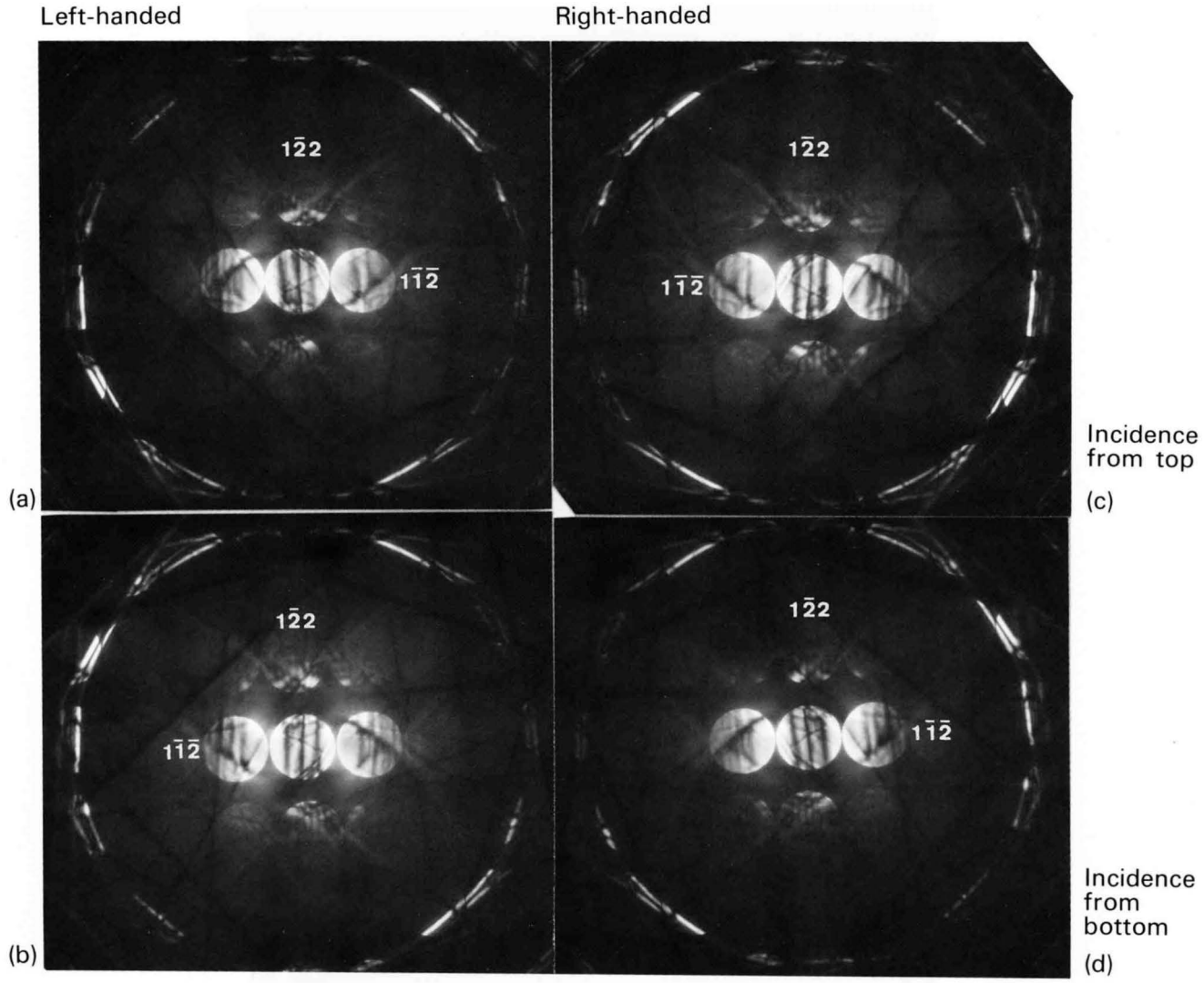

The point groups containing only pure rotation axes, 1, 2, 3, 4, 6, 222, 32, 422, 622, 23 and 432 allow a crystal to have the right-handed or left-handed coordinate system. A famous example is quartz belonging to the space-group of $P3_121$ or $P3_221$. CBED can determine to which system a crystal belongs. [P. Goodman and T.W. Secomb: *Acta Cryst.*, A33 (1977) 126, P.Goodman and A.W.S. Johnson: *Acta Cryst.*, A33 (1977) 997.]

Tellurium also belongs to the space-group of $P3_121$ or $P3_221$. Photos (a) and (b) were obtained from a crystal belonging to the one handed system, which we call the left-handed. Photos (c) and (d) were obtained from a crystal belonging to the other or the right-handed. Photos (b) and (d) were obtained by setting the specimen surface reversed to that for Photos (a) and (c). These four settings give different patterns. The symmetry properties of these patterns are illustrated in the figure.

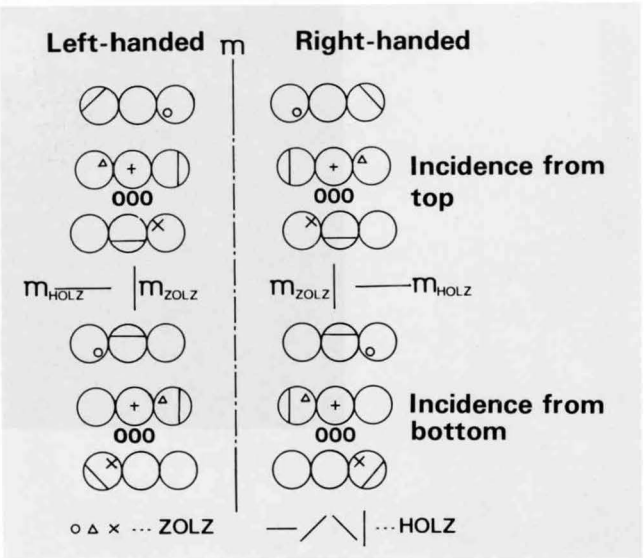

MnSi family [111]

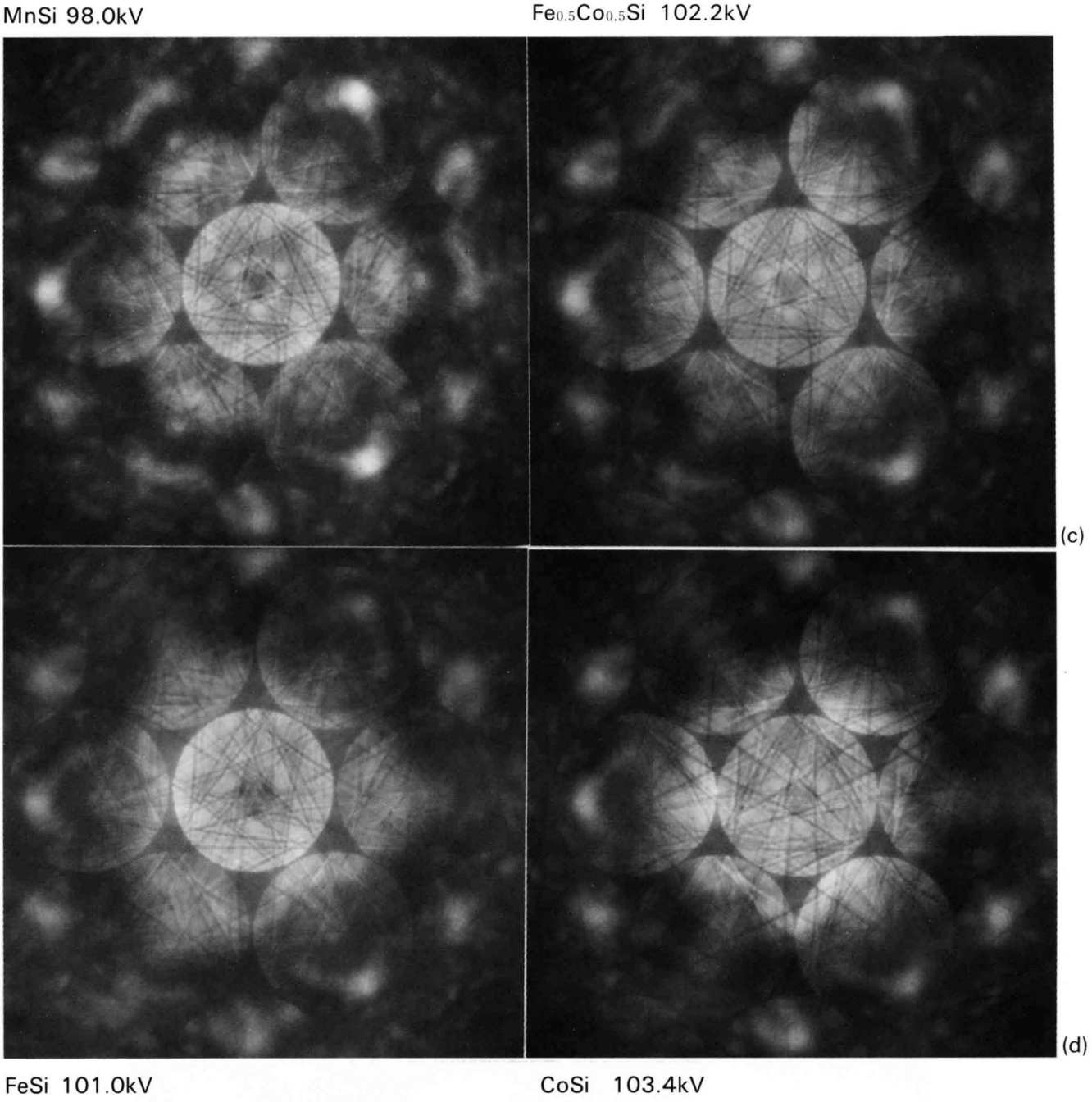

The MnSi family belongs to the crystal space-group of $P2_13$. The crystals of this space-group can have the right-handed or left-handed coordinate system. We found that all the crystals examined belong only to the left-handed system after our definition, although we cannot eliminate the possibility of the existence of right-handed crystals because of small sampling number. [M. Tanaka, H. Takayoshi, M. Ishida and Y. Endoh: *J. Phys. Soc. Jpn.*, 54 (1985) 2970]

Photos (a), (b), (c) and (d) were obtained from MnSi, FeSi, $Fe_{0.5}Co_{0.5}Si$ and CoSi at accelerating voltages of 98.0 kV, 101.0 kV, 102.2 kV and 103.4 kV, respectively. The accelerating voltages were adjusted according to their lattice spacings so as to obtain similar HOLZ line patterns for all the crystals.

Materials Science (4) Phase Transition

$LiTaO_3$

G=20$\bar{2}\bar{4}$

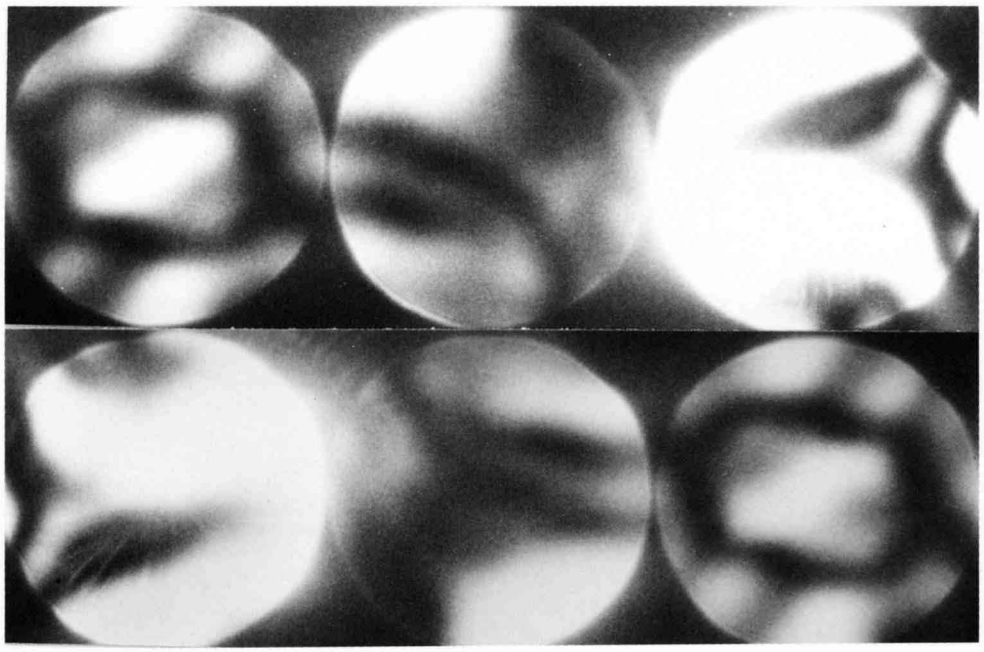

(a)

(b)

710°C $\bar{3}m$ ±DP : 2_R $\bar{G}=\bar{2}024$

G=20$\bar{2}\bar{4}$

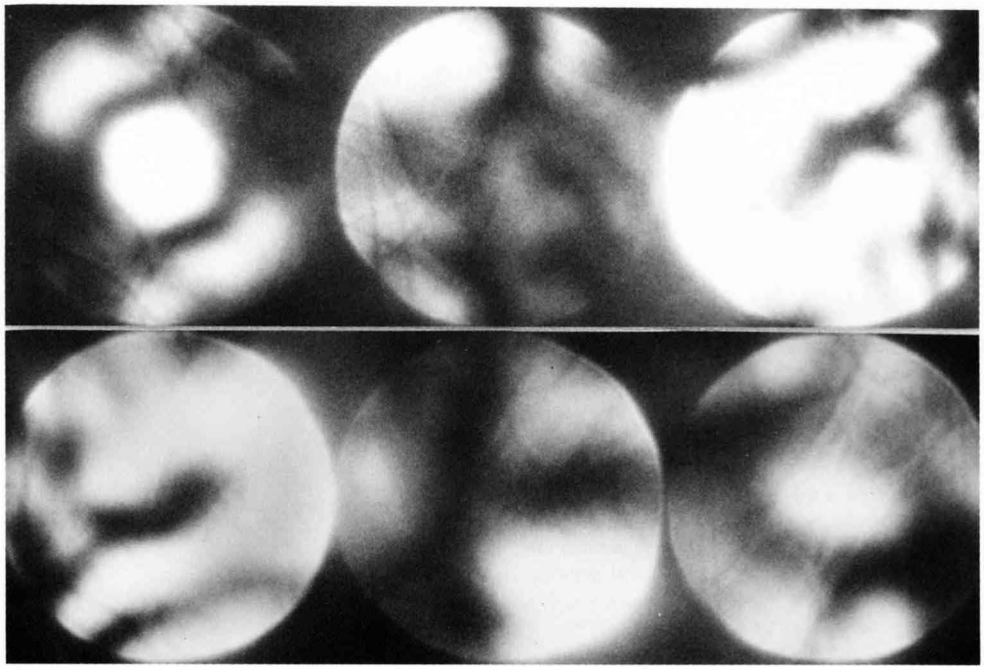

(c)

(d)

R.T. $3m$ ±DP : 1 $\bar{G}=\bar{2}024$

The first study of phase transition by CBED was carried out for barium titanate ($BaTiO_3$) [M. Tanaka and G. Lehmpfuhl: *Jpn. J. Appl. Phys.*, **11** (1972) 1755]. The room temperature phase of $BaTiO_3$ belongs to the tetragonal system of the point group $4mm$ and shows the spontaneous polarization in the c-axis. The substance transforms from the tetragonal phase into the orthorhombic phase of the point group $mm2$ at 273K. A [001] ZAP obtained at room temperature showed that the phase is non-polar in the [010] direction or exhibits the (010) mirror plane, but is polar in the [001] direction. When the temperature was lowered through the transition temperature, the CBED pattern shows that the polar direction was changed by 45° from that in the tetragonal phase into the [101] pseudo cubic direction.

Lithium tantalate ($LiTaO_3$) at 938K undergoes a phase transition from the paraelectric phase of the point group $\bar{3}m$ to the ferroelectric phase of the point group $3m$. Photos (a) to (d) show a symmetry change between the paraelectric and ferroelectric phases of $LiTaO_3$. The patterns (a) and (b) obtained from the high temperature phase show 2_R symmetry or the translational symmetry between $\pm$DP, indicating the presence of an inversion center. The patterns (c) and (d) from the low temperature phase have no translational symmetry between $\pm$DP, revealing that the crystal loses an inversion center through the phase transition.

Appendices

Abbreviations of Technical Terms

CBED	Convergent-Beam Electron Diffraction
HREM	High-Resolution Electron Microscopy
CTEM	Conventional Transmission Electron Microscopy
SAMAG	Selected Area Magnification
SADIFF	Selected Area Diffraction
STEM	Scanning Transmission Electron Microscopy
BR Method	Beam Rocking Method
HCB	Hollow-Cone Beam
FEG	Field Emission Gun
C-O Lens	Condenser-Objective Lens
ZAP	Zone-Axis Pattern
BP	Bright-Field Pattern
WP	Whole Pattern
DP	Dark-Field Pattern
ZOLZ	Zero-th Order Laue-Zone
H(F,S)OLZ	Higher (First, Second) Order Laue-Zone
GM Line	Gjønnes-Moodie Line = Dynamic Extinction Line
LACBED Pattern	Large-Angle CBED Pattern
SMB-CBED Pattern	Symmetrical Many-Beam CBED Pattern

Stereographic Projection

All the crystallographic planes or directions are characterized by a set of normals of these planes which are outgoing radially from a point X in a crystal (Fig. (a)). Thus, the normals are represented by the intersecting points A, B, C, D and E between the normals and the reference sphere centered at the point X as shown in the figure. A projection plane is depicted so as to be in contact with the reference sphere. The normals are represented further by the points A', B', C', D' and E' on the projection plane, which are projections of the points A, B, C, D and E from the projection point P on the reference sphere. This projection is called stereographic projection.

Figure (b) shows the stereographic projection of the outgoing-directions of the transmitted beam O and diffracted beam G in CBED, where the Bragg condition of the reflection G is assumed to be satisfied. The projection disks shown in the lower part of the figure are used for explaining the symmetries of CBED patterns. It should be noted that the possible radial distortion of the diffraction disks is not observed in CBED, since reflection angles in electron diffraction are very small or of the order of 10^{-2} rad.

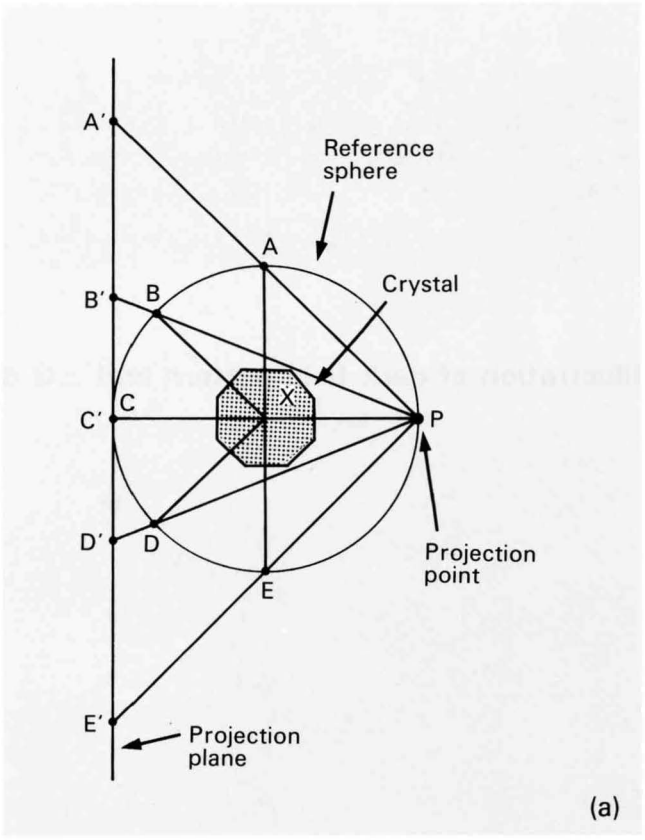

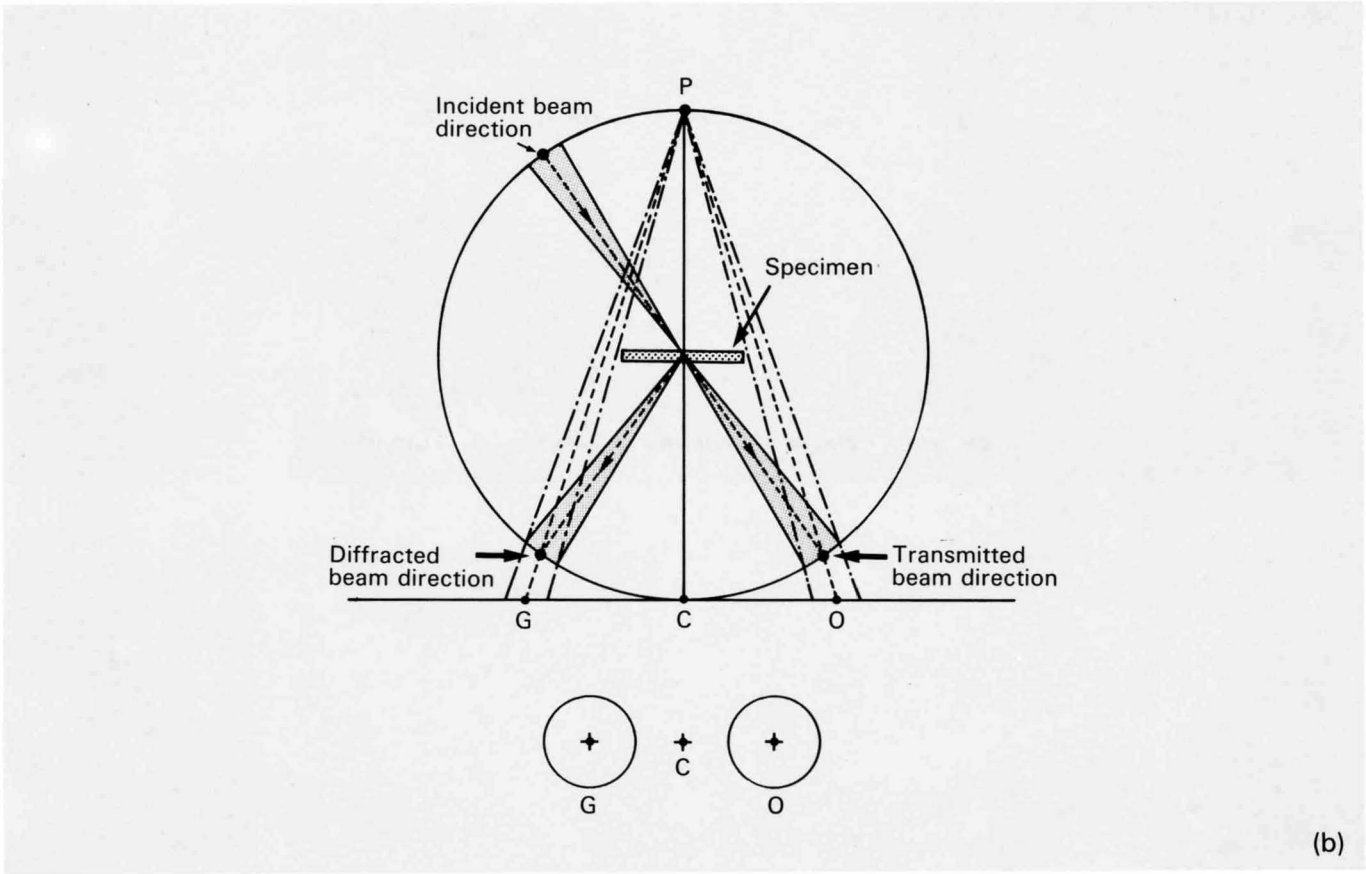

Tables and Figures for Point-Group Determination I

Symmetry elements and diffraction groups of plane-parallel specimen

	1	2	3	4	6	m	$2m(m)$	$3m$	$4m(m)$	$6m(m)$	
1	1	2	3	4	6	m	$2m(m)$	$3m$	$4m(m)$	$6m(m)$	10
$(m')\ 1_R$	1_R	21_R	31_R	41_R	61_R	$m1_R$	$2m(m)1_R$	$3m1_R$	$4m(m)1_R$	$6m(m)1_R$	10
$(i)\ 2_R$	2_R	(21_R)	6_R	(41_R)	(61_R)	$2_Rm(m_R)$	$(2m(m)1_R)$	$6_Rm(m_R)$	$(4m(m)1_R)$	$(6m(m)1_R)$	4
$(2')\ m_R$	m_R	$2m_R(m_R)$	$3m_R$	$4m_R(m_R)$	$6m_R(m_R)$	$(2_Rm(m_R))$ $(m1_R)$	$(2m(m)1_R)$ $(4_R(m)m_R)$	$(3m1_R)$ $(6_Rm(m_R))$	$(4m(m)1_R)$	$(6m(m)1_R)$	5
$(\bar{4})\ 4_R$		4_R		(41_R)		$4_Rm(m_R)$	$(4_Rm(m_R))$		$(4m(m)1_R)$		2

$1_R.2_R = 2,\ 2_R.2_R = 1,\ m_R.2_R = m,\ 4_R.2_R = 4,\ 1_R.m_R = m.m_R,\ 1_R.4_R = 4.1_R,\ m_R.4_R = m.4_R.$

Illustration of dark-field pattern and ±G dark-field pattern symmetries

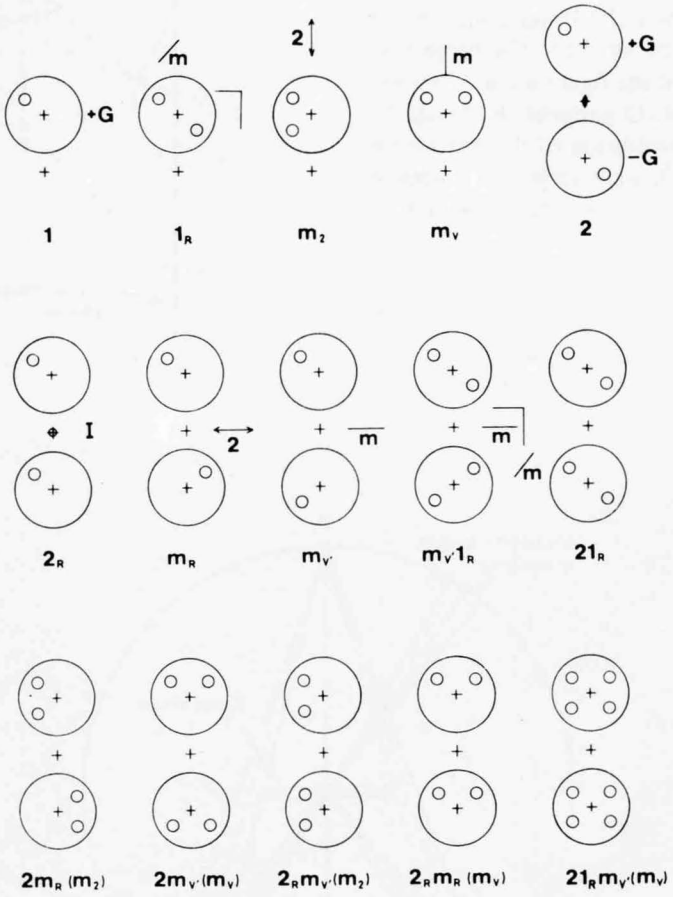

Symmetries of zone-axis and two-beam CBED patterns

I	II	III	IV	V	VI
1	1	1	1	1	
1_R	2 (1_R)	1	$2 = 1_R$	1	1_R
2	2	2	1	2	
2_R	1	1	1	2_R	21_R
21_R	2	2	2	21_R	
m_R	m (m_2)	1	1 m_2	1 m_R 1	
m	m_v	m_v	1 m_v	1 m_v 1	$m1_R$
$m1_R$	$2mm$ $(m_v + m_2 + (1_R))$	m_v	2 $2m_v m_2$	1 $m_v 1_R$ 1	
$2m_R m_R$	$2mm$ $(2 + m_2)$	2	1 m_2	2 $2m_R(m_2)$	
$2mm$	$2m_v m_{v'}$	$2m_v m_{v'}$	1 m_v	2 $2m_{v'}(m_v)$	$2mm1_R$
$2_R mm_R$	m_v	m_v	1 m_2 m_v	2_R $2_R m_{v'}(m_2)$ $2_R m_R(m_v)$	
$2mm1_R$	$2m_v m_{v'}$	$2m_v m_{v'}$	2 $2m_v m_2$	21_R $21_R m_{v'}(m_v)$	
4	4	4	1	2	
4_R	4	2	1	2	41_R
41_R	4	4	2	21_R	
$4m_R m_R$	$4mm$ $(4 + m_2)$	4	1 m_2	2 $2m_R(m_2)$	
$4mm$	$4m_v m_{v'}$	$4m_v m_{v'}$	1 m_v	2 $2m_{v'}(m_v)$	$4mm1_R$
$4_R mm_R$	$4mm$ $(2m_v m_{v'} + m_2)$	$2m_v m_{v'}$	1 m_2 m_v	2 $2m_R(m_2)$ $2m_{v'}(m_v)$	
$4mm1_R$	$4m_v m_{v'}$	$4m_v m_{v'}$	2 $2m_v m_2$	21_R $21_R m_{v'}(m_v)$	
3	3	3	1	1	
31_R	6 $(3 + 1_R)$	3	2	1	31_R
$3m_R$	$3m$ $(3 + m_2)$	3	1 m_2	1 m_R 1	
$3m$	$3m_v$	$3m_v$	1 m_v	1 m_v 1	$3m1_R$
$3m1_R$	$6mm$ $(3m_v + m_2 + (1_R))$	$3m_v$	2 $2m_v m_2$	1 $m_v 1_R$ 1	
6	6	6	1	2	
6_R	3	3	1	2_R	61_R
61_R	6	6	2	21_R	
$6m_R m_R$	$6mm$ $(6 + m_2)$	6	1 m_2	2 $2m_R(m_2)$	
$6mm$	$6m_v m_{v'}$	$6m_v m_{v'}$	1 m_v	2 $2m_{v'}(m_v)$	$6mm1_R$
$6_R mm_R$	$3m_v$	$3m_v$	1 m_2 m_v	2_R $2_R m_{v'}(m_2)$ $2_R m_R(m_v)$	
$6mm1_R$	$6m_v m_{v'}$	$6m_v m_{v'}$	2 $2m_v m_2$	21_R $21_R m_{v'}(m_v)$	

Columns are: I diffraction group; II bright-field pattern; III whole pattern; IV dark-field pattern; V $\pm G$ dark-field patterns: VI projection diffraction group. All the possible symmetries of dark-field and $\pm G$ dark-field patterns are listed. The symmetries expressed by the symbols in this table are visualized by the illustrations on the opposite page.

Relation between diffraction groups and crystal point-groups

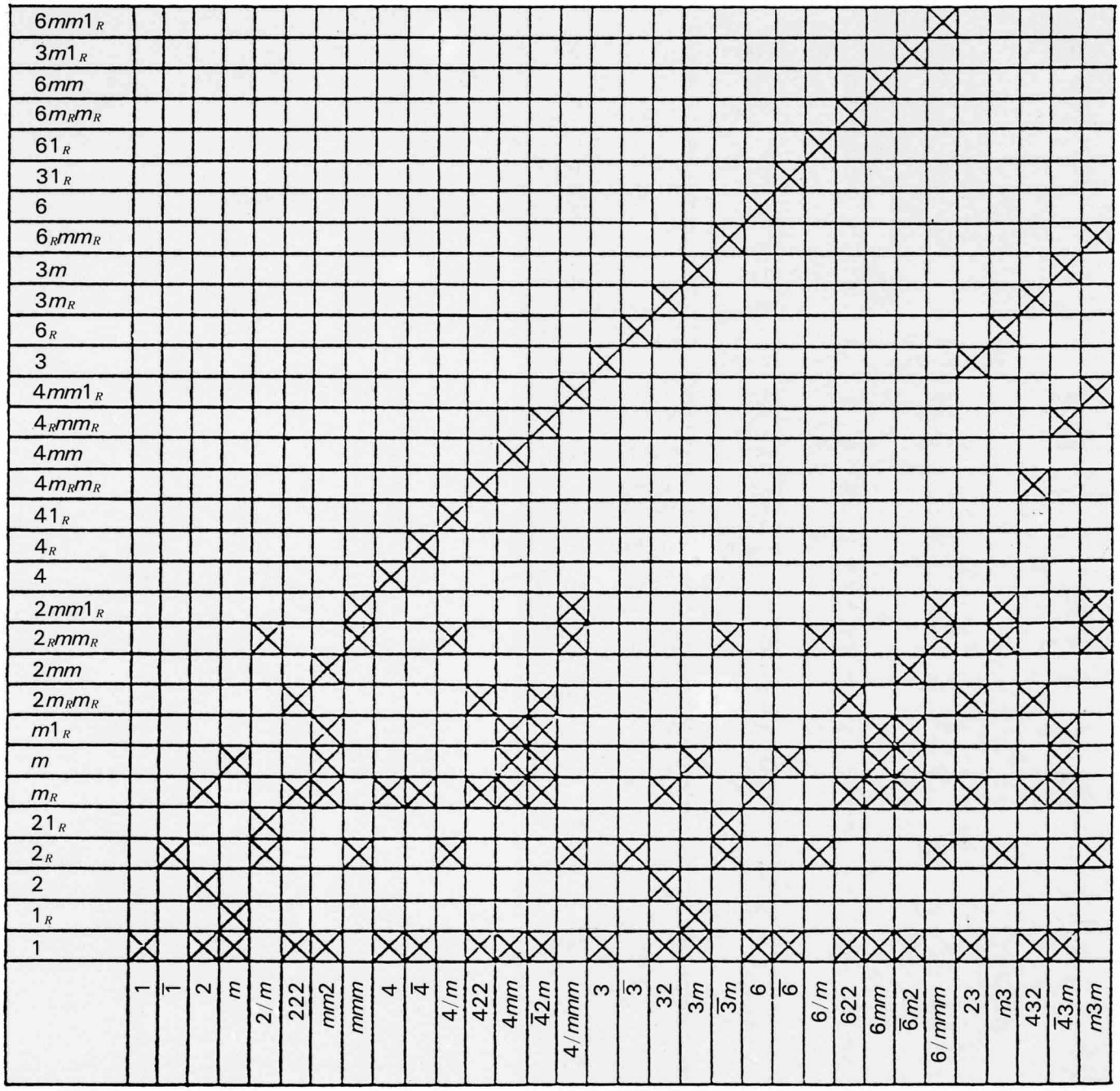

(Courtesy of the Royal Society of London)

Zone-axis symmetries

point group	⟨111⟩	⟨100⟩	⟨110⟩	⟨*uvo*⟩	⟨*uuw*⟩	[*uvw*]
m3m	6_Rmm_R	$4mm1_R$	$2mm1_R$	2_Rmm_R	2_Rmm_R	2_R
$\bar{4}$3m	3m	4_Rmm_R	$m1_R$	m_R	m	1
432	$3m_R$	$4m_Rm_R$	$2m_Rm_R$	m_R	m_R	1

point group	⟨111⟩	⟨100⟩	⟨*uvo*⟩	[*uvw*]
m3	6_R	$2mm1_R$	2_Rmm_R	2_R
23	3	$2m_Rm_R$	m_R	1

point group	[0001]	⟨11$\bar{2}$0⟩	⟨1$\bar{1}$00⟩	[*uv.o*]	[*uu.w*]	[*u*$\bar{u}$*.w*]	[*uv.w*]
6/mmm	$6mm1_R$	$2mm1_R$	$2mm1_R$	2_Rmm_R	2_Rmm_R	2_Rmm_R	2_R
$\bar{6}$m2	$3m1_R$	$m1_R$	2mm	m	m_R	m	1
6mm	6mm	$m1_R$	$m1_R$	m_R	m	m	1
622	$6m_Rm_R$	$2m_Rm_R$	$2m_Rm_R$	m_R	m_R	m_R	1

point group	[0001]	[*uv.o*]	[*uv.w*]
6/m	61_R	2_Rmm_R	2_R
$\bar{6}$	31_R	m	1
6	6	m_R	1

point group	[0001]	⟨11$\bar{2}$0⟩	[*u*$\bar{u}$*.w*]	[*uv.w*]
$\bar{3}$m	6_Rmm_R	21_R	2_Rmm_R	2_R
3m	3m	1_R	m	1
32	$3m_R$	2	m_R	1

point group	[0001]	[*uv.w*]
$\bar{3}$	6_R	2_R
3	3	1

point group	[001]	⟨100⟩	⟨110⟩	[*uow*]	[*uvo*]	[*uuw*]	[*uvw*]
4/mmm	$4mm1_R$	$2mm1_R$	$2mm1_R$	2_Rmm_R	2_Rmm_R	2_Rmm_R	2_R
$\bar{4}$2m	4_Rmm_R	$2m_Rm_R$	$m1_R$	m_R	m_R	m	1
4mm	4mm	$m1_R$	$m1_R$	m	m_R	m	1
422	$4m_Rm_R$	$2m_Rm_R$	$2m_Rm_R$	m_R	m_R	m_R	1

point group	[001]	[*uvo*]	[*uvw*]
4/m	41_R	2_Rmm_R	2_R
$\bar{4}$	4_R	m_R	1
4	4	m_R	1

point group	[001]	⟨100⟩	[*uow*]	[*uvo*]	[*uvw*]
mmm	$2mm1_R$	$2mm1_R$	2_Rmm_R	2_Rmm_R	2_R
mm2	2mm	$m1_R$	m	m_R	1
222	$2m_Rm_R$	$2m_Rm_R$	m_R	m_R	1

point group	[010]	[*uow*]	[*uvw*]
2/m	21_R	2_Rmm_R	2_R
m	1_R	m	1
2	2	m_R	1

point group	[*uvw*]
$\bar{1}$	2_R
1	1

(Courtesy of the Royal Society of London)

Tables and Figures for Point-Group Determination II

Symmetries of hexagonal six-beam CBED patterns

Projection diffraction group		31_R		$3m1_R$				61_R		
Diffraction group		3	31_R	$3m_R$	$3m$	$3m1_R$		6	6_R	61_R
Two-dimensional symmetry		3	3	3	$3m$	$3m$		6	3	6
Three-dimensional symmetry			m'	$2'$		m', $(2')$			$\bar{1}$	m', $(\bar{1})$
Zone-axis pattern	Bright-field pattern	3	6	$3m$	$3m$	$6mm$		6	3	6
	Whole-field pattern	3	3	3	$3m$	$3m$		6	3	6
Hexagonal six-beam pattern	0	1	1	1 m_2	1 m_v	m_2	m_v	1	1	1
	G	1	1_R	m_2 1	1 m_v	1_R	$1_R m_v(m_2)$	1	1	1_R
	F	1	1	m_2 1	1 1	1	m_2	1	1	1
	S	1	1	1 m_2	1 1	m_2	1	1	1	1
	FF'	1	3_R	1 1	1 m_v	3_R	$3_R m_v$	1	1	3_R
	SS'	1	1	1 1	1 m_v	1	m_v	1	6_R	6_R
A pair of symmetrical six-beam patterns	± 0	1	1_R	m_2 1	m_v 1	$m_v 1_R$	$1_R m_2$	2	1	$2(1_R)$
	$\pm G$	1	1	1 m_R	m_v 1	$m_v m_R$	1	2	2_R	21_R
	$\pm F$	1	1	1 1	m_v 1	m_v	1	1	6_R	6_R
	$\pm S$	1	3_R	1 1	m_v 1	$3_R m_v$	3_R	1	1	3_R
	$F'\bar{F}$	1	1	1 m_R	1 1	m_R	1	2	1	2
	$S'\bar{S}$	1	1	m_R 1	1 1	1	m_R	2	1	2
Point group		23, 3	$\bar{6}$	432, 32	$\bar{4}3m$, $3m$	$\bar{6}m2$		6	$m3$, $\bar{3}$	$6/m$

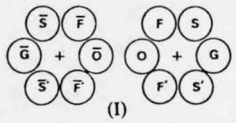

(I)

$6mm1_R$				
$6m_R m_R$	$6mm$	$6_R mm_R$		$6mm1_R$
6	$6mm$	$3m$		$6mm$
$2'$		$\bar{1}$, $(2')$		m', $(\bar{1}, 2')$
$6mm$	$6mm$	$3m$		$6mm$
6	$6mm$	$3m$		$6mm$
m_2	m_v	1	$m_v(m_2)$	$m_v(m_2)$
m_2	m_v	m_2	m_v	$1_R m_v(m_2)$
m_2	1	m_2	1	m_2
m_2	1	1	m_2	m_2
1	m_v	1	m_v	$3_R m_v$
1	m_v	6_R	$6_R m_v$	$6_R m_v$
$2m_2$	$2m_{v'}$	$m_v(m_2)$	1	$2(1_R)m_{v'}(m_2)$
$2m_R$	$2m_{v'}$	$2_R m_v$	$2_R m_R$	$21_R m_{v'}(m_R)$
1	$m_{v'}$	$6_R m_v$	6_R	$6_R m_{v'}$
1	$m_{v'}$	m_v	1	$3_R m_{v'}$
$2m_R$	2	1	m_R	$2m_R$
$2m_R$	2	m_R	1	$2m_R$
622	$6mm$	$m3m$, $\bar{3}m$		$6/mmm$

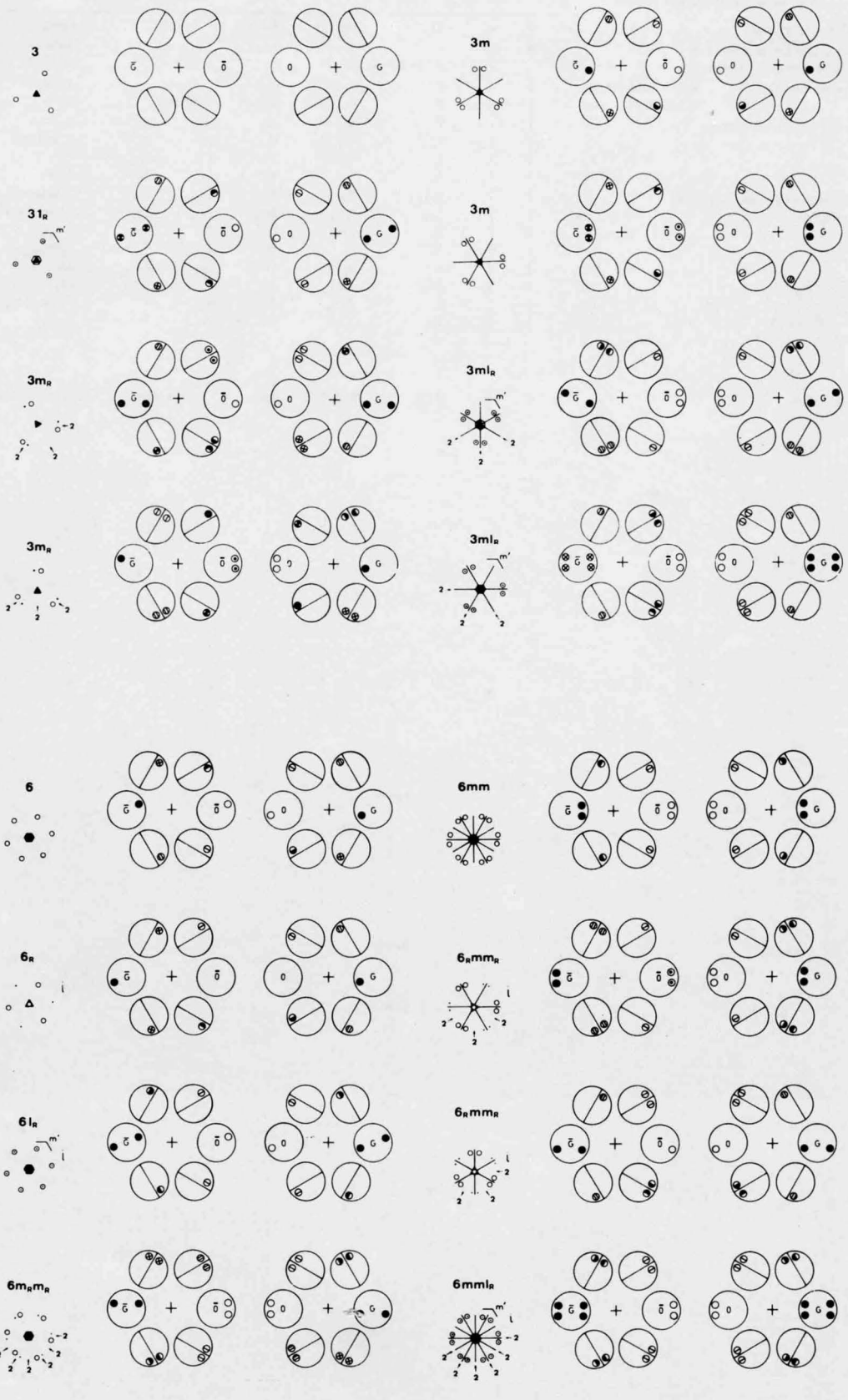
3
3m
$3 1_R$
3m
$3m_R$
$3ml_R$
$3m_R$
$3ml_R$
6
6mm
6_R
6_Rmm_R
$6l_R$
6_Rmm_R
$6m_Rm_R$
$6ml_R$

Symmetries of square four-beam CBED patterns

Projection diffraction group			41_R			$4mm1_R$				
Diffraction group			4	4_R	41_R	$4m_Rm_R$	$4mm$	4_Rmm_R		$4mm1_R$
Two-dimensional symmewtry			4	(2)	4	4	$4mm$	(2mm)		$4mm$
Three-dimensional symmetry				$\bar{4}$	m', $(i, \bar{4})$	2′		$\bar{4}$, 2′		m', $(i, 2', \bar{4})$
Zone-axis pattern	Bright-field pattern		4	4	4	$4mm$	$4mm$	$4mm$		$4mm$
	Whole-field pattern		4	2	4	4	$4mm$	$2mm$		$4mm$
Square four-beam pattern		0	1	1	1	m_2	m_v	m_2	m_v	$m_v(m_2)$
		G	1	1	1_R	m_2	m_v	m_2	m_v	$1_Rm_v(m_2)$
		F	1	1	1	m_2	1	1	m_2	m_2
		FF'	1	4_R	4_R	1	m_v	4_R	4_Rm_v	4_Rm_v
Two pairs of square four-beam patterns		± 0	2	2	$2(1_R)$	$2m_2$	$2m_{v'}$	$2m_2$	$2m_{v'}$	$2(1_R)m_{v'}(m_2)$
	A	$\pm G$	2	2	21_R	$2m_R$	$2m_{v'}$	$2m_R$	$2m_{v'}$	$21_Rm_{v'}(m_R)$
	B	$\pm FF'$	2	2	2	$2m_R$	2	2	$2m_R$	$2m_R$
		$\pm F$	1	4_R	4_R	1	$m_{v'}$	4_R	$4_Rm_{v'}$	$4_Rm_{v'}$
		00′	4	4	4	$4m_2$	$4m_{v''}$	$4m_v$	$4m_2$	$4m_{v''}(m_2)$
	A	GG'	4	4_R	41_R	$4m_R$	$4m_{v''}$	4_Rm_v	4_Rm_R	$41_Rm_{v''}(m_R)$
	C	FS	4	1	4	$4m_R$	4	m_R	1	$41_Rm_{v''}(m_R)$
		FS'	1	1	1_R	1	$m_{v''}$	m_v	1	$1_Rm_{v''}$

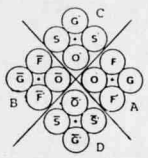

(II)

Point group	4	$\bar{4}$	$4/m$	432, 422	$4mm$	$\bar{4}3m$, $\bar{4}2m$	$m3m$, $4/mmm$

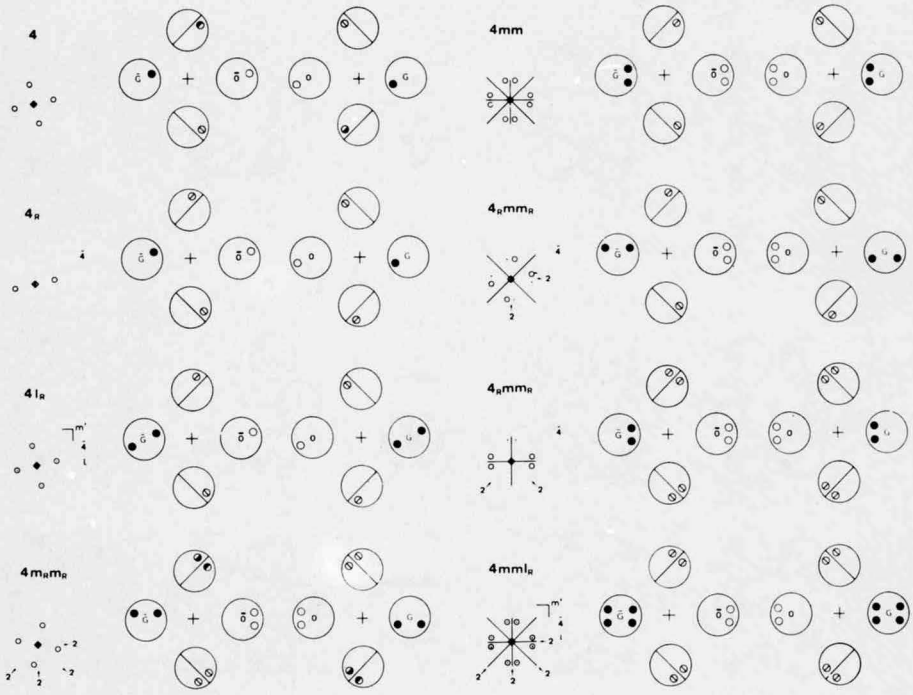

Symmetries of rectangular four-beam CBED patterns

Projection diffraction group			$m1_R$			$2mm1_R$			
Diffraction group			m_R	m	$m1_R$	$2m_Rm_R$	$2mm$	2_Rmm_R	$2mm1_R$
Two-dimensional symmetry				m	m	2	$2mm$	m	$2mm$
Three-dimensional symmetry			$2'$		m', $2'$	$2'$		$2'$, i	m', $2'$, i
Zone-axis pattern	Bright-field pattern		m	m	$2mm$	$2mm$	$2mm$	m	$2mm$
	Whole-field pattern		1	m	m	2	$2mm$	m	$2mm$
Rectangular four-beam pattern		0	1	1	1	1	1	1	1
		G	1	1	1_R	1	1	1	1_R
		F	m_2	1	m_2	m_2	1	m_2	m_2
		S	1	1	m_2	m_2	1	1	m_2
Three pairs of rectangular four-beam patterns		$0_G0_{\bar{H}}$	m_2	1	m_2	m_2	m_v	$m_v(m_2)$	$m_v(m_2)$
	A	$G\bar{H}$	1	1	1	m_R	m_v	m_v	m_vm_R
	B	$F\bar{F}$	1	1	1	1	m_v	2_Rm_v	2_Rm_v
		SS'	1	1	1_R	1	m_v	m_v	m_v1_R
		0_G0_H	1	m_v	m_v	m_2	$m_{v'}$	1	$m_{v'}(m_2)$
	A	GH	m_R	m_v	m_vm_R	m_R	$m_{v'}$	m_R	$m_{v'}m_R$
	C	FF'	1	m_v	m_v1_R	1	$m_{v'}$	1	$m_{v'}1_R$
		$S\bar{S}$	1	m_v	m_v	1	$m_{v'}$	2_R	$2_Rm_{v'}$
		$0_G0_{\bar{G}}$	1	1	1_R	2	2	1	$2(1_R)$
	A	$G\bar{G}$	1	1	1	2	2	2_R	21_R
	D	$F\bar{F}'$	1	1	1	$2m_R$	2	1	$2m_R$
		$S\bar{S}'$	m_R	1	m_R	$2m_R$	2	m_R	$2m_R$
Point group			2, 222, $mm2$, 4, $\bar{4}$, 422, $4mm$, $\bar{4}2m$, 32, 6, 622, $6mm$, $\bar{6}m2$, 23, 432, $\bar{4}3m$	m, $mm2$, $4mm$, $\bar{4}2m$, $3m$, $\bar{6}$, $6mm$, $\bar{6}m2$, $\bar{4}3m$	$mm2$, $4mm$, $42m$, $6mm$, $\bar{6}m2$, $\bar{4}3m$	222, 422, $\bar{4}2m$, 622, 23, 432	$mm2$, $\bar{6}m2$	$2/m$, mmm, $4/m$, $4/mmm$, $\bar{3}m$, $\bar{6}/m$, $6/mmm$, $m3$, $m3m$	mmm, $4/mmm$, $m3$, $m3m$, $6/mmm$

(III)

Illustrations of GM Line Formation

Dynamic extinction lines due to double reflection via the 0-th Laue zone

When an *a*-glide plane in the (010) plane or a 2_1 screw axis in the *a*-direction is present, the equations in the right figure hold between the structure factors. Then, the resultant structure factors for the double reflection "a" has the same magnitude but an opposite sign to the structure factors for the double reflections "b" and "c". The geometrical conditions for the paths "a" and "b" are equivalent when the incident beam lies in the glide plane. The conditions for the paths "a" and "c" are equivalent when a kinematically forbidden reflection due to the screw axis or the glide plane is exactly excited. When these conditions are satisfied, the beams passing through the paths "a" and "b", or "a" and "c", are canceled out each other, resulting in A_2 and B_2 dynamic extinction lines (GM lines). The glide plane and screw axis act equivalently for the double reflection due to ZOLZ reflections. A ZOLZ reflection usually has a large crystal structure factor and a dynamical rocking curve with a large half breadth , compared with a HOLZ reflection. Thus, the dynamic extinction line formed by the double reflection due to ZOLZ reflections has a wide angular breadth resulting in a broard dark line. Figures illustrate the double reflection due to ZOLZ refletions.

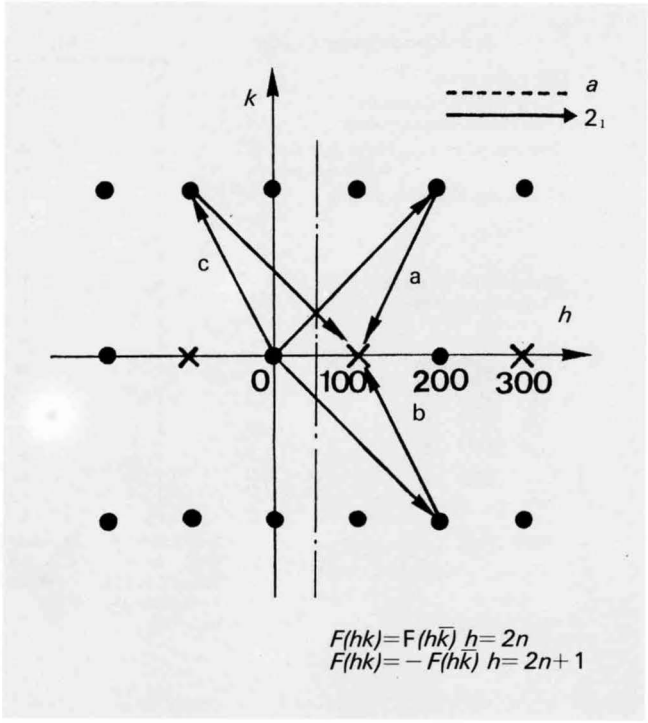

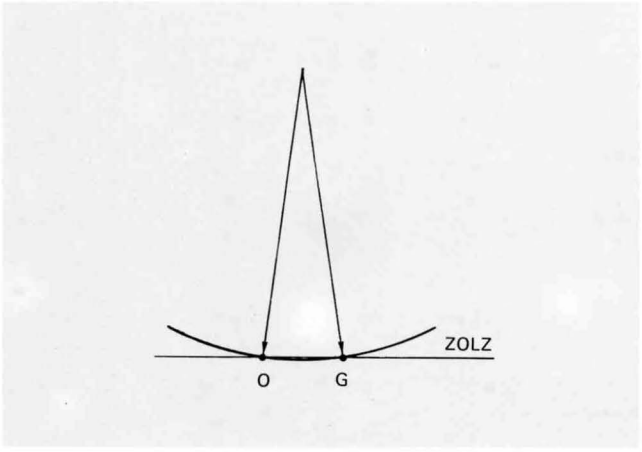

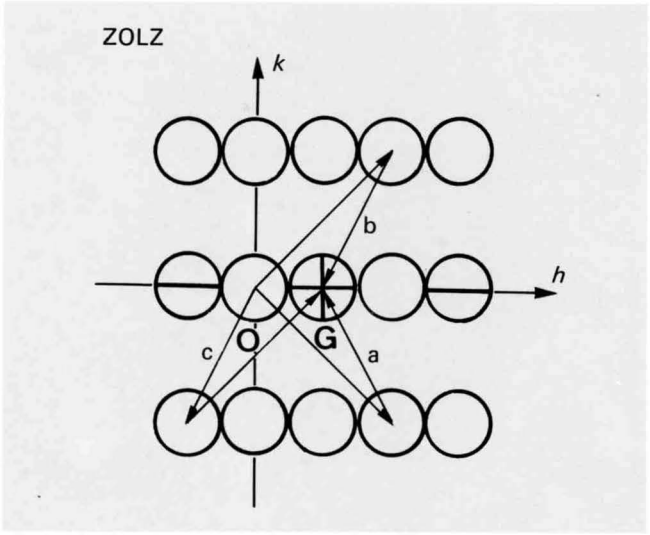

A_2 and B_2 GM lines for 2_1 screw axis and *a*-glide plane.

Dynamic extinction rules for symmetry elements of a plane-parallel specimen

Symmetry elements of plane-parallel specimen	Orientation to specimen surface	GM lines	
		Two dimensional (0-th Laue zone) interaction	Three dimensional (HOLZ) interaction
Glide planes	perpendicular : g	A_2 and B_2	A_3
	parallel : g'	———	Intersection of A_3 and B_3
Twofold screw axis	perpendicular : 2_1	———	———
	parallel : $2_1'$	A_2 and B_2	B_3

Dynamic extinction lines due to double reflection via a higher Laue zone

The figures illustrate the double reflection due to HOLZ reflections. Only the paths "a" and "b" are geometrically equivalent with respect to the glide plane, and only the paths "a" and "c" are geometrically equivalent about the screw axis. The equations on the opposite page hold independently of the index l. Then, an A_3 GM line is formed for the glide plane by the cancelation of the beams passing through the paths "a" and "b".

A B_3 GM line is formed for the screw axis by the cancelation of the beams passing through the paths "a" and "c". Since HOLZ refrections usually have small crystal structure factors, the dynamic extinction due to HOLZ interaction forms a narrow dark line. The GM line rules are given in the table on the opposite page.

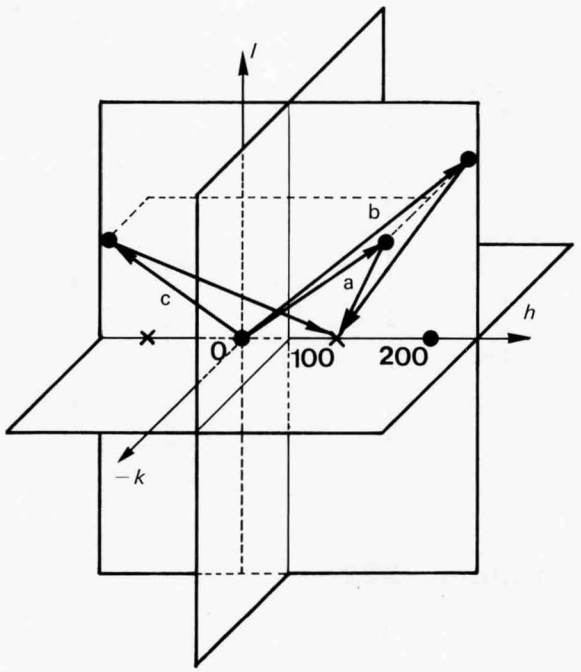

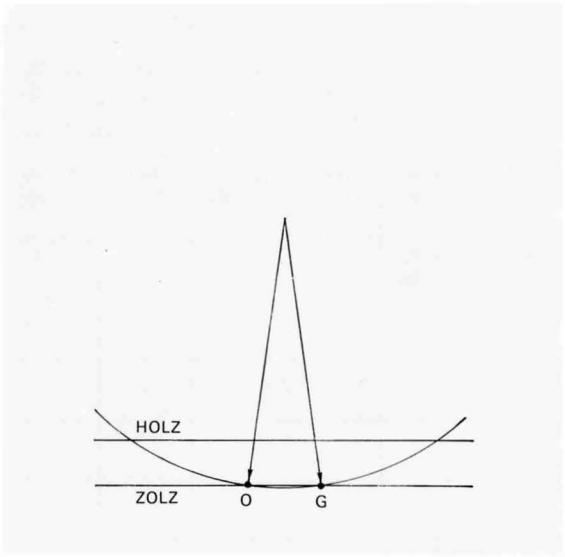

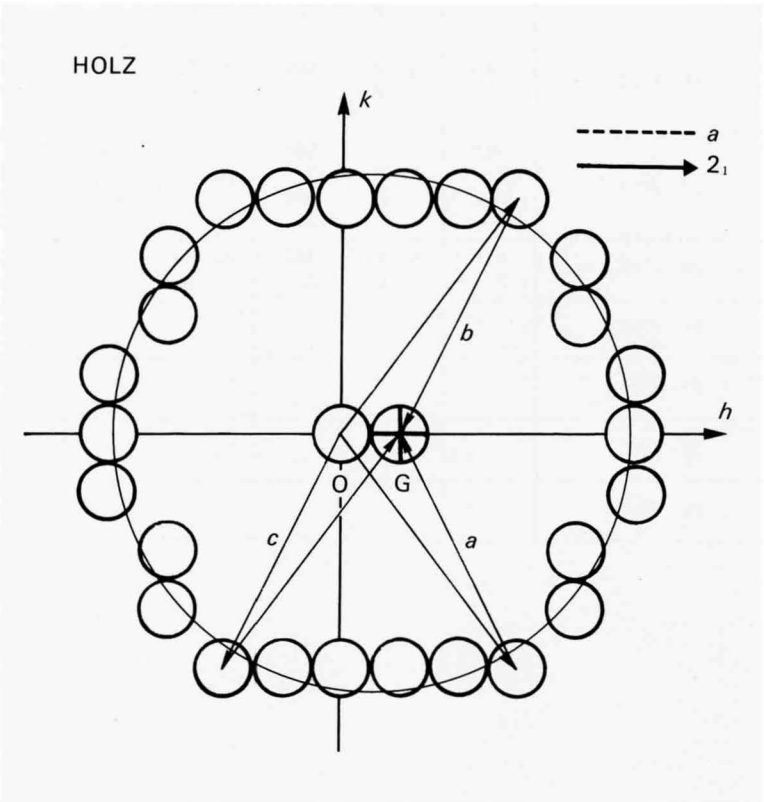

A_3 GM line for a-glide plane. B_3 GM line for 2_1 screw axis.

GM Line Tables for Space-Group Determination

Point-groups 2, *m*, 2/*m*

Incident beam direction / Space group	[h0ℓ]	
3 $P2$		
4 $P2_1$	0k0 2_1	A_2 B_2 B_3
5 $C2$		
6 Pm		
7 Pc	$h0\ell_o$ c	A_2 B_2 A_3
8 Cm		
9 Cc	$h_e0\ell_o$ c	A_2 B_2 A_3

Incident beam direction / Space group	[h0ℓ]	
10 $P2/m$		
11 $P2_1/m$	0k0 2_1	A_2 B_2 B_3
12 $C2/m$		
13 $P2/c$	$h0\ell_o$ c	A_2 B_2 A_3
14 $P2_1/c$	0k0 2_1 $h0\ell_o$ c	A_2 B_2 B_3 A_2 B_2 A_3
15 $C2/c$	$h_e0\ell_o$ c	A_2 B_2 A_3

2nd setting unique axis//b

Point-group 222

Incident beam direction / Space group	[100]		[010]		[001]		[hk0]		[0kℓ]		[h0ℓ]	
16 $P222$												
17 $P222_1$	00ℓ 2_1	A_2 B_2 B_3	00ℓ 2_1	A_2 B_2 B_3			00ℓ 2_1	A_2 B_2 B_3				
18 $P2_12_12$	0k0 2_{12}	A_2 B_2 B_3	h00 2_{11}	A_2 B_2 B_3	h00 2_{11} 0k0 2_{12}	A_2 B_2 B_3			h00 2_{11}	A_2 B_2 B_3	0k0 2_{12}	A_2 B_2 B_3
19 $P2_12_12_1$	0k0 2_{12} 00ℓ 2_{13}	A_2 B_2 B_3	h00 2_{11} 00ℓ 2_{13}	A_2 B_2 B_3	h00 2_{11} 0k0 2_{12}	A_2 B_2 B_3	00ℓ 2_{13}	A_2 B_2 B_3	h00 2_{11}	A_2 B_2 B_3	0k0 2_{12}	A_2 B_2 B_3
20 $C222_1$	00ℓ 2_1	A_2 B_2 B_3	00ℓ 2_1	A_2 B_2 B_3			00ℓ 2_1	A_2 B_2 B_3				
21 $C222$												
22 $F222$												
23 $I222$												
24 $I2_12_12_1$												

Point-group *mm*2

Incident beam direction / Space group	[100]		[010]		[001]		[hk0]		[0kℓ]		[h0ℓ]	
25 *Pmm*2												
26 *Pmc*2$_1$	00ℓ c, 2$_1$	A$_2$ B$_2$ A$_3$ B$_3$	00ℓ 2$_1$	B$_3$			00ℓ 2$_1$	A$_2$ B$_2$ B$_3$			h0ℓ$_o$ c	A$_2$ B$_2$ A$_3$
27 *Pcc*2	00ℓ c$_2$	A$_3$	00ℓ c$_1$	A$_3$					0kℓ$_o$ c$_1$	A$_2$ B$_2$ A$_3$	h0ℓ$_o$ c$_2$	A$_2$ B$_2$ A$_3$
28 *Pma*2					h00 a	A$_2$ B$_2$ A$_3$					h$_o$0ℓ a	A$_2$ B$_2$ A$_3$
29 *Pca*2$_1$	00ℓ 2$_1$	B$_3$	00ℓ c, 2$_1$	A$_2$ B$_2$ A$_3$ B$_3$	h00 a	A$_2$ B$_2$ A$_3$	00ℓ 2$_1$	A$_2$ B$_2$ B$_3$	0kℓ$_o$ c	A$_2$ B$_2$ A$_3$	h$_o$0ℓ a	A$_2$ B$_2$ A$_3$
30 *Pnc*2	00ℓ c	A$_3$	00ℓ n	A$_3$	0k0 n	A$_2$ B$_2$ A$_3$			0kℓ k+ℓ= 2n+1 n	A$_2$ B$_2$ A$_3$	h0ℓ$_o$ c	A$_2$ B$_2$ A$_3$
31 *Pmn*2$_1$	00ℓ n, 2$_1$	A$_2$ B$_2$ A$_3$ B$_3$	00ℓ 2$_1$	B$_3$	h00 n	A$_2$ B$_2$ A$_3$	00ℓ 2$_1$	A$_2$ B$_2$ B$_3$			h0ℓ h+ℓ= 2n+1 n	A$_2$ B$_2$ A$_3$
32 *Pba*2					h00 a 0k0 b	A$_2$ B$_2$ A$_3$			0k$_o$ℓ b	A$_2$ B$_2$ A$_3$	h$_o$0ℓ a	A$_2$ B$_2$ A$_3$
33 *Pna*2$_1$	00ℓ 2$_1$	B$_3$	00ℓ n, 2$_1$	A$_2$ B$_2$ A$_3$ B$_3$	h00 a 0k0 n	A$_2$ B$_2$ A$_3$	00ℓ 2$_1$	A$_2$ B$_2$ B$_3$	0kℓ k+ℓ= 2n+1 n	A$_2$ B$_2$ A$_3$	h$_o$0ℓ a	A$_2$ B$_2$ A$_3$
34 *Pnn*2	00ℓ n$_2$	A$_3$	00ℓ n$_1$	A$_3$	h00 n$_2$ 0k0 n$_1$	A$_2$ B$_2$ A$_3$			0kℓ k+ℓ= 2n+1 n$_1$	A$_2$ B$_2$ A$_3$	h0ℓ h+ℓ= 2n+1 n$_2$	A$_2$ B$_2$ A$_3$
35 *Cmm*2 *ba*2												
36 *Cmc*2$_1$ *bn*2$_1$	00ℓ c, 2$_1$	A$_2$ B$_2$ A$_3$ B$_3$	00ℓ 2$_1$	B$_3$			00ℓ 2$_1$	A$_2$ B$_2$ B$_3$			h$_e$0ℓ$_o$ c	A$_2$ B$_2$ A$_3$
37 *Ccc*2 *nn*2	00ℓ c$_2$	A$_3$	00ℓ c$_1$	A$_3$					0k$_e$ℓ$_o$ c$_1$	A$_2$ B$_2$ A$_3$	h$_e$0ℓ$_o$ c$_2$	A$_2$ B$_2$ A$_3$
38 *Amm*2 *nc*2$_1$												
39 *Abm*2 *cc*2$_1$									0k$_o$ℓ$_o$ b	A$_2$ B$_2$ A$_3$		
40 *Ama*2 *nn*2$_1$					h00 a	A$_2$ B$_2$ A$_3$					h$_o$0ℓ$_e$ a	A$_2$ B$_2$ A$_3$
41 *Aba*2 *cn*2$_1$					h00 a	A$_2$ B$_2$ A$_3$			0k$_o$ℓ$_o$ b	A$_2$ B$_2$ A$_3$	h$_o$0ℓ$_e$ a	A$_2$ B$_2$ A$_3$
42 *Fmm*2												
43 *Fdd*2 2$_1$	00ℓ ℓ=4n+2 d$_2$	A$_3$	00ℓ ℓ=4n+2 d$_1$	A$_3$	h00 h=4n+2 d$_2$ 0k0 k=4n+2 d$_1$	A$_2$ B$_2$ A$_3$			0k$_e$ℓ$_e$ k$_e$+ℓ$_e$= 4n+2 d$_1$	A$_2$ B$_2$ A$_3$	h$_e$0ℓ$_e$ h$_e$+ℓ$_e$= 4n+2 d$_2$	A$_2$ B$_2$ A$_3$
44 *Imm*2 *nn*2$_1$												
45 *Iba*2 *cc*2$_1$									0k$_o$ℓ$_o$ b	A$_2$ B$_2$ A$_3$	h$_o$0ℓ$_o$ a	A$_2$ B$_2$ A$_3$
46 *Ima*2 *nc*2$_1$											h$_o$0ℓ$_o$ a	A$_2$ B$_2$ A$_3$

Point-group *mmm*(I)

Incident beam direction / Space group	[100]		[010]		[001]		[hk0]		[0kℓ]		[h0ℓ]	
47 $P2/m2/m2/m$												
48 $P2/n2/n2/n$	00ℓ n_2 0k0 n_3	A_3	00ℓ n_1 h00 n_3	A_3	0k0 n_1 h00 n_2	A_3	hk0 h+k=2n+1 n_3	A_2 B_2 A_3	0kℓ k+ℓ=2n+1 n_1	A_2 B_2 A_3	h0ℓ h+ℓ=2n+1 n_2	A_2 B_2 A_3
49 $P2/c2/c2/m$	00ℓ c_2	A_3	00ℓ c_1	A_3					0kℓ_o c_1	A_2 B_2 A_3	h0ℓ_o c_2	A_2 B_2 A_3
50 $P2/b2/a2/n$	0k0 n	A_3	h00 n	A_3	0k0 b h00 a	A_3	hk0 h+k=2n+1 n	A_2 B_2 A_3	0k$_o\ell$ b	A_2 B_2 A_3	h$_o$0ℓ a	A_2 B_2 A_3
51 $P2_1/m2/m2/a$			h00 2_1, a	A_2 B_2 A_3 B_3	h00 2_1	B_3	h$_o$k0 a	A_2 B_2 A_3	h00 2_1	A_2 B_2 B_3		
52 $P2/n2_1/n2/a$	00ℓ n_2 0k0 2_1	A_3 B_3	00ℓ n_1 h00 a	A_3	0k0 n_1, 2_1 h00 n_2	A_2 B_2 A_3 B_3 A_3	h$_o$k0 a	A_2 B_2 A_3	0kℓ k+ℓ=2n+1 n_1	A_2 B_2 A_3	h0ℓ h+ℓ=2n+1 n_2 0k0 2_1	A_2 B_2 A_3 A_2 B_2 B_3
53 $P2/m2/n2_1/a$	00ℓ n, 2_1	A_2 B_2 A_3 B_3	h00 a 00ℓ 2_1	A_3 B_3	h00 n	A_3	h$_o$k0 a 00ℓ 2_1	A_2 B_2 A_3 A_2 B_2 B_3			h0ℓ h+ℓ=2n+1 n	A_2 B_2 A_3
54 $P2_1/c2/c2/a$	00ℓ c_2	A_3	00ℓ c_1 h00 a, 2_1	A_3 A_2 B_2 A_3 B_3	h00 2_1	B_3	h$_o$k0 a	A_2 B_2 A_3	0kℓ_o c_1 h00 2_1	A_2 B_2 A_3 A_2 B_2 B_3	h0ℓ_o c_2	A_2 B_2 A_3
55 $P2_1/b2_1/a2/m$	0k0 2_{12}	B_3	h00 2_{11}	B_3	0k0 b, 2_{12} h00 a, 2_{11}	A_2 B_2 A_3 B_3			0k$_o\ell$ b h00 2_{11}	A_2 B_2 A_3 A_2 B_2 B_3	h$_o$0ℓ a 0k0 2_{12}	A_2 B_2 A_3 A_2 B_2 B_3
56 $P2_1/c2_1/c2/n$	00ℓ c_2 0k0 2_{12}, n	A_3 A_2 B_2 A_3 B_3	00ℓ c_1 h00 2_{11}, n	A_3 A_2 B_2 A_3 B_3	0k0 2_{12} h00 2_{11}	B_3	hk0 h+k= 2n+1 n	A_2 B_2 A_3	0kℓ_o c_1 h00 2_{11}	A_2 B_2 A_3 A_2 B_2 B_3	h0ℓ_o c_2 0k0 2_{12}	A_2 B_2 A_3 A_2 B_2 B_3
57 $P2/b2_1/c2_1/m$	00ℓ c, 2_{12} 0k0 2_{11}	A_2 B_2 A_3 B_3 B_3	00ℓ 2_{12}	B_3	0k0 b, 2_{11}	A_2 B_2 A_3 B_3	00ℓ 2_{12}	A_2 B_2 B_3	0k$_o\ell$ b	A_2 B_2 A_3	h0ℓ_o c 0k0 2_{11}	A_2 B_2 A_3 A_2 B_2 B_3
58 $P2_1/n2_1/n2/m$	00ℓ n_2 0k0 2_{12}	A_3 B_3	00ℓ n_1 h00 2_{11}	A_3 B_3	0k0 n_1, 2_{12} h00 n_2, 2_{11}	A_2 B_2 A_3 B_3			0kℓ k+ℓ= 2n+1 n_1 h00 2_{11}	A_2 B_2 A_3 A_2 B_2 B_3	h0ℓ h+ℓ= 2n+1 n_2 0k0 2_{12}	A_2 B_2 A_3 A_2 B_2 B_3
59 $P2_1/m2_1/m2/n$	0k0 n, 2_{12}	A_2 B_2 A_3 B_3	h00 n, 2_{11}	A_2 B_2 A_3 B_3	0k0 2_{12} h00 2_{11}	B_3	hk0 h+k= 2n+1 n	A_2 B_2 A_3	h00 2_{11}	A_2 B_2 B_3	0k0 2_{12}	A_2 B_2 B_3
60 $P2_1/b2/c2_1/n$	00ℓ c, 2_{12} 0k0 n	A_2 B_2 A_3 B_3 A_3	h00 n, 2_{11} 00ℓ 2_{12}	A_2 B_2 A_3 B_3 B_3	0k0 b h00 2_{11}	A_3 B_3	hk0 h+k= 2n+1 n 00ℓ 2_{12}	A_2 B_2 A_3 A_2 B_2 B_3	0k$_o\ell$ b h00 2_{11}	A_2 B_2 A_3 A_2 B_2 B_3	h0ℓ_o c	A_2 B_2 A_3

Point-group *mmm*(II)

Incident beam direction / Space group	[100]		[010]		[001]		[hk0]		[0kℓ]		[h0ℓ]	
61 $P2_1/b2_1/c2_1/a$	00ℓ c, 2_{13} 0k0 2_{12}	A_2 B_2 A_3 B_3 B_3	00ℓ 2_{13} h00 a, 2_{11}	B_3 A_2 B_2 A_3 B_3	0k0 b, 2_{12} h00 2_{11}	A_2 B_2 A_3 B_3 B_3	h_ok0 a 00ℓ 2_{13}	A_2 B_2 A_3 A_2 B_2 B_3	$0k_o\ell$ b h00 2_{11}	A_2 B_2 A_3 A_2 B_2 B_3	$h0\ell_o$ c 0k0 2_{12}	A_2 B_2 A_3 A_2 B_2 B_3
62 $P2_1/n2_1/m2_1/a$	00ℓ 2_{13} 0k0 2_{12}	 B_3	00ℓ n, 2_{13} h00 a, 2_{11}	 A_2 B_2 A_3 B_3	0k0 n, 2_{12} h00 2_{11}	A_2 B_2 A_3 B_3 B_3	h_ok0 a 00ℓ 2_{13}	A_2 B_2 A_3 A_2 B_2 B_3	0kℓ $k+\ell=$ $2n+1$ n h00 2_{11}	 A_2 B_2 A_3 A_2 B_2 B_3	 0k0 2_{12}	 A_2 B_2 B_3
63 $C2/m2/c2_1/m$	00ℓ c, 2_1	A_2 B_2 A_3 B_3	00ℓ 2_1	 B_3			00ℓ 2_1	A_2 B_2 B_3			$h_e0\ell_o$ c	A_2 B_2 A_3
64 $C2/m2/c2_1/a$	00ℓ c, 2_1	A_2 B_2 A_3 B_3	00ℓ 2_1	 B_3			h_ok_o0 a 00ℓ 2_1	A_2 B_2 A_3 A_2 B_2 B_3			$h_e0\ell_o$ c	A_2 B_2 A_3
65 $C2/m2/m2/m$												
66 $C2/c2/c2/m$	00ℓ c_2	 A_3	00ℓ c_1	 A_3					$0k_e\ell_o$ c_1	A_2 B_2 A_3	$h_e0\ell_o$ c_2	A_2 B_2 A_3
67 $C2/m2/m2/a$							h_ok_o0 a	A_2 B_2 A_3				
68 $C2/c2/c2/a$	00ℓ c_2	 A_3	00ℓ c_1	 A_3			h_ok_o0 a	A_2 B_2 A_3	$0k_e\ell_o$ c_1	A_2 B_2 A_3	$h_e0\ell_o$ c_2	A_2 B_2 A_3
69 $F2/m2/m2/m$												
70 $F2/d2/d2/d$	00ℓ $\ell=4n+2$ d_2 0k0 $k=4n+2$ d_3	 A_3	h00 $h=4n+2$ d_3 00ℓ $\ell=4n+2$ d_1	 A_3	0k0 $k=4n+2$ d_1 h00 $h=4n+2$ d_2	 A_3	h_ek_e0 $h_e+k_e=$ $4n+2$ d_3	 A_2 B_2 A_3	$0k_e\ell_e$ $k_e+\ell_e=$ $4n+2$ d_1	 A_2 B_2 A_3	$h_e0\ell_e$ $h_e+\ell_e=$ $4n+2$ d_2	 A_2 B_2 A_3
71 $I2/m2/m2/m$												
72 $I2/b2/a2/m$									$0k_o\ell_o$ b	A_2 B_2 A_3	$h_o0\ell_o$ a	A_2 B_2 A_3
73 $I2/b2/c2/a$							h_ok_o0 a	A_2 B_2 A_3	$0k_o\ell_o$ b	A_2 B_2 A_3	$h_o0\ell_o$ c	A_2 B_2 A_3
74 $I2/m2/m2/a$							h_ok_o0 a	A_2 B_2 A_3				

Point-groups 4, $\bar{4}$, 4/*m*

Incident beam direction / Space group	[hk0]	
75 $P4$		
76 $P4_1$	00ℓ 4_1	A_2 B_2 B_3
77 $P4_2$		
78 $P4_3$	00ℓ 4_3	A_2 B_2 B_3
79 $I4$		
80 $I4_1$		
81 $P\bar{4}$		
82 $I\bar{4}$		
83 $P4/m$		
84 $P4_2/m$		
85 $P4/n$	hk0 h+k=2n+1 n	A_2 B_2 A_3
86 $P4_2/n$	hk0 h+k=2n+1 n	A_2 B_2 A_3
87 $I4/m$		
88 $I4_1/a$	h_0k_00 a	A_2 B_2 A_3

Point-group 422

Incident beam direction / Space group	[hk0]		[0kℓ]	
89 $P422$				
90 $P42_12$			h00 2_1	A_2 B_2 B_3
91 $P4_122$	00ℓ 4_1	A_2 B_2 B_3		
92 $P4_12_12$	00ℓ 4_1	A_2 B_2 B_3	h00 2_1	A_2 B_2 B_3
93 $P4_222$				
94 $P4_22_12$			h00 2_1	A_2 B_2 B_3
95 $P4_322$	00ℓ 4_3	A_2 B_2 B_3		
96 $P4_32_12$	00ℓ 4_3	A_2 B_2 B_3	h00 2_1	A_2 B_2 B_3
97 $I422$				
98 $I4_122$				

Point-group 4*mm*

Incident beam direction / Space group	[100]		[001]		[110]		[h0ℓ]*		[hhℓ]	
99 $P4mm$										
100 $P4bm$			h00 a_2 0k0 b_1	A_2 B_2 A_3			$h_o0\ell$ a	A_2 B_2 A_3		
101 $P4_2cm$	00ℓ c_2	A_3					h0ℓ_o c	A_2 B_2 A_3		
102 $P4_2nm$	00ℓ n_2	A_3	h00 n_2 0k0 n_1	A_2 B_2 A_3			h0ℓ h+ℓ= 2n+1 n	A_2 B_2 A_3		
103 $P4cc$	00ℓ c_{12}	A_3			00ℓ c_2	A_3	h0ℓ_o c_1	A_2 B_2 A_3	hhℓ_o c_2	A_2 B_2 A_3
104 $P4nc$	00ℓ n_2	A_3	h00 n_2 0k0 n_1	A_2 B_2 A_3	00ℓ c	A_3	h0ℓ h+ℓ= 2n+1 n	A_2 B_2 A_3	hhℓ_o c	A_2 B_2 A_3
105 $P4_2mc$					00ℓ c	A_3			hhℓ_o c	A_2 B_2 A_3
106 $P4_2bc$			h00 a_2 0k0 b_1	A_2 B_2 A_3	00ℓ c	A_3	$h_o0\ell$ a	A_2 B_2 A_3	hhℓ_o c	A_2 B_2 A_3
107 $I4mm$										
108 $I4cm$							$h_0 0\ell_0$ c	A_2 B_2 A_3		
109 $I4_1md$			$\underline{h}h0$ $\bar{h}h0$ d	A_2 B_2 A_3	00ℓ $\ell=4n+2$ d	A_3			hhℓ_e $2h+\ell_e=$ 4n+2 d	A_2 B_2 A_3
110 $I4_1cd$			$\underline{h}h0$ $\bar{h}h0$ d	A_2 B_2 A_3	00ℓ $\ell=4n+2$ d	A_3	$h_o0\ell_o$ c	A_2 B_2 A_3	hhℓ_e $2h+\ell_e=$ 4n+2 d	A_2 B_2 A_3

* The symbol "a" in the column of [*h0l*] incidence is equivalent to the symbol "b" in the space groups of the first column.

Point-group $\bar{4}2m$

Incident beam direction / Space group	[100]		[001]		[110]		[h0ℓ]*		[hhℓ]	
111 $P\bar{4}2m$										
112 $P\bar{4}2c$					00ℓ c	A_3			hhℓ$_o$ c	A_2 B_2 A_3
113 $P\bar{4}2_1m$	0k0 2_{12}	A_2 B_2 B_3	h00 2_{11} 0k0 2_{12}	A_2 B_2 B_3			0k0 2_1	A_2 B_2 B_3		
114 $P\bar{4}2_1c$	0k0 2_{12}	A_2 B_2 B_3	h00 2_{11} 0k0 2_{12}	A_2 B_2 B_3	00ℓ c	A_3	0k0 2_1	A_2 B_2 B_3	hhℓ$_o$ c	A_2 B_2 A_3
115 $P\bar{4}m2$										
116 $P\bar{4}c2$	00ℓ c_2	A_3					h0ℓ$_o$ c	A_2 B_2 A_3		
117 $P\bar{4}b2$			h00 a_2 0k0 b_1	A_2 B_2 A_3			h$_o$0ℓ a	A_2 B_2 A_3		
118 $P\bar{4}n2$	00ℓ n_2	A_3	h00 n_2 0k0 n_1	A_2 B_2 A_3			h0ℓ h+ℓ= 2n+1 n	A_2 B_2 A_3		
119 $I\bar{4}m2$										
120 $I\bar{4}c2$							h$_o$0ℓ$_o$ c	A_2 B_2 A_3		
121 $I\bar{4}2m$										
122 $I\bar{4}2d$			hh0 hh0 d	A_2 B_2 A_3	00ℓ ℓ=4n+2 d	A_3			hhℓ$_e$ 2h+ℓ$_e$= 4n+2 d	A_2 B_2 A_3

Point-group $4/mmm$(I)

Incident beam direction / Space group	[100]		[001]		[110]		[h0ℓ]*		[hhℓ]		[hk0]	
123 $P4/mmm$ $P4/m2/m2/m$												
124 $P4/mcc$ $P4/m2/c2/c$	00ℓ c_{12}	A_3			00ℓ c_2	A_3	h0ℓ$_o$ c_1	A_2 B_2 A_3	hhℓ$_o$ c_2	A_2 B_2 A_3		
125 $P4/nbm$ $P4/n2/b2/m$	0k0 n	A_3	h00 a_2 0k0 b_1	A_3			h$_o$0ℓ a	A_2 B_2 A_3			hk0 h+k= 2n+1 n	A_2 B_2 A_3
126 $P4/nnc$ $P4/n2/n2/c$	0k0 n_1 00ℓ n_{22}	A_3	h00 n_{22} 0k0 n_{21}	A_3	00ℓ c	A_3	h0ℓ h+ℓ= 2n+1 n_2	A_2 B_2 A_3	hhℓ$_o$ c	A_2 B_2 A_3	hk0 h+k= 2n+1 n_1	A_2 B_2 A_3
127 $P4/mbm$ $P4/m2_1/b2/m$	0k0 2_{12}	B_3	h00 a_2, 2_{11} 0k0 b_1, 2_{12}	A_2 B_2 A_3 B_3			h$_o$0ℓ a 0k0 2_1	A_2 B_2 A_3 A_2 B_2 B_3				

Point-group 4/*mmm*(II)

Incident beam direction / Space group		[100]		[001]		[110]		[h0ℓ]*		[hhℓ]		[hk0]	
128	$P4/mnc$ $P4/m2_1/n2/c$	00ℓ n_2 0k0 2_{12}	A_3 B_3	h00 n_2, 2_{11} 0k0 n_1, 2_{12}	A_2 B_2 A_3 B_3	00ℓ c	A_3	h0ℓ h+ℓ=2n+1 n 0k0 2_1	A_2 B_2 A_3 A_2 B_2 B_3	hhℓ$_o$ c	A_2 B_2 A_3		
129	$P4/nmm$ $P4/n2_1/m2/m$	0k0 n, 2_{12}	A_2 B_2 A_3 B_3	h00 2_{11} 0k0 2_{12}	B_3			0k0 2_1	A_2 B_2 B_3			hk0 h+k=2n+1 n	A_2 B_2 A_3
130	$P4/ncc$ $P4/n2_1/c2/c$	0k0 n, 2_{12} 00ℓ c_{12}	A_2 B_2 A_3 B_3 A_3	h00 2_{11} 0k0 2_{12}	B_3	00ℓ c_2	A_3	h0ℓ$_o$ c_1 0k0 2_1	A_2 B_2 A_3 A_2 B_2 B_3	hhℓ$_o$ c_2	A_2 B_2 A_3	hk0 h+k=2n+1 n	A_2 B_2 A_3
131	$P4_2/mmc$ $P4_2/m2/m2/c$					00ℓ c	A_3			hhℓ$_o$ c	A_2 B_2 A_3		
132	$P4_2/mcm$ $P4_2/m2/c2/m$	00ℓ c_2	A_3					h0ℓ$_o$ c	A_2 B_2 A_3				
133	$P4_2/nbc$ $P4_2/n2/b2/c$	0k0 n	A_3	h00 a_2 0k0 b_1	A_3	00ℓ c	A_3	h$_o$0ℓ a	A_2 B_2 A_3	hhℓ$_o$ c	A_2 B_2 A_3	hk0 h+k=2n+1 n	A_2 B_2 A_3
134	$P4_2/nnm$ $P4_2/n2/n2/m$	0k0 n_1 00ℓ n_{22}	A_3	h00 n_{22} 0k0 n_{21}	A_3			h0ℓ h+ℓ=2n+1 n_2	A_2 B_2 A_3			hk0 h+k=2n+1 n_1	A_2 B_2 A_3
135	$P4_2/mbc$ $P4_2/m2_1/b2/c$	0k0 2_{12}	B_3	h00 a_2, 2_{11} 0k0 b_1, 2_{12}	A_2 B_2 A_3 B_3	00ℓ c	A_3	h$_o$0ℓ a 0k0 2_1	A_2 B_2 A_3 A_2 B_2 B_3	hhℓ$_o$ c	A_2 B_2 A_3		
136	$P4_2/mnm$ $P4_2/m2_1/n2/m$	00ℓ n_2 0k0 2_{12}	A_3 B_3	h00 n_2, 2_{11} 0k0 n_1, 2_{12}	A_2 B_2 A_3 B_3			h0ℓ h+ℓ=2n+1 n 0k0 2_1	A_2 B_2 A_3 A_2 B_2 B_3				
137	$P4_2/nmc$ $P4_2/n2_1/m2/c$	0k0 n, 2_{12}	A_2 B_2 A_3 B_3	h00 2_{11} 0k0 2_{12}	B_3	00ℓ c	A_3	0k0 2_1	A_2 B_2 B_3	hhℓ$_o$ c	A_2 B_2 A_3	hk0 h+k=2n+1 n	A_2 B_2 A_3
138	$P4_2/ncm$ $P4_2/n2_1/c2/m$	0k0 n, 2_{12} 00ℓ c_2	A_2 B_2 A_3 B_3 A_3	h00 2_{11} 0k0 2_{12}	B_3			h0ℓ$_o$ c 0k0 2_1	A_2 B_2 A_3 A_2 B_2 B_3			hk0 h+k=2n+1 n	A_2 B_2 A_3
139	$I4/mmm$ $I4/m2/m2/m$												
140	$I4/mcm$ $I4/m2/c2/m$							h$_o$0ℓ$_o$ c	A_2 B_2 A_3				
141	$I4_1/amd$ $I4_1/a2/m2/d$			hh0 $\bar{h}$h0 d	A_3	00ℓ ℓ=4n+2 d $\bar{h}$h0 a	A_3			hhℓ$_e$ 2h+ℓ$_e$=4n+2 d	A_2 B_2 A_3	h$_o$k0 a	A_2 B_2 A_3
142	$I4_1/acd$ $I4_1/a2/c2/d$			hh0 $\bar{h}$h0 d	A_3	00ℓ ℓ=4n+2 d $\bar{h}$h0 a	A_3	h$_o$0ℓ$_o$ c	A_2 B_2 A_3	hhℓ$_e$ 2h+ℓ$_e$=4n+2 d	A_2 B_2 A_3	h$_o$k0 a	A_2 B_2 A_3

* The symbol "a" in the column of [*h0l*] incidence is equivalent to the symbol "b" in the space groups of the first column.

Point-groups 3, $\bar{3}$, 32, 3*m*, $\bar{3}$*m*

Incident beam direction / Space group	[11$\bar{2}$0]		[1$\bar{1}$00]	
No. 143 ~ No.155 No GM line				
156 $P3m1$				
157 $P31m$				
158 $P3c1$			00ℓ c	A_2 B_2 A_3
159 $P31c$	00ℓ c	A_2 B_2 A_3		
160 $R3m$				
161 $R3c$			00ℓ ℓ=6n+3 c	A_2 B_2 A_3

Incident beam direction / Space group	[11$\bar{2}$0]		[1$\bar{1}$00]	
162 $P\bar{3}1m$				
163 $P\bar{3}1c$	00ℓ c	A_2 B_2 A_3		
164 $P\bar{3}m1$				
165 $P\bar{3}c1$			00ℓ c	A_2 B_2 A_3
166 $R\bar{3}m$				
167 $R\bar{3}c$			00ℓ ℓ=6n+3 c	A_2 B_2 A_3

Point-groups 6, $\bar{6}$, 6/*m*, 622, 6*mm*, $\bar{6}$*m*2, 6/*mmm*

Incident beam direction / Space group	[11$\bar{2}$0]		[1$\bar{1}$00]	
168 $P6$				
169 $P6_1$	00ℓ 6_1	A_2 B_2 B_3	00ℓ 6_1	A_2 B_2 B_3
170 $P6_5$	00ℓ 6_5	A_2 B_2 B_3	00ℓ 6_5	A_2 B_2 B_3
171 $P6_2$				
172 $P6_4$				
173 $P6_3$	00ℓ 6_3	A_2 B_2 B_3	00ℓ 6_3	A_2 B_2 B_3
174 $P\bar{6}$				
175 $P6/m$				
176 $P6_3/m$	00ℓ 6_3	A_2 B_2 B_3	00ℓ 6_3	A_2 B_2 B_3
177 $P622$				
178 $P6_122$	00ℓ 6_1	A_2 B_2 B_3	00ℓ 6_1	A_2 B_2 B_3
179 $P6_522$	00ℓ 6_5	A_2 B_2 B_3	00ℓ 6_5	A_2 B_2 B_3
180 $P6_222$				
181 $P6_422$				

Incident beam direction / Space group	[11$\bar{2}$0]		[1$\bar{1}$00]	
182 $P6_322$	00ℓ 6_3	A_2 B_2 B_3	00ℓ 6_3	A_2 B_2 B_3
183 $P6mm$				
184 $P6cc$	00ℓ c_2	A_3	00ℓ c_1	A_3
185 $P6_3cm$	00ℓ 6_3	B_3	00ℓ 6_3, c	A_2 B_2 A_3 B_3
186 $P6_3mc$	00ℓ 6_3, c	A_2 B_2 A_3 B_3	00ℓ 6_3	B_3
187 $P\bar{6}m2$				
188 $P\bar{6}c2$			00ℓ c	A_2 B_2 A_3
189 $P\bar{6}2m$				
190 $P\bar{6}2c$	00ℓ c	A_2 B_2 A_3		
191 $P6/mmm$				
192 $P6/mcc$	00ℓ c_2	A_3	00ℓ c_1	A_3
193 $P6_3/mcm$	00ℓ 6_3	B_3	00ℓ 6_3, c	A_2 B_2 A_3 B_3
194 $P6_3/mmc$	00ℓ 6_3, c	A_2 B_2 A_3 B_3	00ℓ 6_3	B_3

Point-groups 23, $m3$

Incident beam direction / Space group	[100] (cyclic)		[110] (cyclic)		[hk0] (cyclic)	
195 $P23$						
196 $F23$						
197 $I23$						
198 $P2_13$	00ℓ 2_{13} 0k0 2_{12}	A_2 B_2 B_3	00ℓ 2_{13}	A_2 B_2 B_3	00ℓ 2_1	A_2 B_2 B_3
199 $I2_13$						
200 $Pm3$ / $P2/m\bar{3}$						
201 $Pn3$ / $P2/n\bar{3}$	00ℓ n_2 0k0 n_3	A_3			$\bar{k}$h0 n	A_2 B_2 A_3
202 $Fm3$ / $F2/m\bar{3}$						
203 $Fd3$ / $F2/d\bar{3}$	00ℓ $\ell=4n+2$ d_2 0k0 k$=4n+2$ d_3	A_3			$\bar{k}$h0 h+k$=$ $4n+2$ d	A_2 B_2 A_3
204 $Im3$ / $I2/m\bar{3}$						
205 $Pa3$ / $P2_1/a\bar{3}$	00ℓ c_2, 2_{13} 0k0 2_{12}	A_2 B_2 A_3 B_3 B_3	00ℓ 2_{13} hh0 a_3	A_2 B_2 B_3 A_2 B_2 A_3	00ℓ 2_1 $\bar{k}$h0 a	A_2 B_2 B_3 A_2 B_2 A_3
206 $Ia3$ / $I2_1/a\bar{3}$			$\bar{h}$h0 a_3	A_2 B_2 A_3	$\bar{k}$h0 a	A_2 B_2 A_3

Point-group 432

Incident beam direction / Space group	[hk0] (cyclic)		Incident beam direction / Space group	[hk0] (cyclic)	
207 $P432$			211 $I432$		
208 $P4_232$			212 $P4_332$	00ℓ 4_3	A_2 B_2 B_3
209 $F432$			213 $P4_132$	00ℓ 4_1	A_2 B_2 B_3
210 $F4_132$			214 $I4_132$		

Point-group $\bar{4}3m$

Incident beam direction / Space group	[100] (cyclic)		[110] (cyclic)		[hhℓ] (cyclic)	
215 $P\bar{4}3m$						
216 $F\bar{4}3m$						
217 $I\bar{4}3m$						
218 $P\bar{4}3n$			00ℓ n	A_3	hhℓ$_o$ n	A_2 B_2 A_3
219 $F\bar{4}3c$					$h_oh_o\ell_o$ c	A_2 B_2 A_3
220 $I\bar{4}3d$	0$\underline{k}$k 0$\bar{k}$k d	A_2 B_2 A_3	00ℓ ℓ=4n+2 d	A_3	hhℓ$_e$ 2h+ℓ$_e$= 4n+2 d	A_2 B_2 A_3

Point-group $m3m$

Incident beam direction / Space group	[100] (cyclic)		[110] (cyclic)		[hk0] (cyclic)		[hhℓ] (cyclic)	
221 $Pm3m$ $P4/m\bar{3}2/m$								
222 $Pn3n$ $P4/n\bar{3}2/n$	00ℓ n_{12} 0k0 n_{13}	A_3	00ℓ n_2	A_3	hk0 h+k= 2n+1 n_1	A_2 B_2 A_3	hhℓ$_o$ n_2	A_2 B_2 A_3
223 $Pm3n$ $P4_2/m\bar{3}2/n$			00ℓ n	A_3			hhℓ$_o$ n	A_2 B_2 A_3
224 $Pn3m$ $P4_2/n32/m$	00ℓ n_2 0k0 n_3	A_3			hk0 h+k= 2n+1 n	A_2 B_2 A_3		
225 $Fm3m$ $F4/m\bar{3}2/m$								
226 $Fm3c$ $F4/m\bar{3}2/c$							$h_oh_o\ell_o$ c	A_2 B_2 A_3
227 $Fd3m$ $F4_1/d\bar{3}2/m$	00ℓ ℓ=4n+2 d_2 0k0 k=4n+2 d_3	A_3			h_ek_e0 h$_e$+k$_e$= 4n+2 d	A_2 B_2 A_3		
228 $Fd3c$ $F4_1/d\bar{3}2/c$	00ℓ ℓ=4n+2 d_2 0k0 k=4n+2 d_3	A_3			h_ek_e0 h$_e$+k$_e$= 4n+2 d	A_2 B_2 A_3	$h_oh_o\ell_o$ c	A_2 B_2 A_3
229 $Im3m$ $I4/m\bar{3}2/m$								
230 $Ia3d$ $I4_1/a\bar{3}2/d$	0$\underline{k}$k 0$\bar{k}$k d	A_3	00ℓ ℓ=4n+2 $\underline{d}$ $\bar{h}h0$ a_3	A_3	h_ok_o0 a	A_2 B_2 A_3	hhℓ$_e$ 2h+ℓ$_e$= 4n+2 d	A_2 B_2 A_3

Space-groups indistinguishable by GM lines

$[P3, (P3_1, P3_2)]$
$[P312, (P3_112, P3_212)]$
$[P321, (P3_121, P3_221)]$
$[P6, (P6_2, P6_4)]$
$[P622, (P6_222, P6_422)]$
$[P6_3, (P6_1, P6_5)]$
$[P6_322, (P6_122, P6_522)]$
$(P4, P4_2)$
$(P4/m, P4_2/m)$
$(P4/n, P4_2/n)$
$(P422, P4_222)$
$(P42_12, P4_22_12)$
$(P432, P4_232)$
$(I4, I4_1)$
$(I422, I4_122)$
$(I432, I4_132)$
$(F432, F4_132)$
$(I23, I2_13)$
$(I222, I2_12_12_1)$

Notes on GM Line Tables

In the GM line tables, the atoms are postulated to occupy the general positions of a space group and the forbidden reflections caused by the special positions are not taken into account. One has to consult the full symbols of space groups; otherwise, one may overlook some glide planes and screw axes.

The space groups are written in the first column of each table. The expected GM lines are listed for various incident-beam directions in the following columns. The definitions needed to understand the tables are given in the following examples.

For [001] incidence of space group $P2_12_12$, A_2 and B_2 GM lines due to the 0-th Laue-zone interaction and a B_3 GM line due to a HOLZ interaction are produced at [001] electron incidence in the odd-order $h00$ and $0k0$ reflections by the 2_1 screw axes of space group $P2_12_12$. The second suffixes 1 and 2 of the symbols 2_{11} and 2_{12} distinguish between the first (in the a direction) and the second (in the b direction) screw axes of the space group. The glide symbols in the third column for space group $P4/nnc$ have two suffixes (n_{21} and n_{22}). The first suffix 2 denotes the second glide plane between two n-glide planes of the space group. The second suffixes 1 and 2, which appear in the tetragonal and cubic systems, distinguish two equivalent glide planes which lie in the x and y planes. The equivalent planes are distinguished only for the cases of [100], [010] and [001] electron incidences (not for more general incidences $[hkl]$) for convenience. The c-glide planes of space group $Pcc2$ are distinguished by the symbols c_1 and c_2, since the equivalent planes are not present. The glide symbol in the third column for space group $P4/mbm$ has a suffix 1 or 2. The suffix distinguishes the equivalent glide planes lying in the x and y planes. Another suffix is not necessary, since the space group has only one symbol b. For a general electron incidence in which the index of the incident-beam direction is represented only by a letter like the $[h0l]$ in the first table, the index h or l can take the value zero. That is, the GM-line rules are applicable to [100] and [001] electron incidences. However, if a table has the columns for [100], [010] and [001] incidneces, as the third has $[hk0]$, $[0kl]$ and $[h0l]$ incidences cover only the incidences of non-zero h, k and l. The reflections in which GM lines appear are always perpendicular to the corresponding incident-beam directions. The indices of the reflections in which GM lines appear are odd, if no remark is given. For c-glide planes of space groups $R3c$ and $R\bar{3}c$ and for a d-glide plane, the reflections in which GM lines appar are specified as $6n + 3$ and $4n + 2$ orders, respectively.

It is found from the tables that 185 space groups can be distinguished by the difference in the GM lines appearing for various electron incidences. It is assumed that the lattice types P, C, I and F are determined kinematically. It is noted that the handedness is determined by a different method [see references below]. The 19 pairs of space groups which cannot be distinguished by GM lines are enumerated in the table on this page. These indistinguishable pairs have to be identified from the intensity change of the forbidden reflections by varying crystal orientation. An example is the pair $I4$ and $I4_1$. If the intensity of the 200 reflection diminishes or decreases appreciably by varying crystal orientation, the space group is identified to be $I4_1$.

P. Goodman and T.W. Secomb: *Acta Cryst.*, **A33** (1977) 126.
P. Goodman and A.W.S. Johnson: *Acta Cryst.*, **A33** (1977) 997.
M. Tanaka, H. Takayoshi, M. Ishida and Y. Endoh: *J. Phys. Soc. Jpn.*, **54** (1985) 2970.

Computer Program Lists for HOLZ-Line Simulations

List for PC8801 (NEC)

```
10 '        ****** HOLZ ******
20 CONSOLE ,,0
30 DEF FNPARITY(X)=2*(X/2-INT(X/2)) '  0 : even , 1 : odd
40 DEF FNPRO(X1,X2,X3,Y1,Y2,Y3)=X1*Y1+X2*Y2+X3*Y3
50 DEF FNPARITY(X)=2*(X/2-INT(X/2))
60 DEF FNCS(X1,Y1,Z1,X2,Y2,Z2)=(X1*X2+Y1*Y2+Z1*Z2)/SQR((X1*X1+Y1*Y1+Z1*Z1)*(X2
 *X2+Y2*Y2+Z2*Z2))
70 DEF FNRL(H,K,L)=SQR((H*AST1)^2+(H*AST2+K*BST2+L*CST2)^2+(H*AST3+L*CST3)^2)
80 DEF FNXABC(H,K,L)=H*AST1+K*BST1+L*CST1
90 DEF FNYABC(H,K,L)=H*AST2+K*BST2+L*CST2
100 DEF FNZABC(H,K,L)=H*AST3+K*BST3+L*CST3
110 DEF FNPROX(X,Y,Z)=(UU*WW*X+VV*WW*Y-FA1*FA1*Z)/(FA1*FA2)
120 DEF FNPROY(X,Y,Z)=(VV*X-UU*Y)/FA1
130 DEF FNPROZ(X,Y,Z)=-(UU*X+VV*Y+WW*Z)/FA2
140 PAI#=3.1415926#
150 OPTION BASE 1
160 DIM HCA(500),KCA(500),LCA(500)
170 '
180 CLS 1
190 LOCATE 18,10 :PRINT "by  PHYS. DEPT. FAC OF SCI. TOHOKU UNIV.
                                  T.KANEYAMA ":CLS 2:CLS 1:PRINT
200 INPUT "   SPECIMEN NAME                                    ";S$
210 PRINT "   CRYSTAL SYSTEM"
220 PRINT "      cubic            ----------------- 1"
230 PRINT "      tetragonal       ----------------- 2"
240 PRINT "      rhombohedral
               (rhombohedral coordinates) --- 3"
250 PRINT "      hexagonal,trigonal,rhombohedral
               (hexagonal coordinates) ------ 4"
260 PRINT "      orthorhombic     ----------------- 5"
270 PRINT "      monoclinic       ----------------- 6"
280 PRINT "      triclinic        ----------------- 7"
290 PRINT "      diamond type     ----------------- 8"
300 INPUT "                                                    ";SYS
310 IF SYS=6 THEN GOSUB *SYS6
320 IF SYS=8 THEN 450
330 IF SYS=3 OR SYS=4 OR SYS=7 THEN 430
340 PRINT "           primitive ------------- 1"
350 IF SYS=2 THEN 370
360 PRINT "           face centered ---------- 2"
370 PRINT "           body centered ---------- 3"
380 IF SYS=1 OR SYS=2 THEN 420
390 PRINT "           A-base centered -------- 4"
400 PRINT "           B-base centered -------- 5"
410 PRINT "           C-base centered -------- 6"
420 INPUT "                                                    ";BRAV:GOTO 460
430 BRAV=1             primitive
440 GOTO 460
450 BRAV=7
460 ON SYS GOSUB *SYS1,*SYS2,*SYS3,*SYS4,*SYS5,*SYS6,*SYS7,*SYS1
470 INPUT "   ACCELERATING VOLTAGE in KV                       ";E
480 INPUT "   ZONE AXIS  u,v,w                                 ";U,V,W
490 INPUT "   DOES EXCITE G-REFLECTION ? (y/n)                 ";GREF$
500 IF GREF$="n" OR GREF$="N" THEN 540
510 INPUT "   INDEX OF G                                       ";HG,KG,LG
520 IF FNPRO(U,V,W,HG,KG,LG)=0 THEN 540
530 INPUT " reinput index of G which IS on the 0th loue zone!
                                                              ";HG,KG,LG:GOTO 520
540 INPUT "   ORDER OF LAUE ZONE                               ";N
550 PRINT "   TWO NONLINEAR VECTORS V1 AND V2 BY WHICH ALL RECIPROCAL"
560 PRINT "   LATTICE POINTS IN THE 0-TH LAUE ZONE ARE COVERED."
570 PRINT "   (V1 DETERMINES HORIZONTAL DIRECTION IN THE OUTPUT)"
580 INPUT "                          X1,Y1,Z1, X2,Y2,Z2 =";X1,Y1,Z1,X2,Y2,Z2
```

```
590    IF X1=0 AND Y1=0 AND Z1=0 THEN 630
600    IF X2=0 AND Y2=0 AND Z2=0 THEN 630
610    IF (FNCS(X1,Y1,Z1,X2,Y2,Z2))^2>.99 THEN 640
620    IF 0=U*X1+V*Y1+W*Z1 AND 0=U*X2+V*Y2+W*Z2 THEN 650
630    PRINT " Reinput vector!" :GOTO 580
640    PRINT " V2 is parallel to V1! Reinput!!":GOTO 580
650 IF FNCS(X1,Y1,Z1,X2,Y2,Z2)=>0 THEN 670
660 X2=X2+X1:Y2=Y2+Y1:Z2=Z2+Z1
670 INPUT "    TWO REFLECTIONS IN THE 0-TH LAUE ZONE (THEY DETERMINE
              THE DISK SIZE)          H1,K1,L1, H2,K2,L2=";HAD1,KAD1,LAD1,HAD2,
KAD2,LAD2
680 IF FNPRO(HAD1,KAD1,LAD1,U,V,W)=0 AND 0=FNPRO(HAD2,KAD2,LAD2,U,V,W) THEN 700
690 PRINT " Reinput disk parameter !" :GOTO 670
700 PRINT "    DIAMETER OF DISKS MEASURED IN UNITS OF
              MIN.[ABS(H1,K1,L1),ABS(H2,K2,L2),ABS(H1-H2,K1-K2,L1-L2)]"
710 INPUT "                                                    ";DA
720 IF DA<0 THEN DA=-DA
730 IF DA=0 THEN DA=1
740 INPUT "    INDEX OF A RECIPROCAL LATTICE POINT IN THE N-TH
              LAUE ZONE.                                       ";HN,KN,LN
750    IF FNPRO(HN,KN,LN,U,V,W)=N THEN 770
760    PRINT " Reinput!  It isn't Nth!" :GOTO 740
770
780 SCREEN 2,0:CLS 3
790 DREA=SQR(1-COS(ALP)^2-COS(BET)^2-COS(GAM)^2+2*COS(ALP)*COS(BET)*COS(GAM))
800 DREC=DREA*DREA/(SIN(ALP)*SIN(BET)*SIN(GAM))
810 VOL=A*B*C*DREA : VOLST=1/VOL
820 AST=B*C*SIN(ALP)/VOL:BST=C*A*SIN(BET)/VOL:CST=A*B*SIN(GAM)/VOL
830 COA=(COS(BET)*COS(GAM)-COS(ALP))/(SIN(BET)*SIN(GAM))
840 COB=(COS(GAM)*COS(ALP)-COS(BET))/(SIN(GAM)*SIN(ALP))
850 COG=(COS(ALP)*COS(BET)-COS(GAM))/(SIN(ALP)*SIN(BET))
860 SIA=DREA/(SIN(BET)*SIN(GAM)):SIB=DREA/(SIN(GAM)*SIN(ALP)):SIG=DREA/(SIN(ALP)
  *SIN(BET))
870 S11ST=(BST*CST*SIA)^2:S22ST=(CST*AST*SIB)^2:S33ST=(AST*BST*SIG)^2
880 S12ST=AST*BST*CST*CST*(COA*COB-COG):S23ST=AST*AST*BST*CST*(COB*COG-COA):
    S31ST=AST*BST*BST*CST*(COG*COA-COB)
890 D=N*VOLST/SQR(S11ST*U*U+S22ST*V*V+S33ST*W*W+2*S12ST*U*V+2*S23ST*V*W+2*S31ST*
  W*U)
900 A1=A:B1=B*COS(GAM):B2=B*DREA/SIN(BET):B3=B*(COS(ALP)-COS(BET)*COS(GAM))/SIN(
  BET):C1=C*COS(BET):C3=C*SIN(BET)
910 AST1=1/A:AST2=(COS(ALP)*COS(BET)-COS(GAM))/(A*DREA*SIN(BET)):AST3=-COS(BET)/
  (A*SIN(BET)):BST2=SIN(BET)/(B*DREA):CST2=(COS(BET)*COS(GAM)-COS(ALP))/(C*DREA*
  SIN(BET)):CST3=1/(C*SIN(BET))
920 UU=A1*U+B1*V+C1*W : VV=A2*U+B2*V+C2*W : WW=A3*U+B3*V+C3*W
930 RD=FNRL(HAD1,KAD1,LAD1)/2  :RD2=FNRL(HAD2,KAD2,LAD2)/2
940 IF RD>RD2 THEN RD=RD2
950 RD3=FNRL(HAD1-HAD2,KAD1-KAD2,LAD1-LAD2)/2
960 IF RD>RD3 THEN RD=RD3
970 DDA=DA*RD : DD=1.2*DDA
980 XX1=DD*1.05
990 XX4=-XX1:XX5=-XX1:XX8=XX1:YY2=-XX1:YY3=-XX1:YY6=XX1:YY7=XX1
1000 INDX=4*DD/240 : INDY=28*DD/240
1010 XY1=-DD*400/240-INDY/2
1020 XY4=XY1:XY5=-XY1-2.1*INDY:XY8=XY5
1030 FA1=SQR(UU*UU+VV*VV) : FA2=SQR(UU*UU+VV*VV+WW*WW)
1040 WN=SQR(1000*E*(1+9.788E-07*1000*E))/12.26
1050 R0=FNRL(HG/2,KG/2,LG/2)
1060 R=SQR(WN*WN-(SQR(WN*WN-R0*R0)-D)^2)
1070 IF UU*UU+VV*VV=0 THEN 1110
1080 X=FNPROX(FNXABC(X1,Y1,Z1),FNYABC(X1,Y1,Z1),FNZABC(X1,Y1,Z1))
1090 Y=FNPROY(FNXABC(X1,Y1,Z1),FNYABC(X1,Y1,Z1),FNZABC(X1,Y1,Z1))
1100 GOTO 1120
1110 X=FNXABC(X1,Y1,Z1):Y=-FNYABC(X1,Y1,Z1)
```

```
1120 CO=FNCS(1,0,0,X,Y,0):SI=FNCS(0,1,0,X,Y,0)
1130 O1=0:O2=0:O3=0:I=0:V2=0:QQ=0:NQ1=0:NQ2=0:NQ3=0:NQ4=0:HV2=0:KV2=0:LV2=0
1140 WINDOW (-R-RD*2.2,-R-RD*2.2)-(R+RD*2.2,R+RD*2.2)
1150 VIEW (205,5)-(595,395)
1160 CIRCLE(0,0),R
1170 IF GREF$="n" OR GREF$="N" THEN 1270
1180 IF UU*UU+VV*VV=0 THEN 1220
1190 HGPROI!=FNPROX(FNXABC(HG/2,KG/2,LG/2),FNYABC(HG/2,KG/2,LG/2),FNZABC(HG/2,
   KG/2,LG/2))
1200 KGPROI!=FNPROY(FNXABC(HG/2,KG/2,LG/2),FNYABC(HG/2,KG/2,LG/2),FNZABC(HG/2,
   KG/2,LG/2))
1210 GOTO 1230
1220 HGPROI!=FNXABC(HG/2,KG/2,LG/2) : KGPROI!=-FNYABC(HG/2,KG/2,LG/2)
1230 HGPRO!=HGPROI!*CO+KGPROI!*SI:KGPRO!=-HGPROI!*SI+KGPROI!*CO
1240 CIRCLE(HGPRO!,KGPRO!),DDA
1250 PUT(192-195*HGPRO!/(R+DD*2!),192-195*KGPRO!/(R+DD*2!)),KANJI(&H14F)
1260 PUT(192+195*HGPRO!/(R+DD*2!),192+195*KGPRO!/(R+DD*2!)),KANJI(&H147)
1270 CIRCLE(-HGPRO!,-KGPRO!),DDA
1280 LOCATE 4,2:PRINT "    ";S$:PRINT
1290 PRINT "  ["U" "V" "W"]":PRINT
1300 PRINT "      "E;"kV":PRINT
1310 PRINT "  ";N;
1320 IF N>3 THEN 1370
1330 ON N GOTO 1340,1350,1360
1340 PRINT "st Laue Zone":GOTO 1380
1350 PRINT "nd Laue Zone":GOTO 1380
1360 PRINT "rd Laue Zone":GOTO 1380
1370 PRINT "th Laue Zone"
1380 PRINT
1390 IF GREF$="n" OR GREF$="N" THEN 1420
1400 PRINT " G reflection :"
1410 PRINT "      ("HG" "KG" "LG")"
1420 PRINT :PRINT "  a ="A:PRINT "  b ="B:PRINT "  c ="C
1430 PRINT "  alpha,beta,gamma ":PRINT "  ="ALPH","BETA","GAMM
1440 PRINT : PRINT " Radius of N-th Laue Zone"
1450 PRINT "  =";R
1460 PRINT " Horizontal Direction"
1470 PRINT "  = ("X1","Y1","Z1")"
1480 '
1490 H=HN : K=KN : L=LN
1500 GOSUB *SOTO
1510 IF FNRL(H-HG/2,K-KG/2,L-LG/2)=>R+DDA THEN  1540
1520 GOTO 1500
1530 '
1540 IF I=3 THEN 1680
1550 LL!=FNRL(H-HG/2,K-KG/2,L-LG/2)
1560 IF LL!>R-DDA AND LL!<R+DDA THEN P=1
1570 IF LL!<=R-DDA THEN P=2
1580 IF LL!>=R+DDA THEN P=3
1590 '
1600 IF P=3 AND O2<>0 THEN P=4
1610 IF P=4 THEN P4=P4+1
1620 ON P GOSUB *HOLZRING , *V2 , *UCHI , *V2
1630 IF P=1 THEN GOSUB *UCHI
1640 IF P=3 AND O2=0 AND O1>30 THEN GOSUB *ORIKAESHI
1650 IF P=2 OR P=4 THEN GOTO 1510
1660 IF P=10 THEN 1680
1670 GOTO 1540
1680 IF O3=0 THEN 1780
1690 COPY 3 :I=0
1700 CLS 3
1710 GOSUB *HOLZ
1720 COPY 3
```

```
1730 LPRINT " "
1740 LPRINT " "
1750 LPRINT " "
1760 GOSUB *INDEX
1770 END
1780 LOCATE 40,3:PRINT " You have no holz."
1790 END
1800 '
1810 '   ((((  sub  ))))
1820 *SYS1 'cubic
1830 INPUT "   LATTICE PARAMETERS (A°)                a=b=c= ";A
1840  B=A:C=A:ALP=PAI#/2:BET=PAI#/2:GAM=PAI#/2:ALPH=90:BETA=90:GAMM=90
1850 RETURN
1860 *SYS2 'tetragonal
1870 INPUT "   LATTICE PARAMETERS (A°)                  a=b= ";A
1880 INPUT "                                             c= ";C
1890  B=A:ALP=PAI#/2:BET=PAI#/2:GAM=PAI#/2:ALPH=90:BETA=90:GAMM=90
1900 RETURN
1910 *SYS3 'rhombohedral
1920 INPUT "   LATTICE PARAMETERS (A°)                a=b=c= ";A
1930 INPUT "                ANGLE (deg)  alpha=beta=gamma= ";ALPH
1940 B=A:C=A:ALP=ALPH*PAI#/180:BET=ALP:GAM=ALP:BETA=ALPH:GAMM=ALPH
1950 RETURN
1960 *SYS4 'hexagonal (trigonal,rhombohedral)
1970 INPUT "   LATTICE PARAMETERS (A°)                  a=b= ";A
1980 INPUT "                                             c= ";C
1990 INPUT "  rhombohedral ? (y/n)                          ";RH$
2000  B=A:ALP=PAI#/2:BET=PAI#/2:GAM=2*PAI#/3:ALPH=90:BETA=90:GAMM=120
2010 RETURN
2020 *SYS5 'orthorhombic
2030 INPUT "   LATTICE PARAMETERS (A°)                    a= ";A
2040 INPUT "                                              b= ";B
2050 INPUT "                                              c= ";C
2060 ALP=PAI#/2:BET=PAI#/2:GAM=PAI#/2:ALPH=90:BETA=90:GAMM=90
2070 RETURN
2080 *SYS6 'monoclinic
2090 INPUT "      UNIQUE AXIS,B or C ?                       ";UNIQ$
2100 INPUT "   LATTICE PARAMETERS (A°)                    a= ";A
2110 INPUT "                                              b= ";B
2120 INPUT "                                              c= ";C
2130 IF UNIQ$="c" OR UNIQ$="C" THEN 2160
2140 INPUT "                ANGLE (deg)                beta= ";BETA:GAMM=90
2150 GOTO 2170
2160 INPUT "                ANGLE (deg)               gamma= ";GAMM:BETA=9
2170 ALP=PAI#/2:BET=BETA*PAI#/180:GAM=GAMM*PAI#/180:ALPH=90
2180 PRINT "          primitive ------------- 1"
2190 IF UNIQ$="b" OR UNIQ$="B" THEN 2220
2200 PRINT "          B-base centered -------- 2"
2210 GOTO 2230
2220 PRINT "          C-base centered -------- 3"
2230 INPUT "                                                 ";BRAV
2240 IF BRAV=2 THEN BRAV=5
2250 IF BRAV=3 THEN BRAV=6
2260 RETURN 470
2270 *SYS7 'tricrinic
2280 INPUT "   LATTICE PARAMETERS (A°)                    a= ";A
2290 INPUT "                                              b= ";B
2300 INPUT "                                              c= ";C
2310 INPUT "                ANGLE (deg)               alpha= ";ALPH
2320 INPUT "                                           beta= ";BETA
2330 INPUT "                                          gamma= ";GAMM
2340 ALP=ALPH*PAI#/180:BET=BETA:PAI#/180:GAM=GAMM*PAI#/180
2350 RETURN
```

```
2360 *HOLZ
2370 WINDOW (-DD,-DD)-(DD,DD)
2380 VIEW (200, 80)-(440,320)
2390 CIRCLE(0,0),DDA
2400 FOR IJ=1 TO O3-1
2410 WINDOW (-DD,-DD)-(DD,DD)
2420 VIEW (200, 80)-(440,320)
2430 IF UU*UU+VV*VV=0 THEN 2470
2440 XI=FNPROX(FNXABC(HCA(IJ)-HG/2,KCA(IJ)-KG/2,LCA(IJ)-LG/2),FNYABC(HCA(IJ)-HG/
2,KCA(IJ)-KG/2,LCA(IJ)-LG/2),FNZABC(HCA(IJ)-HG/2,KCA(IJ)-KG/2,LCA(IJ)-LG/2))
2450 YI=FNPROY(FNXABC(HCA(IJ)-HG/2,KCA(IJ)-KG/2,LCA(IJ)-LG/2),FNYABC(HCA(IJ)-HG/
2,KCA(IJ)-KG/2,LCA(IJ)-LG/2),FNZABC(HCA(IJ)-HG/2,KCA(IJ)-KG/2,LCA(IJ)-LG/2))
2460 GOTO 2480
2470 XI=FNXABC(HCA(IJ)-HG/2,KCA(IJ)-KG/2,LCA(IJ)-LG/2):YI=-FNYABC(HCA(IJ)-HG/2,K
CA(IJ)-KG/2,LCA(IJ)-LG/2)
2480 X=XI*CO+YI*SI:Y=-XI*SI+YI*CO:CIRCLE(-X,-Y),R
2490 WINDOW (-DD*640/240,-DD*400/240)-(DD*640/240,DD*400/240)
2500 VIEW (0,0)-(639,399)
2510 GOSUB *INDEXING
2520 NEXT IJ
2530 RETURN
2540 *V2
2550 GOSUB *SOTO
2560 IF FNRL(H-HG/2,K-KG/2,L-LG/2)>R+DDA THEN 2580
2570 GOTO 2550
2580 H=H+X2*(-1)^I:K=K+Y2*(-1)^I:L=L+Z2*(-1)^I
2590 O1=0 : O2=0
2600 RETURN
2610 *UCHI
2620 H=H-X1*(-1)^I : K=K-Y1*(-1)^I : L=L-Z1*(-1)^I
2630 O1=O1+1
2640 RETURN
2650 *SOTO
2660 H=H+X1*(-1)^I : K=K+Y1*(-1)^I : L=L+Z1*(-1)^I
2670 RETURN
2680 *ORIKAESHI
2690 I=I+1
2700 H=H+(P4+1)*X2*(-1)^I : K=K+(P4+1)*Y2*(-1)^I : L=L+(P4+1)*Z2*(-1)^I
2710 IF FNRL(H-HG/2,K-KG/2,L-LG/2)<=R+DDA THEN 2740
2720 GOSUB *UCHI
2730 GOTO 2710
2740 O1=0 : O2=0 : P=2 : P4=0
2750 RETURN
2760 *DIAMOND
2770 IF 1=FNPARITY(H+K) OR 1=FNPARITY(K+L) OR 1=FNPARITY(L+H) THEN 2810
2780 IF 1=FNPARITY(H) THEN 2800
2790 IF 1=FNPARITY((H+K+L)/2) THEN 2810
2800 AL=0:RETURN
2810 AL=1:RETURN
2820 '                                  AL=0:allowed    AL=1:forbidden
2830 *I
2840 IF 0=FNPARITY(H+K+L) THEN AL=0 ELSE AL=1
2850 RETURN
2860 *P
2870 AL=0
2880 RETURN
2890 *F
2900 IF 0=FNPARITY(H+K) OR 0=FNPARITY(K+L) OR 0=FNPARITY(L+H) THEN AL=0 ELSE AL=
  1
2910 RETURN
2920 *A
2930 IF 0=FNPARITY(K+L) THEN AL=0 ELSE AL=1
2940 RETURN
```

```
2950 *B
2960 IF 0=FNPARITY(H+L) THEN AL=0 ELSE AL=1
2970 RETURN
2980 *C
2990 IF 0=FNPARITY(H+K) THEN AL=0 ELSE AL=1
3000 RETURN
3010 *RHOMBO
3020 AL=3*((-H+K+L)/3-INT((-H+K+L)/3))
3030 RETURN
3040 *INDEXING
3050 FU1=R*R-(X+DD)*(X+DD) : FU2=R*R-(X-DD)*(X-DD) : FU3=R*R-(Y+DD)*(Y+DD) : FU4
=R*R-(Y-DD)*(Y-DD)
3060 IF X=0 AND Y>0 THEN P=3 : GOTO *SEP
3070 IF X=0 AND Y<0 THEN P=5 : GOTO *SEP
3080 IF X>0 AND Y=0 THEN P=4 : GOTO *SEP
3090 IF X<0 AND Y=0 THEN P=1 : GOTO *SEP
3100 RAT=Y/X
3110 IF RAT=>-1 AND RAT<=0 AND X<0  THEN P=1 : GOTO *SEP
3120 IF RAT<-1             AND X<=0 THEN P=2 : GOTO *SEP
3130 IF RAT=>1             AND X=>0 THEN P=3 : GOTO *SEP
3140 IF RAT>0   AND RAT<1  AND X>0  THEN P=4 : GOTO *SEP
3150 IF RAT>-1  AND RAT<0  AND X>0  THEN P=5 : GOTO *SEP
3160 IF RAT<=-1            AND X>0  THEN P=6 : GOTO *SEP
3170 IF RAT=>1             AND X<=0 THEN P=7 : GOTO *SEP
3180 IF RAT>0   AND RAT<1  AND X<0  THEN P=8 : GOTO *SEP
3190 BEEP:RETURN
3200 *SEP
3210 ON P GOSUB *P1,*P2,*P3,*P4,*P5,*P6,*P7,*P8
3220 ON Q GOSUB *Q1,*Q2,*Q3,*Q4,*Q5,*Q6,*Q7,*Q8
3230 RETURN
3240 *P1
3250 IF FU4<0 THEN 3300
3260 EKS=-X-FU4^.5
3270 IF ABS(EKS)>DD THEN GOTO 3300
3280 IF EKS>=0 THEN Q=2 ELSE Q=3
3290 RETURN
3300 EKS=-X-FU3^.5
3310 IF EKS>0 THEN Q=7 ELSE Q=6
3320 RETURN
3330 *P2
3340 IF FU1<0 THEN 3390
3350 WAI=-Y+FU1^.5
3360 IF ABS(WAI)>DD THEN GOTO 3390
3370 IF WAI<0 THEN Q=1 ELSE Q=8
3380 RETURN
3390 WAI=-Y+FU2^.5
3400 IF WAI=<0 THEN Q=4 ELSE Q=5
3410 RETURN
3420 *P3
3430 IF FU2<0 THEN 3480
3440 WAI=-Y+FU2^.5
3450 IF ABS(WAI)>DD THEN 3480
3460 IF WAI<=0 THEN Q=4 ELSE Q=5
3470 RETURN
3480 WAI=-Y+FU1^.5
3490 IF WAI<0 THEN Q=1 ELSE Q=8
3500 RETURN
3510 *P4
3520 IF FU4<0 THEN 3570
3530 EKS=-X+FU4^.5
3540 IF ABS(EKS)>DD THEN 3570
3550 IF EKS>0 THEN Q=2 ELSE Q=3
3560 RETURN
```

```
3570 EKS=-X+FU3^.5
3580 IF EKS>0 THEN Q=7 ELSE Q=6
3590 RETURN
3600 *P5
3610 IF FU3<0 THEN 3660
3620 EKS=-X+FU3^.5
3630 IF ABS(EKS)>DD THEN 3660
3640 IF EKS>0 THEN Q=7 ELSE Q=6
3650 RETURN
3660 EKS=-X+FU4^.5
3670 IF EKS>0 THEN Q=2 ELSE Q=3
3680 RETURN
3690 *P6
3700 IF FU2<0 THEN 3750
3710 WAI=-Y-FU2^.5
3720 IF ABS(WAI)>DD THEN 3750
3730 IF WAI<0 THEN Q=4 ELSE Q=5
3740 RETURN
3750 WAI=-Y-FU1^.5
3760 IF WAI<0 THEN Q=1 ELSE Q=8
3770 RETURN
3780 *P7
3790 IF FU1<0 THEN 3840
3800 WAI=-Y-FU1^.5
3810 IF ABS(WAI)>DD THEN 3840
3820 IF WAI<0 THEN Q=1 ELSE Q=8
3830 RETURN
3840 WAI=-Y-FU2^.5
3850 IF WAI<0 THEN Q=4 ELSE Q=5
3860 RETURN
3870 *P8
3880 IF FU3<0 THEN 3930
3890 EKS=-X-FU3^.5
3900 IF ABS(EKS)>DD THEN 3930
3910 IF EKS>0 THEN Q=7 ELSE Q=6
3920 RETURN
3930 EKS=-X-FU4^.5
3940 IF EKS>0 THEN Q=2 ELSE Q=3
3950 RETURN
3960 *INDEX
3970 IF N=>4 THEN 3990
3980 ON N GOTO 4010,4030,4050
3990 LPRINT "  *"S$"    ("U""V""W")    "N"th zone    "E"kV":LPRINT " "
4000 GOTO 4060
4010 LPRINT "  *"S$"    ("U""V""W")     1 st zone    "E"kV":LPRINT " "
4020 GOTO 4060
4030 LPRINT "  *"S$"    ("U""V""W")     2 nd zone    "E"kV":LPRINT " "
4040 GOTO 4060
4050 LPRINT "  *"S$"    ("U""V""W")     3 rd zone    "E"kV":LPRINT " "
4060 JI=FIX((O3-1)/3)+1
4070 FOR IJ=1 TO JI
4080 IF IJ+JI>O3-1 THEN 4140
4090 IF IJ+JI*2>O3-1 THEN 4120
4100 LPRINT IJ"-"" ("HCA(IJ)","KCA(IJ)","LCA(IJ)")", IJ+JI"-"" ("HCA(IJ+JI)","
  KCA(IJ+JI)","LCA(IJ+JI)")",IJ+JI*2"-"" ("HCA(IJ+JI*2)","KCA(IJ+JI*2)","LCA(IJ+
  JI*2)")"
4110 GOTO 4150
4120 LPRINT IJ"-"" ("HCA(IJ)","KCA(IJ)","LCA(IJ)")", IJ+JI"-"" ("HCA(IJ+JI)","
  KCA(IJ+JI)","LCA(IJ+JI)")"
4130 GOTO 4150
4140 LPRINT IJ"-"" ("HCA(IJ)","KCA(IJ)","LCA(IJ)")"
4150 NEXT IJ
4160 RETURN
```

```
4170 *HOLZRING
4180 O1=0 : O2=O2+1
4190 ON BRAV GOSUB *P,*F,*I,*A,*B,*C,*DIAMOND
4200 IF RH$="Y" OR RH$="y" THEN GOSUB *RHOMBO
4210 IF AL=1 THEN 4350
4220 IF AL<>0 THEN 4350
4230 O3=O3+1
4240 HCA(O3)=H : KCA(O3)=K : LCA(O3)=L
4250 IF O3=0 OR O3=1 THEN 4280
4260 IF (HCA(O3)-HCA(1))^2<.1 AND (KCA(O3)-KCA(1))^2<.1 AND (LCA(O3)-LCA(1))^2<
  .1 AND I=2 THEN P=10
4270 IF P=10 THEN 4350
4280 IF UU*UU+VV*VV=0 THEN 4320
4290 XI=FNPROX(FNXABC(H-HG/2,K-KG/2,L-LG/2),FNYABC(H-HG/2,K-KG/2,L-LG/2),FNZABC(
  H-HG/2,K-KG/2,L-LG/2))
4300 YI=FNPROY(FNXABC(H-HG/2,K-KG/2,L-LG/2),FNYABC(H-HG/2,K-KG/2,L-LG/2),FNZABC(
  H-HG/2,K-KG/2,L-LG/2))
4310 GOTO 4330
4320 XI=FNXABC(H-HG/2,K-KG/2,L-LG/2):YI=-FNYABC(H-HG/2,K-KG/2,L-LG/2)
4330 X=XI*CO+YI*SI:Y=-XI*SI+YI*CO
4340 CIRCLE(X,Y),DDA
4350 RETURN
4360 *Q1
4370 IF NQ1+NQ8>69 THEN BEEP:RETURN
4380 NQ1=NQ1+1 : XX1=XX1+INDX
4390 IF NQ1-3*INT(NQ1/3)<>1 THEN 4410
4400 XY1=XY1-2*INDX+INDY : XX1=XX1+INDX/2
4410 LINE(DD,WAI)-(XX1,WAI) : LINE(XX1,WAI)-(XX1,XY1)
4420 LINE(XX1,XY1)-(2*DD,XY1)
4430 LOCATE 70+3*(NQ1-1-3*INT((NQ1-1)/3)),INT((NQ1-1)/3):PRINT IJ
4440 XY1=XY1+INDX
4450 RETURN
4460 *Q2
4470 IF NQ1+NQ8>69 THEN BEEP:RETURN
4480 NQ1=NQ1+1 : XX1=XX1+INDX : YY2=YY2-INDX
4490 IF NQ1-3*INT(NQ1/3)<>1 THEN GOTO 4510
4500 XY1=XY1-2*INDX+INDY : XX1=XX1+INDX/2 : YY2=YY2-INDX
4510 LINE(EKS,-DD)-(EKS,YY2) : LINE(EKS,YY2)-(XX1,YY2)
4520 LINE(XX1,YY2)-(XX1,XY1) : LINE(XX1,XY1)-(2*DD,XY1)
4530 LOCATE 70+3*(NQ1-1-3*INT((NQ1-1)/3)),INT((NQ1-1)/3):PRINT IJ
4540 XY1=XY1+INDX
4550 RETURN
4560 *Q3
4570 IF NQ4+NQ5>69 THEN BEEP:RETURN
4580 NQ4=NQ4+1 : XX4=XX4-INDX : YY3=YY3-INDX
4590 IF NQ4-3*INT(NQ4/3)<>1 THEN GOTO 4610
4600 XY4=XY4-2*INDX+INDY : XX4=XX4-INDX/2 : YY3=YY3-INDX
4610 LINE(EKS,-DD)-(EKS,YY3) : LINE(EKS,YY3)-(XX4,YY3)
4620 LINE(XX4,YY3)-(XX4,XY4) : LINE(XX4,XY4)-(-2*DD,XY4)
4630 LOCATE 1+3*(NQ4-1-3*INT((NQ4-1)/3)),INT((NQ4-1)/3):PRINT IJ
4640 XY4=XY4+INDX
4650 RETURN
4660 *Q4
4670 IF NQ4+NQ5>69 THEN BEEP:RETURN
4680 NQ4=NQ4+1 : XX4=XX4-INDX
4690 IF NQ4-3*INT(NQ4/3)<>1 THEN 4710
4700 XY4=XY4-2*INDX+INDY : XX4=XX4-INDX/2
4710 LINE(-DD,WAI)-(XX4,WAI) : LINE(XX4,WAI)-(XX4,XY4)
4720 LINE(XX4,XY4)-(-2*DD,XY4)
4730 LOCATE 1+3*(NQ4-1-3*INT((NQ4-1)/3)),INT((NQ4-1)/3):PRINT IJ
4740 XY4=XY4+INDX
4750 RETURN
4760 *Q5
```

```
4770 IF NQ4+NQ5>69 THEN BEEP:RETURN
4780 NQ5=NQ5+1 : XX5=XX5-INDX
4790 IF NQ5-3*INT(NQ5/3)<>1 THEN 4810
4800 XY5=XY5-4*INDX-INDY : XX5=XX5-INDX/2
4810 LINE(-DD,WAI)-(XX5,WAI) : LINE(XX5,WAI)-(XX5,XY5)
4820 LINE(XX5,XY5)-(-2*DD,XY5)
4830 LOCATE 1+3*(NQ5-1-3*INT((NQ5-1)/3)),22-INT((NQ5-1)/3):PRINT IJ
4840 XY5=XY5+INDX
4850 RETURN
4860 *Q6
4870 IF NQ4+NQ5>69 THEN BEEP:RETURN
4880 NQ5=NQ5+1 : XX5=XX5-INDX : YY6=YY6+INDX
4890 IF NQ5-3*INT(NQ5/3)<>1 THEN GOTO 4910
4900 XY5=XY5-4*INDX-INDY : XX5=XX5-INDX/2 : YY6=YY6+INDX
4910 LINE(EKS,DD)-(EKS,YY6) : LINE(EKS,YY6)-(XX5,YY6)
4920 LINE(XX5,YY6)-(XX5,XY5) : LINE(XX5,XY5)-(-2*DD,XY5)
4930 LOCATE 1+3*(NQ5-1-3*INT((NQ5-1)/3)),22-INT((NQ5-1)/3):PRINT IJ
4940 XY5=XY5+INDX
4950 RETURN
4960 *Q7
4970 IF NQ1+NQ8>69 THEN BEEP:RETURN
4980 NQ8=NQ8+1 : XX8=XX8+INDX : YY7=YY7+INDX
4990 IF NQ8-3*INT(NQ8/3)<>1 THEN GOTO 5010
5000 XY8=XY8-4*INDX-INDY : XX8=XX8+INDX/2 : YY7=YY7+INDX
5010 LINE(EKS,DD)-(EKS,YY7) : LINE(EKS,YY7)-(XX8,YY7)
5020 LINE(XX8,YY7)-(XX8,XY8) : LINE(XX8,XY8)-(2*DD,XY8)
5030 LOCATE 70+3*(NQ8-1-3*INT((NQ8-1)/3)),22-INT((NQ8-1)/3):PRINT IJ
5040 XY8=XY8+INDX
5050 RETURN
5060 *Q8
5070 IF NQ1+NQ8>69 THEN BEEP:RETURN
5080 NQ8=NQ8+1 : XX8=XX8+INDX
5090 IF NQ8-3*INT(NQ8/3)<>1 THEN 5110
5100 XY8=XY8-4*INDX-INDY : XX8=XX8+INDX/2
5110 LINE(DD,WAI)-(XX8,WAI) : LINE(XX8,WAI)-(XX8,XY8)
5120 LINE(XX8,XY8)-(2*DD,XY8)
5130 LOCATE 70+3*(NQ8-1-3*INT((NQ8-1)/3)),22-INT((NQ8-1)/3):PRINT IJ
5140 XY8=XY8+INDX
5150 RETURN
```

List for HP-86 (Hewlett-Packard)

```
10 REM 'HOLZ UNIVERSAL'
20 !  **** MAIN ****
30 INTEGER HA(300),KA(300),LA(300),DISK(300)
40 DIM XA(300),YA(300),TK1$[50],TK2$[20]
50 SHORT A,B,C,ALP,BET,GAM,E,RANGE,RANGEA,RR,RD,RD1,RD2,RD3,RDA
60 SHORT HG,KG,LG,INTE,ANG,ANGLE,THET,THETA
70 INTEGER SYSTEM,BRAV,H,K,L,N,H1,K1,L1,H2,K2,L2,U,V,W,X1,Y1,Z1,X2,Y2,Z2
80 INTEGER O1,O2,O3,I,P,P4,HI,KI,LI,HJ,KJ,LJ
90 PLOTTER IS 1 @ GCLEAR @ CLEAR @ GOSUB LAB
100 DISP "  SET A PAPER TO PLOTTER"
110 DISP "     SPECIMEN NAME ";
120 INPUT NAME$
130 DEG
140 DISP "      CRYSTAL SYSTEM "
150 DISP "        Cubic              ------------------------------ 1"
160 DISP "        Hexagonal(Trigonal,Rhombohedral) ------- 2"
170 DISP "        Rhombohedral(Rhombohedral coodinates) - 3"
180 DISP "        Tetragonal         ------------------------------ 4"
190 DISP "        Orthorhombic       ------------------------------ 5"
200 DISP "        Monoclinic         ------------------------------ 6"
210 DISP "        Triclinic          ------------------------------ 7"
220 INPUT SYSTEM
230 BRAV=1
240 IF SYSTEM=2 OR SYSTEM=3 OR SYSTEM=7 THEN 340
250 DISP "    LATTICE TYPE "
260 DISP "                 Primitive          --------- 1"
270 DISP "                 Body centered      --------- 2"
280 DISP "                 Fase centered      --------- 3"
290 DISP "                 A-Base centered      ------- 4"
300 DISP "                 B-Base centered      ------- 5"
310 DISP "                 C-Base centered      ------- 6"
320 DISP "                 Special              ------- 7"
330 INPUT BRAV
340 ON SYSTEM GOSUB SYS1 ,SYS2 ,SYS3 ,SYS4 ,SYS5 ,SYS6 ,SYS7
350 DISP "ACCELERATING VOLTAGE (kV)";
360 INPUT E
370 DISP "TWO REFLECTION IN 0TH LAUE ZONE H1,K1,L1,H2,K2,L2 (NON PARALLEL)";
380 INPUT H1,K1,L1,H2,K2,L2
390 IF FNL(H1,K1,L1)=0 OR FNL(H2,K2,L2)=0 THEN DISP "NON ZERO!" @ GOTO 370
400 IF FNCO(H1,K1,L1,H2,K2,L2)^2>.99 THEN DISP "NON PARALLEL!" @ GOTO 370
410 DISP "ZONE AXIS U,V,W  ";
420 INPUT U,V,W
430 IF 0=FNPRO(U,V,W,H1,K1,L1) AND 0=FNPRO(U,V,W,H2,K2,L2) THEN 450
440 DISP "ZONE AXIS IS NOT PERPENDICULAR TO 0TH LAUE ZONE. REINPUT!" @ GOTO 370
450 DISP "G-REFLECTION HG,KG,LG  ";
460 INPUT HG,KG,LG
470 IF 0=FNPRO(U,V,W,HG,KG,LG) THEN 490
480 DISP "G-REFLECTION IS NOT IN THE 0TH LAUE ZONE. REINPUT!" @ GOTO 450
490 DISP "IN WHICH LAUE ZONE REQUIRED REFLECTIONS ARE? INPUT ORDER N"
500 INPUT N
510 DISP "TWO NONLINEAR VECTORS V1 AND V2 BY WHICH ALL THE RECIPROCAL"
520 DISP "LATTICE POINTS IN THE 0-TH LAUE ZONE ARE COVERED."
530 DISP " (V1 DETERMINES THE HORIZONETAL DIRECTION IN THE OUTPUT)"
540 DISP "X1,Y1,Z1, X2,Y2,Z2=";
550 INPUT X1,Y1,Z1,X2,Y2,Z2
560 IF 0=FNPRO(U,V,W,X1,Y1,Z1) AND 0=FNPRO(U,V,W,X2,Y2,Z2) THEN 580
570 DISP "VECTOR IS NOT 0-TH L.Z.. REINPUT " @ GOTO 540
580 IF .99>FNCO(X1,Y1,Z1,X2,Y2,Z2)^2 THEN 600
590 DISP "VECTOR1 AND VECTOR2 CAN NOT PARALLEL,REINPUT" @ GOTO 540
600 DISP "INPUT TWO NUMBERS,DIAMETER OF DISKS AND SEARCHING AREA,IN UNITS OF"
610 DISP "   MIN[ABS(H1,K1,L1),ABS(H2,K2,L2),ABS(H1-H2,K1-K2,L1-L2)]"
620 INPUT RDA,RANGEA
630 DISP "DRAW HOLZRING (Y/N)";
```

```
640 INPUT HR$
650 IF HR$#"N" THEN GOTO 720
660 DISP "INTENSITY OF THE 'HOLZ' PATTERN.(normal set:10)";
670 INPUT INTE
680 IF INTE=0 THEN INTE=10
690 IF INTE<0 THEN INTE=-INTE
700 DISP "DRAW OUTLINE OF DISK IN THE 'HOLZ' PATTERN (Y/N)";
710 INPUT HD$
720 GOSUB ZONE
730 GOSUB RECIPRO
740 GOSUB DEFINITION
750 GOSUB SEARCH
760 PLOTTER IS 1
770 GCLEAR 60 @ MOVE 80,50 @ LORG 5 @ CSIZE 20 @ LABEL "PLOTTIG"
780 IF HR$="N" THEN 910
790 GOSUB HOLZRING
800 GOSUB LABELING
810 ALPHA
820 DISP "IF DRAW HOLZ , SET A PAPER TO PLOTTER (Y/N)";
830 INPUT HOLZ$
840 IF HOLZ$="N" THEN 930
850 DISP "INTENSITY OF THE 'HOLZ' PATTERN.(normal set:10)";
860 INPUT INTE
870 IF INTE=0 THEN INTE=10
880 IF INTE<0 THEN INTE=-INTE
890 DISP "DRAW OUTLINE OF DISK IN THE 'HOLZ' PATTERN (Y/N)";
900 INPUT HD$
910 GOSUB HOLZ
920 GOSUB LABELING
930 PLOTTER IS 1 @ GRAPH @ GCLEAR 60
940 MOVE 80,50 @ CSIZE 20 @ LORG 5 @ LABEL "END"
950 BEEP @ END
960 !  ** DIFINITION OF USER FUNCTION **
970 DEF FNPRO(X1,Y1,Z1,X2,Y2,Z2) = X1*X2+Y1*Y2+Z1*Z2
980 DEF FNL(X,Y,Z) = SQR (X*X+Y*Y+Z*Z)
990 DEF FNCO(X1,Y1,Z1,X2,Y2,Z2) = (X1*X2+Y1*Y2+Z1*Z2)/(SQR (X1*X1+Y1*Y1+Z1*Z1)*S
QR (X2*X2+Y2*Y2+Z2*Z2))
1000 DEF FNRL(X,Y,Z) = SQR ((X*AX)^2+(X*AY+Y*BY+Z*CY)^2+(X*AZ+Z*CZ)^2)
1010 DEF FNXA(X,Y,Z) = X*AX+Y*BX+Z*CX
1020 DEF FNYA(X,Y,Z) = X*AY+Y*BY+Z*CY
1030 DEF FNZA(X,Y,Z) = X*AZ+Y*BZ+Z*CZ
1040 DEF FNPROX(X,Y,Z) = (UU*WW*X+VV*WW*Y-FA1*FA1*Z)/(FA1*FA2)
1050 DEF FNPROY(X,Y,Z) = (-(VV*X)+UU*Y)/FA1
1060 DEF FNXPP(X,Y) = -X+SQR (R^2-(Y+AREA)^2)
1070 DEF FNXPN(X,Y) = -X-SQR (R^2-(Y+AREA)^2)
1080 DEF FNXNP(X,Y) = -X+SQR (R^2-(Y-AREA)^2)
1090 DEF FNXNN(X,Y) = -X-SQR (R^2-(Y-AREA)^2)
1100 DEF FNYPP(X,Y) = -Y+SQR (R^2-(X+AREA)^2)
1110 DEF FNYPN(X,Y) = -Y-SQR (R^2-(X+AREA)^2)
1120 DEF FNYNP(X,Y) = -Y+SQR (R^2-(X-AREA)^2)
1130 DEF FNYNN(X,Y) = -Y-SQR (R^2-(X-AREA)^2)
1140 !  **** SUB ROUTINE ****
1150 SYS1:
1160  DISP "LATTICE CONSTANT a IN  ";
1170  INPUT A
1180  B=A @ C=A @ ALP=90 @ BET=90 @ GAM=90
1190 RETURN
1200 SYS2:
1210  DISP "             hexagonal,trigonal ----- 1"
1220  DISP "             rhombohedral       ----- 2"
1230  INPUT SYS2
1240  IF SYS2=2 THEN BRAV=8
1250  DISP "LATTICE CONSTANT a,c IN  ";
```

```
1260  INPUT A,C
1270  B=A @ ALP=90 @ BET=90 @ GAM=120
1280 RETURN
1290 SYS3:
1300  DISP "LATTICE CONSTANT a IN  ";
1310  INPUT A
1320  DISP "ANGLE alpha IN DEG";
1330  INPUT ALP
1340  B=A @ C=A @ BET=ALP @ GAM=ALP
1350 RETURN
1360 SYS4:
1370  DISP "LATTICE CONSTANT a,c IN  ";
1380  INPUT A,C
1390  B=A @ ALP=90 @ BET=90 @ GAM=90
1400 RETURN
1410 SYS5:
1420  DISP "LATTICE CONSTANT a,b,c IN  ";
1430  INPUT A,B,C
1440  ALP=90 @ BET=90 @ GAM=90
1450 RETURN
1460 SYS6:
1470  DISP "UNIQUE AXIS b OR c";
1480  INPUT UNIA$
1490  DISP "LATTICE CONSTANT a,b,c IN  ";
1500  INPUT A,B,C
1510  IF UNIA$="C" OR UNIA$="c" THEN 1550
1520  DISP "ANGLE beta IN DEG";
1530  INPUT BET
1540  ALP=90 @ GAM=90 @ GOTO 1580
1550  DISP "ANGLE gamma IN DEG";
1560  INPUT GAM
1570  ALP=90 @ BET=90
1580 RETURN
1590 SYS7:
1600  DISP "LATTICE CONSTANT a,b,c IN  ";
1610  INPUT A,B,C
1620  DISP "ANGLE alpha,beta,gamma IN DEG";
1630  INPUT ALP,BET,GAM
1640 RETURN
1650 LAB:
1660  BEEP
1670  PLOTTER IS 1
1680  TK1$="by   PHYS. DEPT.,FAC OF SCI.,TOHOKU UNIV."
1690  TK2$="T.KANEYAMA"
1700  CSIZE 5 @ LORG 5
1710  MOVE 80,90 @ LABEL TK1$
1720  CSIZE 7 @ MOVE 80,80 @ LABEL TK2$
1730  WAIT 2000
1740  BEEP
1750 RETURN
1760 ZONE:
1770  MOVE 80,50 @ CSIZE 20 @ LABEL "SEARCHING"
1780  FOR HI=0 TO 5
1790  FOR HJ=0 TO 1
1800   H=HI*((-1)^HJ)
1810  FOR KI=0 TO 5
1820  FOR KJ=0 TO 1
1830   K=KI*((-1)^KJ)
1840  FOR LI=0 TO 5
1850  FOR LJ=0 TO 1
1860   L=LI*((-1)^LJ)
1870   IF N#FNPRO(U,V,W,H,K,L) THEN 1900
1880   ON BRAV GOSUB P ,I ,F ,A ,B ,C ,S ,R
```

```
1890   IF AL=1 THEN 2010
1900  NEXT LJ
1910  NEXT LI
1920  NEXT KJ
1930  NEXT KI
1940  NEXT HJ
1950  NEXT HI
1960  DISP "INPUT INDEX OF A RECIPROCAL LATTICE POINT IN NTH LAUE ZONE"
1970  DISP "ALLOWED BY EXTINCTION RULE: H,K,L";
1980  INPUT H,K,L
1990  ON BRAV GOSUB P ,I ,F ,A ,B ,C ,S ,R
2000  IF AL=0 OR N#FNPRO(U,V,W,H,K,L) THEN DISP "  REINPUT!!" @ GOTO 1960
2010 RETURN
2020 !
2030 ! extinction rule
2040 P:
2050  AL=1 @ RETURN
2060 I:
2070  AL=(H+K+L+1) MOD 2 @ RETURN
2080 F:
2090  IF (H+K) MOD 2=0 AND (H+L) MOD 2=0 THEN AL=1 ELSE AL=0
2100 RETURN
2110 A:
2120  AL=(K+L+1) MOD 2 @ RETURN
2130 B:
2140  AL=(L+H+1) MOD 2 @ RETURN
2150 C:
2160  AL=(H+K+1) MOD 2 @ RETURN
2170 R:
2180  IF (-H+K+L) MOD 3=0 THEN AL=1 ELSE AL=0
2190 RETURN
2200 S:
2210 ! SPECIAL CASE : PROGRAM BY YOU YOURSELF!
2220 ! AL=1 --- ALLOWED
2230 ! AL=0 --- FORBIDDEN
2240 ! WHEN X IS ODD NUMBER, X MOD 2 =1
2250 ! WHEN X IS EVEN NUMBER , X MOD 2 =0
2260 AL=1
2270 RETURN
2280 !
2290 RECIPRO:
2300 ! construction of reciprocal lattice
2310  COA=COS (ALP) @ COB=COS (BET) @ COG=COS (GAM)
2320  SIA=SIN (ALP) @ SIB=SIN (BET) @ SIG=SIN (GAM)
2330  DREA=SQR (1-COA^2-COB^2-COG^2+2*COA*COB*COG)
2340  AST=SIA/(A*DREA) @ BST=SIB/(B*DREA) @ CST=SIG/(C*DREA)
2350  COAST=(COB*COG-COA)/(SIB*SIG) @ SIAST=DREA/(SIB*SIG)
2360  COBST=(COG*COA-COB)/(SIG*SIA) @ SIBST=DREA/(SIG*SIA)
2370  COGST=(COA*COB-COG)/(SIA*SIB) @ SIGST=DREA/(SIA*SIB)
2380  AXO=A @ AYO=0 @ AZO=0
2390  BXO=B*COG @ BYO=B*DREA/SIB @ BZO=B*(COA-COB*COG)/SIB
2400  CXO=C*COB @ CYO=0 @ CZO=C*SIB
2410 AX=1/A @ AY=(COA*COB-COG)/(A*DREA*SIB) @ AZ=-(COB/(A*SIB))
2420 BX=0 @ BY=BST @ BZ=0
2430 CX=0 @ CY=(COB*COG-COA)/(C*DREA*SIB) @ CZ=1/(C*SIB)
2440 RETURN
2450 !
2460 DEFINITION:
2470  VOL=A*B*C*DREA @ VOLST=1/VOL
2480 S11ST=(BST*CST*SIAST)^2 @ S22ST=(AST*CST*SIBST)^2
2490 S33ST=(AST*BST*SIGST)^2 @ S12ST=AST*BST*CST^2*(COAST*COBST-COGST)
2500 S23ST=AST^2*BST*CST*(COBST*COGST-COAST)
2510 S31ST=AST*BST^2*CST*(COGST*COAST-COBST)
```

```
2520 WN2=1000*E*(1+.000000978*1000*E)/12.26^2 @ WN=SQR (WN2)
2530 D=N*VOLST/SQR (S11ST*U*U+S22ST*V*V+S33ST*W*W+2*S12ST*U*V+2*S23ST*V*W+2*S31S
T*W*U)
2540 RG=FNRL(HG/2,KG/2,LG/2)
2550 R=SQR (WN2-(SQR (WN2-RG*RG)-D)^2)
2560 RD1=FNRL(H1,K1,L1)/2 @ RD2=FNRL(H2,K2,L2)/2 @ RD3=FNRL(H1-H2,K1-K2,L1-L2)/2

2570 IF RD1<RD2 THEN RD=RD1 ELSE RD=RD2
2580 IF RD>RD2 THEN RD=RD2
2590 DD=RDA*RD @ RANGE=RANGEA*RD
2600 UU=U*AXO+V*BXO+W*CXO @ VV=U*AYO+V*BYO+W*CYO @ WW=U*AZO+V*BZO+W*CZO
2610 FA1=SQR (UU*UU+VV*VV) @ FA2=SQR (UU*UU+VV*VV+WW*WW)
2620 IF FA1<.0001 THEN 2660
2630 X=FNPROX(FNXA(X1,Y1,Z1),FNYA(X1,Y1,Z1),FNZA(X1,Y1,Z1))
2640 Y=FNPROY(FNXA(X1,Y1,Z1),FNYA(X1,Y1,Z1),FNZA(X1,Y1,Z1))
2650 GOTO 2670
2660 X=FNXA(X1,Y1,Z1) @ Y=FNYA(X1,Y1,Z1)
2670 CO=FNCO(1,0,0,X,Y,0) @ SI=-FNCO(0,1,0,X,Y,0)
2680 IF FA1<.0001 THEN 2720
2690 XIG=FNPROX(FNXA(HG,KG,LG),FNYA(HG,KG,LG),FNZA(HG,KG,LG))
2700 YIG=FNPROY(FNXA(HG,KG,LG),FNYA(HG,KG,LG),FNZA(HG,KG,LG))
2710 GOTO 2730
2720 XIG=FNXA(HG,KG,LG) @ YIG=FNYA(HG,KG,LG)
2730 XG=CO*XIG-SI*YIG @ YG=SI*XIG+CO*YIG
2740 LENG=XIG^2+YIG^2
2750 RETURN
2760 SEARCH:
2770 ! searching allowed reflection in the n-th laue zone
2780 I=0 @ O1=0 @ O2=0 @ O3=0 @ P=0 @ P4=0
2790 GOSUB VEX
2800 IF I=3 THEN 2930
2810 LL=FNRL(H-HG/2,K-KG/2,L-LG/2)
2820 IF LL>R-RANGE AND LL<R+RANGE THEN P=1
2830 IF LL<= R-RANGE THEN P=2
2840 IF LL>= R+RANGE THEN P=3
2850 IF P=3 AND O2#0 THEN P=4
2860 IF P=4 THEN P4=P4+1
2870 ON P GOSUB BRAGG ,V2 ,VIN ,V2
2880 IF P=1 THEN GOSUB VIN
2890 IF P=3 AND O2=0 AND O1>20 THEN GOSUB TURN
2900 IF P=2 OR P=4 THEN GOTO 2790
2910 IF P=10 THEN 2930
2920 GOTO 2800
2930 IF O3=0 THEN DISP "COULD NOT FIND EXCITED REFLECTION IN THE NTH LAUE ZONE"
2940 BEEP
2950 RETURN
2960 VEX:
2970 H=H+(X1*((-1)^I)) @ K=K+(Y1*((-1)^I)) @ L=L+(Z1*((-1)^I))
2980 IF FNRL(H-HG/2,K-KG/2,L-LG/2)<= R+RANGE THEN 2970
2990 RETURN
3000 VIN:
3010 H=H-(X1*((-1)^I)) @ K=K-(Y1*((-1)^I)) @ L=L-(Z1*((-1)^I)) @ O1=O1+1
3020 RETURN
3030 V2:
3040 GOSUB VEX
3050 H=H+(X2*((-1)^I)) @ K=K+(Y2*((-1)^I)) @ L=L+(Z2*((-1)^I)) @ O1=0 @ O2=0
3060 RETURN
3070 TURN:
3080 I=I+1
3090 H=H+((P4+1)*X2*((-1)^I)) @ K=K+((P4+1)*Y2*((-1)^I)) @ L=L+((P4+1)*Z2*((-1)^
I))
3100 GOSUB VIN
3110 IF FNRL(H-HG/2,K-KG/2,L-LG/2)>R+RANGE THEN 3100
```

```
3120 O1=0 @ O2=0 @ P=2 @ P4=0
3130 RETURN
3140 DRAGG:
3150 O1=0 @ O2=O2+1
3160 ON DRAW GOSUB P ,I ,F ,A ,B ,C ,S ,R
3170 IF ML=0 THEN RETURN
3180 IF O7=0 THEN 3200
3190 IF (H-HA(1))^2<.1 AND (K-KA(1))^2<.1 AND (L-LA(1))^2<.1 AND I=2 THEN P=10 @
 RETURN
3200 O3=O3+1
3210 XI=FNXA(H-HG/2,K-KG/2,L-LG/2) @ YI=FNYA(H-HG/2,K-KG/2,L-LG/2) @ ZI=FNZA(H-H
G/2,K-KG/2,L-LG/2)
3220 IF FA1<.000001 THEN X=XI @ Y=YI @ GOTO 3240
3230 X=FNPROX(XI,YI,ZI) @ Y=FNPROY(XI,YI,ZI)
3240 HA(O3)=H @ KA(O3)=K @ LA(O3)=L
3250 XA(O3)=CO*X-SI*Y @ YA(O3)=SI*X+CO*Y
3260 IF LL>R-DD AND LL<R+DD THEN DISK(O3)=1 ELSE DISK(O3)=0
3270 RETURN
3280 !
3290 HOLZRING:
3300 ! plot holz ring and index
3310 GRAPH
3320 PLOTTER IS 905
3330 DEG @ PEN 1
3340 LOCATE 46,136.5,95
3350 SHOW -(R+RANGE+5*DD),R+RANGE+5*DD,-(R+RANGE+5*DD),R+RANGE+5*DD
3360 MOVE -(XG/2),-(YG/2)
3370 FOR ANG=0 TO 360 STEP 10
3380 RPLOT DD*COS (ANG),DD*SIN (ANG)
3390 NEXT ANG
3400 IF HG=0 AND KG=0 AND LG=0 THEN 3440
3410 O3=O3+1
3420 HA(O3)=HG @ KA(O3)=KG @ LA(O3)=LG
3430 XA(O3)=XG/2 @ YA(O3)=YG/2
3440 FOR I=1 TO O3
3450 MOVE XA(I),YA(I)
3460  FOR ANG=0 TO 360 STEP 20
3470   RPLOT DD*COS (ANG),DD*SIN (ANG)
3480  NEXT ANG
3490 NEXT I
3500 MOVE 0,0
3510 FOR ANG=0 TO 360 STEP 3
3520 RPLOT R*COS (ANG),R*SIN (ANG)
3530 NEXT ANG
3540 CS=30*DD/R
3550 IF CS<2.5 THEN CS=2.5
3560 CSIZE CS,.4 @ LDIR 0 @ LORG 5
3570 MOVE -(XG/2),-(YG/2)
3580 LABEL "0 0 0"
3590 PEN 1
3600 LORG 5
3610 FOR I=1 TO O3
3620 IF XA(I)=0 AND YA(I)>0 THEN THET=90 @ LDIR 90 @ LORG 2 @ GOTO 3680
3630 IF XA(I)=0 AND YA(I)<0 THEN THET=270 @ LDIR 90 @ LORG 8 @ GOTO 3680
3640 THETA=ATN (YA(I)/XA(I)) @ LDIR THETA
3650 IF XA(I)>0 THEN THET=THETA @ LORG 2 @ GOTO 3680
3660 IF XA(I)<0 THEN THET=THETA+180 @ LORG 8 @ GOTO 3680
3670 GOTO 3710
3680 XRI=XA(I)+DD*COS (THET) @ YRI=YA(I)+DD*SIN (THET)
3690 MOVE XRI,YRI
3700 LABEL " ";HA(I);KA(I);LA(I);" "
3710 NEXT I
3720 RETURN
```

```
3730 !
3740 HOLZ:
3750 ! plot holz line and index
3760 GRAPH
3770 PLOTTER IS 805
3780 LOCATE 57,129,14,86
3790 AREA=DD*1.2 @ THET=1.5*180*AREA/(R*PI ) @ ANGLE=360*DD/(INTE*R*PI )
3800 SHOW -AREA,AREA,-AREA,AREA
3810 DEG @ PEN 2 @ CSIZE 3,.4
3820 IF HR$="N" OR HR$="n" THEN 3850
3830 IF HG=0 AND KG=0 AND LG=0 THEN 3850
3840 O3=O3-1
3850 FOR I=1 TO O3
3860 IF DISK(I)=0 THEN 3960
3870 THETA=(360+ATN2 (-YA(I),-XA(I))) MOD 360
3880 P=THETA DIV 45+1
3890 MOVE -XA(I),-YA(I)
3900 FOR ANG=THETA-THET TO THETA+THET STEP ANGLE
3910 RPLOT -(R*COS (ANG)),-(R*SIN (ANG))
3920 NEXT ANG
3930 ON P GOSUB P1 ,P2 ,P3 ,P4 ,P5 ,P6 ,P7 ,P8
3940 MOVE X,Y
3950 LABEL " ";HA(I);KA(I);LA(I)
3960 NEXT I
3970 IF HD$="N" THEN 4020
3980 MOVE 0,0
3990 FOR ANG=0 TO 360 STEP 3
4000 RPLOT DD*COS (ANG),DD*SIN (ANG)
4010 NEXT ANG
4020 RETURN
4030 P1:
4040 LDIR 90
4050 X=FNXPN(XA(I),YA(I))
4060 IF ABS (X)<= AREA THEN Y=AREA @ LORG 2 @ RETURN
4070 X=FNXNN(XA(I),YA(I)) @ Y=-AREA @ LORG 8
4080 RETURN
4090 P2:
4100 LDIR 0
4110 Y=FNYPN(XA(I),YA(I))
4120 IF ABS (Y)<= AREA THEN X=AREA @ LORG 2 @ RETURN
4130 X=-AREA @ Y=FNYNN(XA(I),YA(I)) @ LORG 8
4140 RETURN
4150 P3:
4160 LDIR 0
4170 Y=FNYNN(XA(I),YA(I))
4180 IF ABS (Y)<= AREA THEN X=-AREA @ LORG 8 @ RETURN
4190 X=AREA @ Y=FNYPN(XA(I),YA(I)) @ LORG 2
4200 RETURN
4210 P4:
4220 LDIR 90
4230 X=FNXPP(XA(I),YA(I))
4240 IF ABS (X)<= AREA THEN Y=AREA @ LORG 2 @ RETURN
4250 X=FNXNP(XA(I),YA(I)) @ Y=-AREA @ LORG 8
4260 RETURN
4270 P5:
4280 LDIR 90
4290 X=FNXNP(XA(I),YA(I))
4300 IF ABS (X)<= AREA THEN Y=-AREA @ LORG 8 @ RETURN
4310 X=FNXPP(XA(I),YA(I)) @ Y=AREA @ LORG 2
4320 RETURN
4330 P6:
4340 LDIR 0
4350 Y=FNYNP(XA(I),YA(I))
```

```
4360 IF ABS (Y)<= AREA THEN X=-AREA @ LORG 8 @ RETURN
4370 X=AREA @ Y=FNYPP(XA(I),YA(I)) @ LORG 2
4380 RETURN
4390 P7:
4400 LDIR 0
4410 Y=FNYPP(XA(I),YA(I))
4420 IF ABS (Y)<= AREA THEN X=AREA @ LORG 2 @ RETURN
4430 X=-AREA @ Y=FNYNP(XA(I),YA(I)) @ LORG 8
4440 RETURN
4450 P8:
4460 LDIR 90
4470 X=FNXNN(XA(I),YA(I))
4480 IF ABS (X)<= AREA THEN Y=-AREA @ LORG 8 @ RETURN
4490 X=FNXPN(XA(I),YA(I)) @ Y=AREA @ LORG 2
4500 RETURN
4510 !
4520 LABELING:
4530 ! label several data
4540 SETGU @ LDIR 0 @ LORG 1 @ CSIZE 10
4550 MOVE 6,87
4560 LABEL NAME$
4570 CSIZE 6
4580 MOVE 7,80
4590 LABEL "[";U;V;W;"]"
4600 MOVE 9,73
4610 LABEL E;"kV"
4620 CSIZE 4
4630 MOVE 9,67
4640 ON N GOTO 4650,4660,4670,4680,4680,4680,4680,4680
4650 LABEL "1st Laue Zone" @ GOTO 4690
4660 LABEL "2nd Laue Zone" @ GOTO 4690
4670 LABEL "3rd Laue Zone" @ GOTO 4690
4680 LABEL N;"th Laue Zone"
4690 CSIZE 5
4700 MOVE 8,61
4710 LABEL "G=(";HG;KG;LG;")"
4720 CSIZE 4
4730 MOVE 9,54
4740 LABEL "a=";A;"(A)"
4750 MOVE 9,50
4760 LABEL "b=";B;"(A)"
4770 MOVE 9,46
4780 LABEL "c=";C;"(A)"
4790 MOVE 9,42
4800 LABEL "alpha=";ALP;"(deg)"
4810 MOVE 9,38
4820 LABEL "beta =";BET;"(deg)"
4830 MOVE 9,34
4840 LABEL "gamma=";GAM;"(deg)"
4850 MOVE 9,28
4860 CSIZE 3
4870 RR=R
4880 LABEL "RADIUS OF HOLZ RING"
4890 MOVE 9,24
4900 LABEL " =";RR;"(1/A)"
4910 MOVE 9,20
4920 LABEL "HORIZONTAL DIRECTION"
4930 LABEL " =(";X1;Y1;Z1;")"
4940 PEN 0 @ BEEP
4950 RETURN
```

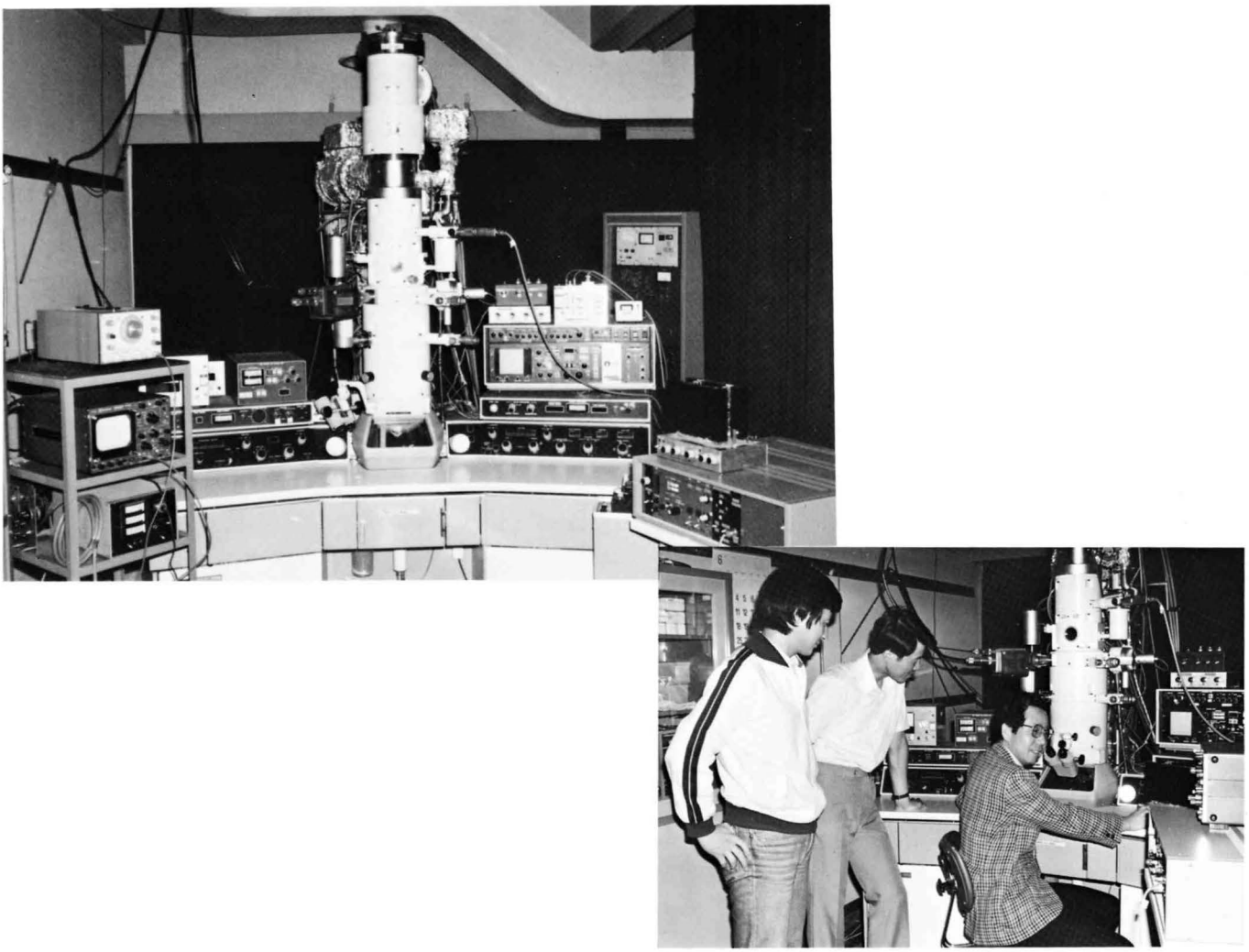

Associate Professor M. Tanaka, Mr. M. Terauchi and Mr. Sato.

Our JEM-100CX was purchased for CBED studies in 1976 with the Grant-in-Aid of Scientific Research No. 142009 from the Ministry of Education, Science and Culture (hereinafter abbreviated to "SR-Grant"). A STEM attachment was purchased in 1978 with SR-Grant No. 346033 for developing STEM- and BR-CBED. The signal processing of CBED patterns was performed with the finantial support of the Kurata Research Grant (1978).

To obtain a cleaner vacuum, a 20 ℓ ion pump was attached to the specimen chamber; an anti-contamination trap was installed at the intermediate lens; conventional aperture holders for the condenser, objective and intermediate lenses were replaced with metal bellows type holders; and a newly developed Fomblin fluorinated grease, YVAC3, was used for viton O-rings. Use was made of square, hexagonal and rectangular condenser apertures. A function was added which can vary the operating voltage in steps of 70 volts from the preset voltage. A bright electron source of LaB_6 was introduced instead of a tungusten hairpin filament.

A preliminary study of BR-LACBED was begun by the support of the Kurata Research Grant, and the final mechanical and electrical devices for BR-LACBED were constructed with the Grant-in-Aid for Developmental Scientific Research No. 56840016 from the Ministry of Education, Science and Culture (1981). A thermal type field-emission-gun (FEG) was installed in our microscope together with an electronically controlled automatic evacuation system for the gun chamber in 1983 with SR-Grant No. 57420014. The effectiveness of the FEG is described in the text. Technical developments, including the HCB technique, are still in progress for the exploitation of all possible CBED techniques.

It is not long before the elapse of ten years since our original JEM-100CX was purchased. In the meantime, a great progress has been achieved in the electron optical and especially in the electronical techniques for electron microscopes. Our instrument has become a little outdated and is not alway very easy to operate, in spite of continuous improvements on the instrument. In 1985, a new instrument, the JEM-2000FX, is to be purchased with SR-Grant No. 60420051. We are going to make efforts to enable this instrument to meet all the needs for CBED work.

Michiyoshi Tanaka

Errata
to
Convergent-Beam Electron Diffraction

Page 3: References

1) References [6] and [7] should be interchanged.

2) (1982) in Reference [11] should read (1980)

Page 25: Photo numbers

The photo numbers shown at the right bottoms of the photos on both sides should be changed as follows:

1 → 5, 2 → 6, 3 → 7,

4 (not changed), 5 → 1,

6 → 2, 7 → 3

Page 136: The word "commensulate" should read "commensurate".

JEOL Ltd.